OCS Study
MMS 91-0083

CALIFORNIA OCS PHASE II MONITORING PROGRAM

FINAL REPORT

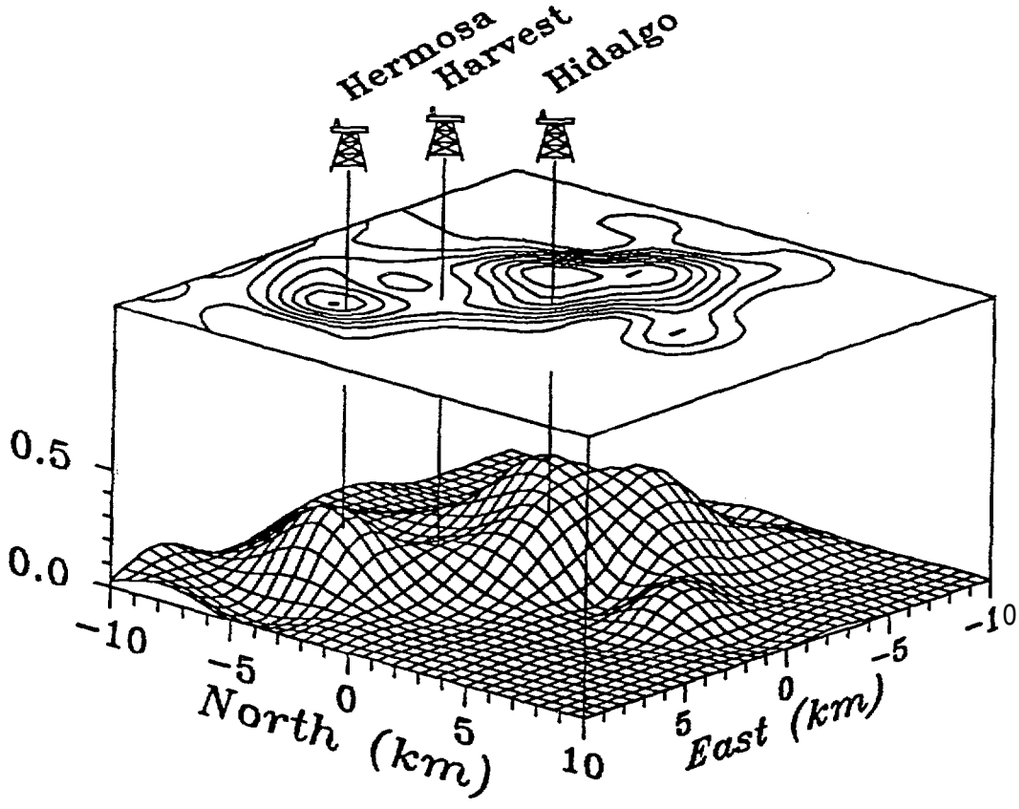

U.S. Department of the Interior
Minerals Management Service
Pacific OCS Region

CALIFORNIA OCS PHASE II MONITORING PROGRAM

FINAL REPORT

Prepared By

Battelle Ocean Sciences
397 Washington Street
Duxbury, Massachusetts 02332

This study was supported by

The Minerals Management Service, Department of the Interior
Pacific OCS Region
770 Paseo Camarillo
Camarillo, California 93010

under

Contract No. 14-12-0001-30262

November 1991

Disclaimer

This report has been reviewed by the Pacific Outer Continental Shelf Region, Minerals Management Service, U.S. Department of the Interior and approved for Publication. The opinions, findings, conclusions, or recommendations expressed in the report are those of the authors, and do not necessarily reflect the views of the Minerals Management Service. Mention of trade names or commercial products does not constitute endorsement or recommendations for use.

TABLE OF CONTENTS

TABLE OF CONTENTS (continued)

TABLE OF CONTENTS (continued)

TABLE OF CONTENTS (continued)

1. INTRODUCTION

WILLIAM STEINHAUER

Battelle
397 *Washington Street, Duxbury, Massachusetts* 02332

EIJI IMAMURA

Marine Research Specialists
3639 *E. Harbor Blvd., Suite 208, Ventura, California 93001*

JEFFREY HYLAND

Marine Science Institute
University of California, Santa Barbara, California 95060

BACKGROUND AND PURPOSE OF THE STUDY

The California Outer Continental Shelf (OCS) Phase II Monitoring Program (CAMP) was a five-year, multidisciplinary study designed to monitor potential environmental changes resulting from oil and gas development in the Santa Maria Basin off the coast of southern California. This program, which was sponsored by the Minerals Management Service (MMS) of the U.S. Department of the Interior, originated in response to requirements under the 1978 OCS Lands Act Amendments (43 U. S. C.-1346) for MMS (then the Bureau of Land Management) to implement studies designed to evaluate environmental impacts of oil- and gas-development activities on human, marine, and coastal resources of the U.S. OCS.

Three additional factors have contributed to the decision to implement this particular study. These factors were

1. The great potential for extensive production of oil and gas from this region of the California OCS.

2. The concern that development of, and production from, a major new oil field on the U.S. OCS may result in cumulative, long-term adverse impacts in the marine environment.

3. The lack of previous oil- and gas-production activities or other major anthropogenic sources in the area.

Recommendations from two panels of experts (one sponsored by the National Research Council of the National Academy of Sciences; the other sponsored by the Interagency Committee on Ocean Pollution Research, Development and Monitoring) have played a part in the scope of CAMP. The panels recommended that monitoring of offshore oil and gas activities focus on evaluation of long-term effects on the marine environment of development of a major oil field in a frontier area of the U.S. OCS (NRC, 1983; Boesch and Rabalais, 1987). During development of a field, much larger volumes of materials (mainly drilling muds and cuttings) are discharged over a longer period of time than during exploratory drilling. Although extensive monitoring of exploratory drilling has revealed few adverse environmental impacts, the long-term cumulative impacts of field development (including drilling and production) can be predicted with much less confidence. Long-term studies also were recommended to gain knowledge about the basic chemical, physical, and biological processes controlling the ecosystems of concern. In summary, the panels recommended long-term studies in order to separate natural ecological variability and long-term natural cycles from those changes actually caused by oil development and production.

This Phase II Monitoring Program extended the pre-drilling baseline sampling conducted in the same study area during the earlier 1983-1984 Phase I Reconnaissance Survey (SAIC, 1986). The Phase I study was conducted to characterize biological, chemical, and geological conditions over a broad region of the Santa Maria Basin and the western Santa Barbara Channel. Results of the Phase II study expanded upon this information, in the process of providing the basis for a definitive evaluation of long-term spatial and temporal impacts of discharges from oil development and production in the southern Santa Maria Basin.

The Phase-II program will provide valuable information for the use in decision-making in the California OCS for years to come. Results from the study will be useful in post-sale steps for existing leases (e.g., approval of development and production plans) and for various pre-sale steps for future sales (e.g., preparation of draft and final environmental impact statements, development of lease conditions or stipulations). In June 1990, President Bush canceled Proposed Lease Sales 91 (Northern Planning Area), 119 (Central California Planning Area), and 95 (Southern California Planning Area). Lease sales in these Planning Areas will not be considered until after the year 2000 except for 87 lease blocks within the Santa Barbara Charnel and the Santa Maria Basin which will not be considered until 1996. Results of the Phase-11 Study also will be useful in the EPA-NPDES permitting process.

Furthermore, the results of this study have expanded our knowledge of basic oceanographic processes and ecological conditions of the Santa Maria Basin region and will provide information to help interpret results of future offshore monitoring programs conducted in other planning areas.

STUDY OBJECTIVES

Specific objectives of the Phase-II program were as follows:

1. To detect and measure potential long-term (or short-term) chemical, physical, and biological 'changes around oil and gas platforms in the southern Santa Maria Basin.

2. To determine whether the observed changes are caused by drilling-related activities or whether they are the product of natural processes.

These objectives were addressed through time-series monitoring of a number of environmental parameters before and after initiation of drilling at various monitoring sites throughout the study area, including control sites and sites where environmental impacts were more likely to occur. An optimal impact study design (Green, 1979) and a-priori hypothesis testing were applied in the process of addressing these objectives so that any conclusions regarding environmental changes could be stated within established levels of statistical confidence. The long-term nature of this program was a unique feature allowing investigators to make comprehensive assessments of the structure of the regional ecosystem and the dynamics of physical, chemical, and biological processes over a time series encompassing both seasonal and repeated annual scales. As a result, knowledge gained from these assessments was used to accomplish the important objective of separating natural background variation from potential low-level cumulative environmental impacts caused by drilling-related activities.

This study focused on examining effects of platform discharges on the benthos. The emphasis has been placed here for two reasons: (1) benthic environments are suspected sinks for the accumulation of discharged drill materials; and (2) because of their relative immobility, benthic organisms should be more susceptible to impacts from exposure to any drilling-related materials that may accumulate on the bottom. Although potential effects of drilling *on* planktonic and pelagic systems should not be ignored, the temporal and spatial variability in these more ephemeral assemblages, relative to the benthos, make hypothesis testing for effects much more difficult (Boesch and Rabalais, 1987).

Specific parameters addressed as part of the time-series monitoring effort consisted of biological community indices and species abundances for hard-bottom and soft-bottom benthic assemblages; concentrations and distributions of trace metals and hydrocarbons in bottom sediments, suspended particulate, animal tissues, and pore waters; water currents and other physical oceanographic features; and various sedimentological properties (e.g., sediment grain size, total organic carbon and carbonate content, sediment shear strength, distribution of mineral types, and redox conditions). Synoptic measurements of these various parameters were taken to permit examination of biological changes in relation to concomitant chemical or physical changes linked to specific drilling events. Additional companion studies focused on sediment-transport processes and animal-sediment-pollutant interactions (which will be reported elsewhere in the literature).

SAMPLING DESIGN AND RATIONALE

The station design for this program was comprised of a series of regional stations and two additional arrays of site-specific stations located in the vicinity of two planned oil development/production platforms off the coast of southern California, in the southern Santa Maria Basin, from Point San Luis (35°06'N) to north of Point Conception (34°28'N; see Figure l-l). The regional stations consisted of three cross-shelf transects of three stations each (encompassing water depths of about 90 to 410 m) and an additional station located approximately 50 km west of Point Sal in a suspected offshore depositional area. Regional stations were selected with two major objectives in mind: (1) to provide an opportunity to compare ecological conditions and potential responses to drilling-related impacts over broad regional areas and bath ymetric zones; and (2) to revisit, wherever possible, previous sampling stations (e.g., sites from the Phase I survey) to provide historical data support. Results of the Phase I Reconnaissance Survey (SAIC, 1986) showed that all regional stations are characterized by soft-bottom benthic assemblages inhabiting sand and mud substrates.

One of the two site-specific sampling arrays was located in unconsolidated substrates offshore of Point Sal, at the anticipated site for Shell Western's Platform Julius. The site-specific study at Platform Julius together with the regional stations comprised the soft-bottom monitoring component of CAMP. Sampling at the regional stations and at the Platform-Julius array was conducted on the following occasions: October 1986, January 1987, May 1987, October 1987, January 1988, May 1988, October 1988, and May 1989. Typically, the 9 regional stations and 19 site-specific stations were sampled on the first three cruises. Because of delays in the installation of Platform Julius, the number

of site-specific stations was reduced to three on the October-1987 cruise, and finally to one station beginning with the May-1988 cruise. With the news of indefinite delays in the installation of Platform Julius, sampling of the soft-bottom benthos was discontinued after May 1989. The Year-3 Annual Report (Steinhauer and Imamura, 1990) summarized the technical activity and results of the soft-bottom monitoring component of CAMP.

The second site-specific sampling array was located offshore of Point Arguello, in the vicinity of Chevron's Platform Hidalgo. Monitoring efforts at this site focused on rocky substrates inhabited by hard-bottom benthic assemblages. Sampling at the hard-bottom stations was conducted October 1986, May 1987, October 1987, October 1988, May 1989, October 1989, and October 1990. There were two important features of these stations: (1) stations consist of both "high-relief" substrates (defined operational y a.. substrates higher than 1 m) and "low-relief" substrates, so that assemblages of epifaunal organisms inhabiting both types of substrates could be monitored to compare their relative susceptibilities and sensitivities to potential impacts; and (2) for each type of substrate, stations were positional at several distances away from the platform so that effects could be monitored along possible "dose-response" gradients.

The sampling design incorporated four major features providing important foundations for statistical and other interpretive analyses. First, replicate sampling was performed at all monitoring sites. The replication approach was selected for several reasons: (1) to support statistical analysis of the data (i.e., variation among samples within sites was used as an error term for testing hypotheses); (2) to enhance within-station coverage (e.g., sampling at a site provided a comprehensive record of species, increasing the probability of encountering rarer species); and (3) to provide a means of revealing any anomalous results within a given station, and thus avoiding the possibility of basing a conclusion on a single outlier. Second, synoptic measurements of a number of biotic and abiotic variables from replicate samples were taken so that within-site variability of the biotic community could be explained as a function of within-site variability of the physical and chemical environment. This approach was particular y important in testing for dose-response relationships between variables representing possible drilling impacts. Third, the replicate samples from each hard-bottom site represented factorial combinations of depth, time, and substrate height. Thus, a number of appropriate statistical models (e.g., unreplicated three-way ANOVAs) were employed to test for the significance of observed differences in any given response variable (e.g., epifaunal abundances) in relation to relevant temporal and spatial factors (e.g., main effects of time, depth, low-relief, or high relief

location) and their interactions. Lastly, an optimal-impact study design (sensu Green, 1979), with a basis for accommodating pre-impact and post-impact sampling at both impact and control sites, was established. This sampling design provided the spatial-by-temporal framework required for powerful and robust testing of impact-related changes in the environment.

The positions and other relevant field data for the various monitoring stations and instrument deployments comprising the hard-bottom monitoring surveys are presented in a series of tables. Table 1 provides information on hard-bottom photosurvey sites; Table 2 provides information on hard-bottom sediment grab stations; Table 3 provides information on hard-bottom animal-trap stations; Table 4 provides information on instrumentdeployment sites for the physical oceanography task; and Table 5 provides information on the sediment-trap stations.

FORMAT OF THE FINAL REPORT

The format of the final report is designed to foster publication of results in a series of peer-reviewed manuscripts. Therefore, this final report does not follow the standard guidelines for an MMS final report. Instead, what follows is a series of related manuscripts by the principal investigators of the Phase-II program that discuss the natural physical processes that control the structure and organization of hard-bottom communities and how drilling discharges influence that structure and organization. These manuscripts have been or will soon be submitted for publication in the scientific literature.

The results and synthesis of findings of the soft-bottom components of the Phase-II program have been reported earlier in the Year-3 Annual Report (Steinhauer and Imamura, 1990) and are not repeated here. Multiple manuscripts or presentations from the soft-bottom study, the special task on sediment transport, or other CAMP-related activities have already been published, or are in the process of being published. These documents are summarized in Table 6. It is the intention of the MMS that all the manuscripts resulting from the Phase-II program be compiled in a single volume of published works.

This program was conducted by a team of scientists and advisors from Battelle; Kinnetic Laboratories, Inc.; University of California, Santa Barbara; Marine Research Specialists; University of Texas; Woods Hole Oceanographic Institution; U.S. Geological Survey; University of Maine; Louisiana State University; Louisiana Universities Marine Consortium; University of Western Ontario; Lawrence Livermore Laboratories, Arthur D. Little, and Scripps Institution of Oceanography. Several independent consultants also were involved. Principal Investigators responsible for various task areas appear as primary authors in the manuscripts that follow.

REFERENCES

Boesch, D.F. and N.N. Rabalais (Eds.). 1987. The *Long-Term Effects of Offshore Oil and Gas Development: An Assessment and a Research Strategy.* Report to the Interagency Committee on Ocean Pollution, Research, Development and Monitoring. Elsevier Applied Sciences Publishing, Barking, Essex, England. 708 pp.

Green, R.H. 1979. *Sampling Design and Statistical Methods for Environmental Biologists.* John Wiley and Sons, Inc., New York, NY. 257 pp.

National Research Council. 1983. *Drilling Discharges in the Marine Environment,* National Academy Press, Washington, DC. 180 pp.

SAIC. Science Applications International Corporation. 1986. Assessment of Long-Term Changes in Biological Communities of the Santa Maria Basin and Western Santa Barbara Channel - Phase I. Final Report to the U.S. Department of Interior, Minerals Management Service, Pacific OCS Region, Los Angeles, CA. Contract No. 14-12-0001-30032. Two volumes (MMS 86-9911 and MMS-9912).

Steinhauer M. and E. Imamura (eds). 1990. California OCS Phase II Monitoring Program: Year Three Annual Report. Volume I. U.S. Department of the Interior, Minerals Management Service, Pacific OCS Region, Camarillo, CA. OCS Study MMS 90-0055.

Table 1. Reference Coordinates of High- and Low-Relief Hard-Bottom Photosurvey Sites.

Station	Latitude Longitude	UTM Coordinates	Depth (m)	Relief Type
PH-E	34°30.26'N 120°42.76'W	N3820250 E710000	119	Low
PH-F	34°30.81'N 120°42.36'W	N3821285 E710580	105	Low
PH-I	34 °29.96'N 120°41.68'W	N3819735 E711665	107	Low
PH-J	34°29.82'N 120°41.82'W	N3819480 E71 1450	117	Low
PH-K	34°29.37'N 120°42.26'W	N3818635 *E710795*	160	High [a]
PH-N	34"29.21'N 120°42.05'W	N3818345 E711125	166	Low
PH-R	34°29.11'N 120°42.67'W	N3818140 E710180	213	High/Low
PH-U	34 °31.48'N 120 °43.51'W	N3822480 E708800	113	Low
PH-W	34°31.52'N 120°45.86'W	N3822480 E705200	195	High/Low

[a] High relief is greater than 1 m

Table 2. Reference Coordinates of Hard-Bottom Grab Stations.

Station	Latitude Longitude	**UTM** Coordinates	Depth (m)
PH-E	**34°30.19'N** **120°42.68'W**	N3820125 E710125	119
PH-F	34"30.79'N 120"42.52'W	**N3821250** E71035O	105
PH-I	**34°29.30'N** 120 **°41.73'W**	**N3819805** E71 1593	107
PH-J	34 °29.83'N 120°41 **.86'W**	**N3819495** E71 1399	117
PH-K	34"29.41'N **120°42.29'W**	**N3818700** E71075O	160
PH-N	**34°29.24'N** 120 **°42.10'W**	**N3818399** E71 1045	166
PH-R	**34°29.18'N** **120°42.45'W**	N381 8266 E710518	213
PH-U	**34°31.41'N** **120°43.47'W**	N3822370 **E708870**	113
PH-W	**34°31.58'N** **120°45.68'W**	**N3822591** E705464	195

Table 3. Reference Coordinates of Hard-Bottom Animal-Trap Stations.

Station	Latitude Longitude	UTM Coordinates	Depth (m)	Location
PHA-1	34 °29.89'N 120°42.37'W	N3819592 E710611	150	500 m N.W. of Platform Hidalgo
PHA-2	34°30.08'N 120°42.60'W	N3819938 E710249	140	1 km N.W. of Platform Hidalgo
PHA-3	34°31.23'N 120°43.99'W	N3822011 E708080	140	4 km N.W. of Platform Hidalgo

Table 4. Reference Coordinates of Current-Meter Moorings.

Station	Latitude Longitude	UTM Coordinates	LORAN Time Delays	Depth (m)	Equipment
PJ-13A	34°56.20'N 120°49.94'W	N3867974 E697983	27792.5 41844.3	140	Primary Current-meter Array
Hidalgo	34°30.27'N 120°43.07'W	N3820267 E709524	27812.8 41844.3	132	Primary Current-meter Array

Table 5. Reference Coordinates of Sediment Traps Deployed at the Hard-Bottom Stations.

Station	Latitude Longitude	UTM Coordinates	Depth (m)
PH-Est	34 °30.19'N 120 °42.68'W	N3820125 E710175	119
PH-Fst	34"30.79'N 120°42.52'W	N3821250 E7103OO	105
PH-Ist	34°29.98'N 120°41 .76'W	N3819770 E71 1579	107
PH-Jst	34°29.83'N 120°41.86'W	N3819550 E711400	117
PH-Kst	34°29.41'N 120 °42.29'W	N381 8700 E7107OO	160
PH-Nst	34"29.24'N 120 °42.10'W	N3818400 E711OOO	166
PH-Rst .	34°29.17'N 120 °42.46'W	N3818250 E7 10550	213
PH-Ust	34°31.42'N 120 °43.47'W	N3822370 E708920	113
PH-Wst	34°31.58'N 120°45.69'W	N3822591 E705514	195
PHAR-ST	34°28.30'N 120°41.12'W	N3816775 E7 12630	213
PH-ST1	34"30.44'N 120°43.00'W	N3820767 E709451	120
PH-ST2	34"30.02'N 120°43.36'W	N3819959 E708912	163
PH-ST3	34°29.68'N 120°43.65'W	N3819337 E708461	212

Table 6. Summary of Publications Resulting from CAMP Phase-Ii Study.

Published:

Brewer, G, D., J. Hyland, and D.D. Hardin. 1991. Effects of oil drilling on deep-water reefs offshore California. *American Fisheries Society, symposium* 11:26-38.

Butman, C.A. and R.J. Chapman. 1989. The 17-meter flume at the Coastal Research Laboratory. Part I: Description and user's manual. Woods Hole oceanographic Institution Technical Report WHOI-89-1O. CRC-89-2. 31 pp.

Chapman, R.J. and R.E. Galat. 1988. cooling the waters of the 17-meter flume at the Coastal Research Laboratory. Woods Hole Oceanographic Institution Technical Report WHOI-88-62. CRC-88-1. 15 pp.

Crecelius, E. A. 1988. Detecting contamination or trends in the concentrations of trace metals in marine environments. *Journal of Research of the National Bureau of Standards* 93(3):321-323.

Fiers, F. 1991. Three new harpacticoid copepods from the Santa Maria Basin off the Californian Pacific coast (Copepoda, Harpacticoida). *Beaufortia 42(2): 13-47.*

Grassle, J.P. and C.A. Butman. 1989. Active habitat selection by larvae of the polychaetes, *Capitella* spp. I and II, in a laboratory flume. Pp. 107-114 *In,* J.S. Ryland & P.A. Tyler (eds.) Reproduction, genetics and distributions of marine organisms. 23rd European Marine Biology Symposium.

Hyland, J., D. Hardin, E. Crecelius, D. Drake, P. Montagna, and M. Steinhauer. 1990. Monitoring long-term effects of offshore oil and gas development along the southern California outer continental shelf and slope: Background environmental conditions in the Santa Maria Basin. Oil *& Chemical Pollution 6:195-240.*

Hyland, J., J. Kennedy, J. Campbell, S. Williams, P. Boehm, A. Uhler, W. Steinhauer. 1989. Environmental effects of the *Pac Baroness* oil and copper spill. Proceedings of the 1989 Oil Spill Conference (Prevention, Behavior, Control, Cleanup). San Antonio, Texas. Pp. 413-419.

Trowbridge, J. H., W.R. Geyer, C.A. Butman, and R.J. Chapman. 1989. The 17-meter flume at the Coastal Research Laboratory. Part II: Flow characteristics. Woods Hole Oceanographic Institution Technical Report WHOI-89-11. CRC-89-3. 37 pp.

Webb, *C.M.* 1989. Larval swimming and substrate selection in the brittle star *Ophioderma brevispinum. Pp. 217-224 In,* J.S. Ryland & P.A. Tyler (eds.) Reproduction, genetics and distributions of marine organisms. 23rd European Marine Biology Symposium.

Table 6. (continued)

Manuscripts *in press:*

Hyland, J., E. Baptiste, J. Campbell, J. Kennedy, R. Kropp, and S. Williams. ma. **Macroinfaunal** communities of the Santa Maria Basin on the California outer continental shelf and slope. ***Marine Ecology Progress Series.***

Kropp, R.K. ma. Repaired shell damage among soft-bottom **molluscs** on the continental shelf and upper slope north of Point Conception, California. ***The Veliger.***

Montagna, P. 1991. **Meiobenthic communities** of the Santa Maria Basin on the California continental shelf. *Continental* ***Shelf Research*** 11.

Manuscripts submitted:

Bachelet, G., **C.A. Butman, C.M.** Webb, **V.R. Starczak,** and **P.V.R. Snelgrove.** Sediment selection **by** settling ***Mercenaria mercenaria (L.)*** larvae: Fact or artifact? ***Journal of Experimental Marine Biology and Ecology.***

Drake, **D.E.** and D.A. **Cacchione.** Wave-current interaction in the bottom boundary layer during storm and non-storm conditions: Observations and model predictions. ***Journal*** *of* ***Geophysical Research.***

Drake, **D.E.** and D.A. **Cacchione.** Storm events on the California continental margin: Bottom boundary layer observations and model predictions. *Continental* ***Shelf*** *Research.*

Findlay, R. L., **S.L.** Kim, and **C.A. Butman. Colonization** of freshly deposited **barite** and silica sediments by marine microorganisms in a laboratory flume flow. ***Marine Ecology Progress Series.***

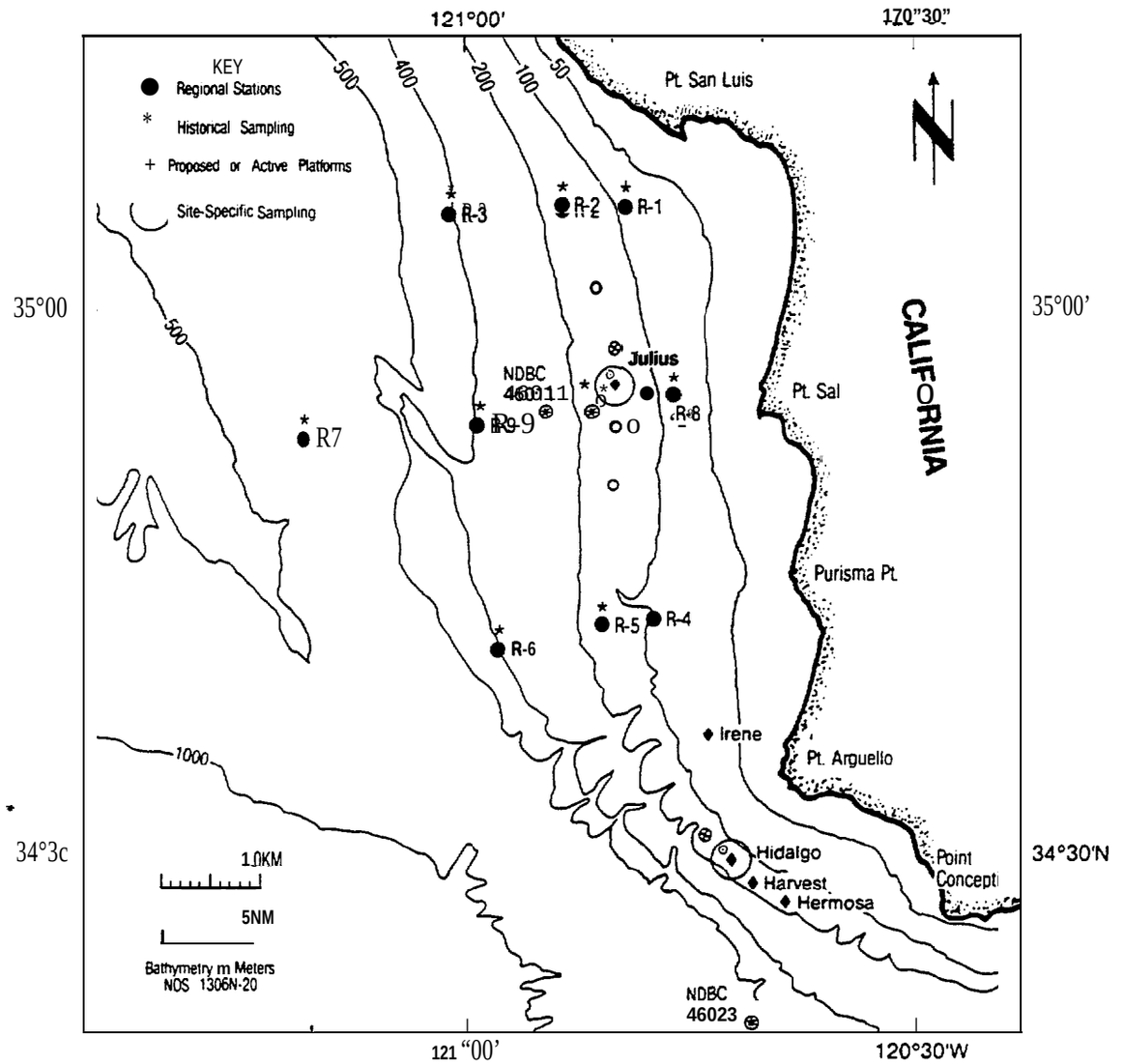

Figure 1. Area of Study and Station Location for the MMS California OCS Phase 11 Monitoring Program. ⊙ = Current-meter moorings; ⊗ = Water-quality stations

2. HISTORY OF DRILLING OPERATIONS AND DISCHARGES IN THE POINT ARGUELLO FIELD, OFFSHORE SOUTHERN CALIFORNIA

WILLIAM STEINHAUER

Battelle Ocean Sciences
397 Washington Street, Duxbury, Massachusetts 02332

EIJI IMAMURA

Marine Research Specialists
3639 East Harbor Boulevard, Suite 208, Ventura, California 93001

JOAN ROBERTS

Minerals Management Service
770 Paseo Camarillo, Camarillo, California 93010

JERRY NEFF

Arthur D. Little Co.
25 Acorn Park, Cambridge, Massachusetts 02140

INTRODUCTION

The Santa Maria Basin figures prominently in U.S. offshore oil and gas development plans. Located off the coast of Southern California, the Santa Maria Basin contains 43 of the 106 active lease tracts in the Minerals Management Service (MMS) Pacific Outer Continental Shelf (OCS) Region. Once the necessary permits are obtained, and the offshore fields in these blocks and associated transportation facilities are fully developed, oil production in the Pacific OCS Region is expected to increase from 78,000 to 178,000 barrels per day by the mid 1990s (MMS, 1987). Future development of the Point Arguello field in the southern Santa Maria Basin and the nearby Santa Ynez Unit (in the western Santa Barbara Channel) is expected to account for a majority of the increased

production. The Point Arguello field is one of the largest fields ever discovered in U.S. OCS waters (Rintoul, 1985). The onshore Gaviota processing serving the Point Arguello field is currently permitted for 100,000 barrels per day. However, issues concerning the transportation of oil and gas from the field have delayed the full development of these producing platforms. These issues have not yet been resolved.

The OCS oil and gas resources are managed by the MMS (part of the U.S. Department of Interior) as mandated by the OCS Lands Act and its Amendments. As part of its overall management of the region, the MMS has been conducting monitoring and process-oriented research in the Santa Maria Basin [California Monitoring Program, Phase II (CAMP) and Effects of OCS Production Platforms on Rocky Reef Fishes and Fisheries] to understand possible long-term environmental effects of oil and gas development (see Hyland et al., 1990 for program overview). As part of CAMP, a site-specific study region was established to determine effects of drilling-related discharges at Platform Hidalgo in the Point Arguello field. Part of the study included collection and review of platform discharge records for Platforms Hidalgo, Hermosa, and Harvest. The discharge records were provided to the U.S. Environmental Protection Agency (EPA) by the platform operators in accordance with National Pollution Discharge Elimination System (NPDES) permit conditions. The constituent composition of the drilling fluids was also obtained from the MMS (Santa Maria District Office). In addition, drilling fluids and drill cuttings were analyzed for metal and hydrocarbon content. This paper summarizes all permitted discharges to date from the three platforms comprising the Point Arguello field, and compares contaminants from platforms and natural sources. Discharges from all three platforms occurred between November 1986 and January 1989.

ENVIRONMENTAL SETTING

The Santa Maria Basin is a coastal and offshore geologic feature extending from Point Conception in the south to Monterey Bay in the north. The Point Arguello field is in the southern portion of the basin between Point Arguello (34°34'N) and Point Conception (34°28'N, Figure I). The Arguello Canyon and adjacent sea valleys are prominent features of the Basin. However, the topography generally lacks the complexity of the southern California borderland south of Point Conception (e.g., Emery, 1960), more closely resembling that of the continental shelf and slope north of Point Conception. The shelf extends seaward to a depth of about 110 m (SAIC, 1986), and varies in width from about 3.7 km in the Point Conception area to about 9.3 km between Point Conception and Point

Arguello. In the Point Arguello area, the seabed rapidly drops to a depth of about 1000 m and is incised by the Arguello Canyon.

There are four major coastal rivers draining into the southern Santa Maria Basin. The coastal rivers from north to south include: (1) the Arroyo Grande Creek, (2) the Santa Maria River, (3) the San Antonio Creek, and (4) the Santa Ynez River. Each drainage basin is distinct geologically and contributes sediments with a distinct mineral and trace elemental signature (Dibblee, 1950; SAIC 1986). The importance of the sediment contribution from these rivers is not known. However, the sediments from these sources combined with those from smaller streams and with suspended sediments carried by littoral transport from the north, contribute to the nearshore and offshore sediments of the study area. Fine-grained sediments are also transported into the study area by currents flowing north from areas east of Point Conception (Parr et al., Chapter 3).

Generally, sediments throughout much of the central and northern California continental margin grade from sands in shallow waters on the inner shelf to silt and clay substrates on the outer shelf and slope. Offshore (> 50 m water depth) substrates are fine sands to very-fine silts and become progressively finer with increasing water depth and distance from shore, however there are variations of this general pattern (MMS, 1983; SAIC, 1986; Steinhauer and Imamura, 1990; Parr et al., Chapter 3). Hard-bottom features are also located principally in shallow nearshore waters and in the offshore area between Point Arguello and Point Conception, at depths of about 100 to 300 m (Steinhauer and Imamura, 1990; Hard in et al., Chapter 7).

The California Current system is a predominant oceanographic feature (Reid et al., 1958; Hickey, 1979; Chelton, 1984), as is seasonal coastal upwelling, caused by wind-induced Ekman circulation (Reid et al., 1958; Brink et al., 1984). Upwelling occurs primarily during the spring and summer (March to June) in response to increased winds from the northwest, bringing deep, cold, nutrient-rich water to the surface along the coast. Coastal upwelling leads to significant increases in new primary biological production (Dugdale and Wilkerson, 1989). Currents near the Point Arguello field are generally aligned with topography and show frequent flow reversals; there are periods of northwest-southeast flow and less frequent periods of south-southwest flow (Coats, Chapter 8; Savoie et al., Chapter 4). The local circulation has a variety of transient phenomena including eddies, swirls, filaments, meanders, and narrow jets that are obscured in time-averaged current data. Some of these

features can be detected in satellite images (Bernstein et al., 1977; Bernstein et al., Chapter 5), and may be responsible for significant cross-shelf transport of heat, nutrients, and pollutants (Mooers and Robinson, 1984). In addition, inter-annual variations such as the El Niño/Southern Oscillation, can obscure or alter the generalized circulation pattern. Thus, the region has a complex circulation, generally consisting of currents that flow northwest or southeast parallel to the coastline with small time components that provide a cross-shelf component.

Natural petroleum seepage rates have not been estimated for the waters north of Point Conception, but, based on previous studies in neighboring Santa Barbara Channel, seepage may be a principal natural source of petroleum to the sediments. Hyland and Neff (1988) and Steinhauer and Imamura (1990) reported macroscopic tar particles in bottom sediments throughout the study region. The hydrocarbon chromatograms of sediments and sediment trap samples from the region display a prominent unresolved complex mixture (UCM) characteristic of petroleum hydrocarbons (Steinhauer et al., Chapter 6). Additional evidence for seeps in the area is provided by reports of fouled fishing gear, and sightings of oil slicks and tar mounds in the area (Danenberger, MMS, personal communication). Tar from natural seeps frequently washes ashore in this region of central California. Wilkinson (1972) cataloged approximately 20 oil and gas seeps along the coast south of the study area, between Point Conception and Coal Oil Point. Allen et al. (1970) estimate that seeps in the Coal Oil Point area alone introduce about 7600 to 11,400 liters of oil per day into surrounding waters of the Santa Barbara Channel.

HISTORY OF DRILLING AND OTHER HUMAN ACTIVITIES IN THE AREA

Compared to other coastal regions, the OCS north of Point Conception is a relatively uncontaminated area (SAIC, 1986; Steinhauer and Imamura, 1990). Although 76 exploratory wells have been drilled in the Santa Maria Basin in the past 25 years, there had been no oil and gas development or production activities in the area until April 1986 when drilling started at Platform Irene in the Pedernales field. There also are few cities and little industrial development along this part of the California coast, so there is little domestic and industrial waste discharge in the region. Channel Islands National Park is located approximately 33 km to the south of the Point Arguello field. The Channel Islands Marine Sanctuary extends 5.6 km into the waters surrounding the national park. The relatively limited public access to the national park, and the marine sanctuary status of the

surrounding area further limit the amount of anthropogenic contaminants reaching the southern Santa Maria Basin.

The first phase of drilling in the Point Arguello field commenced when the first well at Platform Harvest was drilled in November 1986, and ended in January 1989 when the seventh well was completed at Platform Hidalgo (Table 1). Additional production wells are scheduled to be drilled in 1992 and 1993. Production of oil and gas began in the Point Arguello field in May 1991. Drilling at Platform Irene, located approximately 12 nmi north of the Point Arguello field, began in April 1986 and ended in October 1989. Production at Platform Irene commenced in April 1987, and continues. Installation of Platform Julius, approximately *20 nmi* north of the Point Arguello field, has been delayed indefinitely because of issues surrounding the permitting and construction of an onshore oil and gas processing facility in San Luis Obispo county, California.

PLATFORM DISCHARGES AND NPDES PERMIT CONDITIONS

A variety of solid and liquid wastes are generated during well drilling and production of oil and gas. The NPDES permits may allow discharge of these wastes to the ocean. Deck washdown and sanitary waste discharges are relatively minor discharges that continue throughout the lifetime of a production platform. However, during drilling, large amounts of drilling-fluid and drill-cutting discharges are produced and are of most environmental concern and during production it is produced water that is of concern. Discharges at Platforms Harvest, Hermosa, and Hidalgo are allowed under a general NPDES permit issued by EPA Region IX on February 18, 1982, and reissued on December 8,1983 (Table 2, EPA, 1983). The permit covers both mobile exploration activities, and development and production activities. Produced waters are included in the materials permitted for discharge (EPA, 1983) but there have been no produced-water discharges in the Point Arguello field as of this writing and the portion of the NPDES permit concerning produced-water discharge is not presented in Table 2.

Drilling fluids are mixtures of natural clays or polymers, weighting agents, and other materials in freshwater, seawater, or a refined petroleum (Neff et al., 1987). They are specially formulated for several functions in the rotary drilling process (NRC, 1983). The most important functions of drilling fluids are to (1) transport cuttings to the surface, (2) balance subsurface pressures to prevent the influx of formation fluids (oil, gas, and/or water) into the wellbore, or to avoid potential blowout and,

(3) cool, lubricate, and support part of the weight of the drill bit and drill pipe. During drilling, the drilling-fluid engineer on the platform continually evaluates the properties of the drilling fluid and adjusts the fluid composition to match drilling conditions. Thus, the composition of the drilling fluid on a platform changes continual y during drilling and a variety of drilling fluids are produced. Although the use of oil-based drilling fluids is allowed, their discharge to the ocean and the discharge of cuttings produced with them is not permitted anywhere in U.S. territorial waters.

Table 3 summarizes drilling-fluid constituents contained in used drilling fluids discharged in the Point Arguello field during drilling, as compiled from data provided by platform operators as a stipulation of their NPDES permits. The major inorganic constituents discharged during the drilling process at all three platforms were barite ($BaSO_4$) and bentonite clay (sodium montmorillonite). Large amounts of potassium chloride, sodium chloride, and potassium hydroxide were also discharged at Platforms Hermosa and Hidalgo, with lesser amounts discharged at Harvest. It must be emphasized that the relative consumption (discharge) of individual drilling-fluid constituents, particularly the amounts commercial products, is a reflection of the drilling conditions met during drilling, but it is also a reflection of the management philosophy of the platform operator. Many of the major constituents and commercial drilling mud additives perform similar functions during the drilling process and can be used interchangeably. For example, a relatively large amount of Drispac", a polyanionic cellulose polymer used to modify fluid viscosity, was discharged during the drilling at Platform Harvest, whereas a lesser amount was used at Platform Hermosa and none was used at Platform Hidalgo. Chrome lignosulfonate, a drilling fluid additive of environmental concern because of potential chromate toxicity, was not used during the drilling process at any of the platforms. A complete directory of commercial products used to formulate drilling fluids is presented in *Offshore* magazine (1990). Data were not available for the amount of water used to formulate the drilling fluids at the Point Arguello field. The amount of water may range from 76 % for a lowdensity fluid used at shallow well depths to 30 % for a highdensity fluid used near well completion (NRC, 1983).

The drilling-fluid circulation system allows the fluid to be cleaned of debris and recycled down the drill hole many times (NRC, 1983). Drilling fluid is pumped under high pressure from the drilling-fluid holding tanks on the platform down through the hollow drill pipe. It is discharged at high pressure through nozzles on the drill bit and hydraulically removes cuttings produced by the grinding action of the drill bit on the rock being drilled. Drill cuttings are pieces of crushed sedimentary rock

ranging in size from clay to coarse gravel (Neff, et al., 1987). The drilling fluid, carrying cuttings with it, then returns to the surface through the annulus (the space between the drill pipe and the borehole wall or casing) to the drilling-fluid return line. The drilling fluid then passes through several screens (shale shakers) and other devices that remove most of the cuttings from the fluid, before being returned to the fluid storage tank for recirculation down hole. Generally during drilling, the washed cuttings, still carrying some drilling-fluid solids, are discharged to the ocean more or less continuously at a low rate.

The summaries of daily NPDES drilling fluid discharge records for platforms discharging in the Point Arguello field are presented in Figure 2. These records show that drilling fluid discharges into the surrounding waters are intermittent and that volumes can vary from O to over 500 m^3 (3100 bbl) in a single day. Intermittent discharges are common during drilling and reflect the type of activity occurring on a given day. Periodically, when the composition of the drilling fluid is to be changed substantially or when the volume of drilling fluid increases to the capacity of the fluid tanks, some drilling fluid may be discharged in bulk from the platform. Bulk discharges of fluids may occur several times during the drilling of a well. The usual discharge is less than 50 m^3 (310 bbl) although larger volumes are often discharged when fluid is changed substantially or when the volume of drilling fluid increases to the capacity of the fluid tanks. There were 19, 13, and 7 wells drilled at Platforms Harvest, Hermosa, and Hidalgo, respectively, resulting in an average of 220, 280, and 500 metric tons of solids discharged per well. The amounts discharged from these wells appear typical of production wells drilled in the U.S. OCS (200 to 2000 metric tons of solids discharged per well, Neff et al., 1987).

CONTAMINANTS ASSOCIATED WITH DRILLINGFLUID AND DRILL-CUTTING DISCHARGE

The chemical contaminants of environmental concern in discharged drilling fluids and drill cuttings are metals and petroleum hydrocarbons. At Platform Hidalgo, the metals in composite samples of drilling fluid found at concentrations significantly higher than those found in surrounding marine sediments include only zinc and barium (Steinhauer et al., Chapter 6; summarized in Table 4). All metals, except mercury and barium, were present in drill cuttings at concentrations higher than their concentrations in drilling fluids from the same wells. However, only concentrations of lead, zinc, and barium were significantly elevated in drill cuttings relative to concentrations in marine sediments.

The higher concentrations of most metals in cuttings relative to drilling fluids is unusual and is probably an indication that the rock strata being drilled are naturally enriched in mineral-derived metals. Metals associated with natural minerals usually cannot be extracted from the mineral matrix except by strong acid digestion and, therefore, are considered biologically inert (Luoma and Bryan, 1982; Salomons and Förstner, 1984). The high concentrations of lead and zinc in cuttings and zinc in drilling fluids probably are derived, in part, from pipe-thread compound (pipe dope) used to lubricate the threads of the drill pipe. The metals in pipe dope are present as fine metal granules. Elemental metal forms of lead and zinc dissolve readily in soft fresh water at low pH (Patterson, 1965), but are only slightly soluble in seawater due to the presence, at pH ≈ 8.0, of high concentrations of carbonate, hydroxide, and sulfate in seawater (Förstner and Wittmann, 1983). Therefore, metal granules probably are relatively inert in marine sediments, unless ingested by animals with strong] y acidic digestive processes (e.g., birds). Barium is derived from the mineral barite used as a weighting agent in the fluid. Barite is highly insoluble in seawater (about 50 μg/L as barium; Chan et al., 1977). Except for barium, the metals showed no concentration differences with depth (Steinhauer et al., Chapter 6). The barium concentration increased from 25,000 to 180,000 μg/g in drilling fluids from surface to bottom. The increase in barium concentration reflects increased use of barite in drilling-fluid formulations with depth.

Petroleum hydrocarbons were found in all composite drilling-fluid and drill-cutting samples analyzed (Steinhauer et al., Chapter 6; summarized in Table 4). The petroleum hydrocarbons detected in drilling fluids and drill cuttings may be derived from two possible sources: (1) refined oil added intentionally to the drilling fluid and (2) crude oil from the geologic formations being drilled. Refined petroleum products may be added to the drilling fluid to lubricate the drill string, particularly when drill ing a slant hole, and to aid in freeing stuck drill pipe. Traditional] y, diesel fuel (No, 2 fuel oil) has been used for the latter. However, because MMS Pacific OCS Region policy discourages use of diesel fuel in drilling fluids, the oil industry has replaced the diesel oil with a specially-formulated mineral oil. Mineral oil contains low concentrations of aromatic hydrocarbons and is much less toxic than diesel fuel (Breteler et al., 1985). Although as much as 2 to 4 percent mineral oil may be added to the bulk drilling fluid to reduce torque and drag of the drill string (NRC, 1983), drilling-fluid inventories show no such practice occurring at wells in the Point Arguello field. Also, our drilling-fluid analysis for petroleum hydrocarbons shows no indication that any significant concentrations of petroleum products have been added to the fluid used in the Point Arguello field (Table 4). If the

drill string becomes stuck in the hole, a pill of oil or an oil-based drilling fluid may be injected down the drill string and spotted in the area of the annulus where the pipe is stuck. However, oil-based drilling fluids may not be discharged to the ocean and industry practice is to isolate the oil-based pill from the bulk drilling fluid for subsequent onshore disposal.

In the final stages of drilling a development well or during work-over of an existing well, the drill bit penetrates geologic strata containing high concentrations of fossil fuel (the hydrocarbon reservoir). The cuttings generated during this phase may contain relatively high concentrations of crude oil. At Platform Hidalgo, total petroleum hydrocarbon concentrations increased from 160 to 990 μg/g, and polycyclic aromatic hydrocarbons (PAH) concentrations increased from 0.9 to 50 μg/g from surface to bottom in drilling fluids (Steinhauer et al., Chapter 6), The concentration of PAH in drill cuttings also increased from 2.3 to 120 μg/g from surface to bottom, but the concentrations of total petroleum hydrocarbons showed no correlation with well depth (600 and 525 μg/g, respectively). Drilling fluid and drill cuttings, containing small amounts of crude or refined petroleum, may be discharged to the ocean if they can pass the "bucket-sheen" test (i.e., no sheen of oil is visible at the surface of a sample of the material collected in a bucket; EPA, 1985).

The average metal and hydrocarbon input to the marine environment from drilling-fluid and drill-cutting discharges at Platform Hidalgo and from natural sources are presented in Table 5. Although Steinhauer et rd. (Chapter 6) presents the concentrations of metals and hydrocarbons at several well depths, depth-averaged concentrations are used here because the NPDES discharge information is not sufficiently detailed to relate discharges to depth of well penetration, making a more sophisticated discharge analysis impossible at this time. This approach averages the well-to-well concentration differences (seven wells) and within-well depth concentration differences (four depths; surface, two mid-depths, and bottom) and provides only a rough estimate of average metal and hydrocarbon concentrations in the actual discharges. For drilling-fluid constituents other than barium and petroleum hydrocarbons, this approach appears reasonable because concentration differences with depth are small (Steinhauer et al., Chapter 6). However, concentrations of barium and petroleum hydrocarbons in drilling fluid increased dramatically with well depth as more barite was used in the fluid formulation, and higher concentrations of hydrocarbons were found in the formation rock. Thus, the use of average concentrations of barium and petroleum hydrocarbons most likely underestimated the total amounts of barium and hydrocarbons discharged in drilling fluids. For

example, barium discharge, calculated from the drilling-fluid analysis and total discharge data, is 370,000 kg, whereas barium discharge, calculated from the amount of barite consumed on the platform, is considerably more (1,810,000 kg barite consumed at Platform Hidalgo = 1,070,000 kg barium discharged, assuming all the drilling fluid consumed was discharged).

Table 5 also estimates the amounts of metals and hydrocarbons reaching the Santa Maria Basin from riverine input and coastal petroleum seeps. Although significant amounts of metals and hydrocarbons enter the marine environment as a result of drilling operations, except for barium, the amounts are relative] y small compared to the average annual flux of materials entering the southern Santa Maria Basin from natural sources. At Platform Hidalgo, barium was released in amounts roughly comparable to the average annual rate of input from coastal riverine sources *(320,000* to 1,070,000 kg released over 14 months vs 650,000 kg/y from riverine input). The input of other metals, present at only trace levels in drilling fluids, is low compared to the average annual input from natural sources. Concentrations of zinc and lead are relatively elevated in cuttings, probably reflecting high natural levels in the source rock. Because this region of the California coast was undergoing a drought during the drilling period from 1986 to 1989, input of suspended matter from riverine sources was probably below the average low-flow discharge. However, riverine input during low-flow conditions still represents a benchmark against which to compare input from drilling activity.

Although hydrocarbon input to the southern Santa Maria Basin has not been estimated, there are numerous hydrocarbon seeps charted in the nearby Santa Barbara Channel (Wilkinson, 1972; Allen et al., 1970). If the Allen et al. (1970) estimate of 7600 to 11,400 liters/day entering the marine environment at Coal Oil Point is indicative of natural input to the southern Santa Maria Basin, then the average annual input of total hydrocarbons and PAH from natural sources far exceeds input from drilling operations in the Point Arguello field (Table 5).

CONCLUSIONS

The discharge records and the drilling fluid inventories prepared by the operators for the EPA and the MMS summarize the amounts of drilling fluid constituents and drill cuttings discharged to the marine environment. Further, from the analysis of drilling fluids and drill cuttings for metals and petroleum hydrocarbons, the total amounts of these species associated with marine discharges can be estimated. Comparison of the relative metal and hydrocarbon flux to the southern Santa Maria Basin from

drilling operations at Platform Hidalgo to that from natural sources shows that, except for barium, the relative amount of metals and hydrocarbons discharged at sea from drilling operations is small. The metal and hydrocarbon discharge was calculated for only one of the three platforms discharging between 1986 and 1989 in the Point Arguello field. However, assuming concentrations are similar on the other platforms, the combined input of metals and hydrocarbons over the 3-year period is (except for barium) still low compared to the average annual flux from natural sources.

However, comparison of time-averaged metal and hydrocarbon flux from drilling operations over wide spatial scales to that from natural sources does not address issues of localized or event-specific impact to the marine environment (see Hyland et al., 1990). Drilling discharge records show that daily discharges in the Point Arguello field may vary dramatically, from O to over 500 m^3 per day. Drilling-fluid trajectory modelling has shown that most drilling mud is initially rapidly deposited. Initial deposition may cover a broad area, but is concentrated around the platform (Coats, Chapter 8). This deposition pattern is supported by the results of sediment-trap studies (Steinhauer et al., Chapter 6). Thus, although the overall flux of metals and hydrocarbons from drilling operations may be small compared to those from natural sources, there may be localized accumulations of some components of the drilling-fluid and drill-cutting solids.

The California Monitoring Program, Phase II, was designed to detect and determine whether there are localized environmental changes in hard-bottom benthic (reef) communities surrounding the Point Arguello field during drilling, and to determine if any changes are caused by drilling-related activities or whether they are caused by natural processes. Results of the program indicate that most species observed did not undergo population changes during the period of drilling, but that small changes in species abundance could be detected in some hard-bottom epifauna, and that these changes could be related to discharge events in the field (Hyland et al., Chapter 9).

A follow-on program (California Monitoring Program, Phase III) will continue to monitor hard-bottom epifauna near the Point Arguello field for the next 3 years, during which time several more wells at the existing platforms are expected to be drilled. In addition, the program will devote resources to (1) platform-specific monitoring to further define the area of impact and to refine trajectory modelling; and (2) laboratory and field studies designed to resolve issues of natural population change in hard-bottom communities, and (3) determine the toxicity of drilling fluids to

indigenous species of marine animals. These studies will provide knowledge on separating natural background variation from potential low-level cumulative environmental impacts caused by drilling-related activities.

Acknowledgements – We would like to thank Mr. Eugene Bromley, U.S. EPA, Region IX for his efforts in providing NPDES discharge information and Dr. Jeffrey Hyland, University of California at Santa Barbara for providing information about the survey region. We would also like to thank Dr. Fred Weiss, Dr. Donald Boesch, and Dr. Robert Spies for their thoughtful review of the manuscript. his work was carried out under Minerals Management Service Contract No. 14-12-0001-30262 to Battelle Ocean Sciences.

REFERENCES

Allen, A. A., R.S. Schlueter, and P.G. Mikolaj. 1970. Natural oil seepage at Coal Oil Point, Santa Barbara, California. Science 170:974-977.

Bernstein, R. L., L. Breaker, and R. Whirtner. 1977. California Current eddy formation: Ship, air and satellite results. *Science* 195:353-359.

Breteler, R.J., P.D. Boehm, J.M. Neff, and A.G. Requejo. 1985, Acute toxicity of drilling fluids containing hydrocarbon additives and their fate and partitioning among liquid, suspended, and solid phases. Report to American Petroleum Institute, Environmental Affairs Department, Washington, Washington, DC. 107 pp.

Brink, K. H., D.W. Stuart, and J.C. Vanleer. 1984. Observations of the coastal upwelling region near 34°30'N off California: Spring 1981. *J. Phys. Oceanogr.* 14:378-391.

Chan, L. H., D. Drummond, J.M. Edmond, and B. Grant. 1977. On the barium data from the Atlantic GEOSECS expedition. *Deep-Sea Res.* 24:613-649.

Chelton, D.B. 1984. Seasonal variability of alongshore geostrophic velocity off Central California. *J. Geophys. Res.* 89:3472-3486.

Continental Shelf Associates. 1985. Assessment of the long-term fate and effective methods of mitigation of California outer continental shelf platform particulate discharges. Report to U.S. Department of Interior, Minerals Management Service, Pacific OCS Region, Los Angeles, CA.

Dibblee, T. W., Jr. 1950. Geology of southwestern Santa Barbara County, CA. Bulletin 150, Division of Mines and Geology.

Dugdale, R.C. and F.P. Wilkerson. 1989. New production in the upwelling center at Point Conception, California: Temporal and spatial patterns. *Deep-Sea Res.* 36(7):985-1007.

Emery, K.O. 1960. *The Sea Off Southern California.* John Wiley and Sons, Inc., New York, NY. 366 pp.

EPA. 1983. Environmental Protection Agency. Modification of general NPDES permit for oil and gas operations on the outer continental shelf off southern California. Federal Register. 48(237):55029-55043.

EPA. 1985. Environmental Protection Agency. Static Sheen Test, Industrial Technology Division.

Förstner, U. and G.T.W. Wittmann. 1983. *Metals Pollution in the Aquatic Environment.* Second cd., Springer-Verlag, Berlin, Federal Republic of Germany. 486 pp.

Hickey, B.M. 1979. The California Current system - Hypotheses and facts. *Prog. Oceanogr.* 8:191-279.

Hyland, J. and J. Neff (Eds.). 1988. California OCS Phase II Monitoring Program: Year-One Annual Report. Report prepared for the U.S. Department of the Interior, Minerals Management Service, Pacific OCS Region, Los Angeles, CA. Contract No. 14-12-0001-30262. Volume I (MMS 87-01 15) and Volume II (MMS 87-0116).

Hyland, J., D. Hardin, E. Crecelius, D. Drake, P. Montagna, and M. Steinhauer. 1990. Monitoring long-term effects of offshore oil and gas development along the southern California outer continental shelf and slope: Background environmental conditions in the Santa Maria Basin. *Oil Chem. Pollut.* 6: *195-240.*

Luoma, S.N. and G.W. Bryan. 1982. A statistical study of environmental factors controlling concentrations of heavy metals in the burrowing- bivalve *Scrobicularia plana* and the polychaete *Nereis diversicolor. Estuarine Coastal Shelf Sci.* 15:95-108.

MMS. *1983.* Minerals Management Service. Draft Environmental Impact Statement. Proposed 1983 outer continental shelf oil and gas lease sale offshore Central California, OCS Sale No. 73. U.S. Department of the Interior, Minerals Management Service, Pacific OCS Region, Los Angeles, CA.

MMS. 1987. Minerals Management Service. Anticipated Production rates and number of platforms on Federal lands in the Pacific OCS region. US. Department of the Interior, MMS Technical Announcement POCSR-7, Pacific OCS Region, Los Angeles, CA.

Mooers, C.N.K. and A.R. Robinson. 1984. Turbulent jets and eddies in the California Current and inferred cross-shore transports. *Science* 223:51-53.

NRC. 1983. *Drilling Discharges in the Marine Environment.* A report prepared by the National Research Council, National Academy Press, Washington, DC. 180 pp.

Neff, J. M., N.N. Rabalais, and D.F. Boesch. 1987. Biological effects of drilling muds, drill cutting, and produced waters. Pages 469-538 In: D.F. Boesch and N.N. Rabalais (Eds.) *L.mg-Term Effects of Offshore Oil and Gas Development.* Elsevier Applied Science Publishers, London, UK.

Newman, W .A. 1979. California transition zone: Significance of short-range endemics. Pages 399-416 In: J. Gray and A. Boucot (Eds.) *Historical Biogeography, Plate Tectonics, and the Changing Environment.* Oregon State University Press, Corvallis, OR.

Patterson, D.C. 1965. Contaminated and natural lead environments of man. *Arch. Environ. Health* 11:344-360.

Reid, Jr., J. L., G.I. Roden, and J.G. Wyllie. 1958. Studies of the California current system. Pages 27-56 *In:* Cal if. Coop Oceanic. Fish Invest., Progress Report, 1 July-1 January 1958.

Rintoul, B. 1985. Fifteen platforms planned off California. *Offshore* 45(1):60-61.

SAIC. Science Applications International Corporation. 1986. Assessment of Long-Term Changes in Biological Communities of the Santa Maria Basin and Western Santa Barbara Channel - Phase I. Final Report to the U.S. Department of Interior, Minerals Management Service, Pacific OCS Region, Los Angeles, CA. Contract No. 14-12-0001-30032. Two volumes (MMS 86-9911 and MMS-9912).

Salomons, W. and U. Förstner. 1984. *Metals in the Hydrosphere*. Springer-Verlag, Berlin, Federal Republic of Germany. 349 pp.

Steinhauer, M. and E. Imamura. (Eds.) 1990. California OCS Phase II Monitoring Program Year-Three Annual Report. Final report to the U.S. Department of Interior, Minerals Management Service, Pacific OCS Region, Camarillo, CA. Contract No. 14-12-0001-30262. Two Volumes (MMS 90-0055).

Valentine, J.W. 1966. Numerical analysis of marine molluscan ranges in the extratropical northeastern Pacific shelf. *Limnol. Oceanogr.* 11:198-211.

Wilkinson, E.D. 1972. California offshore oil and gas seeps. California Division of Oil and Gas Pub. No. TR-08.11 pp.

Table 1. Summary of Drilling Activities in the Point Arguello Field.

Platform	Drilling Period	Number of Wells Drilled	Drilling Fluid Discharged[a] (m')	Cuttings Discharged" (m^3)
Harvest	11/86 to 05/88	19	16,340	NA[b]
Hermosa	01/87 to 09/88	13	16,373	3,114
Hidalgo	11/87 to 01/89	7	7,963	2,294

'Multiply by 6.29 to obtain barrels.
[b]Data not available.

Table 2. Summary of the General NPDES Permit for Offshore Oil and Gas Operations on the Outer Continental Shelf Off Southern California.
[Source: EPA, 1983]

Effluent Limitations
Drilling Fluids and Drill Cuttings
No discharge of free oil (visual analysis)
No discharge of floating solids (visual analysis)
No discharge of oil-based drilling fluids
No discharge of toxic materials (concentration outside mixing zone will not exceed 0.01 of concentration shown to be acutely toxic [96 h LC50])[a]
Well Completion and Tratment Fluids, Deck Drainage, and Produced Sands
No discharge of free oil (visual analysis)
Sanitary Waste
Minimum of 1.0 mg/L residual chlorine (discharge to be maintained as close to this concentration as possible)
Monitoring Requirements
Drilling Fluids and Drill Cuttings
Monthly monitoring of volume discharged
Bioassay of spent drilling fluids (procedure and schedule determined by Regional Administrator, Region 9)
Annual analysis of barite used in drilling fluid formulation for arsenic, cadmium, chromium, copper, lead, mercury, nickel, vanadium, and zinc
Chemical inventory of all constituents and volume added downhole at each well
Well Completion and Treatment Fluids, Deck Drainage, and Produced Sands
Monthly monitoring of volume discharged

[a]The discharge of generic drilling fluid is preapproved. See following criteria for generic drilling fluid.

Table **2.(continued)** Summary of the General NPDES Permit for Offshore Oil and Gas Operations on the Outer Continental Shelf Off Southern California.
[Source: EPA, 1983]

A generic drilling fluid is one which the components and the heavy metal concentrations do not exceed the following maximum values:

Drilling Mud Components (lb/bbl)		Heavy Metal Concentration (μg/g)	
Barite	176.0	Arsenic	3.0
Bentonite	32.1	Barium	141,000
Chrome lignosulfonate	4	Cadmium	1.0
Lignite	5.0	Chromium	1.0
Polyanionic cellulose	1.0	Copper	26.0
salt	10.0	Lead	24.0
Caustic	1.5	Mercury	1.0
Cellex	0.1	Nickel	8.0
Drill solids	52.0	Vanadium	35.0
Lime	1.5	Zinc	181.0
Extractable organics	0.6 (mg/g)		

Alternatively, a generic drilling mud may be defined as one which 96h LC_{50} concentrations are equal to or greater than 53,000 ppm for suspended particulate phase, or 283,000 ppm for liquid phase.

Source: EPA (1983)

Table 3. Summary of Products Used (kg) for Drilling Fluid Formulations on Three Platforms in the Point Arguello Field Between 1986 and 1989.

MAJOR MUD CONSTITUENTS"	PLATFORM HERMOSA	PLATFORM HIDALGO	PLATFORM HARVEST	TOTAL
Barite	1,470,000	1,810,000	1,840,000	5,120,000
Bentonite Clay	1,230,000	549,000	1,700,000	3,479,000
KCl	31 0,000	348,000	17,000	675,000
NaCl	170,000	57,700	12,700	240,400
KOH	91,500	144,000	0	235,500
Lime	86,700	65,700	71,700	224,100
Drispac®	31,000	0	158,000	189,000
Chrome-free Lignosulfonate	0	41,300	0	41,300
NaOH	7,210	0	*33,400*	40,610
Lignite	8,860	30,300	0	39,160
Drilling Starch	0	36,300	0	36,300
Lubra-Beads®	11,400	22,000	0	33,400
X-Pel-G®	25,500	0	0	25,500
Con-Tone'	14,900	9,000	0	23,900
Perma-Lose HT®	10,600	0	0	10,600
Uni-Cal®	6,910	0	0	6,910
Drispac SuperLo"	0	4,820	0	4,820
Total Mud Constituents[b]	3,650,000	3,470,000	4,100,000	10,425,500

[a]Drispac® and Drispac SuperLo" are polyanionic cellulose products, Lubra-Beads® is a solid polymer bead lubricant, X-Pel-G® is water-dispersible gilsonite, Con-Tone* is a mud conditioner, Perma-Lose HT® is a non-fermenting polymerized starch, and Uni-Cal® is a chrome-modified sodium lignosulfonate.

[b]Total mud constituents used at individual platforms contain some additives not listed on this table.

Table 4. Concentrations (**μg/g** dry weight) of Selected Contaminants in Composite Samples of Drilling Fluids and Drill Cuttings at Platform **Hidalgo** and in Platform Hidalgo Sediments.'

Fluid/Cutting Constituent	Drilling Fluid[b]	Drill **Cutting**[b]	Platform **Hidalgo Sediments**[c]
Silver	0.3	0.6	0.1
Arsenic	6.3	10	8.4
Cadmium	1.2	2.3	0.6
Copper	30	48	15
Chromium	85	150	120
Mercury	0.13	0.10	0.07
Nickel	41	67	42
Lead	19	1900	15
Vanadium	71	110	57
zinc	290	1300	72
Barium	108,000	5200	840
THC[d]	390	490	69
ΣPAH[e]	25	39	0.11

[a]**Data** from **Steinhauer** et al. (Chapter 6).
[b]**Depth** averaged mean concentrations
[c]**Grand** mean, all sediment samples from the Platform **Hidalgo** study region collected 1986 to 1990 (n=62)
[d]**Total** resolved and **unresolved** hydrocarbons as measured by gas chromatography/mass spectrometry **(GC/MS).**
'Sum of **naphthalene,** fluorene, phenanthrene, and dibenzothiophene **(unsubstituted** and **alkylated homologs),** and 4-5 ring PAH

Table 5. Total Contaminant Loading (kg/y) in the Santa Maria Basin From Drilling Operations at Platform Hidalgo and From Natural Sources

Mud/Cutting Constituent	Drilling Fluid Discharge[a]	Drill Cutting Discharge[b]	Riverine and Petroleum Seep Input[c]
Silver	0.9 (1.0)	3.1 (3.6)	*88*
Arsenic	19 (22)	5.1 (6.0)	*6,700*
Cadmium	3.6 (4.2)	11.7 (13.7)	460
Copper	89 (104)	250 (290)	12,000
Chromium	260 (300)	780 (910)	99,200
Mercury	0.3 (0.4)	0.5 (0.6)	56
Nickel	120 (140)	340 (400)	33,600
Lead	57 (66)	9,400 (11,000)	12,000
Vanadium	210 (250)	540 (630)	45,600
Zinc	860 (1OOO)	6,900 (8000)	57,600
Barium	320,000 (370,0009	27,000 (31,000)	670,000
THC	1,100 (1,300)	2,500 (2,900)	2,230,000
ΣPAH	74 (86)	200 (230)	18,500

[a]Computed from the average concentration of analytes in composite drilling-fluid samples and total drilling fluid discharge data. Total amount of drilling fluids discharged (kg) are presented in parenthesis.
[b]Computed from the average concentration of analyte in composite drill-cutting samples and the estimated drill-cutting discharge. Assumed drill-cutting density of 2.6 g-cm^{-3}; 2,294 m^3 of drill-cuttings discharged at Platform Hidalgo. Total amount of drill cuttings discharged (kg) are presented in parenthesis.
'Estimated flux of suspended sediment to southern Santa Maria Basin under low flow conditions is 8 x 10^8kg yr^{-1} (continental Shelf Associates, 1985). Based on ^{210}Pb data and similarity between elemental composition of sediments and sediment traps, the concentrations of crustal elements in riverine-sourced suspended sediment is assumed to be the same as the average concentrations in surface sediment in survey area (Crecelius, Battelle, personal communication). Flux of oil into region estimated to be 7570 liter/day (Allen et al., 1970). Density of oil =0.89 g/cc. Concentration of ΣPAH in seep oil is 8,300 μg/g (Battelle, unpublished data).
'Barium discharge calculated from barite consumed on the platform during drilling is 1,070,000 kg.

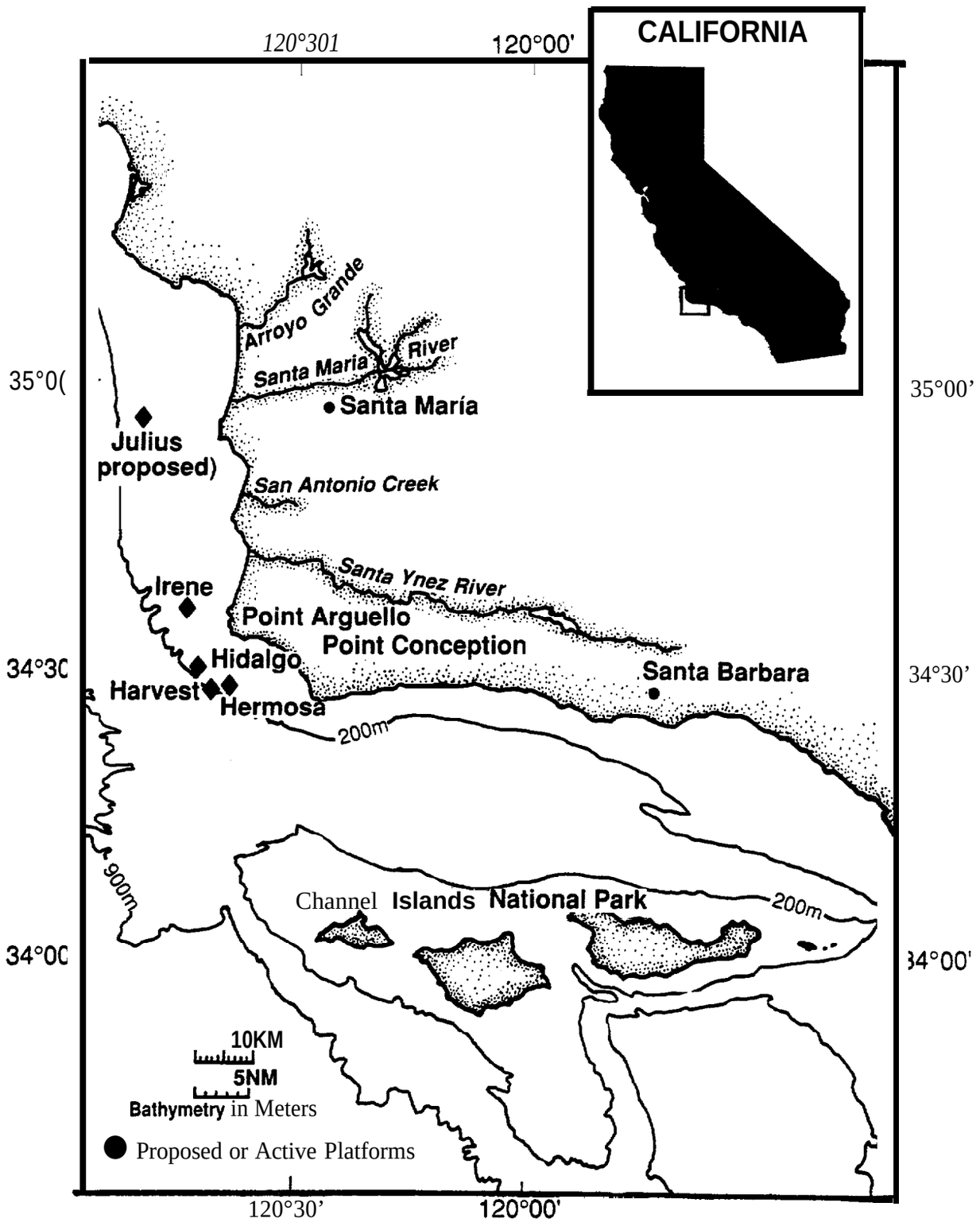

Figure 1. Production Platforms in the Southern Santa Maria Basin, Offshore California.

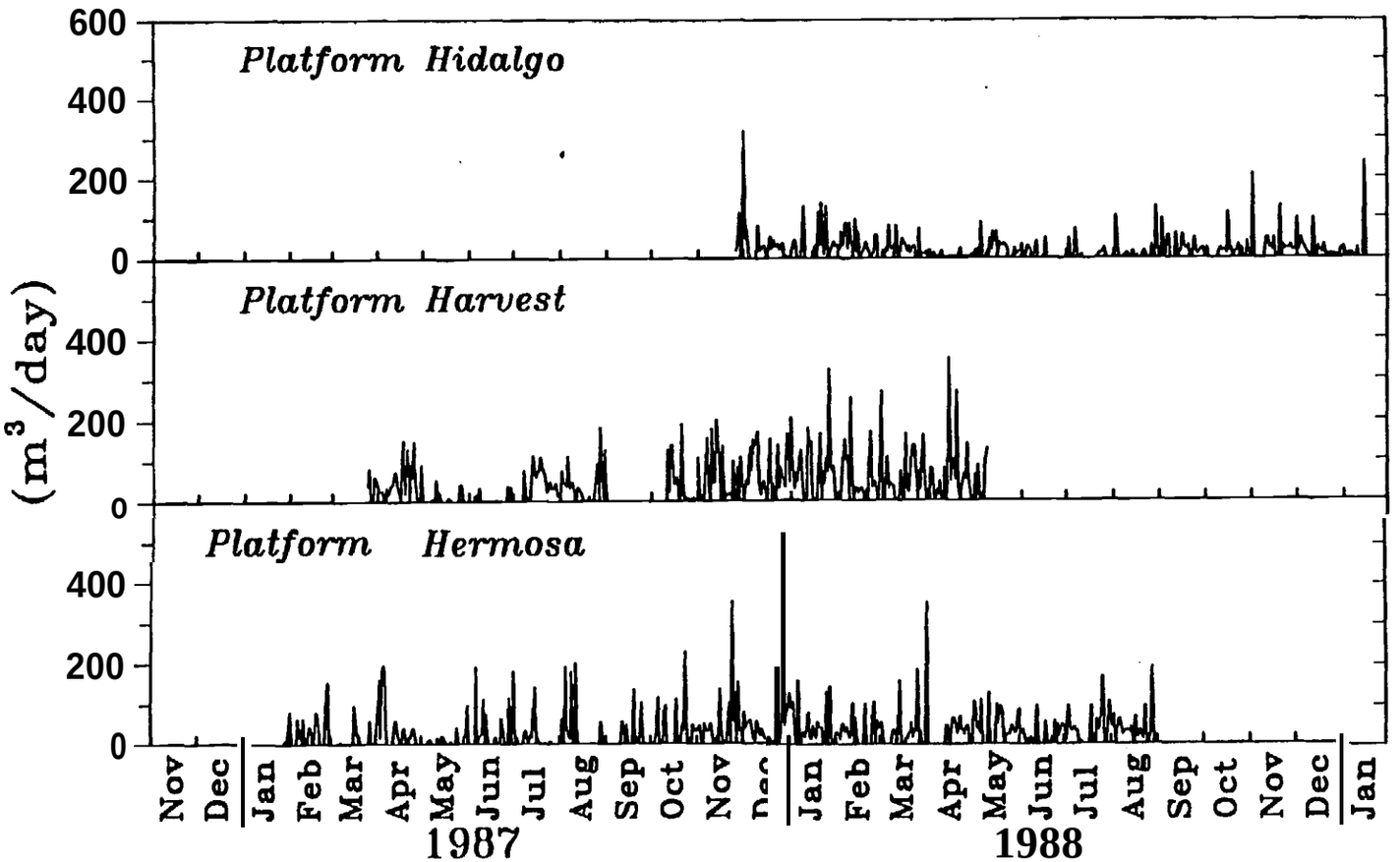

Figure 2. Daily Drilling-Mud Volumes Discharged From Production Platforms in the Point Arguello Field.

3. Spatial and Temporal Variation of Bottom Sediments Near Rock Reefs Exposed to Drilling Discharges off Point Arguello, California

TERENCE PARR, F.C. NEWTON

Kinnetic Laboratories, Inc.
5225 Avenida Encinas, Suite H, Carlsbad, California 92008

DANE HARDIN, PATRICK KINNEY

Kinnetic Laboratories, Inc.
307 Washington Street, Santa Cruz, California 95060

INTRODUCTION

The offshore Arguello Oil Field may be the largest ever discovered in continental U.S waters. Located in the southern Santa Maria Basin off southern California (Fig. 1), its production is like] y to exceed 100,000 bbl per day (Rintoul 1985; Hyland *et al.*, 1990).

The U.S. Minerals Management Service (MMS) has been sponsoring multidisciplinary research and monitoring in the Santa Maria Basin since 1973 as described by SAIC (1986); Hyland and Neff (1988); Hyland *et al.*, (1990); and Steinhauer and Imamura (1990).

While examining broad-scale variability of the offshore environment to assess natural processes, MMS has emphasized localized monitoring to assess potential sublethal, chronic and cumulative impacts of drilling muds upon benthic biological populations (Hyland *et al.*, 1990). Discharged drill mud particulate sink and accumulate at the benthic boundary layer where immobile benthic populations are susceptible to impacts from increased particulate deposition and exposure to contaminants.

The thin-veneered sediments of the Arguello shelf-break region are characterized by intermittent rock outcropping that host well developed and diverse attached invertebrate populations. These reefs typify depths between 100 and 250 m and provide habitat for a number of commercial y valued rockfish species.

Since 1986, MMS monitoring and research efforts in the Arguello region have focused upon hard substrate communities in the vicinity of Platform Hidalgo (Fig. 2) where the benthic layer has been in the downstream path of bulk drill mud dispersal from three clustered production platforms (Fig. 1). Platform drilling mud loading curves are shown in Figure 3.

Attached epifaunal invertebrates near Hidalgo are primarily suspension feeders (Hardin *et al.*, 1990) and may be distributional y controlled by hydrodynamic processes affecting deposition and resuspension of particulate at the sea-floor (see Jumars and Nowell 1984; Loya 1976; La Barbera 1984; Mullineaux 1988). Because of the importance of sedimentary processes to rocky reef communities, sediments have been monitored in the Platform Hidalgo vicinity, including physical and chemical properties of sediments and particulate flux into sediment traps from soft bottom habitats, primarily adjacent to reef areas (Fig. 2). Near bottom currents have also been recorded.

A primary goal of the MMS monitoring program has been to 1) describe the natural variation in the hard bottom assemblages with time and between localities and attempt to assess causes of variation, and 2) determine whether variation in hard bottom assemblages is associated with the introduction of contaminants from drilling discharges. Because of the importance of sedimentary processes to rocky reef communities, their sampling at Hidalgo has been conducted in conjunction with measurements of currents, physical and chemical properties of sediments and particulate flux into sediment traps from soft bottom habitats, primarily adjacent to reef areas (Figure 2). MMS sediment program objectives were to 1) describe temporal and spatial variations in sediments collected from the bottom and in boundary layer sediment traps, 2) assess the flux rate of sediments into the traps, 3) determine whether sediment flux is affected by proximity to rock habitat, and 4) determine whether the above were related to either distance from Platform Hidalgo or the period icity of drill mud disposal. The relationship between sediment traps particulate and bottom sediments was not determined due to lack of coincident sampling (Figure 3).

Sampling locations and dates are shown in Tables 1 and 2 and Figure 2. Current meter measurements were recorded from depths of 12, 54, and 126 meters above the bottom (130 m) at a site located approximately 1 km to the northwest of Platform Hidalgo.

Regional Environmental Setting

The Arguello shelf region makes up a sedimentary depositional unit of about 400 square miles deriving its detrital (coastal) sediments from riverine sources which introduce sediments to the coastal zone at rates ranging from about 1 to 19 $kgm/m^2/yr$, varying with episodic flood conditions (CSA 1985). Nearshore littoral drift is downcoast. Transport to the outer shelf is primarily through nearshore deposition and offshore transport by bedload resuspension. Sediments on the shelf are typically characterized by fine sands grading into silts offshore. The major rivers supplying coastal sediments are located upcoast of Point Conception, with the Santa Ynez providing major inputs (Fig. 1). Each drainage unit has a distinct mineralogical signature. Common minerals include kaolinite, chlorite, illite and smectite. Regional sediment overburden is not generally well developed and offshore areas near the shelf break and deeper are typified by rocky outcropping.

METHODS AND MATERIALS

Currents

The current meter mooring, equipped with conductivity and temperature sensors consisted of three Neil Brown Smart acoustic vector-averaging current meters located at the surface, middle and bottom of the water column. Extensive details of mooring configuration, telemetering and data analysis are reported by Kinney *et al.,* (1990). Sampling sites and schedules are summarized in Tables 1 and 2.

Collection and Analysis of Surface Sediments for Sedimentology Measurements

Sedimentology methods are provided in detail by Kinney *et al.*, (1990a).

Surface (O -2 cm) sediments were collected with a O. $1\text{-}m^2$ modified Van-Veen grab sampler. Three replicate grabs were obtained from soft-bottom substrates adjacent to hard-bottom sites that were sampled by photoquadrat techniques. Subsamples for grain size, total organic carbon (TOC), and carbonate analyses were taken from each of the three replicates at a station and pooled prior to analysis.

Grain size variables were determined by a standard (EPA Method 2) combination sieve and pipette anal ysis as described by Plumb (1981). TOC and carbonate concentrations in sediment samples were determined by the procedures of Kolpack and Bell (1968).

Sediment Traps

Sediment trap design and methods of deployment and retrieval are detailed by Hardin *et al.*, (1990).

With respect to baffling and height/diameter ratio (H/D), sediment traps were designed to minimize bias in determining depositional particulate flux (Gardner 1988a, b). Cylindrical traps of 7:1 H/D ratio and 6.6 cm internal diameter were constructed of butyrate tubing. Hexcel baffles (1 cm opening) were employed to minimize turbulence in the trap. Each trap monitoring array (Figure 4) contained four traps connected to a concrete anchor by stiff stainless-steel springs which allowed them to lay over and return upright if disturbed by passing fishing nets. Traps were positioned seven diameters apart. Arrays were lowered to the seabed with a line from the surface vessel. A pelican hook released the array after reaching the bottom.

Sodium azide (Knauer et *al.*, 1984) was used as a preservative and was dispensed into each trap throughout the deployment from a nalgene bottle, through a cellulose acetate 0.45 μm filter (Bothner *et* a/., 1986). Sodium azide does not interfere with the chemical analyses.

Each sediment trap array was retrieved with a remotely operated vehicle (ROV) equipped with video and guided by surface shore-to-ship and underwater acoustic ship-to-ROV navigation, supplemented by color-imaging sonar on the ROV. The ROV carried in its manipulator a snap-hook which was attached to a reel of line on the ROV. The snap-hook was connected to a lift ring on each trap array. When the ROV returned to the surface, the line was used to hoist the sediment trap array onto the vessel. Traps were capped immediatel y upon their retrieval and frozen for Laboratory analysis.

At two selected sites each survey (Table 2), Aandera current meters without the vane assembly were deployed on sediment-trap moorings. The meters recorded current speeds versus time at a height 1 m above the bottom.

Data Analysis and Statistical Methodology

Data were summarized by both sites and survey period. Tests for differences in sediment variables between sites and surveys utilized procedures of analysis of variance (ANOVA); in particular, a Student Newman Keuls (SNK) testing procedures, by which significant sites or stations or homogeneous groupings can be delineated. SNK procedures are described by Sokal and Rohlf (1969). To fit assumptions of

linearity in the data, percentage estimates were arc sine transformed for ANOVA. Significance criteria were set at the five percent level. Null hypotheses of no significant difference between sites and times (including drill mud dispersal) were tested. When significant differences were evident, appropriate a posteriori tests (regression analyses) were utilized to further explore the source of the variation and examine correlations between sediment variables. Correlations with depth were also examined. Regression analysis is a form of ANOVA (Sokol and Rohlf 1969; Snedecor and Cochran 1967).

Hard Substrate Sedimentation

Hard substrate biological assemblages and cover by sediments were sampled photographically with a remote] y operated vehicle (ROV), which was equipped with a CM80 video camera, a Photosea 70-mm still camera, a Photosea 1500S strobe light, two split-beam lasers, and a five-function manipulator. Navigation and laser methodology are detailed in Hardin *et al.*, (1990).

Approximate] y 80 photographic samples were taken at each station to allow for the analysis of 60 samples per station, Some samples were rejected for having too little relief and some were rejected for having less than 30-percent cover of rock.

Photographic samples were anal yzed by a random point-contact method. Each photograph was projected onto a screen upon which 50 points were randoml y distributed. The species or substrate type under each point was noted and recorded.

RESULTS AND DISCUSSION

The Hydrodynamic Regime

Monthly means of current speeds from the period of mud disposal from mid-depth and near-bottom (Table 3) ranged from 3-10 cm/sec near the bottom and from 1-15 cm/sec in mid-water. Motion was most frequent! y directed to the north and west in mid-water and to the west with a sl ight southerly direction near the bottom as indicated in Figure 5. Current speed frequencies from 4 m above the bottom were.

cm/sec	Frequency
o-1o	.348
10-20	.480
20-30	.147
>30	.025

Currents recorded from station-survey rotated Aandera meters located on sediment traps 1 m above bottom showed comparative reductions in speed, with about 70% frequency in the 0-10 cm range, thus indicating that flow is significantly influenced by form drag adjacent to the boundary layer. Chriss and Caldwell (1982) provided detailed evidence of this phenomenon over a similar textured bottom on the Oregon shelf. They attributed form drag, as opposed to skin friction from sediment grains, to textural features such as mounds, depressions and furrows, irregularly spaced and having vertical relief of a few cm or more. Hidalgo region slopes are typified by such features, especially near rocky habitats where motile macrofauna such as the urchin (Allocentrotus) occur.

Sediments

Sediment data from bottom grabs are summarized in Tables 4 through 7 and Figures 6 and 7. Two extremes of granulometry are evident (Table 4) as delineated by very fine sands on steeper (9° - 120, slopes at the deeper stations (N, K and R) and by coarse silts from shallower depths on lesser inclined slopes (1.5” - 3°) from stations F, E, I, J and U. Platform Hidalgo occupies an intermediate position near the shelf break. The far-removed station W is intermediate in grain character, and is located at about 5-10” slope near the sill of an Arguello finger canyon drop-off (Fig. 2).

Grain Size

Platform Hidalgo regional sediments consisted of very fine sand and coarse silt with station averages ranging from 33 to 91 μ. Coarser sediments typified the deeper stations. The positive correlation of increased grain size with depth ($r = .707$, $p < .0001$) was evidenced by significant differences between deep and shallow site groupings as indicated by ANOVA-SNK results.

	coarser sediments				freer sediments				
Station	N	K	R	W	u	J	E	I	F
depth (m)	160	166	213	195	113	117	119	107	105

Stations not underscored by the same line differ at the p < .05 level. Sediment fine fractions (silt + clay, <62 μ) also decreased significantly with depth (Table 7). There were no significant differences in grain size or sediment fine fractions between survey periods. However, the clay fraction (<4 μ) differed by a factor of about two between survey extremes (Fig. 6), ranging from 12.5 to 26.6 %.

Clay content was significantly higher in the May, 1989 survey (3-4) and lower in the October, 1988 survey (3-1) following a peak period of drill mud disposal (Fig. 3; Fig, 6), thus a signature of the heavy clays present in drill muds was not evident in bottom sediments following platform mud disposal. Temporal ANOVA-SNK patterns for clay are presented below. Surveys following disposal periods are enclosed.

Clay

Lowest							Highest
3-1	1-1	1-3	2-3				3-4
10/88	10/86	5/87	87	11/87	10/90	10/89	5/89

Percentage silt and clay was significantly greater at shallower depths (Table 7). The phenomenon of increased coarseness and reduced fine fractions with depth indicates that surface waves do not routinely dominate boundary layer resuspension over the sampling depth range.

Total Organic Carbon (TOC) and Carbonates

TOC values ranged between 0.3 and 1.4 % of sediment dry weight (Table 6). These levels are similar to those summarized for southern California island and mainland shelves (Emery 1960). TOC was positively associated with sediment tines and clay (Table 7) and therefore was higher in the shallower sediments as indicated by ANOVA-SNK results. The TOC values decreased with depth.

	Lowest TOC							Highest TOC	
Station	N	K	R	W	J	u	E	I	F
depth (m)	166	160	213	195	117	113	119	107	105

Carbonate values did not differ significantly between stations, ranging from 2.2 to 3.4 percent dry wt. Sediment dispersion values were similar between stations; station means ranging between 1.81 and 2.33. Sediments were better sorted from the deeper more steeply inclined sites, as evidenced by a correlation with depth of r = -.393 (p = .018).

***Sediment** Tmp Estimates of Deposition*

Sediment depositional flux estimates and sediment trap granulometry, TOC, and carbonate are summarized in Tables 8 and 9. Significant sediment trap correlations are shown in Table 7. Sediment flux station averages (Table 8) ranged from 25 to 49 $gm/m^2/day$ and were greatest at the shallower stations where bottom sediments are finer (depth correlation, r = -.483; p = .001) Flux rate was positively associated with trapped fine fraction and clay (Table 7). Flux to traps on isolated sediment habitat did not significantly differ from sites ST1, ST2, and ST3, adjacent to reefs. ANOVA-SNK results examining site differences in the Platform Hidalgo vicinity revealed the following:

	Lowest Flux								Highest Flux			
Station	R	K	ST3	W	N	ST2	ST1	E	J	F	I	U
Depth (m)	212	160	212	195	166	163	120	119	117	105	109	113

A significant infusion of clay particulate occurred after the May, 1989 trap deployment when average clay content from all sites nearly doubled from 10 to 19 percent by October, 1989 (Table 8). This condition persisted through two more trap retrievals, ending in May, 1990. The phenomenon was not site or depth restricted and was probably related to regional downslope transport processes, as opposed to mud disposal, since it was not evident four months after the cessation of disposal and appeared more than one year after the peak disposal period (Fig. 3).

The particulate flux to traps at one meter elevation above the seabed is significantly greater than flux recorded in the overlying water column from sites in the Santa Barbara Channel (Dunbar and Berger 1981; Dymond *et* al., 1981). They measured deposition into traps elevated 190 m or more above a 570

m bottom and reported flux from six traps placed at depths of 162 to 381 m, as ranging from 0.2 to 2.1 gm/m^2/day. This represents onl y 0.4 to 8.4 percent of flux recorded from bottom traps at Hidalgo. Thus a significant resuspension fraction into Hidalgo bottom traps is indicated. This has been substantiated by Coats (in prep) who utilized downwelling barium from drill muds as a tracer to show that resuspension accounts for more than 98 percent of flux to traps located a meter above the seafloor.

The recorded flux at the Hidalgo site is about half of that recorded from near-bottom traps at four shallower sites (25-60 m) off southern California by Hendricks (1986).

TOC in Hidalgo traps was consistent between sites and surveys with station averages ranging from 1.9 to 2.4 percent dry wt. (Table 9). Dymond *et al.*, (1981) recorded values between 3 to 4 percent from the Santa Barbara Channel water column, indicating a relatively greater contribution from primary production and organic detritus, primarily in the form of fecal pellets (Dunbar and Berger 1981). Hidalgo bottom trap carbonates all exceeded 3 percent, representing sedimentary contribution, whereas column carbonates (Dymond *et* al., 1981) did not exceed 1 percent.

Sedimentation of Hard Substrates

Observations of sedimentation of hard substrates are summarized in Table 10.

Low Relief. Percent sediment cover of low relief rock ranged from site averages of 20 to 39 percent and was greater at the deeper sites (_ W, N, R). ANOVA-SNK results are shown as follows:

Lowest Sediment Cover							Highest Sediment Cover
I	E	J	F	R	N	W	U

Correlation with depth was significant (r= .338, p= .01). This pattern is counter-intuitive in relation to observed reduced sediment trap flux and coarser bottom sediments at the deeper sites (Table 7). Unknown factors including rock inclination and topography may explain the observed differences. Differences between surveys were not significant.

High Relief. High relief showed comparative] y little sedimentation, averaging 3-5 percent for all surveys at the three sites. Differences between sites and surveys were insignificant. The lower levels of sedimental ion on higher relief substrate may be attributed to their more vertically exposed surface and to the possibility of resuspension from the acceleration of currents as they are forced onto the reef areas. This latter phenomenon has been noted over large seamounts where coral distributions are enhanced in regions of accelerated flow (Genin *et al.,* 1986) At the Hidalgo site, where suspension feeders are more prevalent on high relief (Hard in *et al.,* 1990), photoquadrats of epifauna have revealed that high relief fauna are positively associated with directional exposure to highest-energy currents while the low relief fauna tends to be associated with directional exposure to lower energy currents (Hardin *et al.,* in prep).

CONCLUSIONS

Platform Hidalgo region sediments between depths of 105 to 213 m are characterized by very fine sands and coarse silts. Sediments containing 60 to 70 percent sand typify deeper sites on steep (9° -120, slopes offshore of the shelf break. Nearshore sites on more gradual (1 .5 °- 30, slopes are typified by sediments consisting of 60-70 percent silt. Higher levels of TOC characterize finer nearshore sediments.

Grain size patterns appear to be patterned by localized effects from hydrodynamic forces associated with inclination of exposure topography and slope in coupling with larger-scale episodic introductions of fine sediments. A region-wide deposition of clay occurred in Spring 1989, indicating that episodic bed-load resuspension transport had occurred. This was evident from both trap and bottom sediment clay signatures. Increases in sediment clay levels were not significant y influenced with drill mud disposal.

Depositional flux to sediment traps ranged up to 49 gm/m²/day with highest flux occurring at the finer grained shallow sites. Flux was not significantly influenced by proximity to rocky reef habitat. Flux levels were not significantly related to drill mud disposal.

Average percent cover by sediment of low-relief rocky habitats ranged from 20 to 39 percent between sites, and was counter-intuitively greater at deeper sites characterized by coarser sediments and reduced flux into traps. Temporal changes were not evident. High relief sedimentation averaged 3 to 5 percent. Accelerated current flow and greater vertical exposure may limit deposition on elevated surfaces.

Sediments, flux and habitat sedimentation did not provide evidence of a lasting depositional imprint from drill mud disposal. Water column advection (typically krns per day) and boundary layer resuspension transport are primary factors in dissipation of platform particulate.

ACKNOWLEDGEMENTS

We gratefully acknowledge the important contributions of several people. Special assistance in the field was provided by Jim Campbell, Janet Kennedy and Jay Shrake. Laboratory grain size measurements were conducted by Art Currier, Bill Schmitz, Robin Gartman, Denise Howard and Jay Shrake. Carbon measurements were conducted at the University of Southern California at the laboratory of Dr. Donald Gorsline. Word processing was performed by Teri McLeod. This work was performed under a contract to Kinnetic Laboratories from Battelle, with funding provided by the U.S. Department of Interior, Minerals Management Service (MMS) through contract number 14-12-0001-30262. Dr. Gary Brewer of MMS has ably directed the multidisciplinary program, of which this study was a part.

REFERENCES

Berry, R.W. and B. Nocita. 1977. Clay mineralogy of recent marine sediments around the southern California outer continental shelf. Cal. Div. Mines and Geology, Sp. Rep. 129, pp. 101-106,

Bothner, M. H., C.M. Parmenter, R.R. Rendigs, and M. Rubin. 1986. The flux and composition of resuspended sediment in submarine canyons off the northeastern United States: Implications for pollutant scavenging. Chapter 6 In: B. Butman (Ed.) North Atlantic Slope and Canyon Study. Draft Final Report to U.S. Dept. of the Interior, Minerals Management Service. Interagency Agreement IA 14-12-0001-30180.

Brindley, G. W. and G. Brown. 1980. Crystal structures of clay minerals and their X-ray identification. Mineralogical Society Special Publication No. 5.

Chriss, T.M. and D.R. Caldwell. 1982. Evidence of the influence of form drag on bottom boundary layer flow. *J. Geophys. Res.* 87(6): 4148-4154.

CSA (Continental Shelf Associates). 1985. Assessment of the long-term fate and effective methods of mitigation of California outer continental shelf platform particulate discharges. Vol. I: Final Report. U.S. Dept. of the Interior, Minerals Management Service, Pacific OCS Region, Los Angeles, CA. Contract No. 14-12-001-30056.

Crisp, P. T., S. Brenner, M.I. Venkatesan, E. Ruth, and I.R. Kaplan. 1979. organic chemical characterization of sediment-trap particulate from San Nicolas, Santa Barbara, Santa Monica, and San Pedro Basins, California. *Geochim. Cosmochim.* Acts 43:1791-1801.

Dodge, R.E. and J.R. Vaisyns. 1977. Coral populations and growth patterns. Responses to sedimentation and turbidity associated with dredging. *J. Mar. Res.* 35(4): 715-730.

Drake, D. E., P. Fleisher, and R.L. Kolpack. 1971. Transport and deposition of flood sediment, Santa Barbara Channel, California. pp. 181-217 In: R.L. Kolpack (Ed.) Biological and Oceanographic *Survey* of the Santa Barbara Channel Oil Spill, 1969-1970. Vol. II, Physical, Chemical and Geological Studies. Allan Hancock Foundation, Los Angeles, CA.

Dunbar, R.B. and W.H. Berger. 1981. Fecal pellet flux to modem bottom sediment of Santa Barbara Basin (California) based on sediment trapping. *Geol.* Sot. *Ameer. Bull.* 92:212-218.

Dymond, J., K. Fischer, M. Clauson, R. Cobler, W. Gardner, M.J. Richardson, W. Berger, A. Soutar and R. Dunbar. 1981. A sediment trap intercomparison study in the Santa Barbara Basin. *Earth and Planet. Sci. Let.* 53:409-418.

Emery, K.O. 1960. The Sea Off Southern California. John Wiley and Sons, Inc., New York, 366 pp.

Gardner, W .D.1980a. Sediment trap dynamics and calibration: A laboratory evaluation. *J. Mar. Res.* 38(1): 17-39.

Genin, A., P.K. Dayton, P.F. Lonsdale, and F.N. Spiess. 1986. Corals on seamount peaks provide evidence of current acceleration over deep-sea topography. *Nature 322:59-61.*

Hardin, D., J. Teal, P. Wilde and T. Parr. 1990. Hard-bottom epifaunal assemblages. Chapter 12 In: M. Steinhauer and E. Imamura (Eds.) California OCS Phase 11 Monitoring Program Year-Three Annual Report. U.S. Dept. Interior, Minerals Management Service, Pacific OCS Region, Camarillo, CA. Contract No. 14-12-0001-30262.

Hardin, D., R. Spies and T. Parr. 1987. Hard bottom epifaunal assemblages. Chapter 4 In: Hyland, J. and J. Neff (Eds.). California OCS Phase II Monitoring Program: Year-One Annual Report. U.S. Dept. Interior, Minerals Management Service, Pacific OCS Region, Los Angeles, CA. Contract No. 14-12-0001-30262.

Hendricks, T. 1986, Sedimentation, resuspension and transport of particulate. Southern California Coastal Water Research Project, 1986 Rept: 26-28.)

Hyland, J. and J. Neff (Eds.). 1988. California OCS Phase II Monitoring Program: Year-One Annual Report. U .S, Dept. Interior, Minerals Management Service, Pacific OCS Region, Los Angeles, CA. Contract No. 14-12-0001-30262. Volume I (MMS 87-0115) and Volume II (MMS 87-01 16).

Hyland, J., D. Hard in, E. Crecelius, D. Drake, P. Montagna and M. Steinhauer. 1990. Monitoring long-term effects of offshore oil and gas development along the southern California outer continental shelf and slope: Background environmental conditions in the Santa Maria Basin. *Oil Chem. Pollut. 6:195-240.*

Jackson, M.L. 1956. Soil chemical analysis - Advanced course. Published by the author, Dept. of Soil Science, Univ. of Wisconsin, Madison, WI.

Jumars, P.A. and A.R.M. Newell. 1984. Fluid and sediment dynamic effects on marine benthic community structure. *Amer. Zool.* 24:45-55.

Kimey, P., D. Hardin, T. Parr, F. Newton and R. Kolpack. 1990. Sedimentology. Chapter 4 In: M. Steinhauer and E. Imamura (lMs.) California OCS Phase II Monitoring Program Year-Three Annual Report. U.S. Dept. Interior, Minerals Management Service, Pacific OCS Region, Camarillo, CA. Contract No. 14-12-0001-30262.

Kinney, P., P. Wilde, D. Beard, D. Coats and R. Bernstein. 1990. Physical oceanography. Chapter 3 In: M. Steinhauer and E. Imamura (Eds.) California OCS Phase II Monitoring Program Year-Three Annual Report. U.S. Dept. Interior, Minerals Management Service, Pacific OCS Region, Camarillo, CA. Contract No. 14-124001-30262.

Kolpack, R.L. and S. A. Bell. 1968. Gasometric determination of carbon in sediments by hydroxide absorption. *J. Sedimental. Petrol. 28(2): 617-620.*

Knauer, G. A., D.M. Karl, J.H. Martin, and C.N. Hunter. 1984. In situ effects of selected preservatives on total carbon, nitrogen and metals collected in sediment traps. *J. Mar. Res.* 42:445-462.

La Barbara, M. 1984. Feeding currents and particle capture mechanisms in suspension feeding animals. *Amer. Zool. 24:71-84.*

Loya, Y. 1976. Effects of water turbidity and sedimentation on the community structure of Puerto Rican corals. *Bull. Mar. Sci. 26(4): 450466.*

Martin, J.H. and G. A. Knauer. 1973. The elemental composition of plankton. *Geochim. Cosmochim. Acts 37: 1639-1653.*

Mull ineaux, L.S. 1988. The role of settlement in structuring a hard-substratum community in the deep sea. *J. Exp. Mar. Biol. Ecol. 120:247-261.*

Mull ineaux, L.S. 1989. Vertical distributions of the epifauna on manganese nodules: Implications for settlement and feeding. *Limnol. Oceanogr. 34(7):* 1247-1262.

Plumb, R.H. Jr. 1981. Procedure for Handling and Chemical Analyses of Sediment and Water Samples. Technical Report EPA/CE-81 -1. USACOE Waterways Exp. Station, Vicksburg, MS, 487 pp.

Rintoul, B. 1985. Fifteen platforms planned off California. *Offshore* 45(l): 60-61.

Science Applications International Corporation (SAIC). 1986. Assessment of long-term changes in biological communities of the Santa Maria Basin and western Santa Barbara Channel -Phase 1. Vol. 11: Synthesis of findings. U.S. Dept. Interior, Minerals Management Service, Pacific OCS Region, Los Angeles, CA. Contract No. 14-12-0001-30032 Two volumes (MMS 86-9911 and MMS-9912).

Simmons, G .M. 1979. Abundance and distribution of particulate matter fractions near a Caribbean Bank Barrier Reef. *Mar. Ecol. Prog. Ser.* 1:7-11.

Snedecor, G. W. and W .G. Cochran. 1967. Statistical Methods. Iowa State Univ. Press, Ames, Iowa, 6th cd., 593 pp.

Sokal, R.R. and F.J. Rohlf, 1989. Biometry, The Principles and Practice of Statistics in Biological Research. W.H. Freeman Co., San Francisco, 776 pp.

Steinhauer, M. and E. Imamura (Eds.). 1990. California OCS Phase II Monitoring Program Year-Three Annual Report. U.S. Dept. Interior, Minerals Management Service, Pacific OCS Region, Camarillo, CA. Contract No. 14-12-0001-30262. Two volumes (MMS 90-0055).

Table 1. Summary of grab, sediment trap and hard bottom photoquadrat sampling.

		GSP - Stations									S - StatIons			
		PHF	PHI	PHU	PHJ	PHE	PHK	PHN	PHW	PHR	PHST1	PHST2	PHST3	PHAR
Depth (m)		105	109	113	117	119	160	166	195	212	120	163	212	195
Distance from Hidalgo (km)		2.1	0.8	3.8	0.5	1.2	0.6	0.9	6.4	1.1	1.9	1.9	2.3	3.0
Date	Survey													
Ott 86	1-1	G P	G P	G P	G P	G P	G P	G P	G P	G P				
May,Jul 87	1-3	G P	G P	G P	G P	G P	G P	G P	G P	G P				
Nov 87	2-3	G P	G P	G P	G P	G P	G P	G P	G P	G P				
May 88	2-5		S		S	S	S	S	S	S	S	S	S	
Ott 88	3-1	GS P	GSP	GSP	GSP	GS P	G P	GSP	GSP	GS P	s	s	s	s
May 89	3-4	GS P	GS P	GSP	GSP	GSP	GSP	GS P	GSP	GSP				
Ott 89	4-1	GS P	GSP	GS P	GS P	G P	GS P	G P	G P	GS P	s		s	S
May 90	4-2	S	s	s	S	s	s	s	s	s	s	S	s	s
Ott 90	5-1	GS P	GS P	GS P	GS P	GS P	G P	GS P	GS P	GS P	s	s	s	s

G = Grab Sample; S = Sediment Trap; P = Photoquadrat

Table 2. Sampling periods for sediment traps and current meters mounted on sediment trap assemblies

Sediment Traps

Survey	Retrieved	Number of Days Deployed	Number of stations
2-5	May 17-25,1988	115-117	10
3"1	October 6-18,1988	140-144	12
3-4	May 12-22,1989	216-220	9
4-1	October --1989	163-167	9
4-2	May ---1990	192-195	13
5-1	October --1990	170"173	13

Bottom Mounted Current Meters on Sediment-Trap Assemblies

Deployment	Recovery	Station
Jan 26,1988 Jan 26,1988	May 21,1988 May 21,1988	ST3 R
May 22,1988 May 22,1988	Ott 9,1988 Ott 12,1988	ST2 K
Ott 10,1988 Ott 13,1988	May 15,1989 May 16,1989	ST2 K
May 15,1989 May 16,1989	Ott 29,1989 Ott 28,1989	ST1 J

Table 3. Monthly current speeds and directions from mid-water and near-bottom current meters near Platform Hidalgo (bottom depth = 130 m).

Year	Month	Bottom (126 m)		Mid Water (50 m)	
		Mean Speed (cm/s)	Direction (degrees)	Mean Speed (cm/s)	Direction (degrees)
1987	Feb	5.0	299	1,4	312
	Mar				
	Apr	3.2	244		
	May			13,4	136-
	June	6.4	110	2.9	348
	July	10.5	98	9.8	318
	Aug	8.4	98	10,2	321
	Sept			13.1	318
	Ott			3.8	312
	Nov	6.8	257	15.4	79
	Dec	6.4	249	10.8	309
1988	Jan	6.8	263	7.0	322
	Feb*	5.9	264	15.0	317
	Mar'	5.3	244	5.6	333
	Apr*	4.2	229	2.9	2
	May'				
	Jun	3.5	209		
	Jul	4.7	263		
	Aug	3.0	240		
	Sept	6.4	276		
	Ott			15.2	320
	Nov	5.8	271	4.4	332
	Dec	5.4	286	11.8	326
1989	Jan	11.4	281	18.0	321

● = peak disposal periods

Table 4. Station groups for sediments in the Platform Hidalgo vicinity.

Location: North, East, West 0.5- 3.8 km from Platform Hidalgo Slopes: Est. 1 .5-3%	33-39 Coarse Silt	19-26	60-68	
DEEPER STATIONS (K,N,R) Depths: 160-213 m Location: South and West 0.6- 1.1 km from Platform Hidalgo Slopes: Est. 9-12%	71-91 Very Fine Sand	60-66	27-32	6-8
DEEP STATION (W) Depth: 195 m Location: Northwest, farthest removed 6.4 km from Platform Hidalgo Slope: Est. 5% Near sill area of Arguello - finger contour	56 Coarse Silt	*44*	44	11

Table 5. Median grain size, fine fraction (silt+ clay) and clay in bottom sediments from the Platform" Hidalgo vicinity.

		Stations									Mean	Std. Error
		PHF	PHI	PHU	PHJ	PHE	PHK	PHN	PHW	PHR		
Depth		106	102	113	117	119	160	166	195	212		
Distance		2.1	0.8	3.8	0.5	1.2	0.6	0.9	6.4	1.1		
Date	Survey	Median (μ										
Oct86	1-1	34.94	35.11	33.58	36.68	36.44	70.94	121.35	4s.03	67.54	53.78	9.72
May-Jul87	1-3	33.11	37.09	34.66	35.15	35.64	68.61	91.39	40.85	73.85	53.46	8.99
Nov87	2-3	17.34	28.34	39.48	43.37	37.47	72.16	92.12	64.64	75.13	52.36	8.23
Oct88	3-1	37.50	35.73	33.76	36.02	38.80	67.27	62.26	64.52	72.62	54.30	7.40
May89	3-4	31.21	28.76	55.65	32.35	32.16	88.91	79.00	33.26	88.67	49.54	7.68
Oct89	4-1	37.93	37.50	37.44	39.41	41.07	92.41	62.02	68.44	71.85	56.45	7.38
Oct90	5-1	37.52	38.85	38.51	41.38	38.64	91.20	90.65	69.00	72.35	57.57	7.74
Mean		32.79	34.63	39.00	37.68	37.18	85.79	91.28	65.56	71.43		
Standard Error		2.75	1.51	2.90	1.46	1.07	4.01	5.40	5.53	1.19		
Date	Survey	% Fne (Sit + Clay)									Mean	Std. Error
Oct86	t-1	92.85	88.55	95.08	86.38	67.91	46.58	13.95	61.85	44.61	68.64	9.48
May-Jul87	1-3	85.14	81.30	64.43	77.64	74.95	33.20	37.92	65.52	38.66	84.31	7.21
Nov87	2-3	80.06	84.41	67.22	67.46	81.16	45.31	33.61	47.80	35.68	80.32	6.68
Oct88	3-1	84.18	88.19	82.42	76.88	77.29	37.09	36.98	47.80	37.73	82.39	7.23
May89	3-4	77.19	78.94	53.19	70.70	75.48	39.93	39.88	80.91	45.88	82.44	5.83
Oct89	4-1	71.86	67.16	72.27	71.52	68.11	35.58	38.67	43.84	40.08	58.5s	5.46
Oct90	5-1	76.23	74.64	76.21	89.88	76.02	35.29	33.25	43.10	38.80	58.39	6.67
Mean		81.36	79.46	75.83	74.35	77.28	39.00	33.49	55.83	40.18		
Standard Error		2.55	2.62	5.09	2.44	2.30	1.96	3.38	5.33	1.38		
Date	Survey	% clay									Mean	Std. Error
Oct86	I-t	5.76	5.79	5.44	9.71	5.33	2.87	0.75	2.98	15.63	6.03	1.46
May-Jul87	1-3	15.35	4.05	15,07	17.15	16.05	2.88	2.s3	19.23	2.33	10.50	2.44
Nov87	2-3	16.17	13.3$	16.12	11.21	9.11	18.10	2.89	11.92	4.80	11.60	1.73
Oct88	3-1	3.26	3.87	11.30	10.82	3.53	1.60	4.33	5.05	2.08	5.12	1.17
May89	3-4	24.27	27.40	16.81	24.71	25.78	14.79	13.37	20.26	15.30	20.30	1.79
Oct89	4-1	14.41	16.19	15.76	13.41	13.78	9.01	11.46	10.42	10.07	12.95	0.99
Oct90	5-1	15.72	15.79	13.95	14.87	15.92	8.98	6.02	9.78	9.08	12.46	1.13
Mean		13.58	12.72	13.49	14.55	12.76	8.32	6.22	11.3a	8.47		
Standard Error		2.66	3.30	1.51	1.95	2.87	2.40	1.62	2.47	2.14		

Table 6. Dispersion, total organic carbon and carbonate in bottom sediments from the Platform Hidalgo vicinity.

		Stations										
		PHF	PHI	PHU	PHJ	PHE	PHK	PHN	PHW	PHR		
	Depth	105	108	113	117	119	160	166	195	212		
	Distance	2.1	0.8	3.8	0.5	1,2	0.6	0.9	6.4	1.1		
Data	Survey	Dispersion (Φ)									Mean	Std. Error
Oct86	1-1	1.13	1.15	1.177	1135	1.14	1.89	1.14	1.22	2.34	1.39	0.14
May-Jul87	1-3	1.90	1.35	1.89	2.37	2.27	1.87	1.64	2.60	1.07	1.93	0.17
Nov87	2-3	2.13	1.789	2.64	1186	1.45	3.76	1.71	1.67	1.04	2s)3	0.26
Oct88	3-1	1.07	1.27	1.499	1.66	1.24	1.76	1.71	1.21	0.97	1.37	0.10
May89	3-4	3.15	3.40	2.61	3.31	3.36	2.89	2.37	2.70	2.17	2.66	0.15
Oct89	4-1	2.26	2.864	2229	1.89	1.99	2.16	2.09	1.46	1.29	2.03	0.15
Oct90	5-1	2.14	2.22	1.89	2.16	2220	2000	1.64	1.36	1.17	1.67	0.13
	Mean	1.97	2000	1.88	2009	1955	2233	1.79	1.61	1.44		
	Standard Error	0.27	0.32	0.21	0.24	0.29	0228	0.15	0.26	0.22		
Date	Survey	% Total Organic Carbon									Mean	Std. Error
Oct86	1-1	0.93	0.74	0.78	0.85	0990	0.41	0332	0663	0.52	0.68	0.06
May-Jul87	1-3	0.86	1.07	1.09	0.64	0.92	1.15	0.93		0.92	0.95	0.06
Nov87	2-3	1.22	1.03	0.75	0.73	1.05	0.30	0225	1.00	0.79	0.79	0.11
Oct88	3-1	1.04	1.17	1.07	1.20	1.12	0.76	0.75	0.59	0.63	0.93	0.06
May69	3-4	1.07	1.09	0.98	1199	0999	0.66	0755	0669	0.65	0.92	006
Oct89	4-1	1.15	1.06	1.06	0.63	0.87	0.74	0.74	0.73	0.76	0.66	0.06
Oct90	5-1	1.37	1.19	1.17	1188	1130	0.92	0.95	0.79	0.64	1.08	0.07
	Mean	1.05	0.96	0.95	0960	1000	0.67	0.59	0.71	0.66		
	Standard Error	0.06	0.06	0.06	0.06	0.06	0.12	0.10	0.07	0.07		
Date	Survey	% carbonate (CaCO)									Mean	Std. Error
Oct86	1-1	0.38	0.36	0.31	0.37	0.39	0.51	0.35	0.32	0.36	0.36	0.02
May-Jul87	1-3	3.14	3.43	3.01	3.40	2.93	3.50	2.65		2.22	3.06	0.15
Nov87	2-3	1.27	3.94	2.76	3.32	3.41	5.30	3.63	2.47	1.94	3.12	0.39
Oct88	3-1	2.87	3.07	3.30	2.93	2.93	3.52	2.42	4.53	3.22	3.20	0.20
May89	3-4	2.34	3.20	2.68	3.76	2.89	3.64	2.10	4.96	3.31	3.24	0.29
Oct89	4-1	2.57	3.96	3.51	4.17	4.02	3.64	2.53	3.84	2.70	3.47	0.23
Oct90	5-1	3,{1	3.22	3.71	4.13	3.37	3.19	1.40	4.24	2.92	3.25	0.28
	Mean	1.83	2.44	2.21	2.54	2.31	2.74	1.78	2.64	1.84		
	Standard Error	0.41	0.53	0.49	0.56	0.49	0.59	0.41	0.73	0.42		

Table 7. **Significant ($p \leq 0.05$) correlations between sediment variables in bottom sediments and in sediment traps from the Platform Hidalgo Region. Correlation coefficient (r) and probability value (parentheses).**

Bottom Sediments

	Median Grain	Percent Silt/Clay	Percent Clay	Dispersion	TOC	Carbonate	Depth	Distance from Hidalgo
Median Grain								
Percent Silt/Clay	-.967 (<0.001)							
Percent Clay	-.521 (.001)	.433 (.008)						
Dispersion			.900 (<.001)					
TOC	-.632 (<.001)	.685 (<.001)	.334 (.046)					
Carbonate								
Depth	.707 (<.001)	-.769 (<.001)	-.375 (.024)	-.393 (.018)	-.796 (<.001)			
Distance from Hidalgo						.439 (.007)		

Sediment Traps

	Flux	Median Grain	Percent Silt/Clay	Percent Clay	Dispersion	TOC	Carbonate	Depth	Distance from Hidalgo
Flux									
Median Grain	-.231 (.001)								
Percent Silt/Clay	.190 (.006)	-no (<.001)							
Percent Clay	.228 (.001)	..421 (<.001)	.18s (.007)						
Dispersion	.315 (<.001)		-.279 (<.001)	.433 (<.001)					
TOC									
Carbonate					.169 (.014)				
Depth	-.483 (<ml)		-.155 (.025)			.255 (<.001)			
Distance from Hidalgo			.163 (.018)		..140 (.044)			289 (<.001)	

Table 8. Sediment trap depositional flux, median grain size, fine fraction (silt+ clay) and clay from the Platform Hidalgo vicinity.

		Stations														
		PHF	PHI	PHU	PHJ	PHE	PHST1	PHK	PHST2	PHN	PHw	PHAR	PHST3	PHR		
Depth		105	109	113	117	119	120	160	163	166	195	213	212	212		
Distance		2.1	0.8	3.8	0.5	1.2	1.9	0.6	1.9	0.9	6.4	3	2.3	1.1		
Date	survey	Flux (gm/m²/day) dry weight													Mean	Std. Error
May88	2-5	.	35.75	.	31.05	28.16	27.19	22.66	26.63	29.14	19.71	.	26.05	24.29	27.80	0.86
Oct88	3-1	28.76	26.06	30.14	23.73	28.71	28.83	.	58.64	24.45	21.41	23.17	24.26	21.12	26.44	1.71
May89	3-4	39.77	44.57	42.59	39.41	32.24	36.90	23.37	21.96	29.19	23.14	27.41	23.98	24.42	31.61	1.35
Oct89	4-1	32.55	32.94	36.65	31.46	.	37.77	23.61	.	.	.	22.91	35.34	23.68	30.77	1.11
May90	4-2	81.56	85.70	81.60	69.94	58.41	60.45	35.47	36.44	35.87	36.34	34.80	18.59	27.60	52.68	4.32
Oct90	5-1	51.15	45.31	52.46	45.54	46.76	40,84	31.34	36.26	37.70	34.76	27.69	29.15	30.04	39.48	1.43
Mean		44.27	45.39	4669	43.53	40.96	39.00	26.06	36.39	31.27	26.20	27.23	26.56	25.22		
Standard Error		4.62	4.66	4.95	5.42	4.20	2.68	1.38	3.64	1.45	2.04	2.61	1.37	0.79		
Dale	survey	Median Grain Size													Mean	Std. Error
May88	2-5		22.65	.	25.61	24.23	24.11	19.04	20.67	31.24	20.22	.	29.32	29.64	25.07	1.76
Oct88	3-1	26.06	19.77	22.58	18.37	24.93	.	.	.	18.38	29.25	18.85	.	18.70	21.68	1.58
May89	3-4	22.69	20.95	17.26	15.02	23.17	.	25.87	.	22.42	23.42	22.32	.	22.34	21.57	1.07
Oct89	4-1	21.78	20.68	22.90	21.35	.	.	20.96	.	62.07	.	21.23	.	20.41	26.42	2.84
May90	4-2	14.99	15.76	14.94	14.03	13.93	.	36.96	.	14.06	15.11	16.12	.	14.05	16.99	1.60
Oct90	5-1	20.62	15.66	22.06	17.08	22.11	.	18.68	.	20.18	19.98	24.15	.	19.58	20.07	0.62
Mean		21.27	19.28	19.96	18.58	21.26	24.11	24.30	20.67	28.06	21.81	20.65	29.32	20.79		
Standard Error		1.06	1.15	1.51	1.50	1.32	1.44	3.59	4.05	4.21	1.68	1.54	7.43	1.65		

Table 8 (Continued)

		Stations														
		PHF	PHI	PHU	PHJ	PHE	PHST1	PHK	PHST2	PHN	PHW	PHAR	PHST3	PPHR		
	Depth	105	109	113	117	119	120	160	163	166	195	213	212	212		
	Distance	2.1	0.8	3.8	0.5	1.2	1.9	0.6	1.9	0.9	6.4	3	2.3	1.1		
Date	Survey	Fins (Sill + Clay)													Mean	Std. Enor
May88	2-5	.	90.45		89.25	60.26	68.14	90.02	90.27	95.55	94.67	.	91.76	90.32	90.76	1.13
Oct88	3-1	90.26	92.20	86.90	91.94	66.54		.		66.99	92.18	87.82		88.66	69.47	1.17
May89	3-4	85.95	91.33	93.17	93.45	65.71		81.85		82.56	91.69	65.75		62.22	87.37	1.21
Oct89	4-1	09.72	92.56	89.00	90.34	.		87.69		49.87	.	82.42		84.98	83.32	2.73
May90	4-2	93.03	90.51	94.46	93.86	93.58		67.72		91.85	95.94	90.10		89.86	90.10	1.60
Oct90	5-1	91.27	92.62	66.09	90.20	86.64		86.71		65.76	92.21	79.45		85.69	68.29	0.63
	Mean	90.05	91.65	90.32	91.51	68.59	66.14	63.20	90.27	82.39	93.13	65.11	91.76	86.96		
	Standard Error	1.19	0.93	1.05	0.76	1.00	2.74	3,19	4.91	3.85	0.99	1.99	4.12	1.09		
Date	Survey	Clay													Mean	Std. Error
May88	2-5	.	7.17	.	7.51	9.46	8.15	30.26	24.96	1.33	5.57	.	3.61	7.13	11.00	3.71
Oct88	3-1	3.31	3.16	8.65	6.16	4.56		.		37.17	4.03	4.61	.	6.86	6.73	3.59
May89	3-4	6.98	23.09	4.93	6.42	8.45		10.76	.	11.13	8.74	3.20	.	9.71	9.54	1.61
Oct89	4-1	18.46	22.61	16.92	1950	.		21.42	.	12.27	.	19.84	.	20.58	18.83	0.65
May90	4-2	4.52	24.99	22.77	25.99	28.49		19.92	.	27.12	25.07	25.89	.	26.32	25.46	0.61
Oct90	5-1	6.35	30.97	18.54	30.67	14.35		21,96	.	17.76	17.06	14.98	.	1796	19.57	1.39
	Mean	13.92	18.41	13.76	16.36	13.62	6.15	20.87	24.96	17.80	13.10	13.70	3.81	1509		
	Standard Error	2.16	3.07	1.96	2.46	2.61	1.24	5.60	12.61	5.22	2.42	2.57	1.93	2.19		

Table 9. Sediment trap grain dispersion, total organic carbon and carbonate content from the Platform **Hidalgo** vicinity.

		Stations														
		PHF	PHI	PHU	PHJ	PHE	PHST1	PHK	PHST2	PHN	PHw	PHAR	PHST3	PHR		
	Depth	105	109	113	117	119	120	160	163	166	195	213	212	212		
	Distance	2.1	0.8	3.8	0.5	1.2	1.9	0.6	1.9	0.9	6.4	3	2.3	1.1		
Dale	Survey	Dispersion													Maan	Std. Error
May88	2-5	.	1,24	.	1.35	1.22	1.02	0.91	1.72	0.75	1.07	.	1.08	1.05	1.14	0.09
Oct88	3-1	0.96	1.29	1.28	1.36	1.220	.	.	.	1.07	0.60	1.29		1.40	1.16	0.08
May89	3-4	1.52	1.54	0.99	1.21	1.566	.	1.66	.	1.97	1.37	1.46		1.83	1.51	0.09
Oct89	4-1	2.14	2.38	2.01	2.26	.	.	2.395	.	2.17		2.45		2.32	2.26	0.03
May90	4-2	2.39	2.44	2.34	2.44	2.53	.	2.631	.	2.55	2.26	2.46		2.53	2.46	0.03
Oct90	5-1	1.90	2.69	1.75	2.98	1.831	.	2.392	.	208	1.91	2.51		2.17	2.23	0.09
	Mean	1.78	1.96	1.67	1.94	1.73	1.02	1.97	1.72	1.76	1.55	2.04	1.06	1.89		
	Standard Error	0.15	0.15	0.14	0.18	0.15	0.17	0.19	0.13	0.16	0.17	020	0.37	0.14		
Date	Survey	Total Organic Carbon													Mean	Std. Error
May88	2-5	.	2.20	.	2.57	1.83	2.11	2.22	2.02	2.35	2.60	.	2.41	2.50	2.29	0.05
Oct88	3-1	2.32	2.16	2.07	1.68	2.465	.	.	.	2.65	2.45	2.25		2.32	2.26	0.06
May89	3-4	1.67	1.98	1.80	2.16	2.17	.	2.35	.	2.20	1.98	2.50		2.45	2.13	0.05
Oct89	4-1		.	.		.	.	.	.	.						
May90	4-2		.	.		.	.	.	.	.						
Oct90	5-1		.	.		.	.	.	.	.						
	Maan	1.99	2.11	1.94	2.20	2.24	2.11	2.28	2.02	2.40	2.27	2.37	2.41	2.42		
	Standard Enor	0.15	0.06	0.09	0.13	0.10	0.15	0.06	0.08	0.12	0.11	0.12	0.15	0.07		

Table 9 (Continued)

		Stations														
		PHF	PHI	PHU	PHJ	PHE	PHST1	PHK	PHST2	PHN	PHW	PHAR	PHST3	PHR		
	Depth	105	109	113	117	119	120	160	163	166	195	213	212	212		
	Distance	2.1	0.8	3.8	0.5	1.2	1.9	0.6	.9	0.9	0.4	3	2.3	.1		
[illegible]	[illegible]rve	Carbonate (CaCO)													Mean	Std. Error
May88	2-5	.	3.88	.	4.20	4.60	3.42	3.03	4.15	3.53	3.12	.	4.40	3.73	3.80	0.13
Oct88	3-1	3.87	3.48	3.31	4.00	3.07	.	.	.	2.73	2.88	4.10	.	2.46	3.32	0.13
May89	3-4	3.86	3.99	3.45	4.44	3.37	.	4.10	.	6.14	4.15	9.78	.	3.77	4.71	0.49
Oct89	4-1	.	.	.	.	.	.	.	.	.	.	.	.	.	.	.
May90	4-2	.	.	.	.	.	.	.	.	.	.	.	.	.	.	.
Oct90	5-1	.	.	.	.	.	.	.	.	.	.	.	.	.	.	.
	Mean	3.87	3.78	3.38	4.21	3.42	3.42	3.57	4.15	4.13	3.46	6.94	4.40	3.32		
	Standard Error	0.15	0.16	0.13	0.19	0.22	0.23	0.33	0.35	0.52	0.27	2.28	0.30	0.27		

Table 10. Percent coverage of sediment on high and low relief rock[1]

		Low Relief Stations										High Relief Stations				
		J	I	N	R	E	F	U	W			K	u	W		
	Depth	117	107	166	213	119	105	113	195			160	113	195		
	Distance	0.5	0.8	0.9	1.1	1.2	2.1	3.6	6.4			0.6	3.6	6.4		
Date	Survey									Mean	Std. Error				Mean	Std. Error
Oct 86	1-1	36.7	31.8	39.9	37.3	39.4	40.4	26.9	36.3	36.6	1.5	7.6	1.9	3.0	4.2	1.8
Jul 87	1-3	20.8	27.4	28.3	36.6	25.6	26.5	32.0	34.3	29.2	1.8	5.6	7.2	6.6	6.5	0.5
Nov 87	2-3	38.2	11.4	39.4	39.8	35.1	36.6	47.9	37.9	35.8	3.7	10.0	2.7	2.6	5.2	2.4
Oct 88	3-1	31.4	19.6	35.8	29.2	33.9	28.9	48.7	33.1	32.6	2.9	4.1	3.2	4.0	3.6	0.3
May 89	3-4	24.5	24.1	25.1	32.0	25.8	29.7	31.6	40.4	29.2	2.0	2.8	1.4	3.0	2.4	0.5
Oct 89	4-1	27.0	19.9	49.2	35.8	26.7	29.6	47.0	41.8	34.6	3.7	5.6	6.0	6.6	6.1	0.3
Oct 90	5-1	29.8	7.2	35.6	29.3	20.2	16.4	39.1	35.7	26.7	3.9	1.4	1.1	0.1	0.9	0.4
	Mean	29.8	20.2	36.2	34.3	29.5	30.0	39.3	37.4			5.3	3.4	3.8		
	Standard Error	2.4	3.3	3.0	1.6	2.5	2.6	3.2	1.2			1.1	0.9	0.9		

60 pho oq pe surve

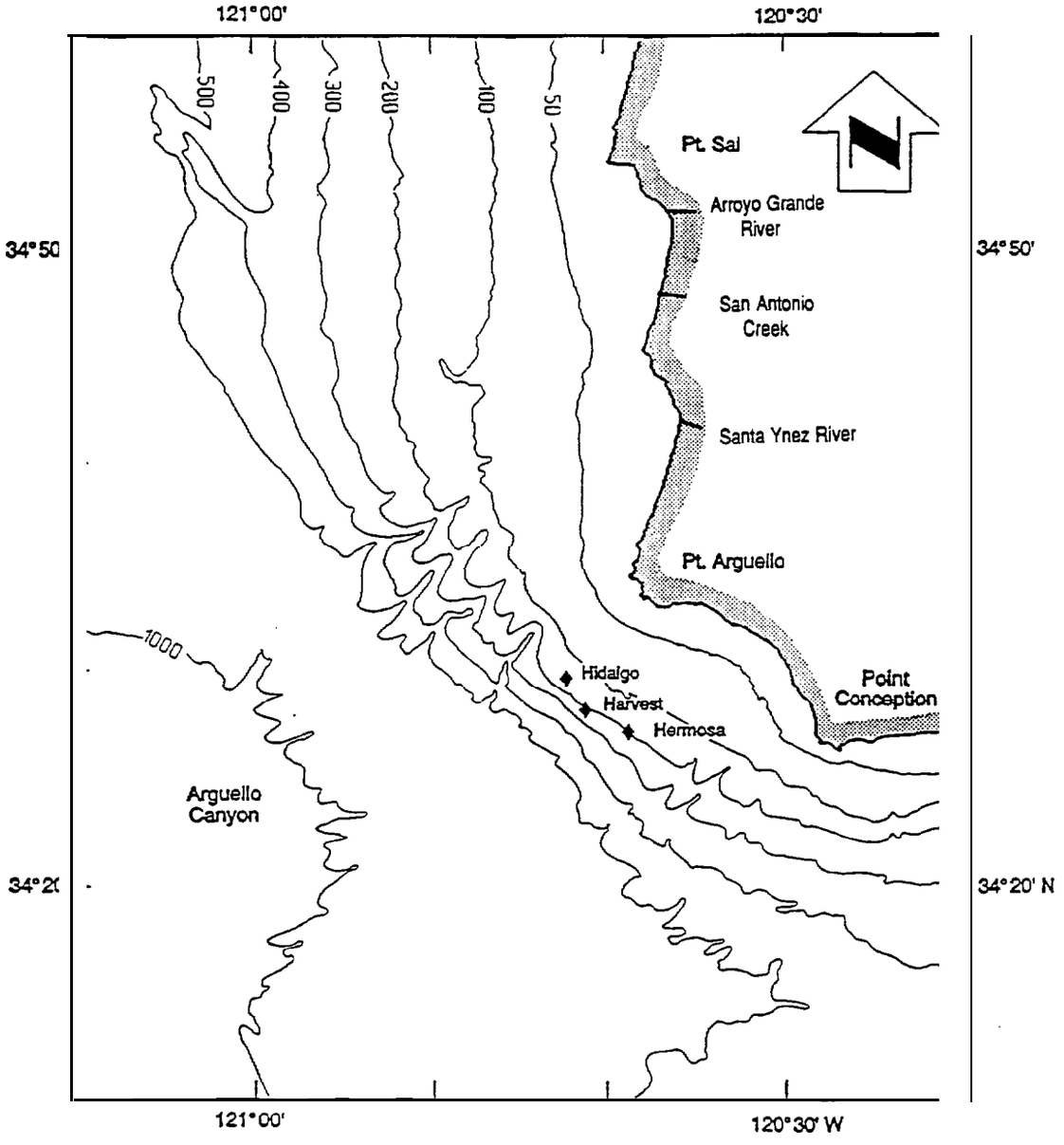

Figure 1. The CAMP region and bathymetry. The three petroleum production platforms lie approximately 12 km offshore of Point Conception.

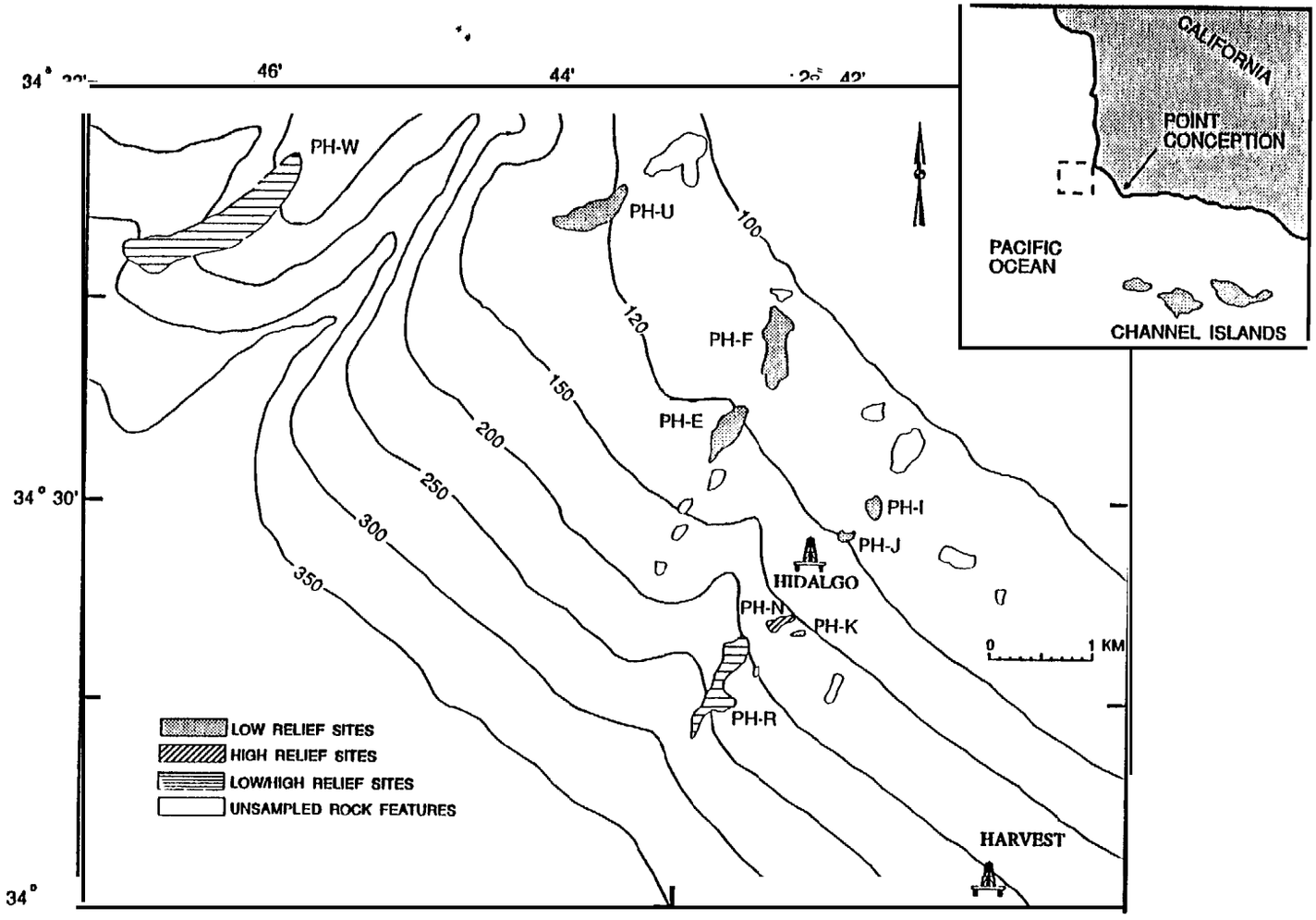

Figure 2. Hard-bottom features sampled in the Santa Maria Basin.

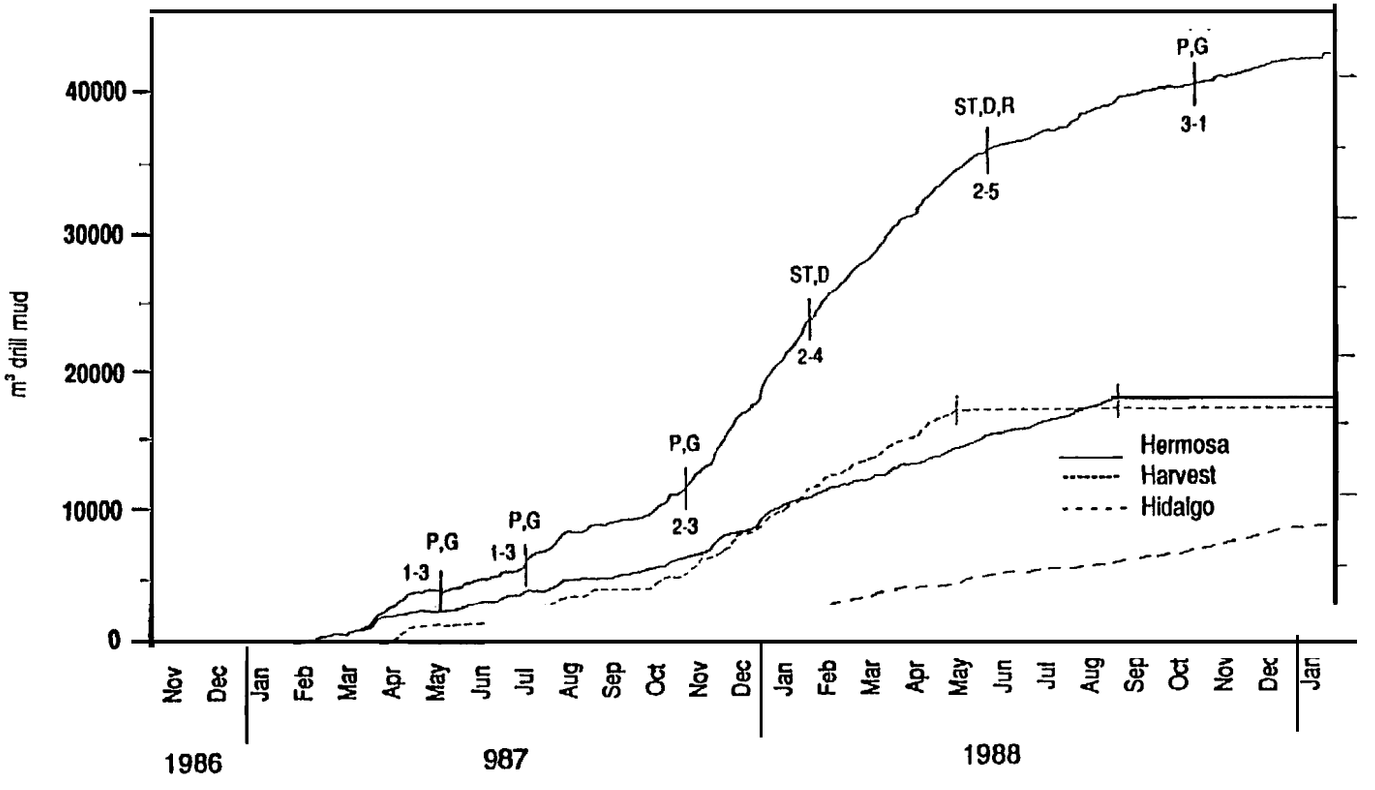

Figure 3. Cumulative and individual drill mud loading curves from Platforms Harvest, Hermosa and Hidalgo.
G = bottom sediment grab; P = hard bottom photoquadrat sampling; ST,D,R = sediment trap, deployment, retrieval

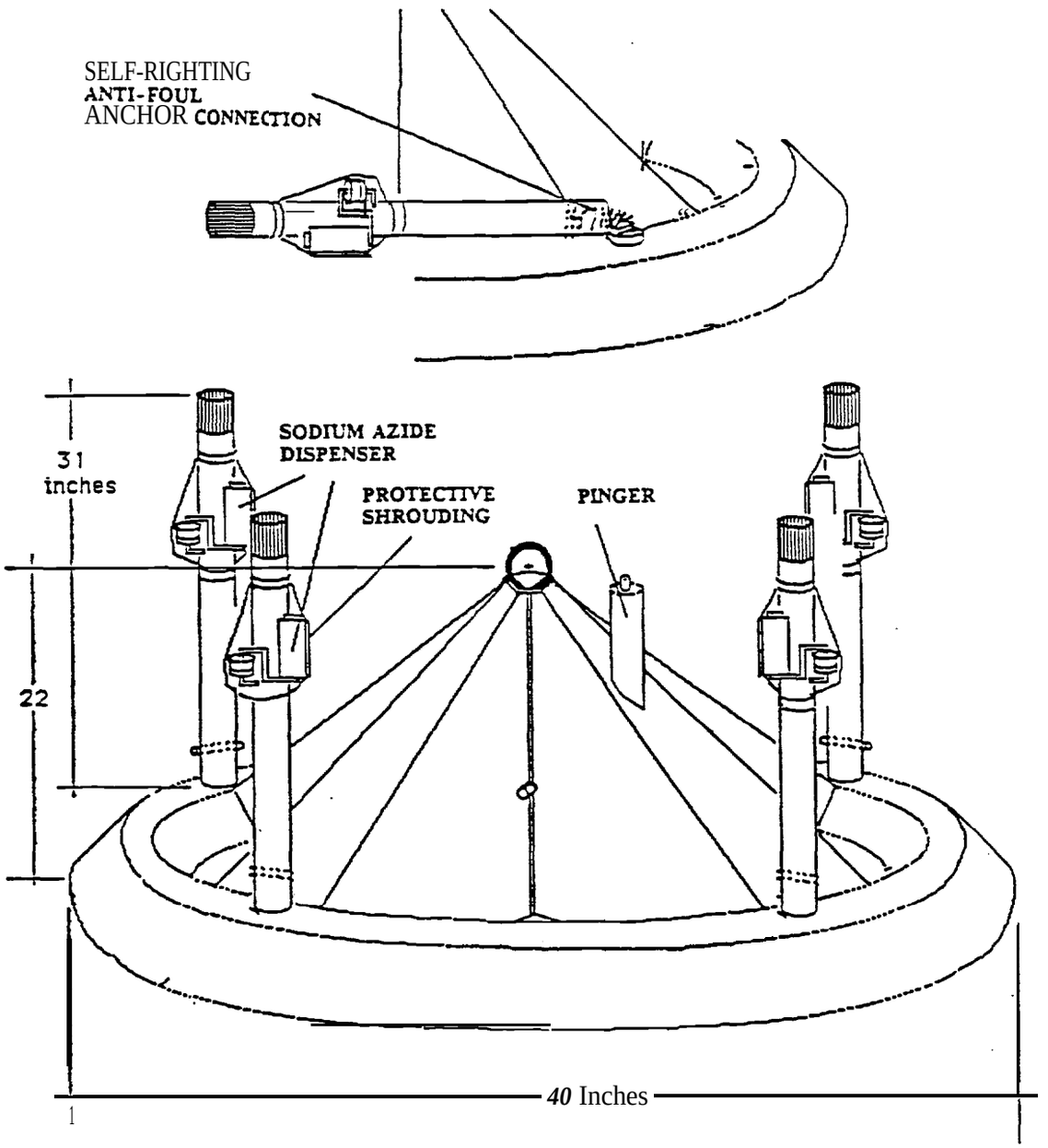

Figure **4.** Sediment trap assembly.

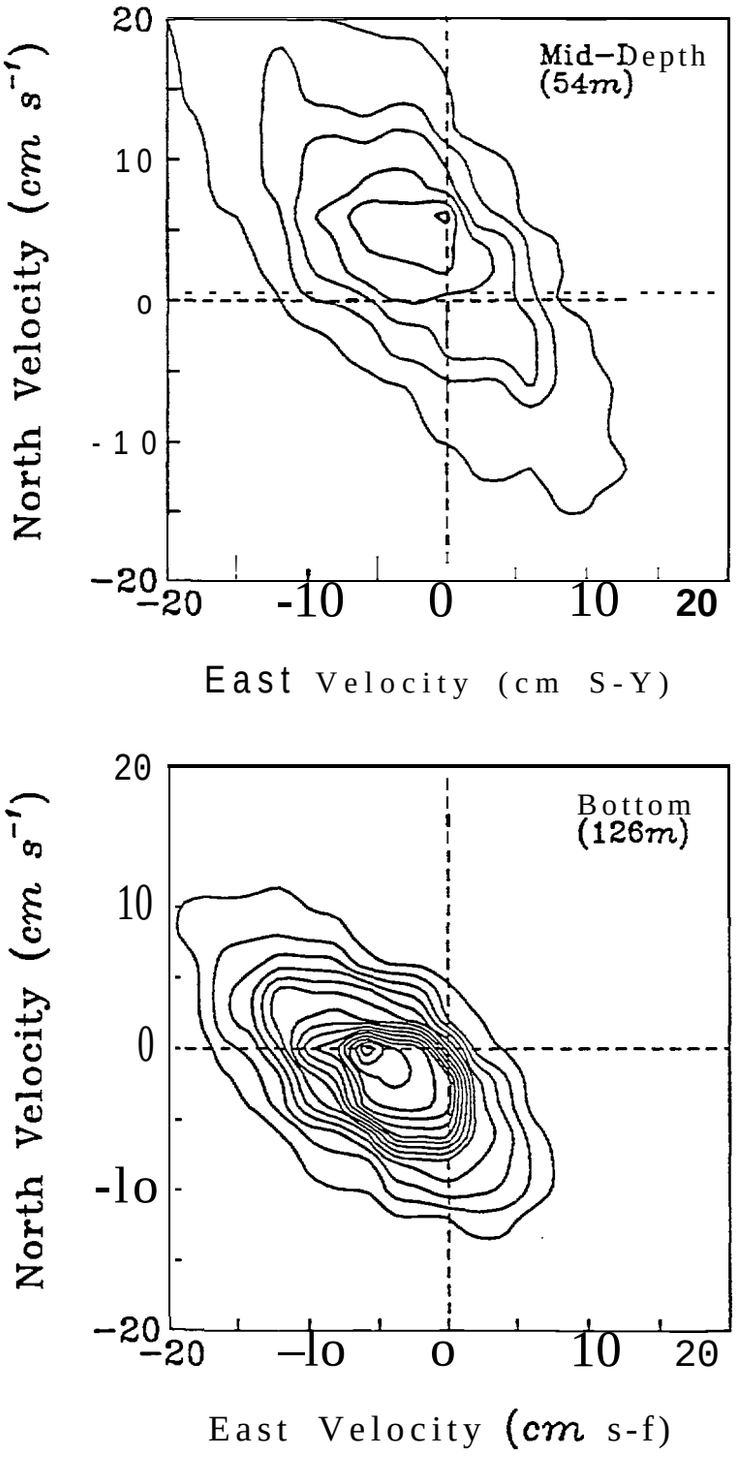

Figure 5. Joint probability of occurrence for current velocity determined from the moored current meters near Platform Hidalgo (bottom = 130 m). The contour interval is 0.05 where the amplitude represents the probability of observing a particular value of north and east velocity with a 1 cm s-' square.

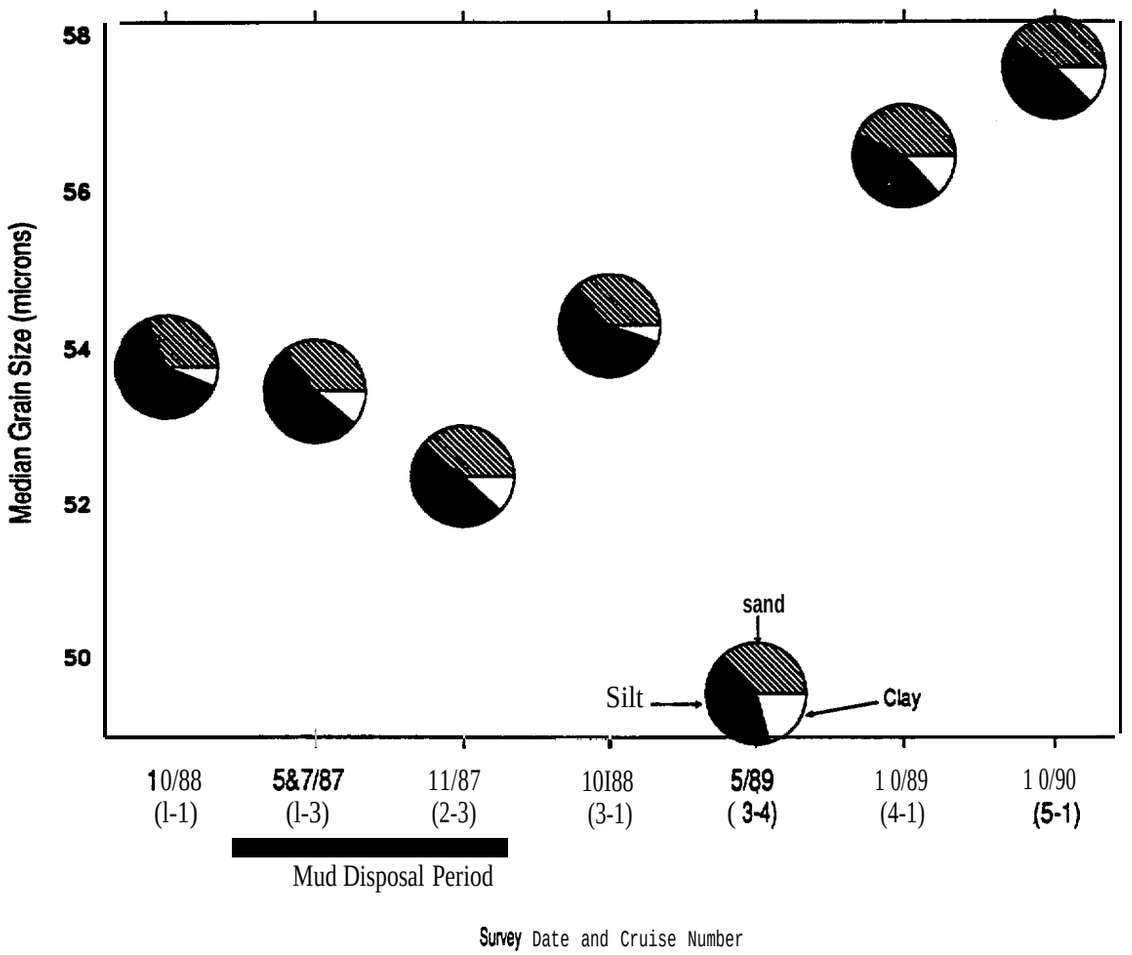

Figure 6. Temporal variation ingrain size from Platform Hidalgo region sediments.

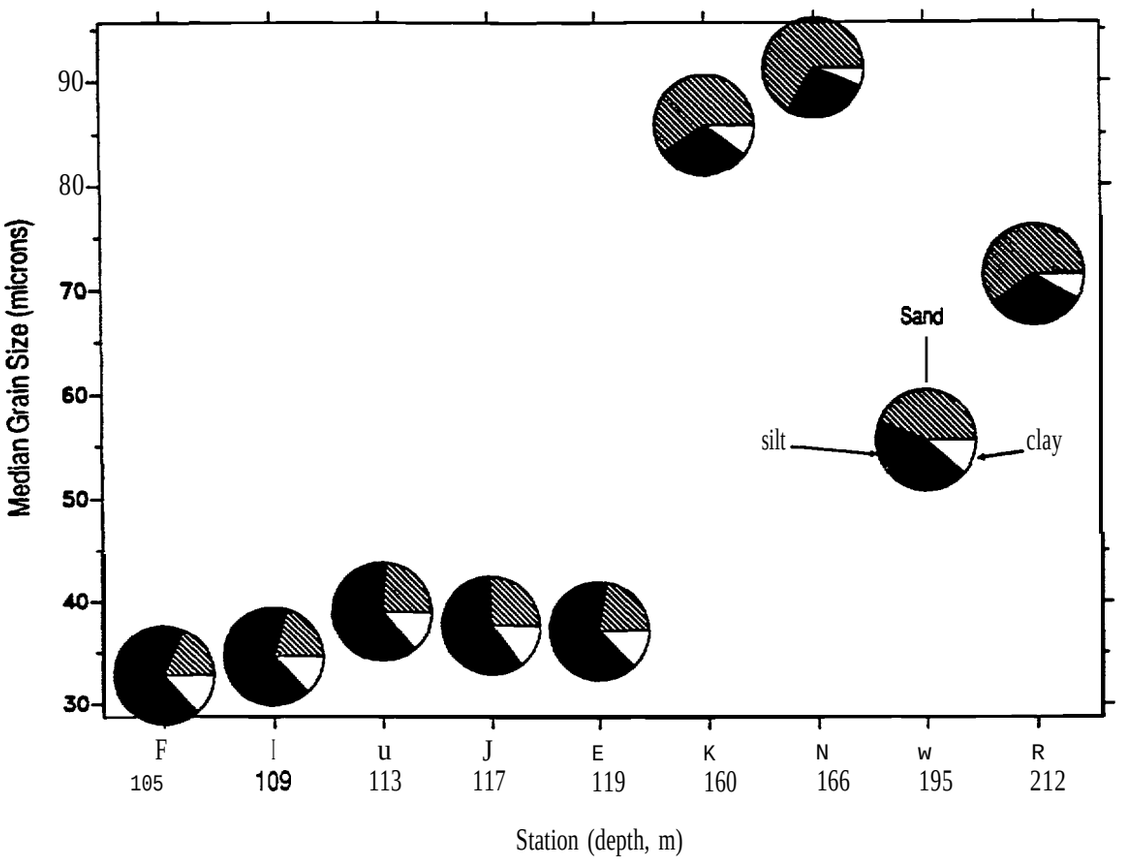

Figure 7. Median gainsize patterns related todepth in the Hidalgo vicinity.

4. LOW-FREQUENCY FLOW VARIABILITY ON THE CONTINENTAL SHELF OFFSHORE POINT CONCEPTION, CALIFORNIA

MARK A. SAVOIE

Kinnetic Laboratories, Inc.
403 West Eighth Avenue, Anchorage, AK 99501

DOUGLAS A. COATS

Marine Research Specialists
3639 E. Harbor Blvd., Suite 208, Ventura, CA 93001

PETER WILDE and PATRICK KINNEY

Kinnetic Laboratories, Inc.
307 Washington Street, Santa Cruz, CA 95060

INTRODUCTION

Four years (December 1986- October 1990) of physical oceanographic time-series observations were collected as part of the interdisciplinary California Outer Continental Shelf Phase II Monitoring Program (CAMP) which was sponsored by the Minerals Management Service (MMS) of the U.S. Department of Interior. This study was designed to assess the long-term impacts on benthic biological communities resulting from oil and gas development in the Santa Maria Basin off the coast of Southern California. Site-specific oceanographic sampling was conducted at two locations: one between Points Conception and Arguello (34°30.3'N 120 °43.1 'W) in a water depth of 130 m, and another offshore of Point Sal (34 °56.2'N120°49.9'W), 43 km to the north in a similar water depth (Figure 1). A single mooring was located at each site and consisted of three vector-averaging current meters (near-surface, mid-depth, and bottom) and a bottom pressure recorder. Data were obtained from December 1986- October 1990 at the southern-most mooring (1-I idalgo) and from December 1986- September 1988 at the northern mooring

(Julius). Site-specific data were augmented with satellite sea surface temperature (SST) imagery, meteorological buoy data, and coastal sea level data to define the spatial scales and forcing mechanisms of the observed currents. Objectives of the sampling were to quantify low-frequency variability in the flow field at each site on scales of days to seasons and to document episodic events that may influence the biology.

BACKGROUND

The four years of moored current-meter data that were collected in support of the CAMP study represent the longest time series of direct measurement of flow on the Point Conception continental shelf, Because of the record length, it was possible to quantify the long-term character of individual flow events identified in previous field investigations. Three flow regimes have been identified in past studies. First, there is a poleward-directed coastal jet that dominates much of the long-term surface flow field. Superimposed are intermittent events of cross-shelf and equatorward flow associated with propagating meso-scale features such as transient eddies and jets. Finally, persistent upwelling is driven by local winds in the region between Points Arguello and Conception. This investigation characterizes the occurrence of these flow features for comparison with biological and chemical variability over the long term. In the process, it also provides insight into local and remote forcing mechanisms responsible for flow variability on time scales of weeks to months.

A sustained poleward flow over the central California continental slope has been identified in climatological maps of geostrophic velocity determined from h ydrographic surveys of the California Cooperative Oceanic Fisheries Investigations (CalCOFI) (Wyllie, 1966). Designated the Davidson Current, the poleward surface flow normally reverses in spring and summer, responding to increased equatorward wind stress (Chelton, 1984). Farther offshore, seasonal cycles in the California Current have been described by Hickey (1979). At distances beyond 100 km from shore, the California Current is southward throughout the year, increasing in strength in spring and summer and weakening in fall and winter when equatorward winds are weakest.

Chelton et al. (1988) obtained direct current observations at 70-m depths on the Point Conception continental shelf and slope as part of the array of moorings from the Central California Coastal Circulation Study (CCCCS). They found that poleward flow was largely sustained throughout the first

half of 1984 when a flow reversal was normally expected. As will be shown in this study, reversals in the poleward shelf flow are relative] y brief and restricted to surface currents.

Poleward flow near Point Conception may be related to outflow from the Santa Barbara Channel which lies to the southeast of the study region (Figure 1). Waters transported from the Santa Barbara Channel are warmer, more saline, and less oxygenated than waters carried southward by the California Current farther offshore (Reid, 1965). Consequently, the frequency and intensity of poleward flow events affect site-specific water chemistry and by extension, the local biology. Point Conception marks the transition between the Southern California Bight and the Central California Coast with a coastline that executes a nearly right-angle change in direction (Figure 1). The westward jet exiting the northern reaches of the Santa Barbara Channel often appears in satellite imagery to separate from the coast and recirculate to the south (e.g., Sheres and Kenyon, 1989). An analysis of drift bottles from 1955 through 1971 also suggested a flow separation at Point Conception, with water exiting the Santa Barbara Charnel often recirculated to the south (Crowe and Schwartzlose, 1972). Nevertheless, Santa Barbara Channel outflow that follows isobaths to the northwest has been observed in acoustic doppler velocity profiles during the 1983 Organization of Persistent Upwelling Structures (OPUS) field program (Barth and Brink, 1987) and during the same year with current meter measurements (Brink and Muench, 1986).

Upwelling is another physical process for which the study region is well known. Infrared satell ite imagery reveals a cold-water plume extending offshore from an upwelling center located between Points Conception and Arguello close to the southern-most current-meter mooring of CAMP (e.g., Svejkovsky, 1988). The OPUS study revealed that the cold-water plumes emanating from this upwelling center generated new primary production over large areas of the shelf (Dugdale and Wilkerson, 1989). Spatial analyses of SST patterns along the northern California coast indicated similar cold water plumes extending from wind-driven upwelling centers anchored to coastal promontories (Kelly, 1985).

Another feature which is evident in the low-frequency coastal flow is a southward-directed coastal jet associated with the California Current that occurs mainly during the summer "upwell ing" season. In this paper we document the possible existence of meso-scale eddies that are advected through the region by the California Current. The two moorings from this study, which were situated on the inshore edge of these warm-core anticyclonic eddies, documented counter-clockwise rotating velocities during these southward flow events.

In recent years there has been increased interest in the interaction of the pressure field with local and regional wind stress forcing and flow measurements on the continental shelf. As part of the Coastal Ocean Dynamics Experiment (CODE) along the northern California shelf, Brown et al. (1987) found that the cross-shelf pressure gradient was in geostrophic balance with the alongshore currents and transport and highly coherent with the regional wind stress. At low frequencies of 0.05 cycles per day (cpd), the alongshore pressure gradient was more important than the local winds in driving the currents, while at higher frequencies (0.2 cpd), local winds were more coherent with the currents. Reid and Mantyla (1976) analyzed coastal tide gauge and steric height data and found that seasonal variations in the California Current were highly correlated with sea level response and that the long-term mean sea level slopes downward toward the north along the southern and central California coast to about 38 "N. Enfield and Allen (1980) and Chelton (1980) analyzed a 25-year period of mean monthly sea level anomalies along the entire west coast and found high correlation of anomalies both between stations and with wind stress. Correlations between sea level and wind stress were found to be lowest along the southern California coast with no significant correlation at San Diego (Enfield and Allen, 1980).

High coherence has been found between wind stress, currents, and sea level records along the California Coast, and sea level records have shown the existence of both forced and free continental shelf waves propagating along the shelf (Halliwell and Allen, 1987; Hickey, 1984; Huyer et al., 1975; and Osmer and Huyer, 1978). Poleward propagation seems to dominate the coastal sea level response in all seasons regardless of the direction of the wind stress (Halliwell and Allen, 1987). Hickey and Pola (1983) found good agreement between observations and the barotropic models of Csanady (1978) and Enfield and Allen (1980) north of Point Conception and a lower correlation to the south extending down to San Diego. Chelton (1984) found the poleward semi-annual varying pressure gradient on the slope to be unrelated to the seasonally-varying wind forcing off Point Conception. The semi-annual pressure gradient was found to be highly coupled with the currents inside the Southern California Bight. In this paper we examine the coupling of the flow near Point Conception and a mooring 43 km to the north with the wind stress forcing and adjusted sea level gradients.

MEASUREMENTS

Continuous measurements of currents, bottom pressure, temperature, and conductivity were made at two sites using moored instrumentation (refer to Figure 1). The Hidalgo mooring was in place from December 1986 through October 1990. The Julius mooring was only deployed during the first two years

of the program (December 1986 through October 1988). The Hidalgo mooring was located just south of a series of submarine canyons and was in a region of fair] y uniform bathymetry (130-m water depth) with an offshore slope of 1:50 out to the shelf break at the 150-m isobath, then increasing to a slope of 1:10. The Julius mooring was located 43 km to the north along the same depth contour and at the shelf break with a slope of 1:100.

The continuous time-series measurements were obtained from one mooring at each site. Each mooring consisted of three Neil Brown Smart vector-averaging current meters (top, middle, and bottom), equipped with conductivity and temperature sensors, and a SeaData 635-11 bottom pressure recorder equipped with a high-precision Pares Scientific 'Digi-Quartz' pressure transducer (Figure 2). To ensure maximum data recovery and to monitor the integrity of the mooring instrumentation, data from the current meters were telemetered to shore via an ARGOS-satellite link. The data were also internally stored by each meter. Currents were sampled at 0.5-s intervals, vector-averaged over a 5-rein period, and recorded every 30 min. One instantaneous reading of temperature and conductivity was taken every 30 min. Bottom pressure data were recorded every 7.5 min for tidal and subtidal information, with a burst averaging every 6 h at 1-s intervals with 1024 samples/burst for long- period ($\tau > 8$ s) wave information. Bottom pressure data were obtained at the Julius mooring during only the fourth mooring deployment period (May 1988 through September 1988), at which point the instrumentation was lost as a result" of commercial fishing activities.

Moorings were picked up and redeployed at six-month intervals over the four-year program. During each of these cruises, supplemental hydrographic information was obtained at each mooring location with a conductivity, temperature, and depth (CTD) meter equipped with pressure, temperature, conductivity, pH, and transmissivity sensors.

Satellite SST imagery was obtained for each day of the four-year period when weather conditions allowed and correlated with the site-specific measurements to better define the spatial extent of water movement. Detailed anal yses of the satellite SST anomalies are presented in Bernstein et al. (1991). Measurements collected as part of this study were augmented with local offshore atmospheric and oceanographic buoy data and coastal sea level data obtained from the National Oceanic and Atmospheric Administration (NOAA); surface atmospheric pressure field information was provided by the National Marine Fisheries Service (NMFS) as determined by the Fleet Numerical Weather Central.

DATA ANALYSIS

Current and wind velocity time series were pre-processed by application of filters to eliminate high-frequency noise. A low-pass Fourier-transform filter described by Forbes (1988) and Elgar (1988) was used. Three optimal tapering coefficients were selected from results of iterative analyses performed by Rabiner et al. (1970). Low-pass filtering was utilized to eliminate frequencies above 0.333 cph (cycles per hour) or periods greater than 3 h. Spectral energy at the higher frequencies was substantially lower than at other frequencies; consequently, the signal-to-noise ratio was lower. To eliminate these potentially unreliable data, only frequencies below the low-pass filter were retained for further analyses; thus, fine-scale turbulence was removed from the data while still retaining motions associated with internal waves, inertial motion, and tides.

To examine flow-field events, the time series of wind, current, and temperature were further filtered with a subtidal low-pass filter having a cutoff near the frequency of 0.025 cph or a period greater than 40 h. The vector velocity analyses that were low-pass filtered to eliminate tidal-inertial motions retained the long-period flow variability and were designated as subtidal flows.

Wind stress was examined to determine the influence of winds on current dynamics and sea level variations. Wind speed and direction were obtained from three National Data Buoy Center (NDBC) buoys located in the study region (Buoys 46011, 46023, and 46025; refer to Figure 1). Winds were adjusted to a common 10-m level above the sea surface to conform to the standard frequent] y used in nondimensionalization of wind parameters. The formalism applied follows that of Liu and Schwab (1987), Liu et al. (1979), and Liu and Blanc (1984) and employs an estimate of the Monin-Obukhov stability length.

Bottom pressure and coastal sea level data were processed to obtain the adjusted sea level (ASL, or alternately called synthetic subsurface pressure) for each location after the detailed methods described by Brown et al. (1987). Bottom pressure was first pre-processed to correct for the temperature sensitivity of the pressure sensor itself by utilizing the external temperature recorded by the bottom pressure gauge. Density anomalies were calculated for each of the three current meters from the temperature time series and a constant salinity of 33 parts per thousand (ppt). Conductivity time series were not utilized to calculate density anomalies due to the low precision and biofouling of the sensors, The internal pressure was then calculated by integrating the density anomalies over the depth of the mooring assuming the

density derived from each of the three current meters was representative of the depths surrounding the current meters (top: 0-40 m; middle: 40-80 m; bottom: 80-130 m). The total internal pressure difference anomaly contribution to the bottom pressure was then removed from the bottom pressure time series to obtain the ASL.

Coastal sea level data were processed by first converting to an equivalent pressure utilizing a constant σ_t (25.0) for each of the three coastal stations (Monterey, Port San Luis, and Rincon Island). The ASL for each station was then determined by adding the atmospheric pressure variation to remove the inverted barometer effect. The ASL time series derived for the bottom pressure and coastal sea level stations were low-pass filtered with a Doodson tidal filter and decimated to 6-h intervals.

Satellite images consisted of a square, 280 km on a side, centered on 35°N 121 "W and encompassing the western portion of the Santa Barbara Channel, Points Conception and Arguello, and the area northward to Point Sal. All advanced very high resolution radiometer (AVHRR) data from the NOAA-satellite afternoon overpasses (overpass time approximately 1330 PDT) were examined using available quick-look imagery to select those images having sufficiently cloud-free views of the sea surface. For those overpasses selected, three of the five spectral channels of the AVHRR were extracted, namely Channel 2 (1.0 μm) to identify clouds, and Channels 4 (11 μm) and 5 (12 μm) for SST. A detailed description of analyses and results of the satellite SST data obtained by this study is contained in Bernstein et al. (1991).

RESULTS AND DISCUSSION

Seasonal Variability

Because of the four-year duration of the time series at Hidalgo, seasonal flow cycles on the continental shelf can be quantified. Previous seasonal analyses have relied on hydrographic measurements collected farther offshore as part of CalCOFI. Past direct measurements of flow on the Point Conception continental shelf, including CCCCS and OPUS, have been too brief to adequately resolve the seasonal variability. In addition to specifying the flow on annual time scales, determination of seasonal cycles is important for defining shorter-term meso-scale variability. For example, the amplitude of annual near-surface temperature fluctuations is comparable to the meso-scale variability (Figure 3). Thus, the presence of these fluctuations masks variability associated with upwelling events which are also of interest in this study. Also, if the seasonal cycle is not removed, adjacent observations are not statistically

independent and the degrees of freedom must be reduced along with the statistical reliability of time-series correlations.

Harmonic analyses similar to those used to process tidal records (Dennis and Long, 1971) were utilized to quantify the large-amplitude annual cycle in temperature and weaker seasonal cycles in flow and wind fields. This is necessary because of the uneven temporal distribution of data and the limited realizations of seasonal cycles in the four-year data set. Because of data gaps, frequency-domain analysis cannot resolve this longer-term variability. Similar] y, the few realizations prevent determination of the seasonal signal by monthly averaging, an approach applied to much longer-term CalCOFI data sets (Wyllie, 1966). Instead, we perform a multiple regression with a model of the form:

$$\hat{y}(t) = A_0 + \sum_{j=1}^{N} A_j \cos(f_j t - \phi_j) \qquad (1)$$

where:

t is time in days;

N is 1 for annual and 2 for semi-annual regressions;

f_j are discrete frequencies given by $2\pi j/365.26$ radians per day;

A_0 is the regression coefficient for the mean amplitude, and A_j is the regression coefficient for the annual and semi-annual amplitude, where j is 1 or 2, respectively.

ϕ_j is the phase regression coefficient in radians for annual and semi-annual regressions, where j is 1 or 2, respectively.

Confidence limits established on the amplitude coefficients serve to test the statistical significance of annual and semi-annual signals in the time series. If 95-percent confidence limits on all coefficients are significantly different from zero, then the full regression with $N=2$ defines the long-term seasonal cycle. If the regression is not statistically significant, then a purely annual cycle is fit to the time series with N= 1 in (l).

As discussed above, the presence of a strong seasonal cycle reduces the statistical reliability of correlation estimates. Similarly, narrow-band processes in the residuals of (1) reduce the number of purely independent observations and increase the effective size of confidence limits. To account for this, we

define an equivalent number of degrees of freedom (Davis, 1977) based on the number of independent observations. These are established from the ratio of total record length and correlation time scale following Beardsley et al. (1985).

Table 1 presents the results of the regression analysis, The strong annual signal in surface temperature decays with depth and generates the seasonal thermocline ('Figure 3). With the summer increase in sea surface insolation, higher mixed-layer temperatures in late summer and early fall are coupled to the developing thermocline. Some of this seasonal downward flux of heat reaches the bottom, since a small but statistically significant annual variation is evident there. Although the signal amplitude is reduced by a factor of 3 at the bottom, it is consistent with the monotonic increase in time lag. Thus, the annual peak in temperature is progressively later in the year with increasing depth. At the shallowest buoy depth, peak annual temperatures are achieved around July 22, whereas temperatures at the bottom of the mooring reach their maximum at the end of November.

The pattern of annual temperature maxima during the October to November time period and minima during the April to May time period is substantially different from that seen on the shelf of Washington, Oregon, and Northern California. Strub et al. (1987a) found the annual temperature maxima and minima off Washington and Oregon to lag those in the south by 2-3 months. The temperature structure in the CAMP study region more closely follows the annual heating and cooling cycle (since the currents are poleward throughout the year except for short periods of reversal), whereas in the more northern latitudes, currents exhibit an annual cycle of reversal with equatorward flow during the summer months as seen by Lentz and Chapman (1989) and Strub et al. (1987a). This annual cycle results in southward advection and upwelling of colder water onto the shelf during the summer months causing a temperature minima 2-3 months later than that seen offshore Point Conception.

The lack of statistically significant semi-annual variability in the temperature and wind time series contrasts with currents (Table 1). This probably is a result of the low signal amplitude rather than an artifact of the lower equivalent degrees of freedom. The F-distribution used to establish the confidence limits is not particularly sensitive to changes in the degrees of freedom across the range reported in Table 1. Nevertheless, these differences provide insight into the different time scales associated with temperature and flow fluctuations.

With nearly identical record lengths, the differences in equivalent degrees of freedom arise from differences in time-lagged correlation functions (Figure 4). Temperature variability has a much longer time scale (-24 days); nearly four times longer than along-shelf flow (-6 days) and eight times longer than cross-shelf flow (-3 days). These along- and cross-shelf time scales of flow match those determined by Davis (1985) from moored current meters on the inner-shelf off northern California. The similar time scales for shelf flow suggest similar eddy field statistics for the two regions. In this study, time-lagged correlation of temperature indicates that meso-scale temperature features are much longer-lived than the flow field features.

Some low-frequency departures from the annual harmonic are evident in the temperature field (Figure 3). This inter-annual variability is primarily reflected by anomalously high temperatures in the summer and fall of 1987. These departures maybe related to the mild El Niño conditions that induced global climate variations at that time (Kousky and Leetmaa, 1989). Because of larger meso-scale variability in along-shelf winds and currents, similar inter-annual variation is not clearly evident in Figure 5.

Low-frequency winds ($\tau <$ 40 h) are nearly always directed equatorward. A phase lag of 341 days indicates that the weakest winds are observed near the beginning of December, and the strongest winds are observed in June. This variability is consistent with canonical views of the wind variability in the region (Hickey, 1979). This annual variability in wind stress approximate] y corresponds to the variabil ity in along-shelf surface currents (Figure 5). In the spring and early summer when equatorward winds are strongest, the largely poleward surface currents reverse for about two months. Although currents at mid-depth (54 m) and at the bottom (126 m) do not exhibit a clear reversal, they do weaken around the same time. In contrast to other time series, along-shelf current velocity exhibits a weak but statistically significant semi-annual variability ('Table 1). The addition of the semi-annual component serves to extend the duration of poleward surface currents and limit the reversal time, At the bottom, only the annual signal is resolved.

Four years of adjusted sea level variations are presented in Figure 6 for the three coastal stations (Monterey, Port San Luis, and Rincon Island) and the Hidalgo mooring at Point Conception, along with the Hidalgo internal pressure, along-shelf ASL variations, and the atmospheric pressure at Point Conception (NDBC Buoy 46023). Seasonal fluctuations of approximately 0.1 dbar (-1 m) can clearly be seen in all of the ASL records. Adjusted sea levels were lowest during the period of March through

June during all four years of the study, corresponding to the annual relaxation in the poleward shelf flow and southward flow reversals due to strengthening of the southward alongshore wind stress along the California Coast and at Point Conception (Figure 5). Adjusted sea levels were highest during the August through January period, corresponding to a relaxation in the equatorward alongshore wind stress and poleward flow on the shelf as evidenced in the current meter and local wind stress records (Figure 5). The seasonal ASL cycle is consistent with the general pattern of poleward flow on the shelf with southward flow reversals and upwelling events along the California Coast during the spring as reported by Chelton (1980), Enfield and Allen (1980), Hickey (1979), and others.

Annual internal pressure fluctuations due to changes in water density were small: c 0.01 dbar and 180° out-of-phase with the ASLS as a result of the annual heating and cooling cycle (Figure 6). This annual signal is consistent with steric heights being in-phase with ASLS near the coast as seen by Reid and Mantyla (1976). Seasonal atmospheric pressure variations at the Hidalgo mooring at Point Conception were highest during the period of December through February and lowest during July through September, lagging the annual ASL signal by approximately three months. A similar pattern was seen by Reid and Mantyla (1976) at La Jolla in the long term record (1950-1969).

Seasonal variations in the alongshore pressure difference were determined by subtracting the ASL variations between the coastal sites (Figure 6). No attempt was made to determine the absolute pressure gradient between sites due to the unknown height of each tide station. The annual alongshore difference signal between Monterey and Port San Luis was found to be highest during the months of December through April and lowest during June through September, similar to that found by Hickey and Pola (1983) between Port San Luis (Avila, 35°N) and San Diego (33°N). Long-term mean steric height data from Reid and Mantyla (1976) indicate a downward slope between Port San Luis and Monterey of approximately 0.04 dbar (4 dyn cm) on the shelf, which would result in a poleward-directed pressure gradient for most of the year that would accelerate the poleward shelf flow. The alongshore pressure difference between Port San Luis and Rincon Island exhibited only small annual variations.

Spring Transition

Oceanographic conditions on the shelf off the coast of Washington, Oregon, and Northern California change rapidly from winter to summer conditions as temperatures and sea levels drop and currents shift from northward to southward corresponding to a shift in wind stress from northward to southward (Strub

et al. 1987b). This "spring transition" was found to be less pronounced south of 37 'N where wind stress was southward throughout the year except for short periods of reversal. Strub et al. (1987b) found the sea level to decrease more gradually at the southern sites near Point Conception with the drop in sea level progressing from south to north for the periods of 1971-75 and 1980-83.

Adjusted sea levels at Monterey, Port San Luis, and Rincon Island exhibited noticeable decreases (10-15 mb) during the years of 1987, 1988, and 1990, but not during 1988 during the period of March through May (Figure 6). Water temperatures at Hidalgo and at NDBC Buoy 46023 dropped 1-2 °C during the same time periods (Figure 3). Local wind stress and currents at Hidalgo did not exhibit any noticeable "spring transition" other than a general increase in southward wind stress and a decrease in poleward currents during the spring time frame (Figure 5). During the Northern California Coastal Circulation Study (NCCCS) pilot experiment, Magnell et al. (1990) found that during mid-March of 1987, the northward wind stress reversed to southward and the adjusted sea level decreased dramatically along the Northern California Coast. Decreases in adjusted sea levels during 1987 corresponding to the "spring transition" at Monterey, Port San Luis, and Rincon Island preceded the northern NCCCS sites by 2-3 days (Figure 6). Based on the low correspondence between local winds and sea level response with respect to the spring transition and the high correlation with the Northern California spring transition during 1987, it would seem that the spring transition in the Point Conception region is being remotely forced by large-scale weather systems with alongshore length scales of 500-1000 km.

Upwelling

Considerable meso-scale wind variability occurs at 2-5-day periods offshore Point Conception. This contrasts with coastal regions in the Santa Barbara Channel which are dominated by diurnal variability (Caldwell et al., 1986). These fluctuations in the weather band that drive persistent upwelling in the region between Points Arguello and Conception were also seen by Atkinson et al. (1986). This upwelling increases rates of new biological production (Dugdale and Wilkerson, 1989) and affects the distribution of water-mass properties (Reid, 1965). One obvious manifestation of upwelling is locally depressed sea surface temperature. Upwelling often causes the formation of cold-water plumes extending offshore from Point Conception (Svejkovsky, 1988).

In this study, we quantify the degree of coupling between the local wind field and upwelling over the long-term with cross-spectral anal ysis of sea surface temperature and wind stress. As described above,

the strong seasonal signal in temperature can mask low-frequency variability associated with upwelling events. Consequent y, the annual signal specified in Table 1 is removed prior to cross-spectral analysis.

Results for both the NDBC meteorological Buoy 46023 and near-surface Hidalgo mooring temperatures are similar (Figure 7). In addition to coupling at diurnal and semi-diurnal tidal frequencies, temperature and wind stress exhibit statistical y significant coherence at periods longer than about two days (three days for mooring temperature). Negative phase lag indicates that the wind variability leads the temperature variability as expected for a ph ysicall y realizable linear system, Phase lags for NDBC buoy temperatures near 60" at 4-day periods (-0.01 cph) indicate that wind perturbations precede temperature changes by about 17 h. Maximum transfer function amplitudes, near 0.6, indicate that a 1 dyn cm^{-2} pulse in equatorward wind stress induces a 0.6°C decrease in sea surface temperature. Figure 8 shows a typical wind-induced upwell ing event. The time lag is close to one day and the temperature response is on the order of 1 "C, in approximate agreement with the cross-spectral analyses.

Remotely-Forced Flow

Near-surface current velocities at subtidal ($\tau >$ 1 day) periods are strongly polarized along isobaths. This is evident from the statistically-significant measures of directional stability derived from rotational auto-spectra (Figure 9). At the Hidalgo mooring, principal directions are stable across a broad subtidal frequency band. Principal directions are measured clockwise relative to true north and there is a 180° ambiguity in their specification. Consequently, Point Conception current directions near 150° (330°T) closely correspond to the along-shelf orientation of local isobaths near 324"T. Similarly, subtidal currents at the Julius mooring at Point Sal are consistently directed toward O^{o}T (1 80°) and aligned with the north-south orientation of the coastline and shelf.

Rotary cross-spectral anal ysis (Mooers, 1973) provides a convenient approach for quantifying rotational motions that are anticipated in a vigorous eddy field. Energetic meso-scale features near Point Conception are evident in satellite imagery (Sheres and Kenyon, 1989) and direct measurements (Barth and Brink, 1987). Rotary auto-spectra (Figure 9) and cross-spectra (Figure 10) summarize the energy distribution of these transient phenomena over the long-term at the two mooring locations. There is a considerable y higher fraction of rotational energy (-40%) at subtidal periods at Hidalgo than at Julius. This additional rotational energy arises from clockwise motions as indicated by elevated clockwise spectral levels. The additional clockwise energy at Hidalgo is the result of eddies being formed on the

lee side of Point Conception during Santa Barbara Channel outflow events as seen by Bernstein et al. (1991). At Julius, the clockwise rotational energy is nearly equivalent to counter-clockwise motions.

It is the counter-clockwise rotating components, however, that are coherent between the two mooring sites. Figure 10 shows that clockwise co-rotating components are not significantly coherent except perhaps at the lowest frequencies. In contrast, counter-clockwise co-rotating components exhibit significant coherence across a broad subtidal frequency band at periods longer than 100 h. The negative phase associated with this subtidal rotary cross-spectrum indicate-s that the counter-clockwise motions at Julius lead the motions at Hidalgo. The 450 phase at periods of 500 h implies a time lag of 2.6 days. Over the 43-km separation distance between moorings, the inferred propagation speed is approximate] y 20 cm s-'. This propagation speed is somewhat faster than the 2-4 cm S-l determined by Davis (1985) for a single cold-core eddy in the CODE region. Also, the counter- clockwise rotation is more suggestive of southward-propagating warm-core eddies. Motions reminiscent of a south ward-propagating onshore meander or frontal eddy begin at Julius with southwestward flow that rotates around to the east, eventually dissipating along a northwestward direction. The process is repeated a few days later at Hidalgo to the south.

Coastal ASL Variability

Subtidal variability in ASLS was examined by spectral and cross-spectral analyses over the four-year period of record. Seasonal signals were removed prior to analysis. Auto-spectra and autocorrelations for each of the three coastal ASL records are presented in Figure 11. Peaks in the individual spectra are evident at frequencies of 0.016 cpd (τ=62 days) and 0.073 cpd (τ= 13.7 days) with most of the energy at frequencies < 0.4 cpd (τ > 2.5 days). Time-1 agged autocorrelations indicate time scales of -20 days, which is 3-4 times longer than along-shelf flow and similar to that found for the temperature variability (Figure 4). Cross-correlations between coastal ASLS were relatively high: 0.75 for Monterey vs. Port San Luis and 0.68 for Port San Luis vs. Rincon (Figure 12). Coastal ASLS were found to be highly coherent at frequencies < 0.1 cpd (τ> 10 days) with significant but less coherence at higher frequencies. A large peak in the coastal ASL coherence spectra is evident at 0.07 cpd which probably corresponds to the lunar fortnightly tidal constituent (τ= 13.66 days), since wind stress forcing was not evident at that frequency (Figure 12). Port San Luis and Rincon ASLS were found to be in-phase (O lag) at maximum cross-correlation. Monterey lagged Port San Luis by 6 h, indicating a northward propagation. The northward propagation speed (680 cm S-l) is approximate] y 40% higher than the

propagation speed of a free-first mode shelf wave (490 cm S-l, Brink, 1982) but consistent with speeds found by Hickey (1984) for the Pacific Northwest.

The maximum cross-correlation between the alongshore differences was low (0.2) with the Port Sari Luis-Rincon difference leading the Monterey-Port San Luis difference by 1.75 days (Figure 13). The coherence between the two along-shelf pressure differences was only marginally significant at periods greater than 15 days. The coherence levels at periods between 1.2 and 5 days ranged from 0.2 to 0.7 and were for the most part 180° out-of-phase.

Wind-Driven Flow

In addition to remote forcing, a portion of surface current is linearly related to local winds at Hidalgo. Along-shelf winds and surface currents exhibit statistically significant coherence levels across a broad subtidal frequency band (Figure 14). However, coherence levels are rather low, near 0.2, and it is only because of the long record length that the coupling can be resolved. This may account for the apparent lack of coupling between winds and currents offshore Point Conception determined from shorter duration time series of the CCCCS (Chelton et al., 1988). Cross-shelf flow is not significant] y coherent with cross-shelf wind stress at any subtidal frequency.

At periods between 30 and 300 h, phase is largely negative and wind stress variability leads along-shelf currents. The -600 phase for 4-day oscillations implies a 17-h time lag between winds and currents, identical to the relationship between wind stress and temperature. At periods longer than 300 h (12.5 days), the phase is positive and inconsistent with a simple physical relationship between local wind and current. Instead, it is possible that remotely-forced propagating coastal] y-trapped waves are responsible for current variability at the lowest frequencies. Because of large-scale coherence in the wind field, it is difficult to separate local wind forcing from long-wave modes in the site-specific analysis described here. Based on an analysis of along-shelf current velocity in CODE, Denbo and Allen (1987) have suggested that remote forcing becomes increasingly important at lower frequencies ($\tau >$ 170 h).

The coherence between along-shelf wind stress and mid-depth (54 m) currents is, however, not statistically significant in this lowest frequency band (Figure 15). In the weather band, between 1 and 12 days, transfer function amplitudes and phase lags are similar to cross-spectra between wind-stress and surface currents. In contrast, the coupling between wind stress and bottom currents is only marginally

significant over a narrow portion of the weather band (Figure 16). As with the cross-spectra at other depths, the cross-shelf flow does not exhibit any clear relationship to the wind stress. It is more likely that cross-shelf exchange is driven by remotely forced eddies and jets that are responsible for the large fraction of rotational energy at Point Conception (Figure 9).

Alongshore winds and ASL variations at Port San Luis had a maximum cross-correlation of 0.5 with winds leading the ASL by 6 h (Figure 12), The coherence for periods greater than 35 days was low. At periods of 3-30 days, coherence levels were about 0.5. The low coherence between Port San Luis ASL and wind stress at lower frequencies is similar to that seen between the wind stress and currents, which would suggest that remotely-forced winds or propagating coastal] y-trapped waves may be driving the currents at the lower frequencies.

Cross-Shelf ASL Variations and Flow

The five-month period of December 1987 through April 1988 was examined to determine the degree of forcing between currents and ASL variations at Hidalgo (Figure 17). Two low pressure systems that passed through the area are highlighted in the time-series plots. The first occurred during mid-December 1987 causing strong poleward flow at the surface and mid-depth for Julius and Hidalgo respectively, and a corresponding increase in the cross-shelf ASL difference between Hidalgo and Port San Luis. The second low pressure system had the opposite effect, currents were directed equatorward and ASLS dropped along with a decrease in the cross-shelf ASL difference.

Middepth (54 m) currents at Hidalgo were found to be highly coherent with the cross-shelf ASL difference between Port San Luis and Hidalgo across a fairly broad band of frequencies except for a narrow band at 0.3-0.5 cpd (2-3 days) and at frequencies c 0.065 cpd ($\tau >$ 15 days) (_Figure 18). The maximum correlation was 0.4 at O lag with most frequency bands being in-phase. In contrast, the coupling between the cross-shelf ASL difference and Hidalgo bottom currents was only marginally significant except at low frequencies > 0.65 cpd, which correspond with those frequencies where coherence with the mid-depth currents was low. Thus, it would seem that the cross-shelf ASL difference at Hidalgo accounts for much of the low-frequency signal in the bottom currents but not in the mid-depth currents.

The cross-shelf ASL difference was also highly correlated with the near-surface (12 m) currents at the Julius mooring with a cross-correlation of 0.63 (Figure 18). Coherence between the alongshore currents at Julius and ASL difference was found principally at the lower frequencies (< 0.4 cpd) or periods greater than 2.5 days. In contrast, the coupling between the bottom currents and cross-shelf ASL differences was onl y marginally coherent at any frequency.

COnClUSiOnS

The measured wind stress in the Point Conception region is directed equatorward throughout the year with only short periods of reversal. Wind stress is strongest in the spring and weakest in the fall, exhibiting annual but no semi-annual signal, whereas Strub et al. (1987a) found evidence of a semi-annual signal in the measured wind stress at the same latitude. Surface currents are poleward throughout the year, reversing in the spring when southward-directed wind stress is maximum and exhibiting both an annual and semi-annual signal of similar magnitude. Middepth and bottom-depth currents were also directed poleward throughout the year, with the annual signal four times as strong as the semi-annual signal at mid-depth and only an annual signal in the bottom currents. A strong seasonal thermocl ine developed each year during late summer and fall, 1-2 months earlier than that seen off the coast of Washington and Oregon. Anomalously high (- 2°C) surface and mid-depth temperatures were observed in 1987, reflecting the mild El Niño conditions during that year as seen by Kousky and Leetmaa (1989).

The Point Conception region is well known as an area of persistent upwelling. In this study, a 1 dyn cm^{-2} pulse in equatorward wind stress induced a surface temperature response of approximately -1 “C with a lag of almost 1 day. Coherence between local wind stress and temperature was statistically significant at periods longer than 2-3 days.

Near-surface and mid-depth currents were strongly polarized along the isobaths with local wind forcing accounting for less than 30% of the along-shelf current variability at periods longer than 1 day. In contrast, the coupling between wind stress and bottom currents was only marginally significant across a narrow portion of the weather band. Coherence between local winds and ASLS was higher than that observed for the currents but still only accounted for less than 50% of the ASL variability at subtidal frequencies, with wind leading the ASL by 6 hours. The low coherence between local wind stress and currents and between local wind stress and ASLS suggest that remotely-forced winds or propagating

coastally-trapped waves may be driving the currents at the lower subtidal frequencies in the Point Conception region.

Remote forcing of currents was examined through rotary spectral analysis at the two current mooring locations. At Hidalgo (Point Conception), there is a considerably higher fraction of rotational energy (-40%) at subtidal periods than at Julius (Point Sal). The additional rotational energy at Hidalgo arises from clockwise motions which are believed to be caused by eddies being formed on the lee side of Point Conception during Santa Barbara Channel northward-outflow events. Counter-clockwise motions for the two sites were similar in magnitude and highly coherent across a broad subtidal frequency band at periods longer than 4 days, with Julius leading Hidalgo by 2-3 days. It is hypothesized that this southward-propagating counter-clockwise motion is due to southward-propagating warm-core eddies or onshore meanders of the California Current.

Coastal ASLS between Monterey and Rincon Island were highly coherent with Port San Luis leading Monterey by 6 hours, indicating a northward propagation of 680 cm s^{-1} which is consistent with speeds found by Hickey (1984) for the Pacific Northwest. Near-surface and mid-depth currents were found to be highly coherent with the cross-shelf ASL difference between Hidalgo and Port San Luis at periods of 3-15 days. In contrast, the coupling between bottom currents and cross-shelf ASL difference was only marginally coherent at the two sites.

A clear "spring transition" as described by Strub et al. (1987b) was seen in the ASLS for Monterey, Port San Luis, and Rincon Island during the years of 1987, 1988, and 1990, but not during 1988. Surface temperatures at Hidalgo and the NDBC Buoy 46023 dropped 1-2 "C during the same time periods. Local wind stress and currents at Hidalgo did not exhibit any noticeable spring transition. ASL data from the NCCCS pilot experiment (Magnell et al. 1990) showed a spring transition during mid-March of 1987 which lagged that seen at Monterey, Port San Luis, and Rincon Island by 2-3 days. Based on the low correspondence between local winds and sea level response with respect to the spring transition and the high correlation with the Northern California spring transition during 1987, it would seem that the spring transition in the Point Conception region is being remotely forced by large-scale weather systems with alongshore length scales of 500-1000 km.

REFERENCES

Atkinson, L. P., K.H. Brink, R.E. Davis, B.H. Jones, T. Paluszkiewicz, and D.W. Stuart, 1986, Mesoscale hydrographic variability in the vicinity of Points Conception and Arguello during April-May 1983: The OPUS 1983 experiment, *J. Geophys. Res.*, 91(C11):12899-12918.

Barth, J. A., and K.H. Brink, 1987, Shipboard acoustic doppler profiler velocity observations near Point Conception: Spring 1983, *J. Geophys. Res.*, 92, 3925-3943.

Beardsley, R. C., D.C. Chapman, K.H. Brink, S.R. Ramp, and R. Schlitz, 1985, The Nantucket Shoals Flux Experiment (NSFE79), Part I: A basic description of the current and temperature variability, *J. Phys. Oceanogr.*, 15:713-748.

Brink, K. H., 1982, A comparison of long coastal trapped wave theory with observations off Peru, *J. Phys. Oceanogr.*, *12, 897-913.*

Brink, K. H., and R.D. Muench, 1986, Circulation in the Point Conception-Santa Barbara Channel region, *J. Geophys. Res.*, 91, 877-895.

Brown, W. S., J.D. Irish, and C.D. Winant, 1987, A description of subtidal pressure field observations on the northern California continental shelf during the Coastal Ocean Dynamics Experiment, *J. Geophys. Res.*, 92, 1605-1635.

Caldwell, P. C., D.W. Stuart, and K.H. Brink, 1986, Mesoscale wind variability near Point Conception, California during Spring 1983, *J. Climate and Applied Meteor., 25:1241-1254.*

Chelton, D. B., 1980, Low frequency sea level variability along the West Coast of North America, Ph. D. thesis, 212 pp., Univ. of Calif., San Diego.

Chelton, D. B., 1984, Seasonal variability of alongshore geostrophic velocity off Central California, *J. Geophys. Res.*, 89, 3473-3486.

Chelton, D. B., A.W. Bratkovich, R.L. Bernstein, and P.M. Kosro, 1988, Poleward flow off Central California during the spring and summer of 1981 and 1984, *J. Geophys. Res.*, 93, 10604-10620.

Crowe, F. J., and R.A. Schwartzlose, 1972, Release and recovery records of drift bottles in the California region, 1955 through 1971, *California Cooperative Oceanic Fisheries Atlas # 16, Marine Fisheries Committee*, State of California.

Csanady, G.T., 1978, The arrested topographic wave, *J. Phys. Oceanogr., 8, 47-62.*

Davis, R. E., 1977, Techniques for statistical anal ysis and prediction of geophysical fluid systems, *Geophys. and Astrophysical Fluid Dynamics*, 8:245-277.

Davis, R. E., 1985, Drifter observations of coastal surface currents during CODE: The statistical and dynamical views, *J. Geophys. Res.,90(C3):4756-4772.*

Denbo, D. W., and J. S. A1len, 1987, Large-scale response to atmospheric forcing of shelf currents and coastal sea level of the west coast of North America: May-July 1981 and 1982, *J. Geophys. Res.*, 92(C2): 1757-1782.

Dennis, R. E., and E.E. Long, 1971, A user's guide to a computer program for harmonic analysis of data at tidal frequencies, Technical report NOS 041, National Oceanic and Atmospheric Administration Rockville, Md. 31 pp.

Dugdale, R. C., and F.P. Wilkerson, 1989, New production in the upwelling center at Point Conception, California: Temporal and spatial patterns, *Deep-Sea Res., 36, 985-1007.*

Elgar, S., 1988, Comment on "Fourier transform filtering: A cautionary note by A. M. G. Forbes", *J. Geophys. Res.*, 93, 15755-15756.

Enfield, D. B., and J.S. Allen, 1980, On the structure and dynamics of monthly mean sea level anomalies along the Pacific Coast of North and South America, *J. Phys.Oceanogr.*, 10, 557-578.

Forbes, A. M. G., 1988, Fourier transform filtering: A cautionary note by A. M. G. Forbes, *J. Geophys. Rex.*, 93, 6958-6962.

Hall iwell, G. R., and J.S. Allen, 1987, Wave number-frequency domain properties of coastal sea level response to alongshore wind stress along the West Coast of North America, *J. Geophys. Res.*, 92, 11761-11788.

Hickey, B. M., 1979, The California Current System--hypotheses and facts, *Prog.Oceanogr.*, 8, 191-279.

Hickey, B., and N.E Pola, 1983, The seasonal alongshore pressure gradient on the West Coast of the United States, *J Geophys. Res.*, 88, 7623-7633.

Hickey, B., 1984, The fluctuating longshore pressure gradient on the Pacific Northwest Shelf A dynamic analysis, *J. Phys. Oceanogr.*, 14, 176-293.

Huyer, A., B.M. Hickey, J.D. Smith, R.L. Smith, and R.D. Pillsbury, 1975, Alongshore coherence at low frequencies in currents observed over the continental shelf off Oregon and Washington, *J. Geophys. Res.*, 80, 3495-3505.

Kelly, K. A., 1985, The influence of winds and topography on the sea surface temperature patterns over the northern California slope, *J. Geophys. Res.*, 90, 11783-11798.

Kousky, V. E., and A. Leetmaa, 1989, The 1986-87 Pacific warm episode: Evolution of oceanic and atmospheric anomaly fields, *J. Climate,* 2(3):254-267.

Lentz, S. J., and D.C. Chapman, 1989, Seasonal differences in the current and temperature variability over the northern California shelf during the Coastal Ocean Dynamics Experiment, *J. Geophys. Res.,* 94(C9): 12571-12592.

Liu, T. W., K.B. Katsaros, and J.A. Businger, 1979, Bulk parametrization of air-sea exchanges of heat and water vapor including the molecular constraints at the interface, *J. Atmos. Sci.,* 36, 1722-1738.

Liu, T. W., and T.V. Blanc, 1984, The Liu, Katsaros, and Businger (1979) bulk atmospheric flux computational iteration program in FORTRAN and BASIC, *NRL Memo. Rep.,* 5291.

Liu, P. C., and D.J. Schwab, 1987, A comparison of methods for estimating u_* from given u_z and air-sea temperature differences, *J. Geophy. Res.,* 92, 6488-6494.

Magnell, B. A., N.A. Bray, C.D. Winant, C.L. Greengrove, J. Largier, J.F. Borchardt, R.L. Bernstein, and C.E. Dorman, 1990, Convergent shelf flows at Cape Mendocino, *Oceanogr.,* April, 4-11 and 64.

Mooers, C. N. K., 1973, A technique of the cross-spectrum analysis of pairs of complex-valued time series, with emphasis on properties of polarized component and rotational invariants, *Deep-Sea Res.,* 23:613-628.

Osmer, S .R., and A. Huyer, 1978, Variations in the alongshore correlation of sea level along the West Coast of North America, *J. Geophys. Res.,* 83, 1921-1927.

Rabiner, L. R., B. Gold, and C.A. McGonegal, 1970, An approach to the approximation problem for non-recursive digital filters, *IEEE Trans. Audio Electroacout.,* AU-18(2), 83-106.

Reid, J. L., 1965, Physical oceanography of the region near Point Arguello, *Technical Report, Institute of Marine Resources, University of California,* La Jolla, IMR Ref. 75-19, 30 pp.

Reid, J. L., and A.W. Mantyla,)976, The effect of the geostrophic flow upon coastal sea elevations in the northern North Pacific Ocean, *J. Geophys. Res.,* 81, 3100-3110.

Sheres, D., and K.E. Kenyon, 1989, A double vortex along the California Coast, *J. Geophys. Res.,* 94, 4989-4997.

Strub, P. T., J.S. Allen, A. Huyer, and R.L Smith, 1987a, Seasonal cycles of currents, temperatures, winds, and sea level over the northeast Pacific continental shelf: 35 "N to 48 'N, *J. Geophys. Res.,* 92(C2): 1507-1526.

Strub, P. T., J.S. Allen, A. Huyer, and R.L Smith, 1987b, Large-scale structure of the spring transition in the coastal ocean off western North America, *J. Geophys. Res.*, 92(C2): 1527-1544.

Svejkovsky, J., 1988, Sea surface flow estimation from advanced very high resolution radiometer and coastal zone color scanner satellite imagery: A verification study, *J. Geophys. Res.*, 93, 155-164.

W yllie, J. B., 1966, Geostrophic flow of the California Current at the surface and at 100 m, *California Cooperative Oceanic Fisheries Investigations Atlas*, Volume 4, La Jolla, California.

Table 1. Results of the multiple regression on the seasonal model (l). 95% confidence limits are also shown.

Measurement	Amplitude			Phase Lag (days from beginning of year)		Equivalent Degrees of Freedom
	Mean	Annual	Semi-Annual	Annual	Semi-annual	
			Temperature (°C)			
NDBC Buoy 46023 (5 m)	14.0420.05	1.63 AO.10	0.29±0.10	270	71	45
Hidalgo Mooing (12 m)	13.18±0.05	1.70*0.11	NS[1]	298	NS	34
Hidalgo Mooring (54 m)	11.23*0.04	0.99±0.08	NS	330	NS	36
Hidalgo Mooring (126 m)	9.50±0.02	0.54±0.04	0.06±0.04	331	27	38
			Along-shelf Wind Stress (dyn cm^{-2})			
NDBC Buoy 46023	-0.91 *0.03	0.25±0.07	NS	341	NS	230
			Along-shelf Current Velocity (cm s^{-1})			
Hidalgo Mooring (12 m)	3.93±0.81	6.17± 1.67	5.07±1.52	317	25	12%
Hidalgo Mooring (54 m)	730*0.60	5.20± 1.22	1.26±1.16	289	14	113
Hidalgo Mooring (126 m)	1.40± 0.30	1.21±0.61	0.75 ±0.58	342	174	137
			Pressure (millibars]			
NDBC Buoy 46023 (Atmospheric)	NS	3.1 O*030	0.73*030	21	180	—
Point Conception (ASL)	NS	2.79±0.27	1.69±0.25	276	42	
Monterey (fML)	NS	4.87 ±0.55	1.07*0.54	307	40	
Port San Luis (ASL)	NS	5.40±0.50	1.30±0.50	293	31	
Rincon (ASL)	NS	4.5420.48	1.01 *0.47	301	22	

[1] Not statistically significant.

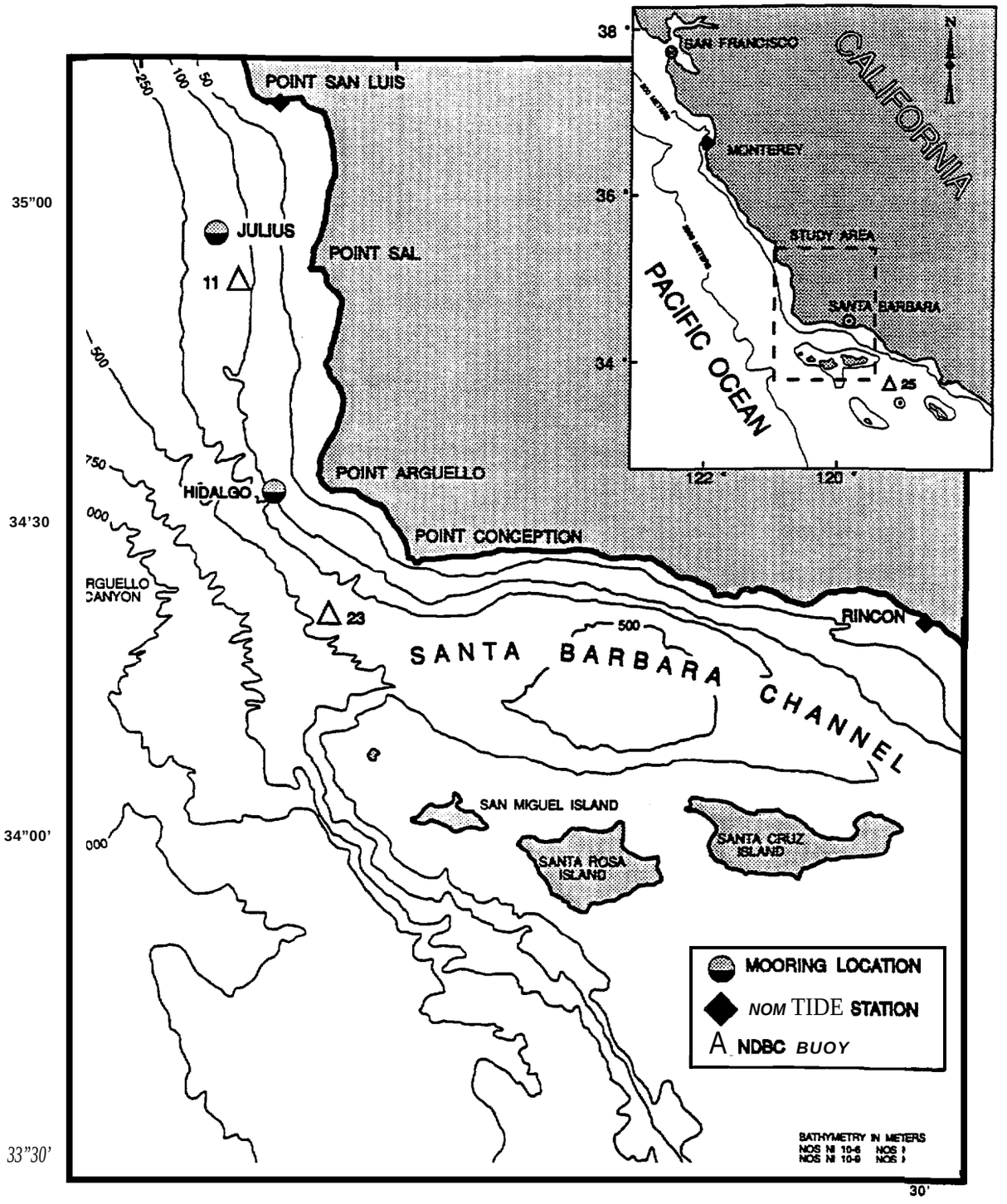

Figure 1. CAMP study location map of the Point Conception region with instrument locations and detailed bathymetry.

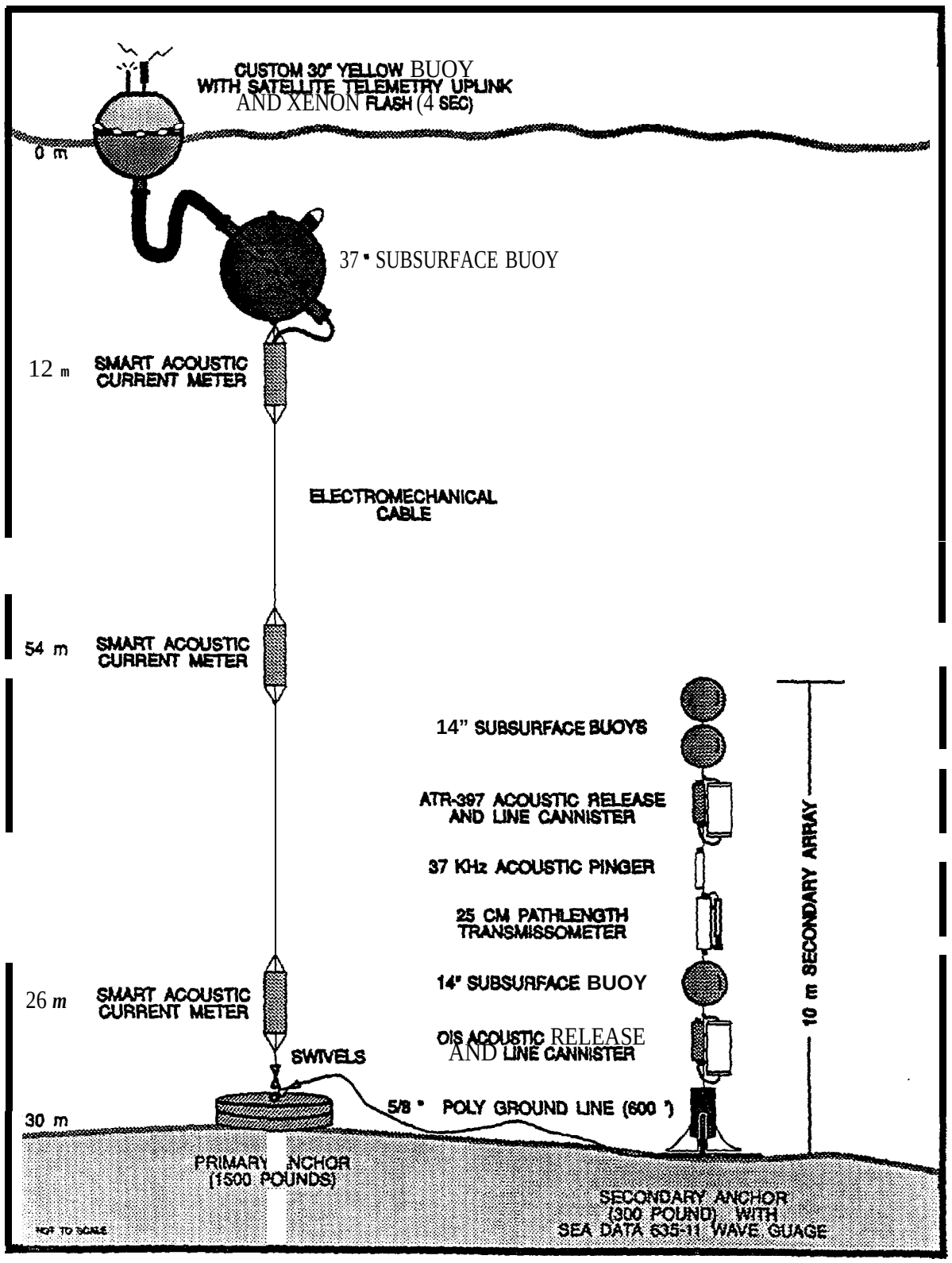

Figure 2. Current and bottom pressure mooring with surface ARGOS-satellite transmission buoy.

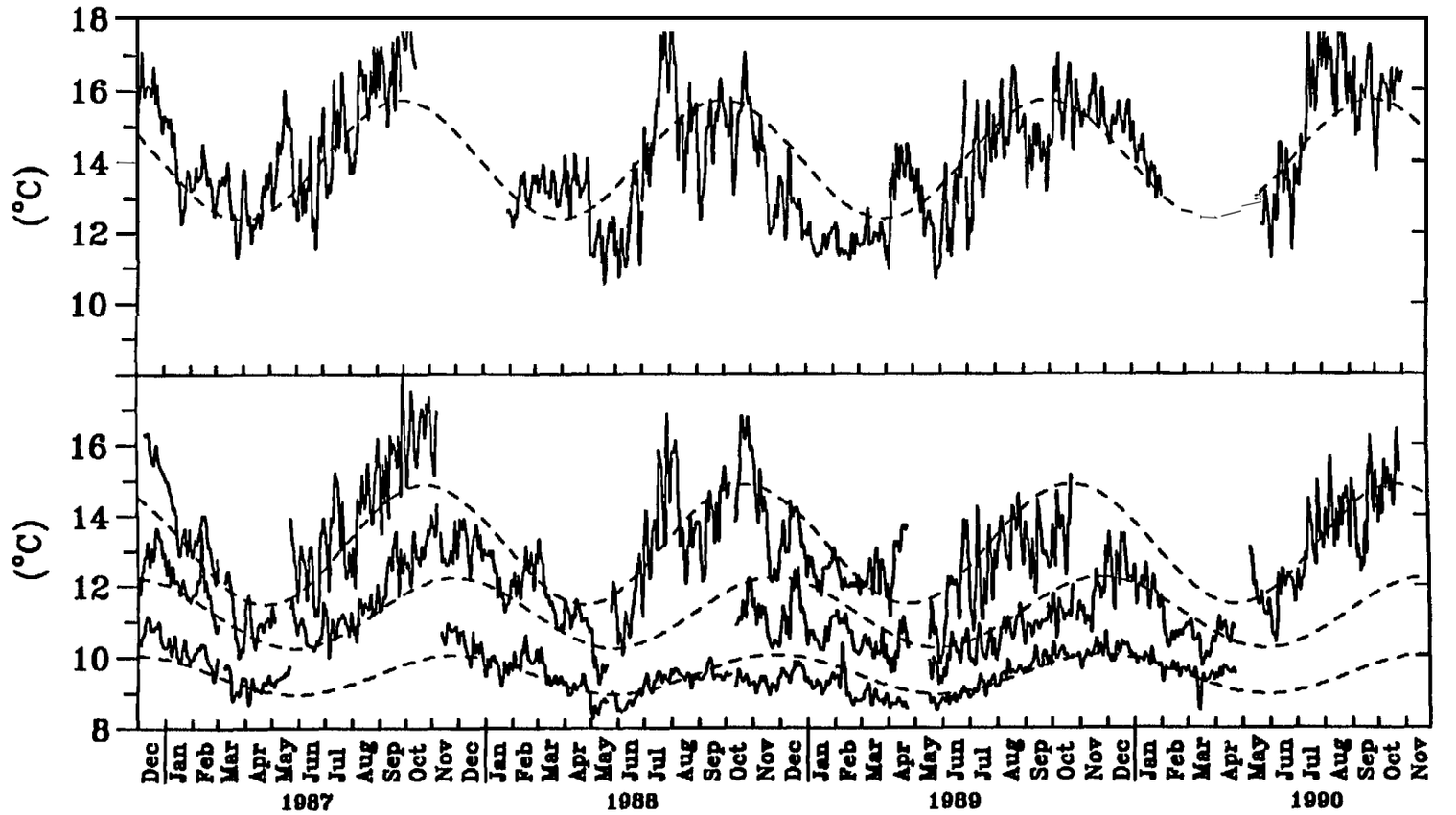

Figure 3. Point Conception temperature time series. Solid lines are 40–h low–pass temperatures and dashed lines are the annual harmonic determined from the regression model (1). The top frame shows the temperature recorded at a depth of 5 m on the NDBC Buoy 46023. The bottom frame shows progressively colder temperatures associated with current meters located at 12, 54, and 126 m on the Hidalgo mooring.

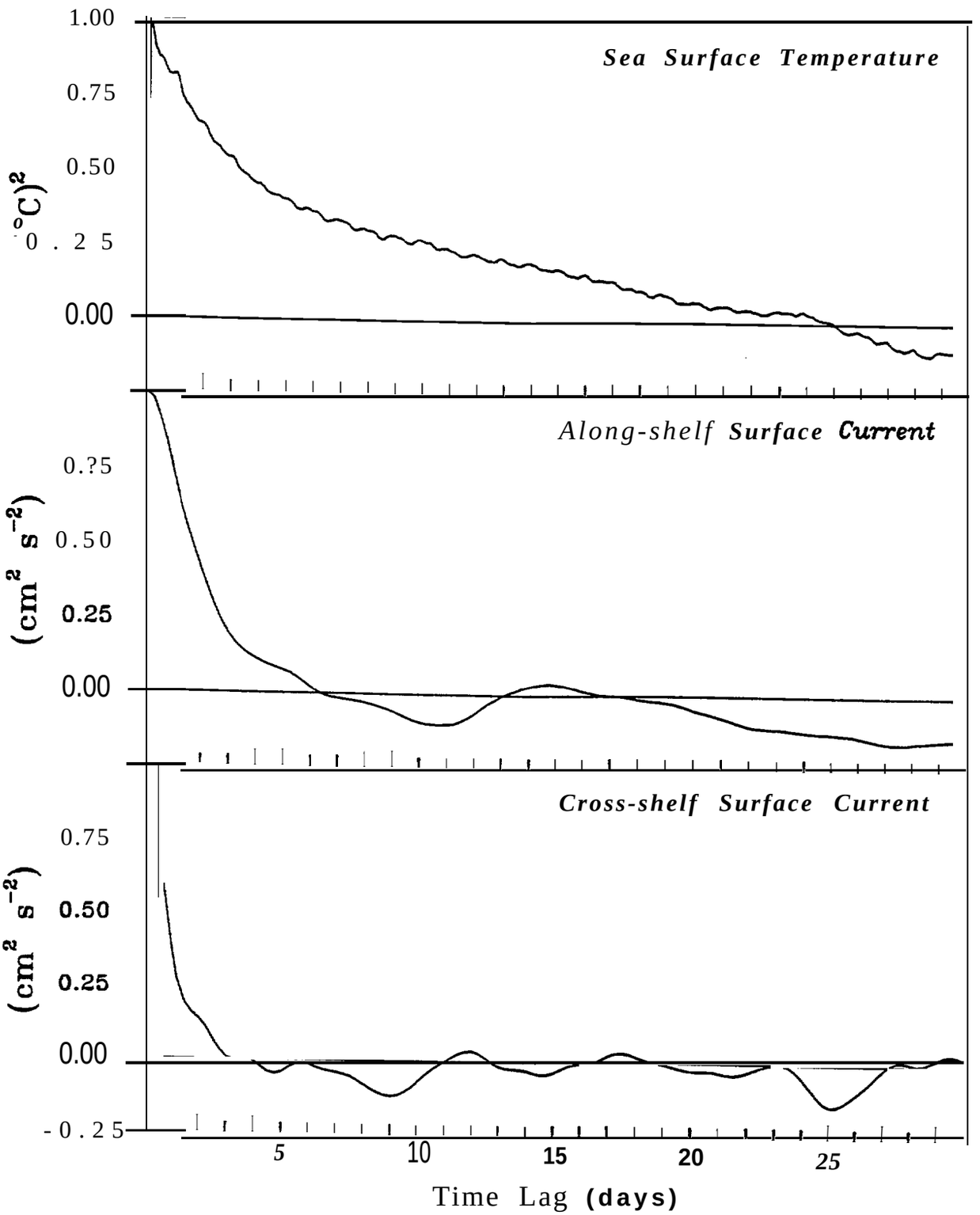

Figure 4. Time-lagged auto-correlation of surface currents and temperature recorded at the Hidalgo mooring. Along-shelf velocity is directed toward 324°T.

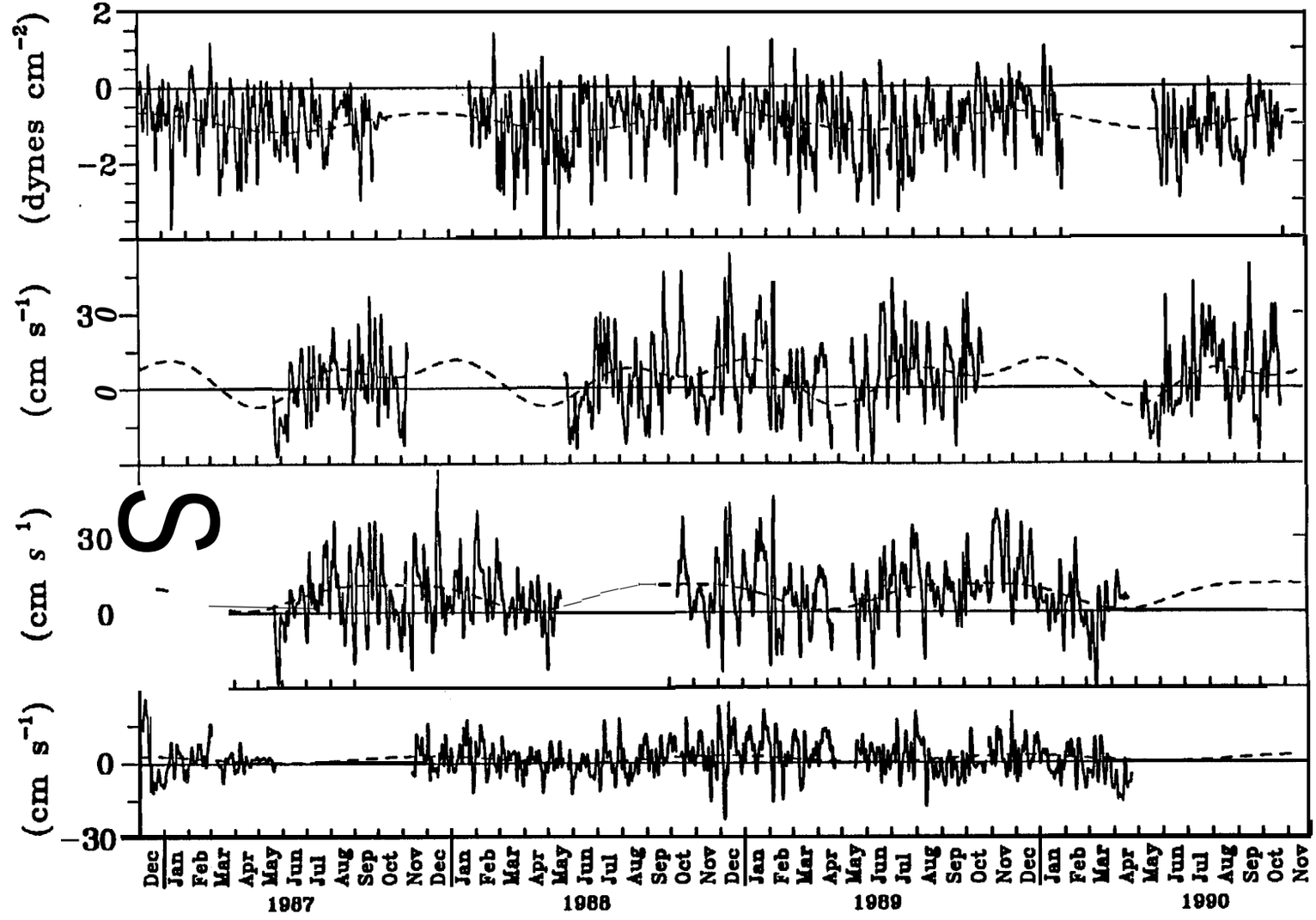

Figure 5. Time series of along-shelf wind stress and currents at Point Conception. The top frame shows 40-h low-pass wind stress determined from NDBC Buoy 46023 (solid) along with the annual harmonic (dashed) determined from a least-squares regression on (1). The second and third frames show along-shelf current flow at depths of 12 and 54 m on the Hidalgo mooring. The least-squares regressions (dashed) include semi-annual as well as annual harmonics as shown in Table 1. Along-shelf currents at 126 m (bottom frame) include only an annual harmonic.

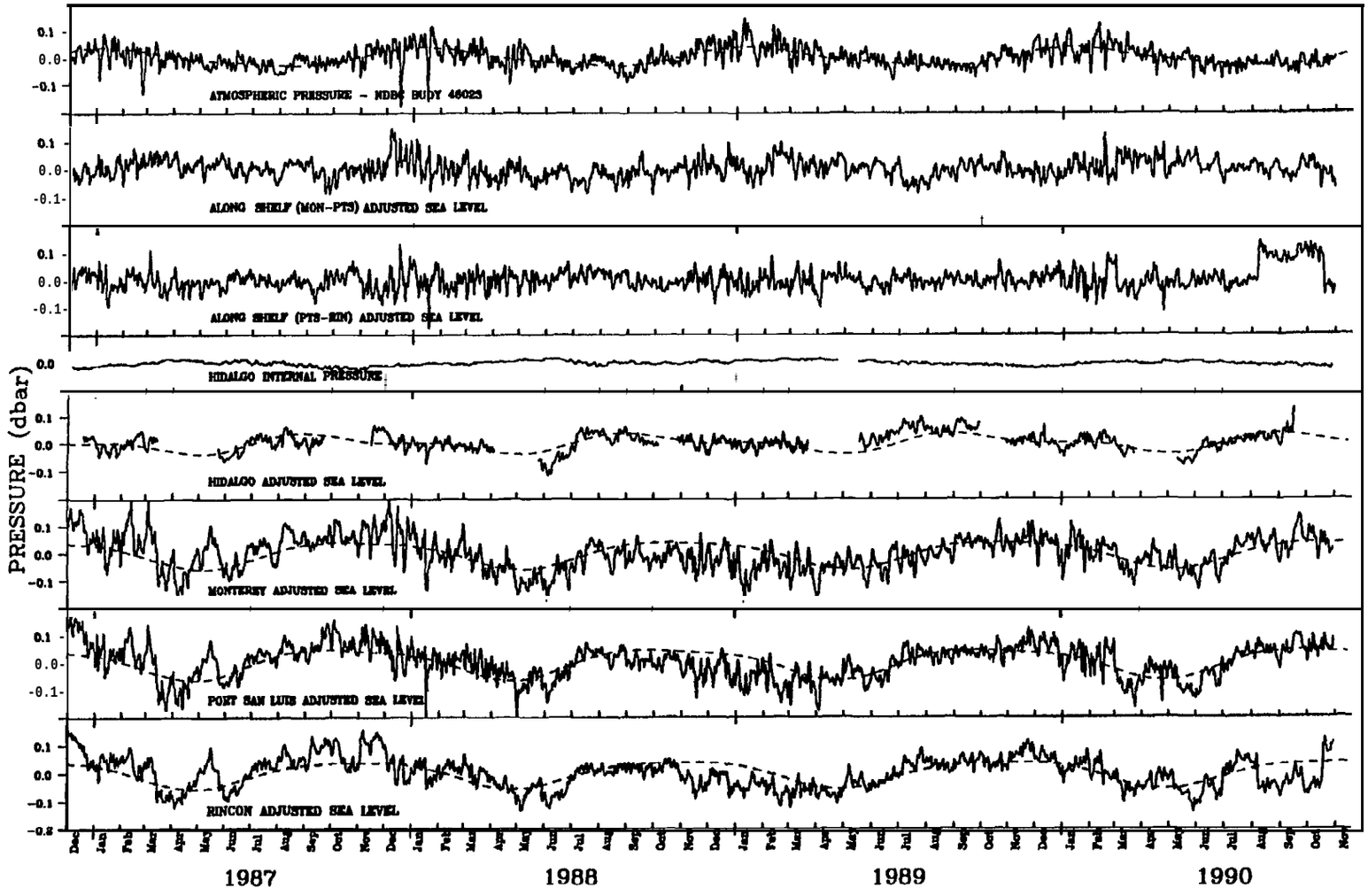

Figure 6. Time series of atmospheric pressure from NDBC Buoy 46023; along-shelf adjusted sea level differences; internal pressure at Hidalgo; and adjusted sea level variations at Hidalgo, Monterey, Port San Luis, and Rincon Island for the period of December 1986 through October 1990. Dashed lines&e the annual harmonic determined from the regression model (l).

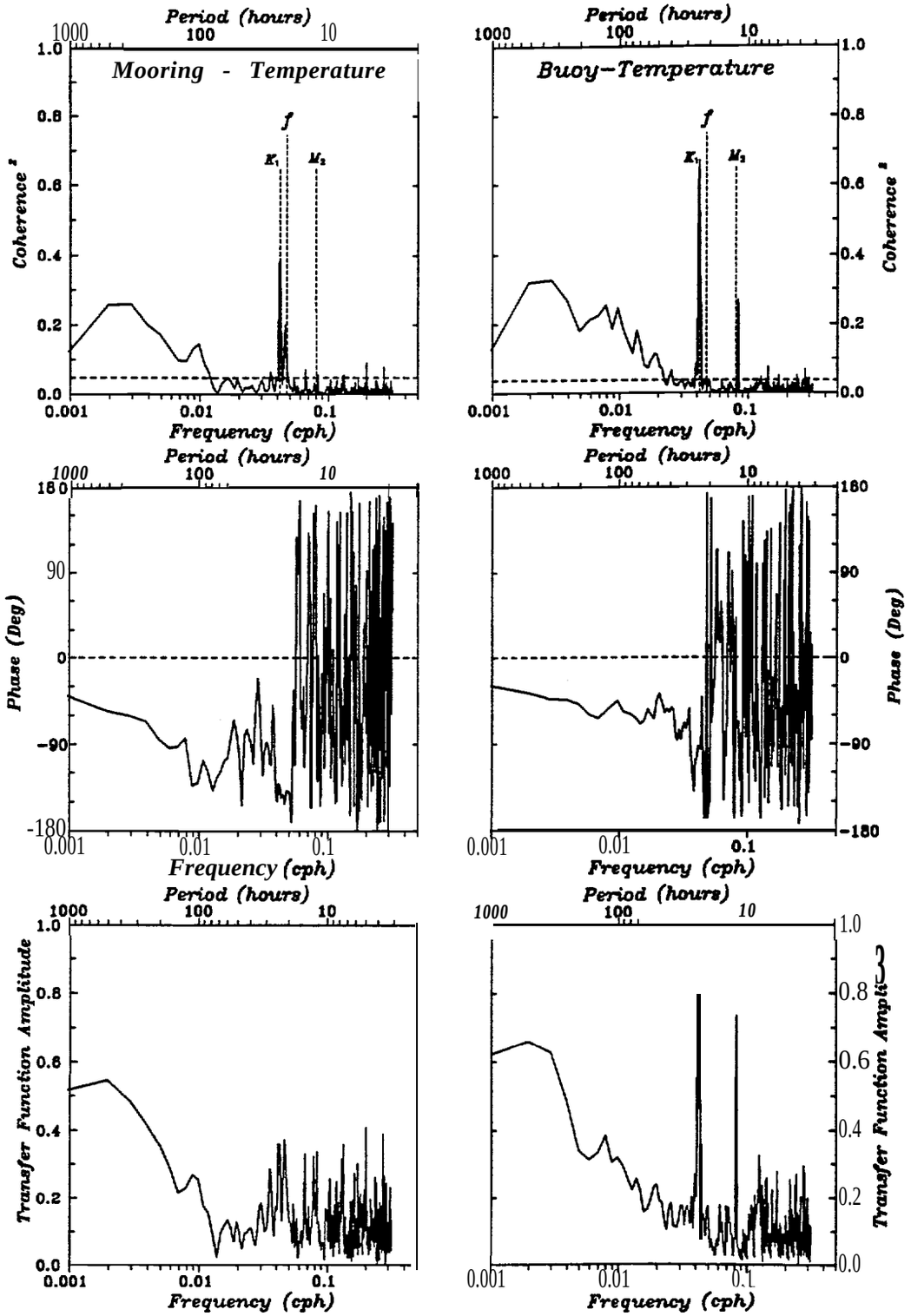

Figure 7. Cross-spectral analysis between along-shelf wind stress (dyn cm-z) and sea surface temperature (°C). Plots at the left are based on temperature data collected by the uppermost current meter (12 m) on the Hidalgo mooring. Plots on the right are based on-near-surface (5 m) temperature from the NDBC Buoy 46023, farther offshore. The transfer function units are °C cm^2 dyn^{-1}.

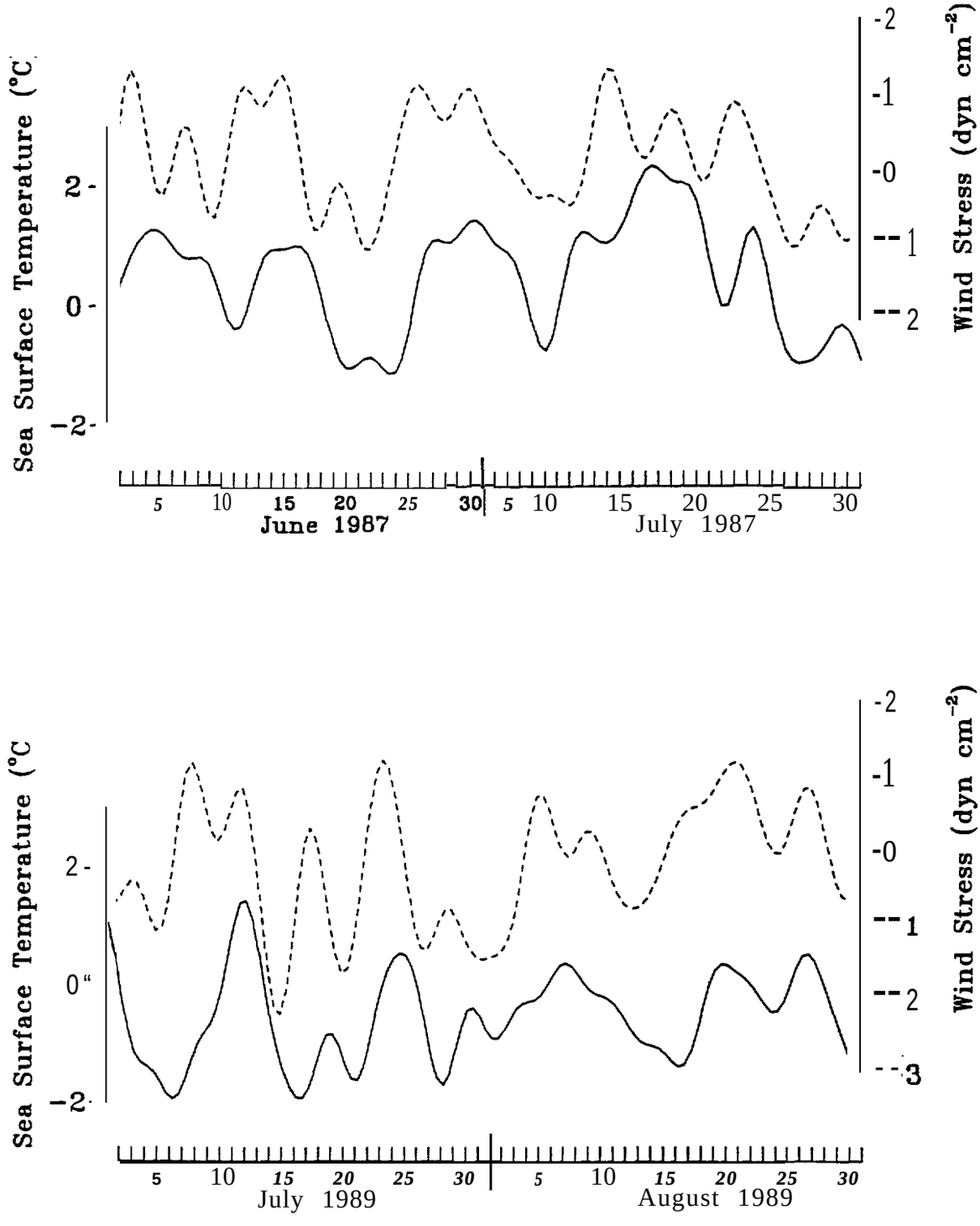

Figure 8. Time series of along-shelf wind stress (dashed) and near-surface (12 m) temperature (solid) from the Hidalgo mooring during two periods of vigorous upwelling.

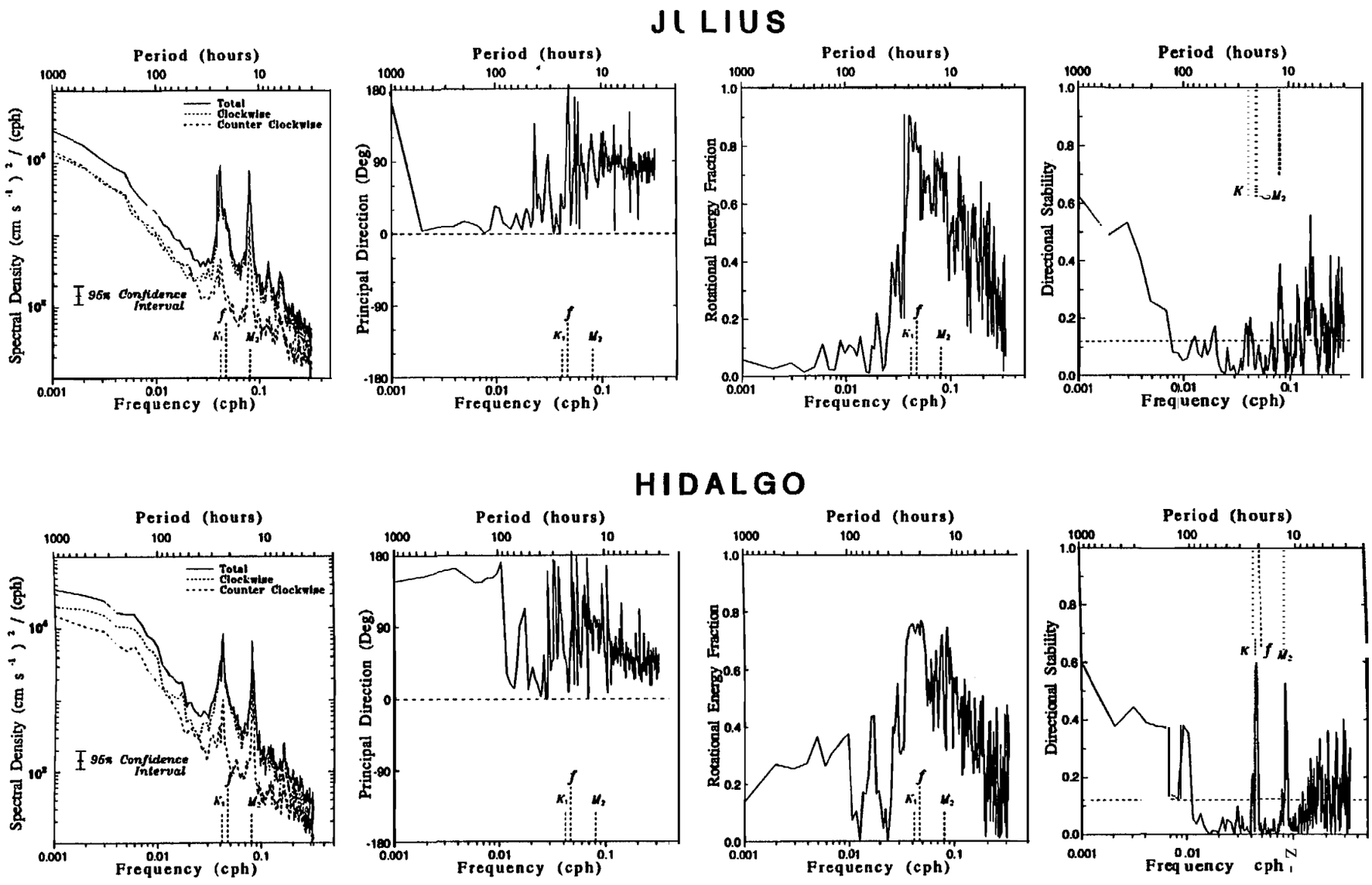

Figure 9. Rotary auto-spectral analysis of near-surface currents at the Julius and Hidalgo moorings.

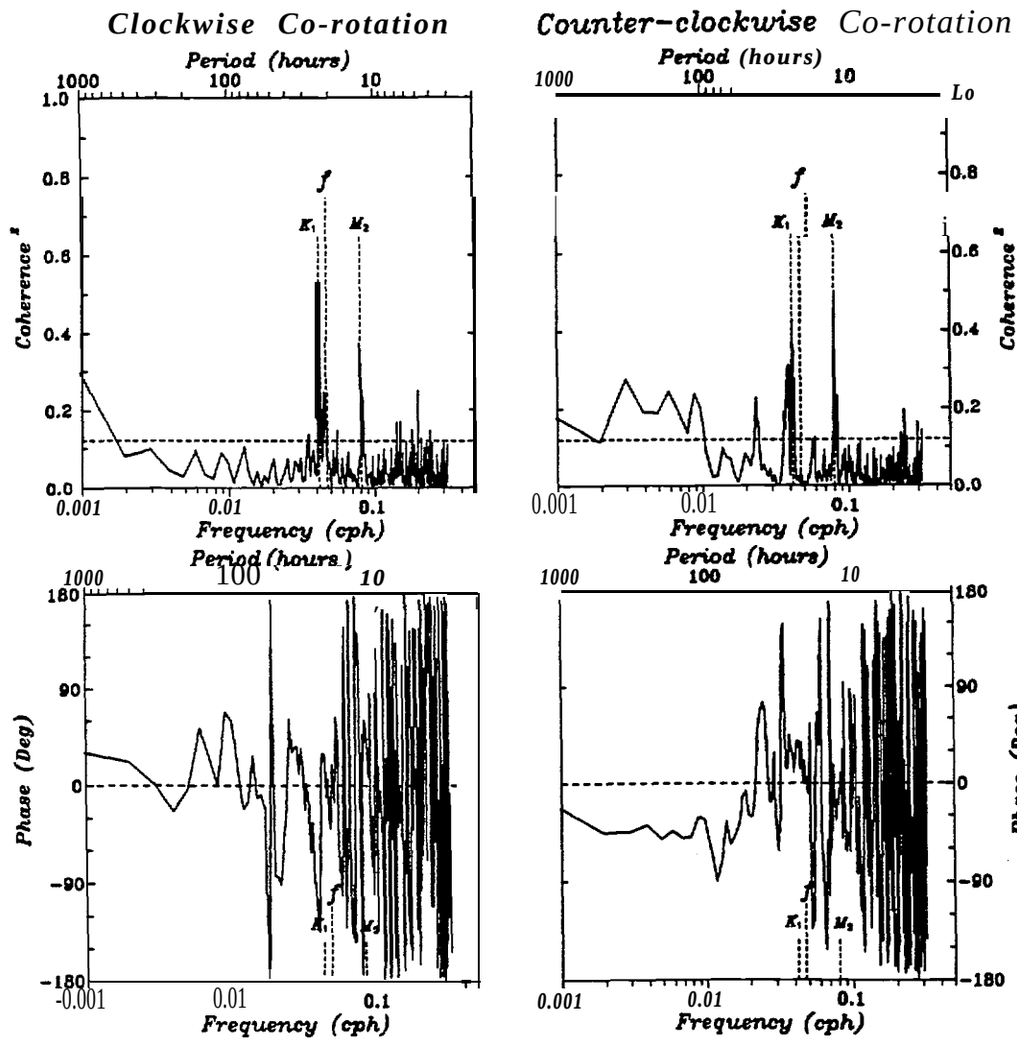

Figure 10. Rotary cross-spectral analysis between near-surface currents at the Julius and Hidalgo moorings.

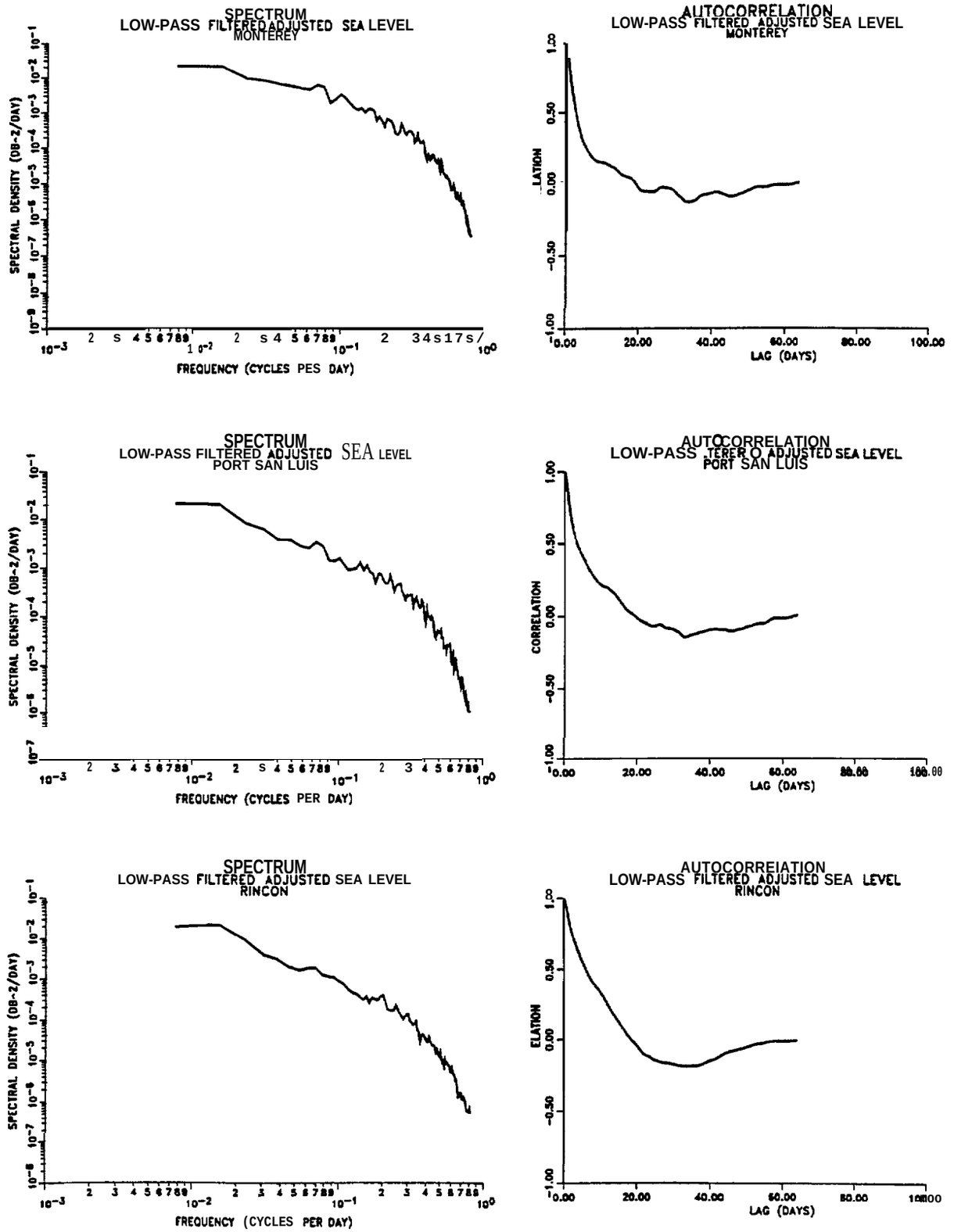

Figure 11. Auto-spectral analysis of coastal adjusted sea levels (decibars) from Monterey, Port San Luis, and Rincon Island for the period of November 1986 through October 1990.

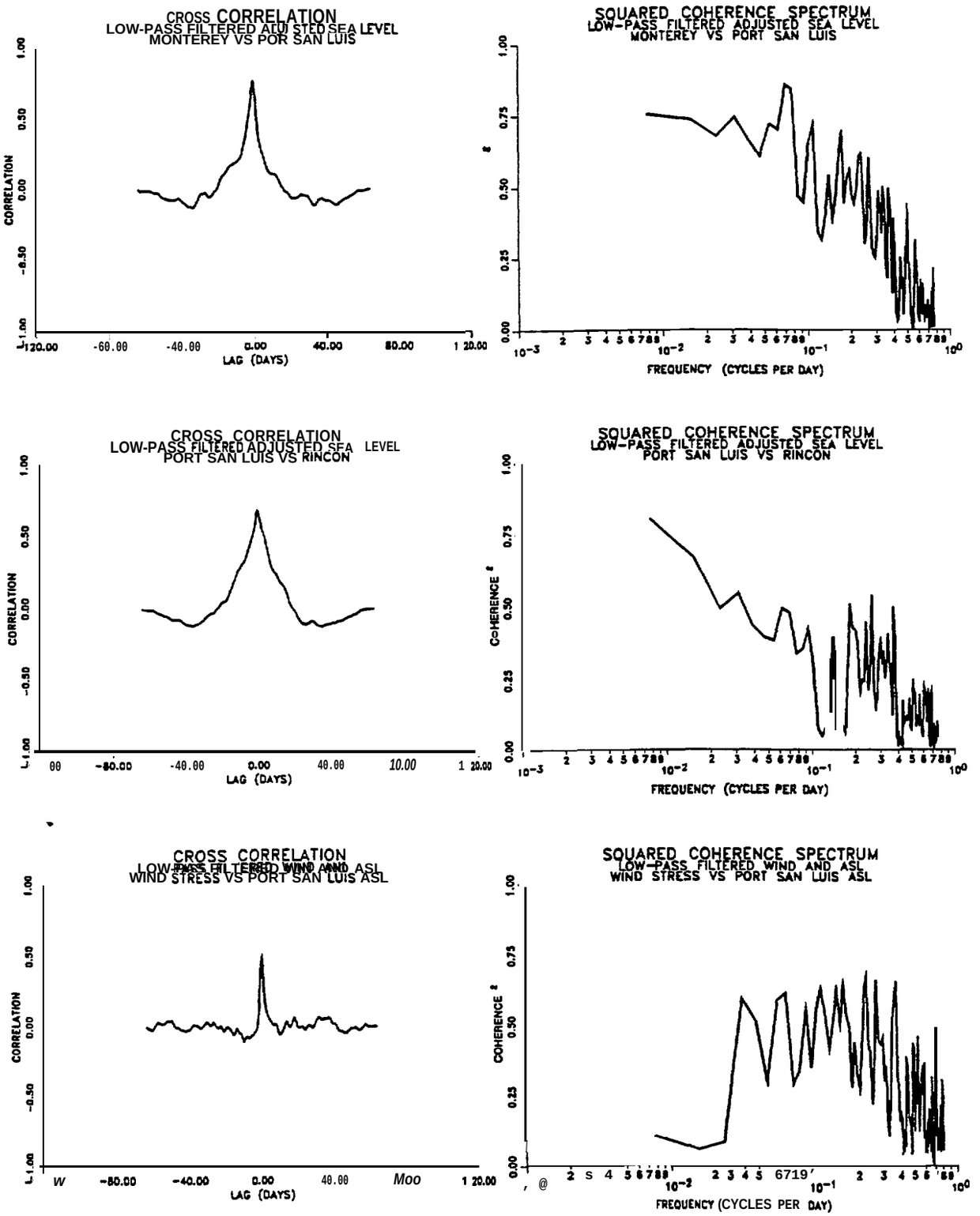

Figure 12. Cross-spectral analysis between coastal adjusted sea levels (decibars) and between alongshore wind stress (dyn cm^{-2}) and Port San Luis ASL.

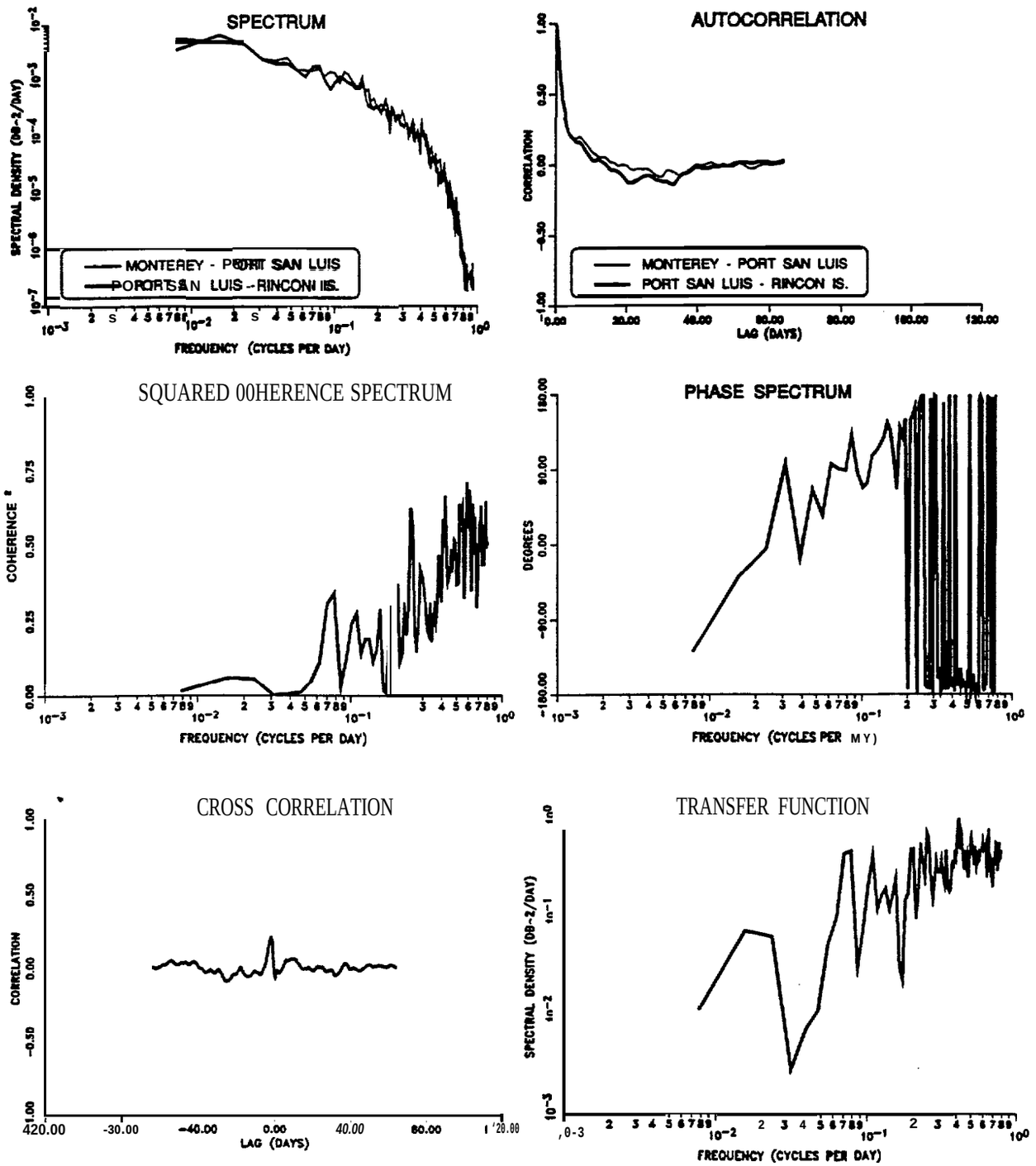

Figure 13. Auto- and cross-spectral analysis for along-shelf coastal ASL differences (Monterey - Port San Luis and Port San Luis - Rincon Island).

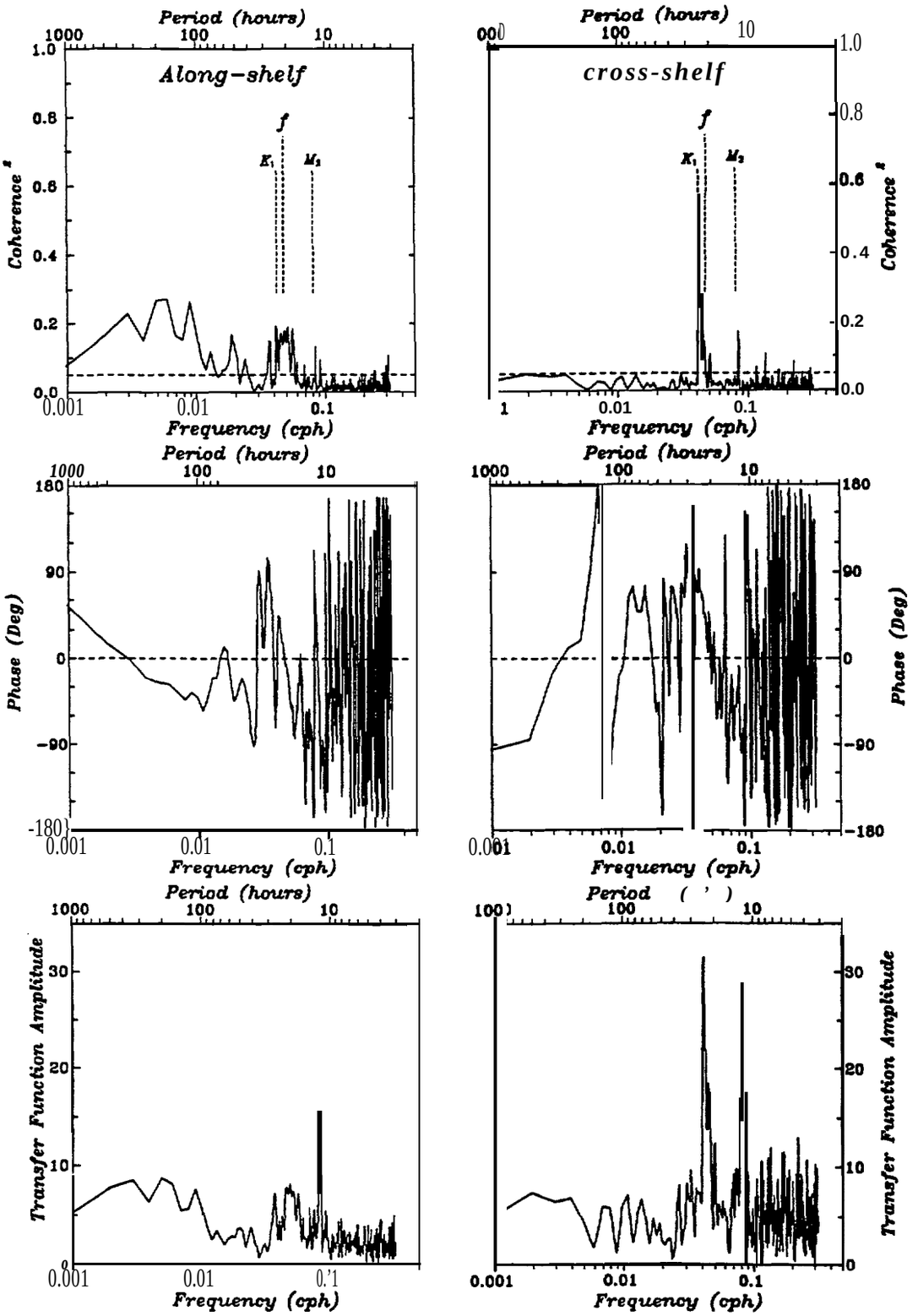

Figure 14. Cross-spectral analysis between wind stress (dyn cm^{-2}) and near-surface (12 m) currents at Hidalgo (cm S-l). The transfer function units are cm^{3} dyn^{-1} s-'.

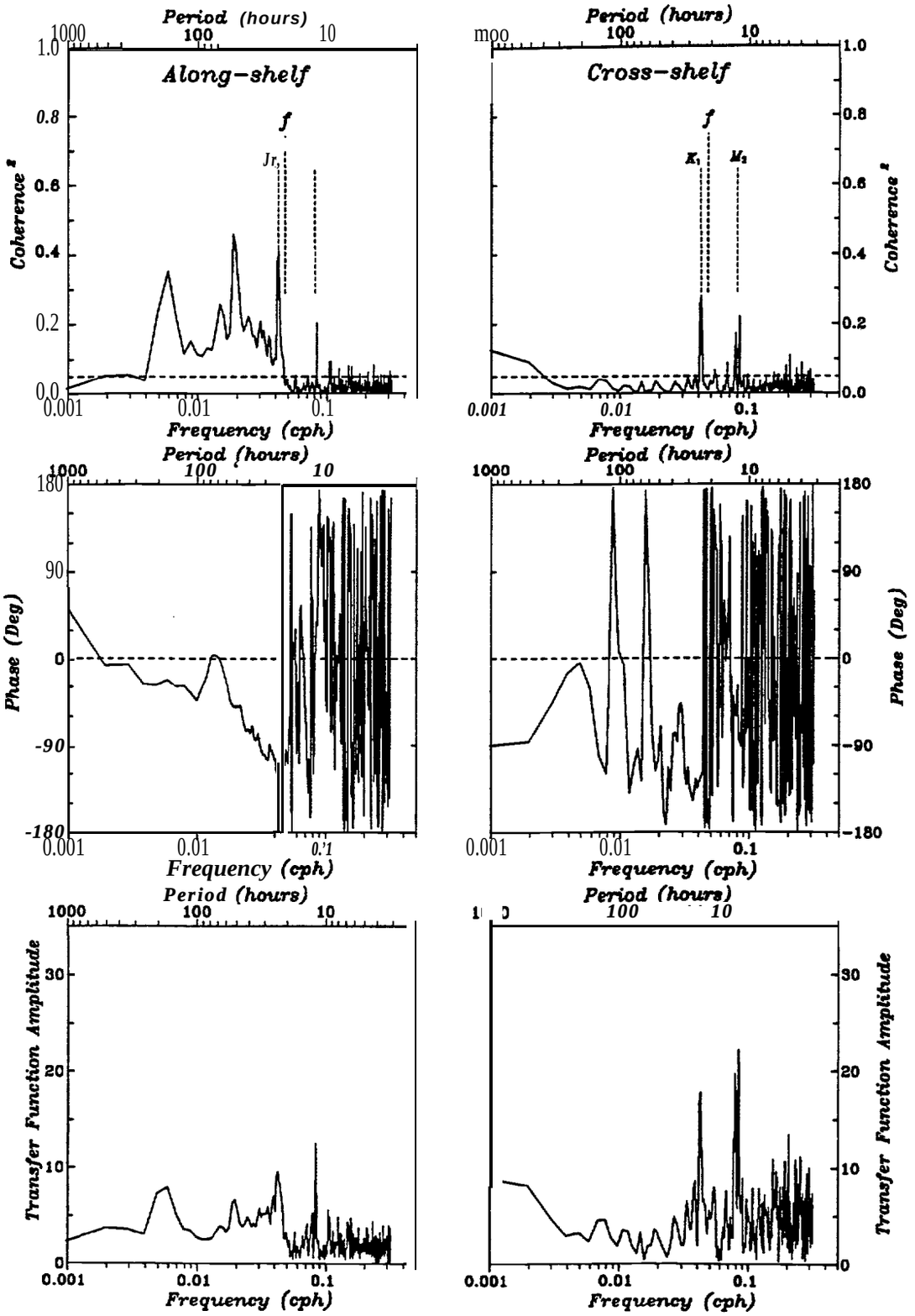

Figure 15. Cross-spectral analysis between wind stress (dyn cm-z) and mid-depth (54 m) currents at Hidalgo (cm S-l). The transfer function units are $cm^3 dyn^{-1}$ S-l.

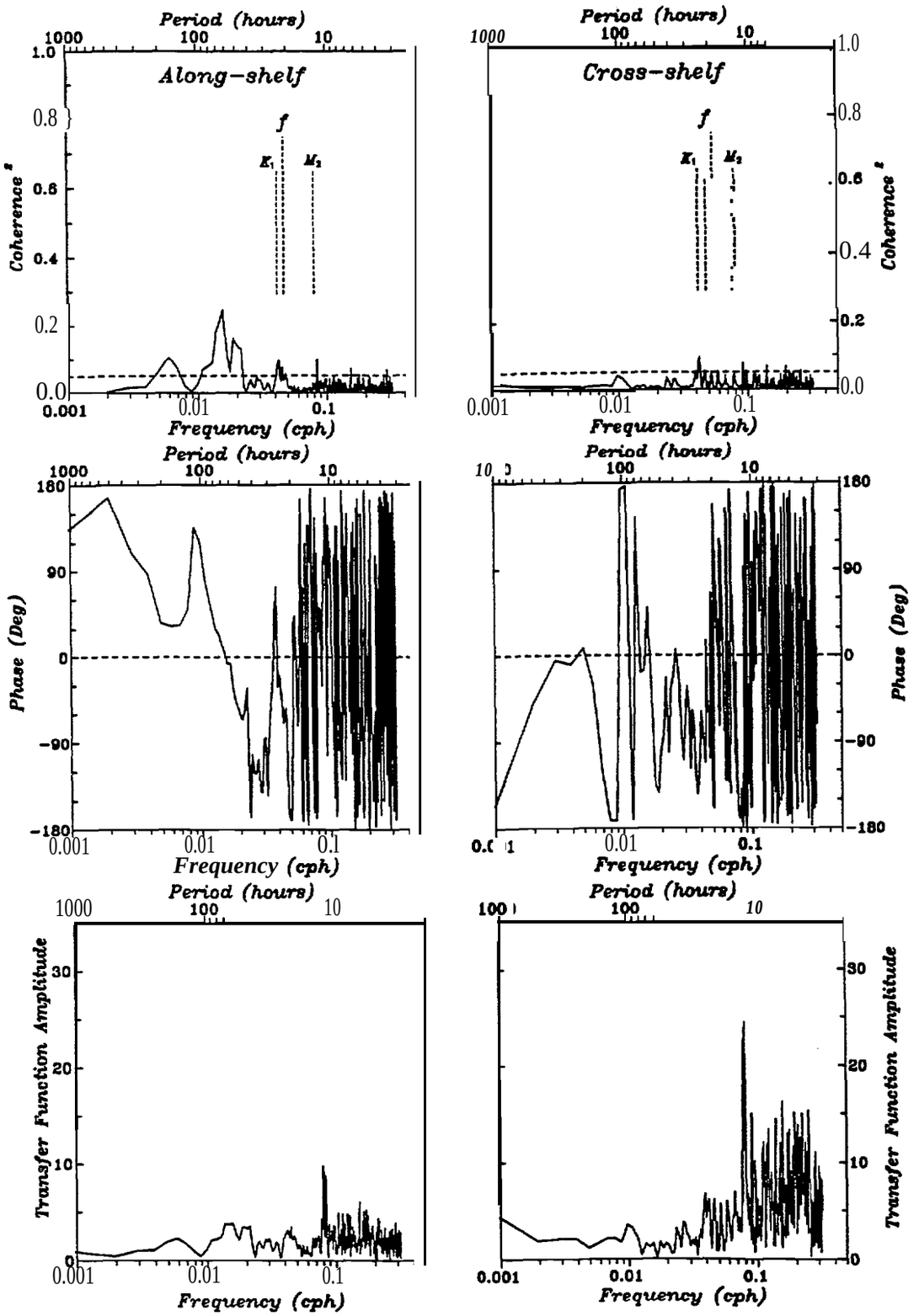

Figure 16. Cross-spectral analysis between wind stress (dyn cm^{-2}) and bottom (126 m) currents at Hidalgo (cm S-l). The transfer function units are cm^{3} dyn^{-1} s^{-1}.

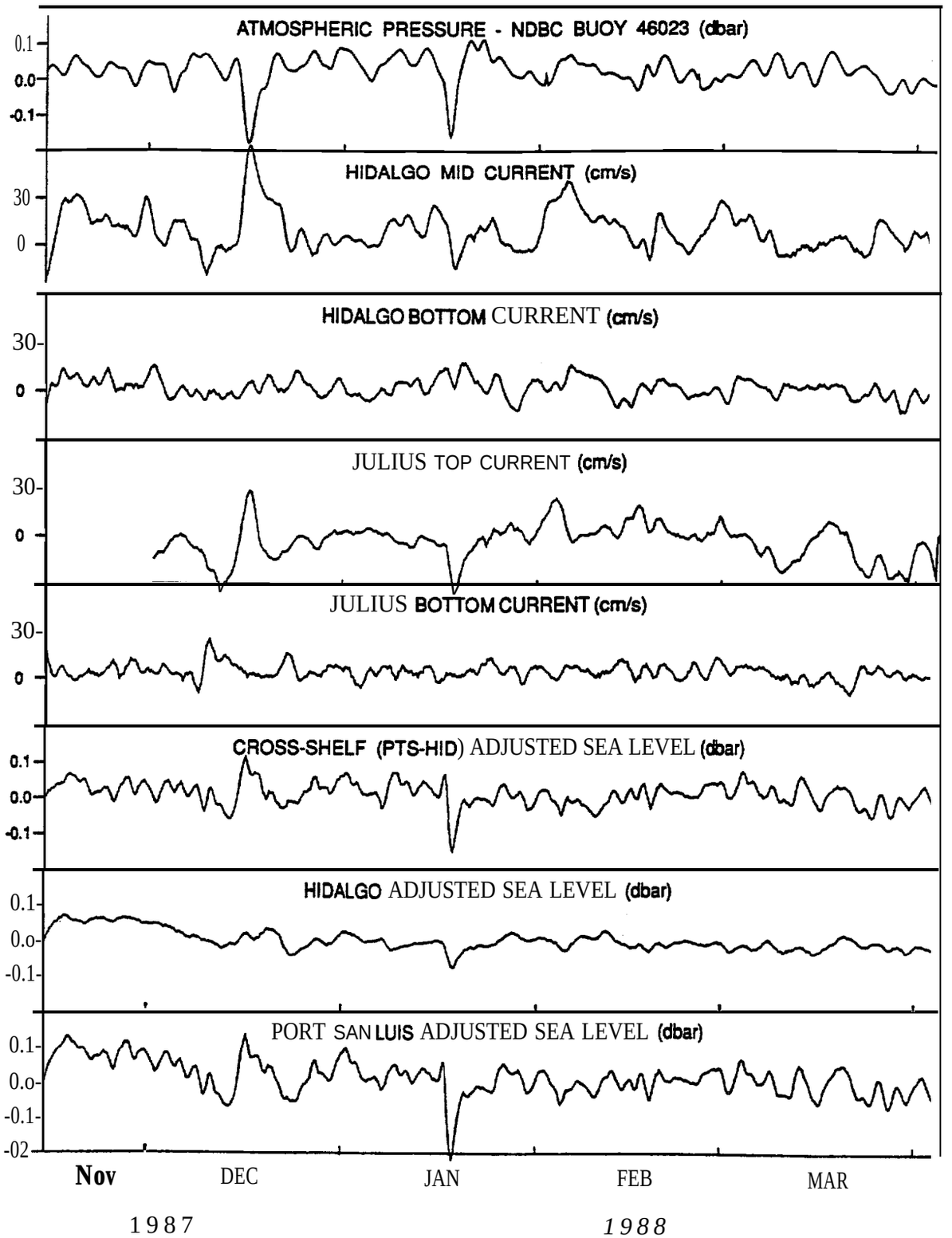

Figure 17. Time series of atmospheric pressure at NDBC Buoy 46023, alongshore currents (cm/s) measured at Hidalgo and Julius, cross-shelf adjusted sea level difference (Port San Luis - Hidalgo), and ASLs from Hidalgo and Port San Luis for the 5-month period of November 1987 through March 1988.

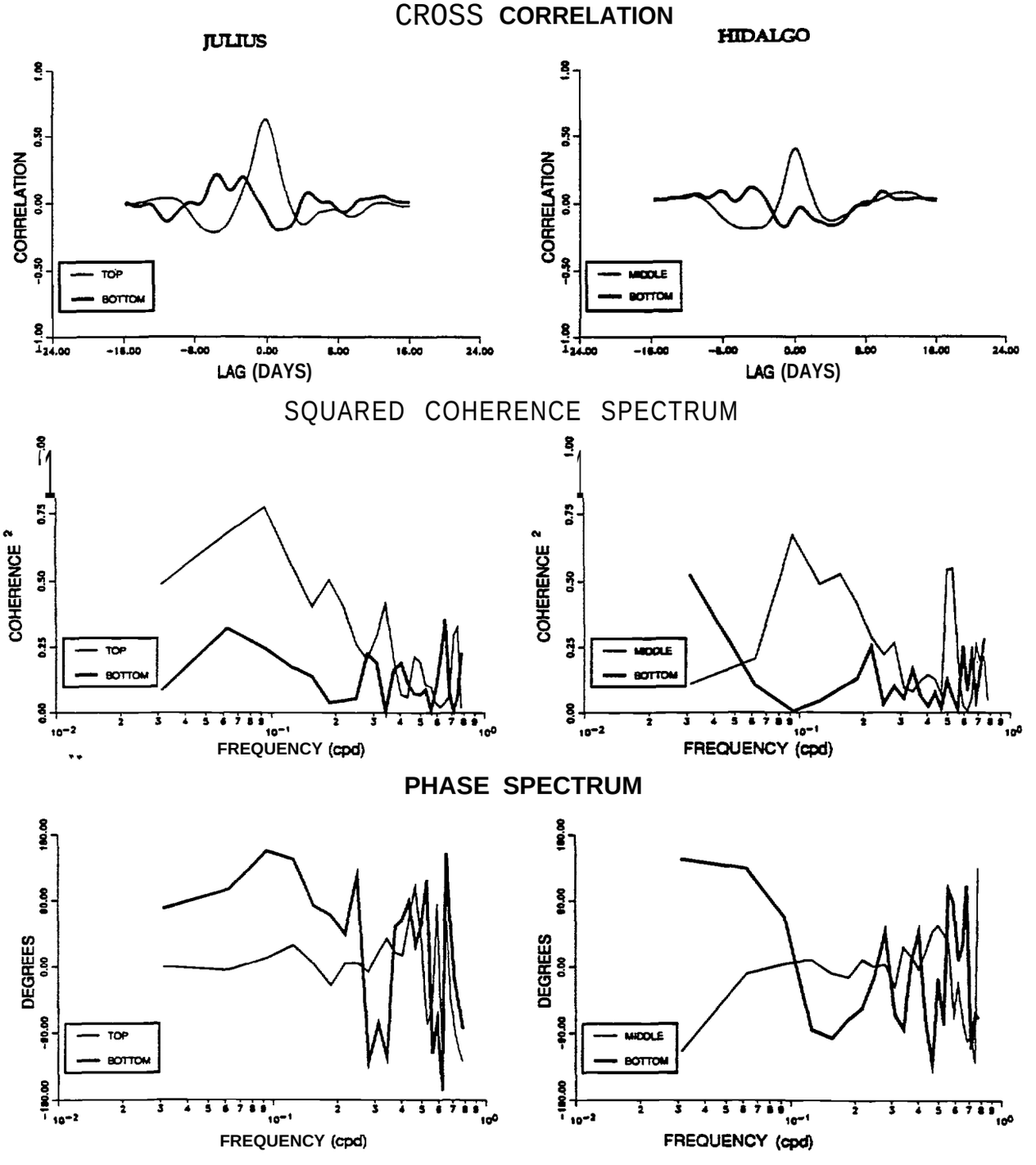

Figure 18. Cross-spectral analysis between the cross-shelf ASL difference (decibars) and alongshore currents (cm/s) at Hidalgo and Julius.

5. ANALYSIS OF A FOUR-YEAR SATELLITE SEA SURFACE TEMPERATURE IMAGING SEQUENCE NEAR POINT CONCEPTION, CALIFORNIA

ROBERT L. BERNSTEIN

SeaSpace
365.5 *Nobel Drive Suite 160, San Diego, California 92122*

GARY S. LAGERLOEF

Science Applications International Corporation
13400 Northup Way, Suite 36, Bellevue, WA 98005

MARK A. SAVOIE

Kinnetic Laboratories
307 Washington Street, Santa Cruz, California 95061

INTRODUCTION

Four years (December 1986- November 1990) of satellite sea surface temperature (sst) imagery were collected and produced, as part of the California Outer Continental Shelf Monitoring Program (CAMP), sponsored by the Minerals Management Service (MMS) of the U.S. Department of the Interior. This study, designed to examine the impact on benthic biological communities of oil and gas development in the Santa Maria Basin off the central California coast, included a physical oceanographic component consisting of multi-year surface wind measurements, currents measured at two sites near Point Conception, and 1 km resolution satellite sst imagery covering a *280* km square region, derived from the AVHRR (Advanced Very High Resolution Radiometer) of the NOAA series of polar-orbiting satellites. The objective of the imagery collection component was to provide a spatial context to the essentially single point time series of current and wind measurements.

This paper focuses on the method used to derive the sst imagery, and an analysis of the principal modes of sst variability, using empirical orthogonal functions, which are then interpreted in terms of the dominant larger scale patterns of flow occurring in the region around Point Conception. The paper is intended to serve as a companion to Savoie et al. (Chapter 4), which discusses the four-year CAMP time series of in situ wind, current, temperature, and sea level observations.

A rather complete discussion of previously published work on the regional winds and currents and their seasonal variation is discussed in Savoie et al. (Chapter 4), and therefore only briefly summarized here. Surface winds are persistently directed toward the southeast, seasonally strongest during late spring and early summer, and weakest during late fall and early winter (Figure 1). The four-year CAMP time series of wind stress, derived from a NOAA meteorological buoy located just 20 km off Point Conception, shows a 1.5 dyn/cm^2 long-term mean along-shelf component of wind stress (Figure 2). Superposed on this is a 0.5 dyn/cm^2 seasonal modulation. Higher frequency fluctuations, in the band 2-10 days, create 1 to 2 dyn/cm^2 fluctuations on this seasonal pattern, but only rarely does the along-shelf stress reverse toward the northwest.

Surface and subsurface temperatures also describe a seasonal variation. From the NOAA buoy four-year measurements of sst, an annual mean temperature of 14 "C is modulated with seasonal variation of 1.8 "C, with minimum temperatures occurring in the spring.

These patterns of wind and temperature are consistent with the classical picture of coastal upwelling, and southeasterly y coastal surface currents would be expected. However, the four-year CAMP time series (Figure 2) of flow at 12 m depth shows a seasonal variation having a southeastward component only for two months of the year, when winds are strongest in that direction. The remainder of the year, poleward flow occurs. CAMP time series of flow at 54 and 126 m depth show consistent y poleward seasonal currents. This tendency for sustained poleward flow is referred to as the Davidson Current; it is associated with larger scale patterns of coastal sea level, which decreases poleward, and larger scale wind patterns, particularly in the positive curl of the wind stress field along the California coast, as discussed by Hickey (1979) and Chelton (1984).

Poleward flow is particularly persistent at all depths along the mainland portion of the Santa Barbara Channel (Lagerloef and Bernstein, 1988), and is associated with the westward advection of warmer water

toward Point Conception. When this flow passes Point Conception, there are occasions where it retains its westward orientation and separates from the coast to form a jet-like feature (Sheres and Kenyon, 1989). At other times, the coastal flow exiting the western portion of the Santa Barbara Channel remains attached to the coast, or only partially separates, thus carrying warmer water north into the Santa Maria Basin.

The oceanographic flow patterns in the region surrounding Point Conception thus reflect three apparent modalities: (i) a strong tendency for persistent upwelling through local wind forcing; (ii) a tendency for persistent poleward coastal flow and its associated advection of warmer water from the south; and (iii) the interaction of these dynamical factors to create a detached jet at the western exit of the Santa Barbara Channel. The satellite sst imagery will be examined with this background in mind.

Imagery Production Methodology

During the four-year period 1 December 1986-30 November 1990, the NOAA-9 (and then NOAA-11) polar orbiting weather satellites provided twice-daily overpasses of the U.S. west coast, at 0130AM and PM local time. Each satellite carries an AVHRR sensor, making nominally 1. l-km resolution radiometric measurements at five different channels in the visible and thermal infrared portions of the spectrum. Only data from the daytime (1:30 PM) overpass, for which visible channel data is available, was used to produce sst imagery, because of the superior cloud detection and screening afforded by visible data. For the first three years, the data were obtained from analog tape telemetry recordings provided by a National Weather Service receiving station located at Redwood City, California; the first year of data were derived from a local reception antenna installed at SeaSpace in San Diego, California.

Each daily overpass was inspected for cloud cover, and days with heavy or complete cloud cover were eliminated from further consideration. Also, overpasses with poor viewing geometry were ignored. The remaining overpasses having some or all of the ocean area around Point Conception free of clouds were subjected to the following processing steps, for the region centered about 35 ‘N, 121 ‘W and enclosing a 256 x 256 array of 1.1132 km^2 pixels: (1) radiometric calibration and earth location and (2) cloud screening and atmospheric corrections. The portion of each pass encompassing the above area was extracted, radiometrically calibrated using AVHRR internal calibration information, and earth-located using satellite ephemeris data, using procedures developed at SeaSpace. Earth location was checked, and adjusted by a few kilometers, if necessary, using Point Conception or other local points of reference.

The AVHRR channels 2 (1.0 urn), 4 (11 urn) and 5 (12 urn), respectively in the reflective (Channel 2) and thermal infrared (channels 4 and 5), were used to determine those over-ocean pixels that were free of cloud. Several sequential cloud tests were employed, following procedures described in McClain et al. (1985):

(a) gross cloud checks - pixels with channel 2 albedo values exceeding those determined by visual inspection; and (b) local cloud checks - each pixel surviving the above test was compared against its immediate neighbors in a 3x3 array. Local variations within the 3x3 array in excess of 0.25% albedo (charnel 2), and 1.5 "C (channel 4) were screened out. Screened-out pixels were set to a designated "bad" value and surviving cloud-free pixels' thermal infrared brightness temperature measurements were linearly combined using weighting coefficients to give the best estimate of sea-surface temperature. The weighting coefficients were those determined by NOAA/NESDIS to give best agreement against a global set of in situ sst measurements (Pichel, pers. comm.). The coefficients included terms dependent upon the local viewing angle.

As described in McClain et al.(1985), these cloud/atmospheric procedures are expected to yield sate]] ite sst accuracies of about 0.7 'C, although the original sensor radiometric resolution, retained in the final results, is 0.1 'C. For a selected set of similar satellite sst results, coinciding with about 30 high-quality in situ sst measurements (CTD at l-m depth), satellite-CTD agreement was at the 0.4 'C rms level.

Finally, the resulting array of cloud-screened sst pixels was spatially mapped to a fixed rectangular map projection, as defined above. The digital arrays were saved for subsequent analysis, and also photographed onto 35-mm slides, and annotated with coastline and latitude-longitude grid, date/time, and a color/temperature calibration wedge.

Over the December 1986- November 1990 period, a total of551 images were obtained, distributed in time as indicated in Table 1. Averaged over the four years, the percentage of retained images varied between about 25 and 50%, depending primarily upon cloud cover.

Examples of satellite sst imagery appear in Figures 3 and 4. In Figure 3a, taken during the period of minimum seasonal wind stress, the warm poleward coastal flow of the Davidson current is apparent. Several weeks later (Figure 3b), the warmer water exiting the Santa Barbara Channel separates from the coast and moves west of Point Conception. Several months later (Figure 3c), with the buildup of

alongshore wind stress, cooler water brought to the surface by upwelling processes, appears along the entire central California coast. These three images illustrate the three apparent modal ities of flow and associated sea surface temperature distribution for the region.

Similarly, Figure 4 illustrates how the upwelling pattern can quickly relax, during a period of weakening winds, with westward flow again exiting the Santa Barbara Channel, This one week transition in late June/early July 1988 appears as a significant wind and current reversal event (Figure 2).

Empirical Orthogonal Analysis

While examination of individual images, and short sequences of images, is useful and informative, statistical methods must be applied for a study of the variability contained within an sst imagery data set of this size. Empirical orthogonal function (EOF; also known as principal component) analysis is the appropriate statistical tool. For California coastal sst imagery, this method was first employed by Ken y (1985), and subsequently by Lagerloef and Bernstein (1988). The spatial EOF procedure is described in detail in the latter paper. In this procedure, the spatial mean is first removed from each image, and the residual for each image is decomposed into a weighted sequence of orthogonal modal amplitude functions. The complete time-series of images thus provides a time-series of each of the modal weights.

The method for determining the modal functions and weights is based upon solving for the eigenfunction and eigenvalue matrices of an autocovariance matrix derived from the de-meaned original image set. Most of the original 551 images were cloud-obscured over half or more of their ocean pixels. Best results in determining a reliable autocovariance matrix thus require images that are most] y cloud-free. A subset of 76 images (Table 2) with minimal cloud obscuration was extracted from the full set, while also attempting to keep approximate] y 20-day time separation between images. Finally, for computation efficiency, the 256 x 256 arrays were subsampled by a factor of two, to 128 x 128 arrays having 2.2264 km pixel resolution.

The overall four-year time-mean of the 76 images listed in Table 2 appears in Figure 5, with the CAMP moorings, NOAA weather buoy, and bathymetric contours superposed for reference. The mean field portrays the persistent upwelling with coolest temperatures along the central coast north of Point Conception. Warmest temperatures are located inshore along the eastern portion of the Santa Barbara Channel, with a strong gradient occurring just at Point Conception. The cooler water upwelled along the

central coast extends southeast (parallel to the prevailing wind) to the western Santa Barbara Channel islands, with a portion actually entering the channel along the north shore of these islands. The mean field spans a 5 ‘C temperature range; 12 to 17 “C.

As noted earlier, the average temperature of each of the above 76 images was computed and subtracted to produce a de-meaned image data set. The variance of these residual temperature values is depicted in Figure 6. Note that variances are higher for all areas south and east of Point Arguello. Within the lower variance region west (and north) of Point Arguello is a smaller subarea of slightly higher variability. This appears to correlate with upwelling jet-like plumes that can originate along the central coast north of Point Arguello, as were seen in the individual images of Figure 4. These plumes grow, decay, and shift laterally, and thus increase the local variability of sst in this region.

The next step in examining the image set is to group it into four 90-day seasons centered on days 1, 90, 180 and 270 (winter, spring, summer, fall). The mean sst for each season (Figure 7) show a large scale pattern similar to the annual mean of Figure 5, but with seasonal offsets. Note that a wider temperature range spanning 11 to 18 °C is used here.

Attention is focused on the winter mean, where spatial gradients are weaker. Figure 8 presents the mean sst for this season, using an appropriate] y narrowed 3 °C range of temperature spanning 12 to 15 ‘C. The tendency for warmer water to advect west out of the Santa Barbara Charnel and then north beyond Point Arguello appears in the winter mean distribution of sst.

Spatial EOF Modes

The EOF decomposition of sst variability across the 76-image data set yields the results displayed in Figure 9. Note that the first EOF mode, which accounts for nearly half of the sst variance, strongly resembles the four-year mean (Figure 5). Since it assumes the pattern associated with upwell ing along the central coast, it will be referred to as the upwelling mode.

The second EOF mode, accounting for 14% of the variance, resembles the pattern of warmer water that appears along the coast during the periods of weaker wind, and especially during the winter when the Davidson Current is present at the surface. For this reason, the second mode will be referred to as the Davidson mode.

The third EOF mode, accounting for only 4.7% of sst variance, is less distinct, but in the vicinity of Point Conception bears some similarity to those situations where flow detaches from the western exit of the Santa Barbara Channel, to form a westward flowing jet. While this may be an arguable distinction, this third mode will be referred to as the Channel jet mode.

The fourth and fifth modes respectively account for 2.6 and 2.4% of the variance, and all higher modes individual] y correspond to less than 2% of variance.

The EOF analysis provides a decomposition of each of the 76 images in the above data set into a weighted sum of all modes. Figure 10 presents the time sequence of these weights for modes 1, 2, and 3. Note that the weights are expressed as dimensionless quantities, which the modes themselves are expressed in "C, consistent with the formalism adopted in Lagerloef and Bernstein (1988).

The time sequence of the mode 1(upwelling mode) weights are separately replotted in Figure 11, along with the 4-year time sequence of alongshore wind stress. From this figure, it is clear that the annual cycle in upwell ing mode weights corresponds well with the seasonal cycle in buoy-measured wind stress, with weakest modal amp] itude coinciding with periods of weakest alongshore windstress.

Examination of the time sequence of mode 2 and 3 weights reveals no clear annual variation, although it may be noteworthy that mode 3 (Channel jet mode) peaks sharply around mid-year in 1987, 1988, 1989, and to a lesser degree in 1990. While this may be without significance, this peaking occurs at a time of year where a longshore wind stress has peaked and is beginning to relax. From inspection of Figure 2, this corresponds to a period of poleward acceleration in surface flow at the CAMP Hidalgo mooring. There may also be a tendency for semi-annual variations in the mode 2 and 3 weights.

CONCLUSIONS

In the vicinity of Point Conception, seasonally recurrent, as well as shorter period fluctuations, in a four-year set of sea surface temperature satellite imagery, demonstrate some consistency with moored in situ single-point observations of wind and current over the same multi-year interval.

Empirical orthogonal function analysis, when applied to a selected subset of this imagery spanning the four-year period, identifies a dominant coastal upwelling mode, accounting for nearly half of the total

variance and exhibiting a well-defined annual cycle coincident with the annual cycle in alongshore wind stress. The next two modes appear to emulate patterns of coastal warming associated with the wintertime Davidson Current, and the jet-like behavior of flow exiting the Santa Barbara Channel and separating from the coast at Point Conception.

REFERENCES

Chelton, D. B., Seasonal variability of alongshore geostrophic velocity off Central California, J. Geophys. Res., 89, 3473-3486, 1984.

Hickey, B. M., The California Current system--hypotheses and facts, Prog. Oceanogr., 8, 191-279, 1979.

Kelly, K. A., The influence of winds and topography on the sea surface temperature patterns over the northern California slope, J. Geophys. Res., 90, 11783-11798, 1985.

Lagerloef, G. S. E., and R. L. Bernstein, Empirical orthogonal function analysis of Advanced Very High Resolution Radiometer surface temperature patterns in Santa Barbara Channel, J. Geophys. Res., 93,6683-6873, 1988.

McClain, E. P., W. G. Pichel, and C. C. Walton, Comparative performance of AVHRR-based multichannel sea surface temperatures, J. Geophys. Res., 90, 11587-11601, 1985.

Sheres, D., and K. E. Kenyon, A double vortex along the California Coast, J. Geoph ys. Res., 94, 4989-4997, 1989.

Table 1. SST Image Distribution

Year	D	J	F	M	A	M	J	J	A	S	O	N	Total
86/87	*14*	*14*	*15*	*16*	*14*	*8*		*14*	*12*	6	5	10	132
87/88	13	8	18	22		11	14	14	19	18	22	8 12	179
88/89	10	16	11	10	14	9	11	14	5	5	14	16	135
89/90	15	11	5	8	19	8		6	4	4	5	8 12	105
Total	53	49	49	56	53	44	37	51	39	37	33	50	551

Table 2. EOF 76-Image Subset
(year; day of year; % cloud-free)

	yr.day	%		yr.day	%		yr.day	%
1.	86.275	91	26.	88.045	95	51.	89.182	95
2.	86.298	73	27.	88.069	99	52.	89.200	78
3.	86.313	96	28.	88.086	98	53.	89.213	97
4.	86.336	96	29.	88.099	99	54.	89.242	78
5.	86.351	98	30.	88.123	98	55.	89.262	84
6.	87.010	98	31.	88,141	93	56.	89.277	98
7.	87.031	96	32.	88.188	99	57.	89.299	92
8.	87.050	97	33.	88.197	93	58.	89.320	95
9.	87.068	78	34.	88.218	83	59.	89.338	96
10.	87.086	97	35.	88.236	75	60.	89.363	99
11.	87.110	98	36,	88.271	96	61.	90.004	83
12.	87.122	97	37.	88.282	99	62.	90.025	98
13.	87.150	88	38.	88.309	99	63.	90.045	84
14.	87.168	82	39.	88.325	93	64.	90.065	72
15.	87.184	96	40.	88.335	99	65.	90.079	94
16.	87.210	95	41.	88.343	98	66.	90.102	88
17.	87.231	75	42.	89.002	99	67.	90.120	93
18.	87.249	86	43.	89.017	94	68.	90.144	89
19.	87.276	96	44.	89.042	70	69.	90.155	98
20.	87.278	98	45.	89.062	85	70.	90.183	98
21.	-87.311	95	46.	89.076	99	71.	90.228	91
22.	87.331	97	47.	89.096	98	72.	90.242	91
23.	87.347	85	48.	89.121	98	73.	90.267	90
24.	87.359	92	49.	89.145	72	74.	90.282	98
25.	88.023	99	50.	89.164	96	75.	90.309	98
						76.	90.326	97

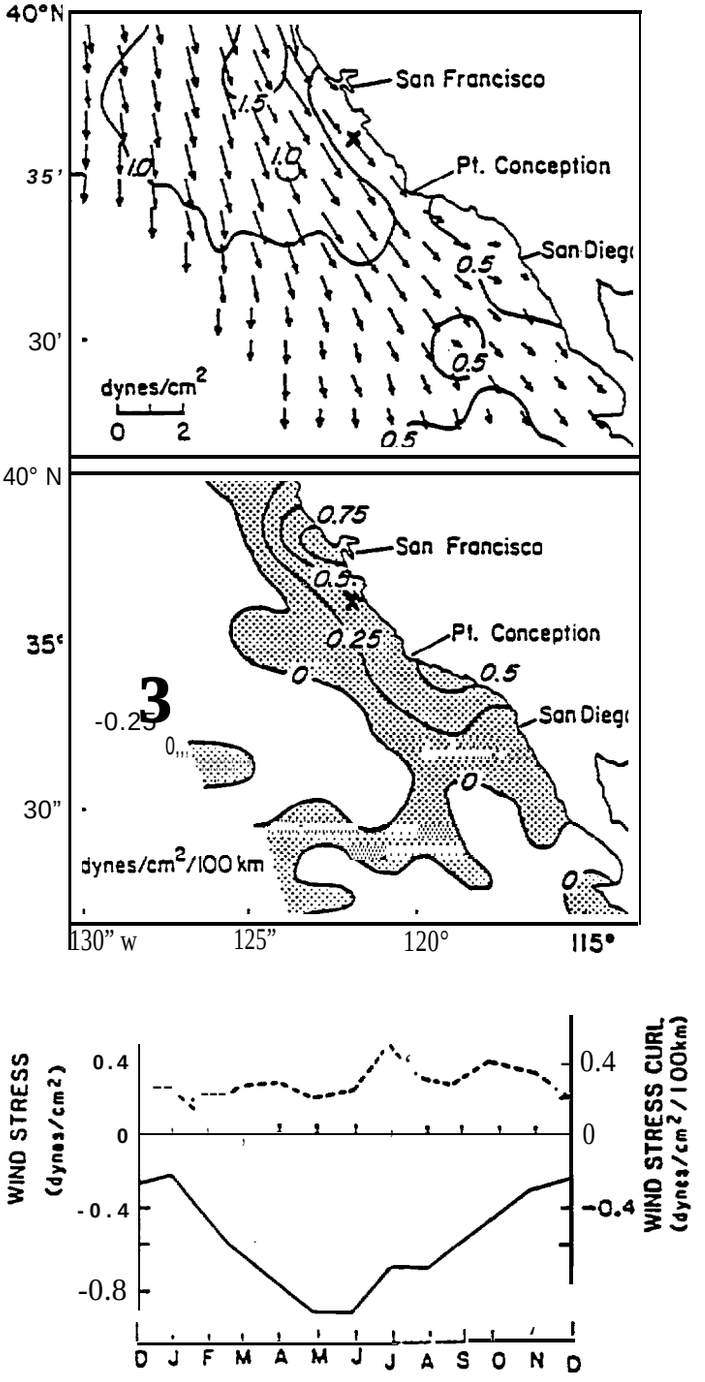

Figure 1. Climatological mean wind stress and stress curl along California; annual variation of same atapoint just offshore Monterey (from Shelton, 1984).

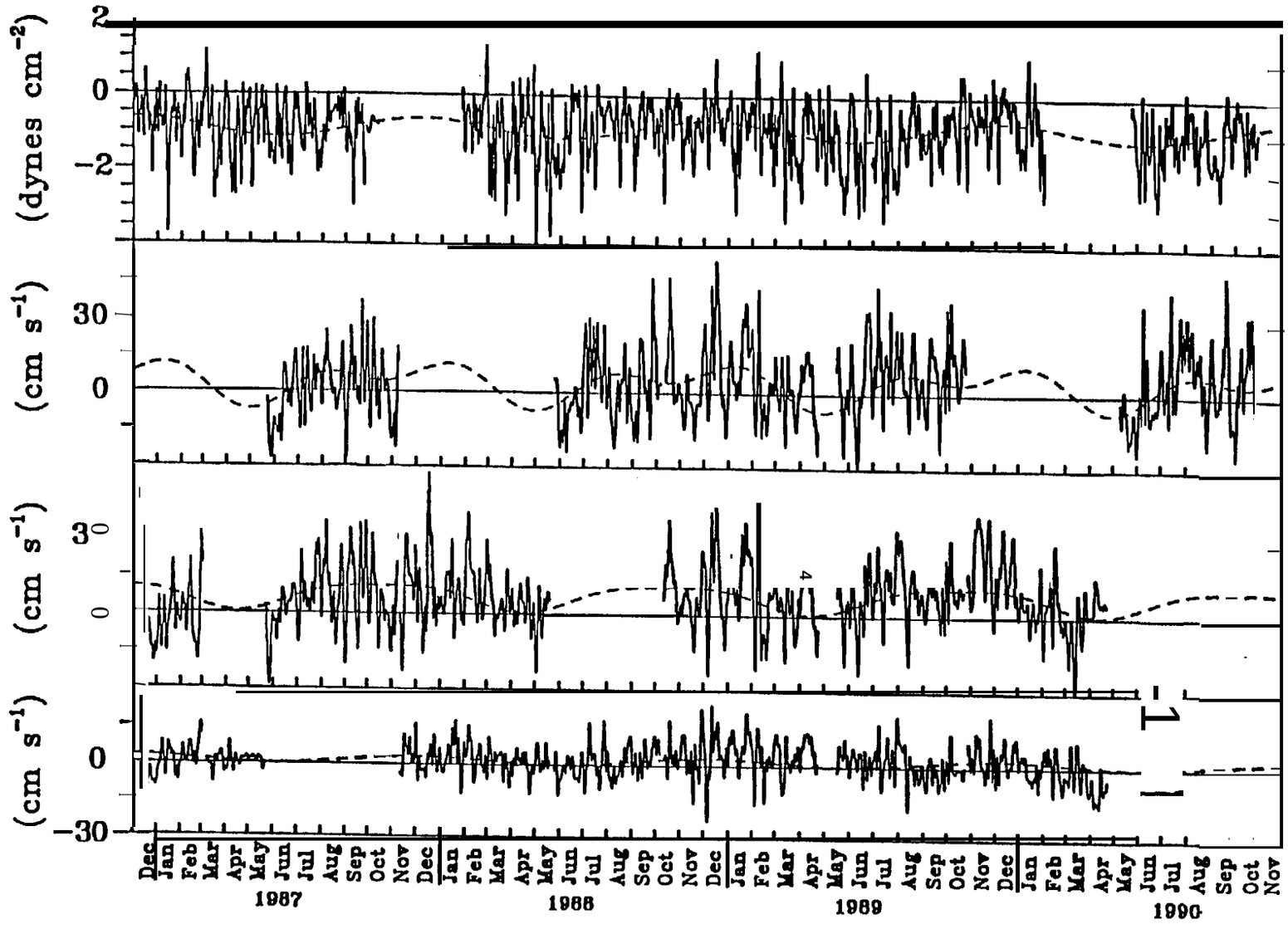

Figure 2. Four-year time sequence of alongshore surface wind stress, and currents at 12, 54, and 126 m depth, at locations 20 km offshore Point Conception, California (from Savoie et al., 1991).

SST
°C
22
20
18
16
14
12
10
8
°N
34
35
36
120
121
122
121°W
DEC 86
1
7
14
21
28

SST
°C
22
20
18
16
14
12
10
8
°N
34
35
36
120
121
122
121°W
DEC 86
1
7
14
21
28

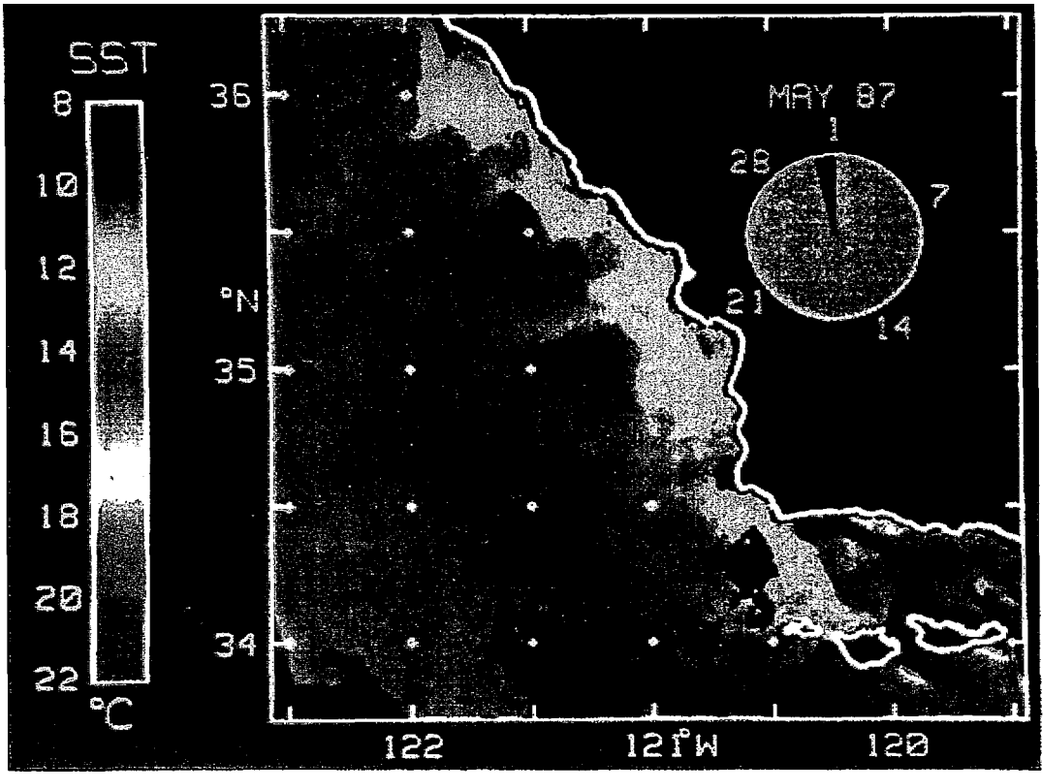

Figure 3c. Satellite sst imagery from 30 May 87, illustrating temperature patterns associated with upwelling along the California central coast.

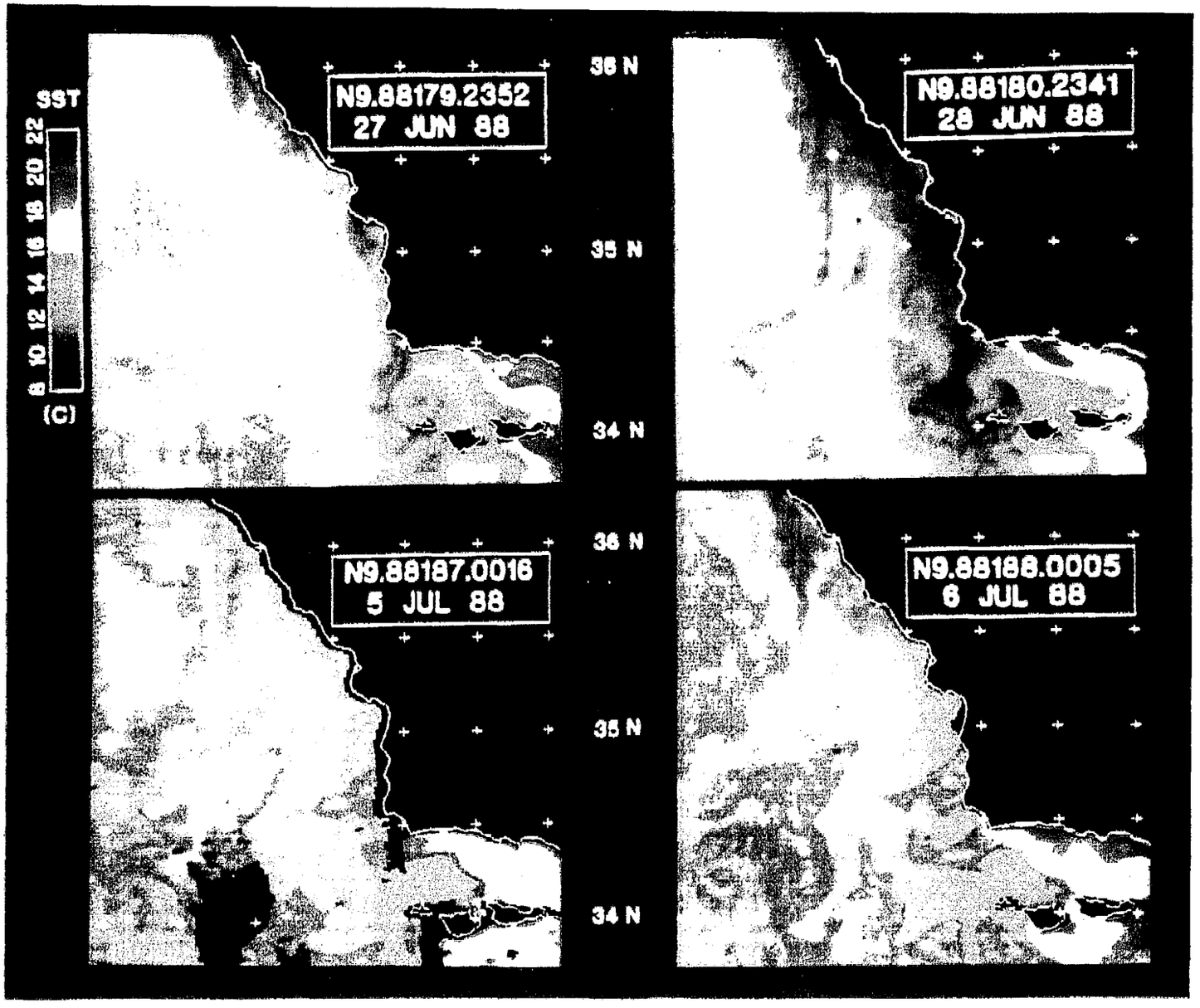

Figure 4. Satellite sst imagery from 27 and 28 Jun, 5 and 6 Jul 1988 illustrating short-term relaxation of upwelling patterns.

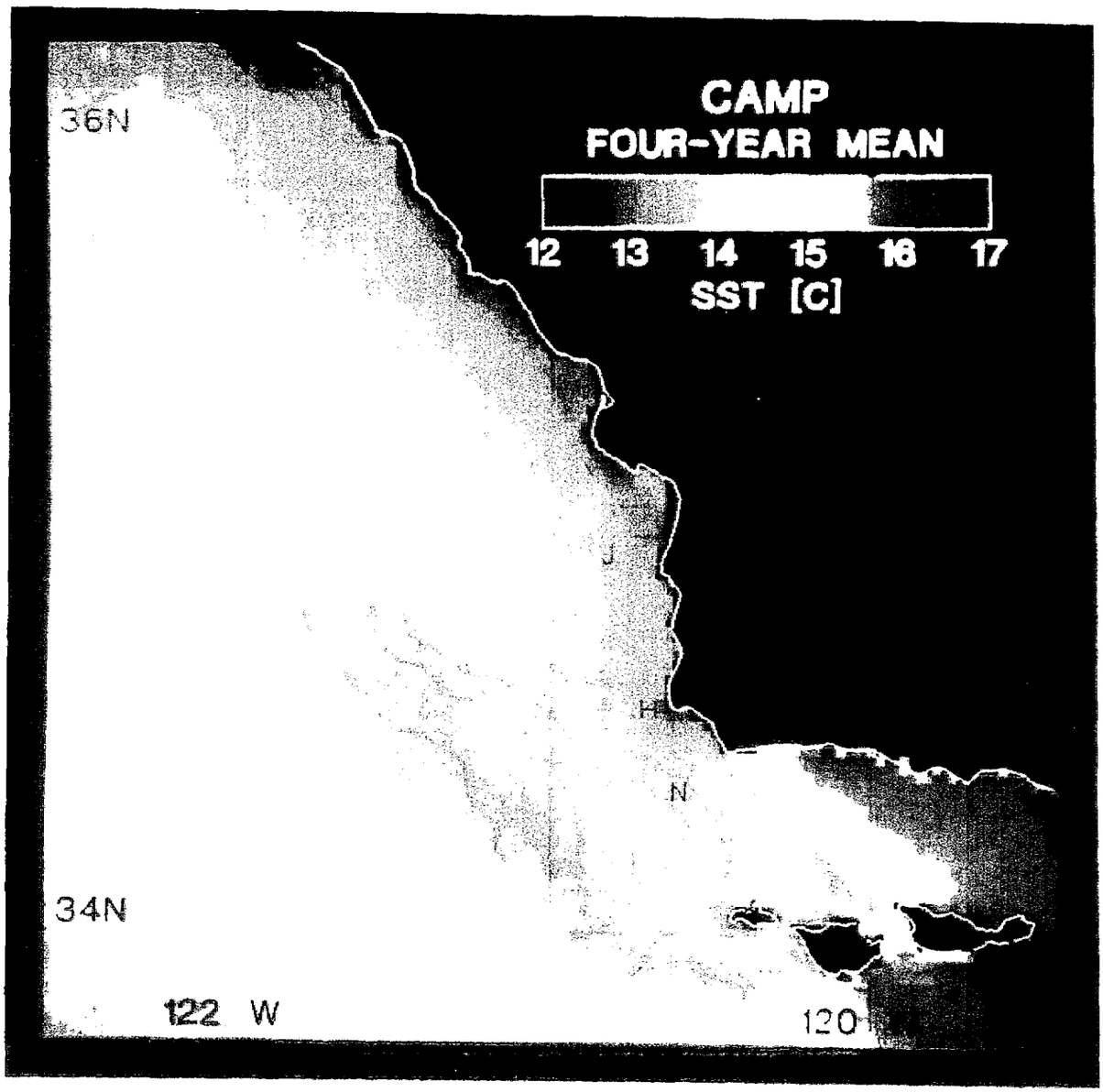

Figure 5 Four-year mean of 76 selected sst images

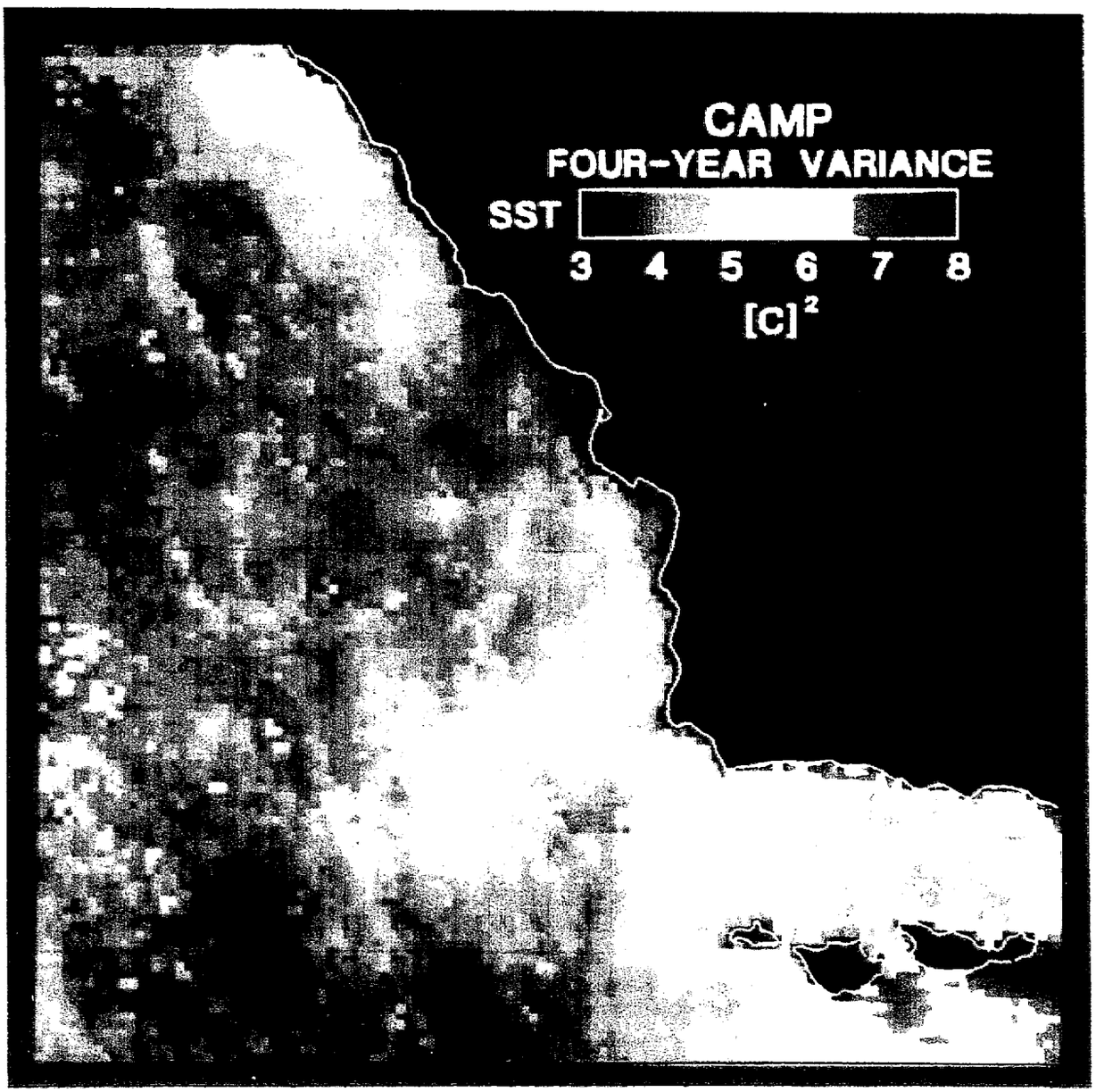

Figure 6. SST variance derived from four-year set of 76 selected sst images.

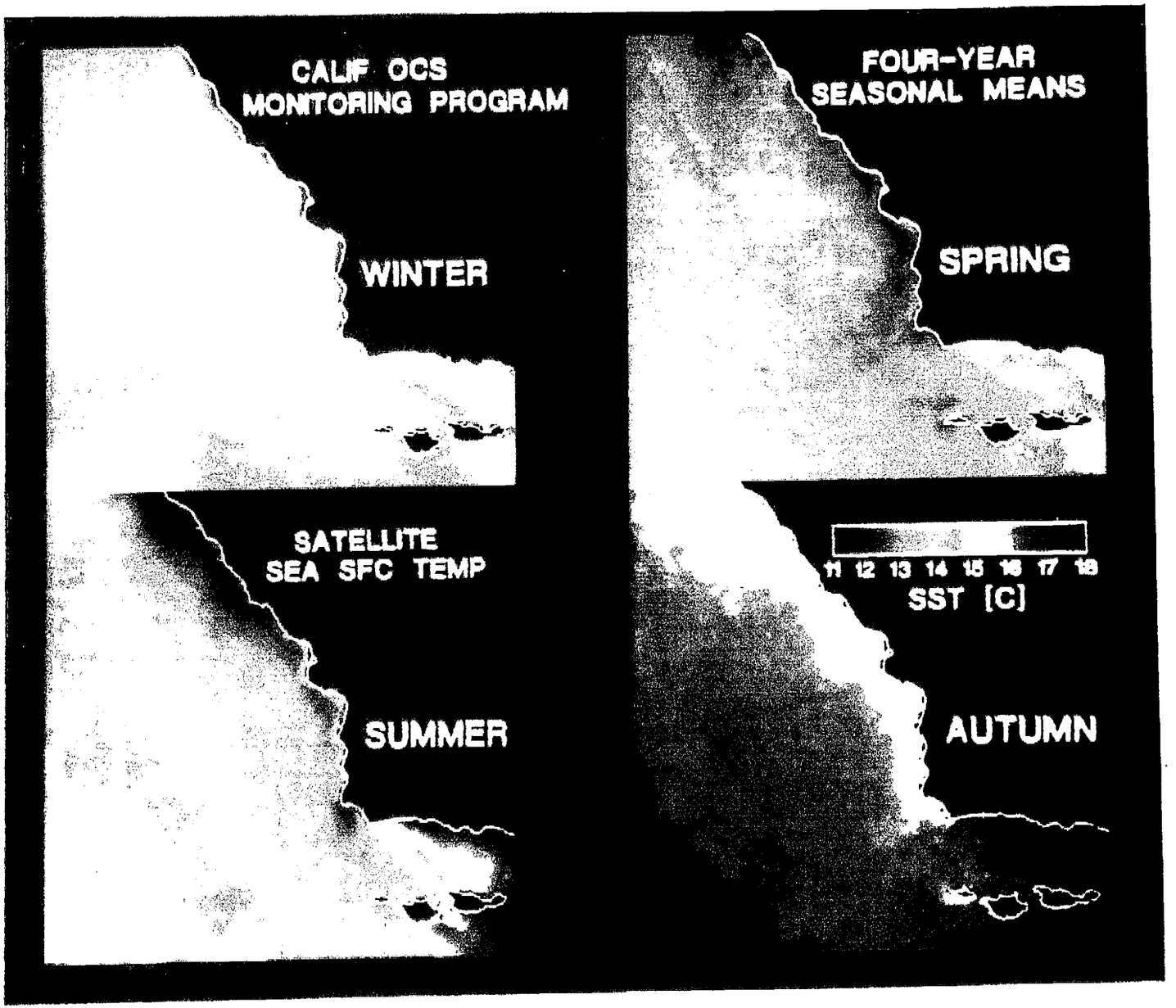

Figure 7. Winter, spring, summer, and autumn means, constructed from selected 76-image data set.

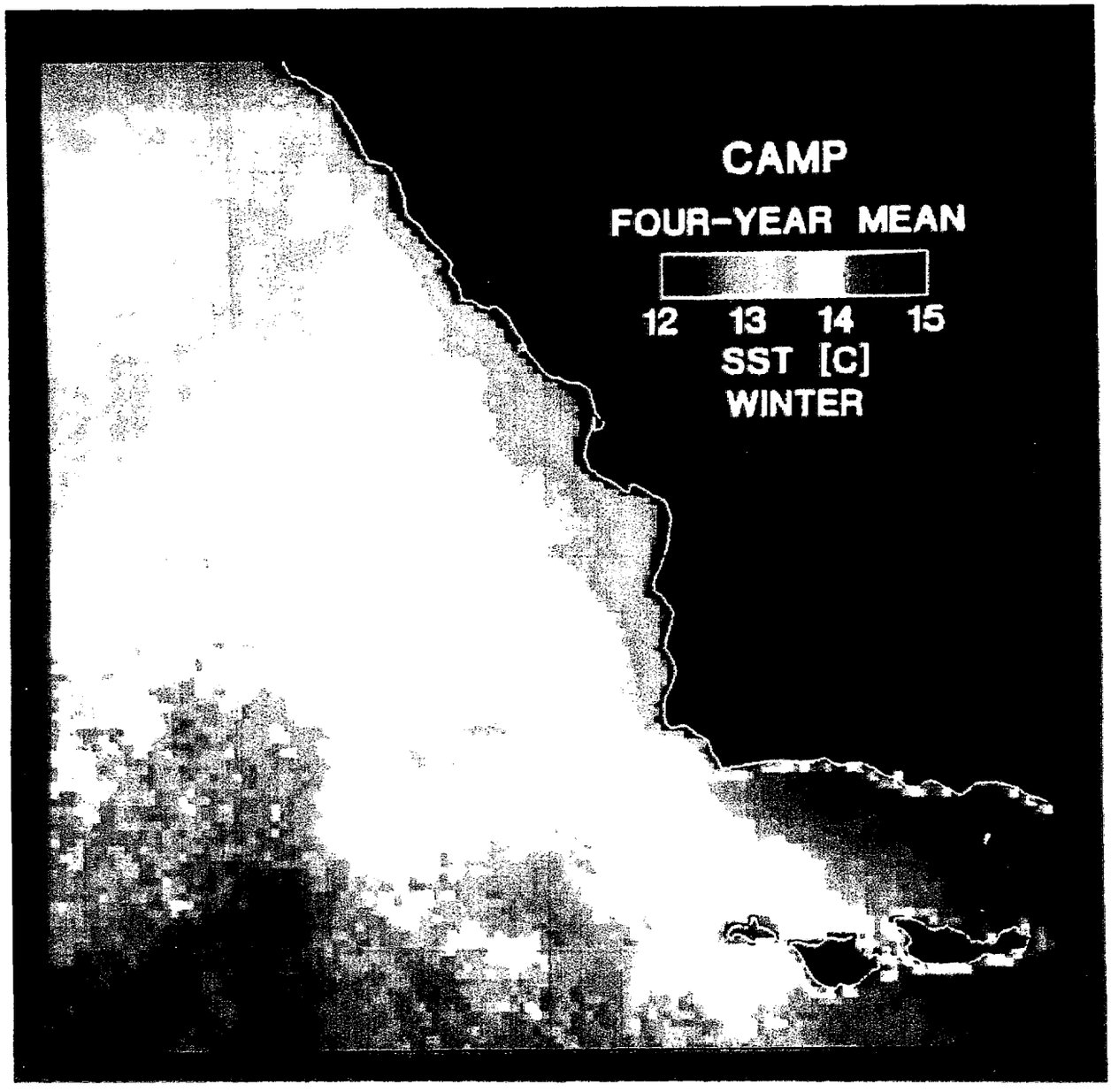

Figure 8. Winter mean image of Figure 7, enhanced over narrower temperature range.

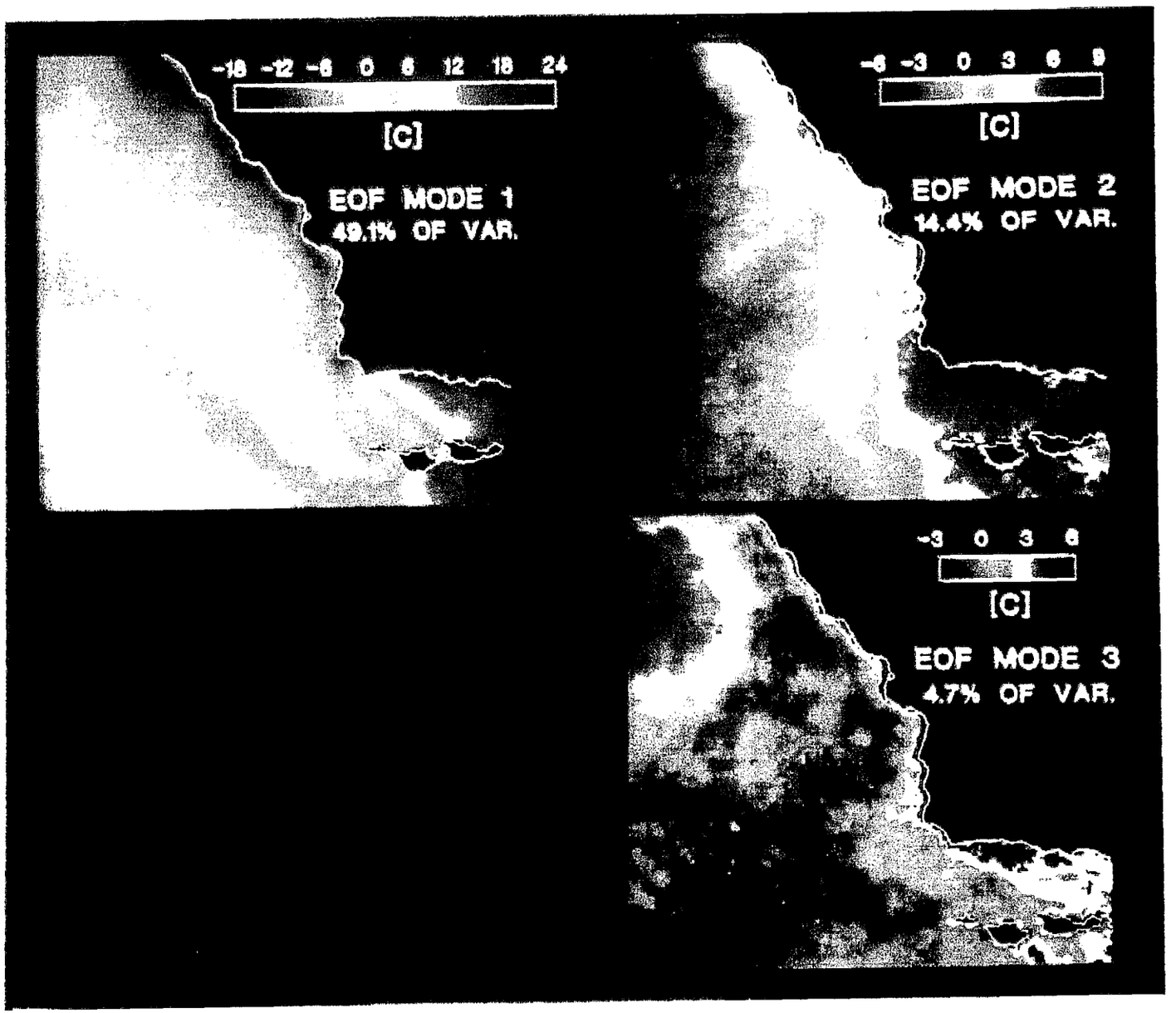

Figure 9. First three dominant spatial EOF modes derived from 76-image data set.

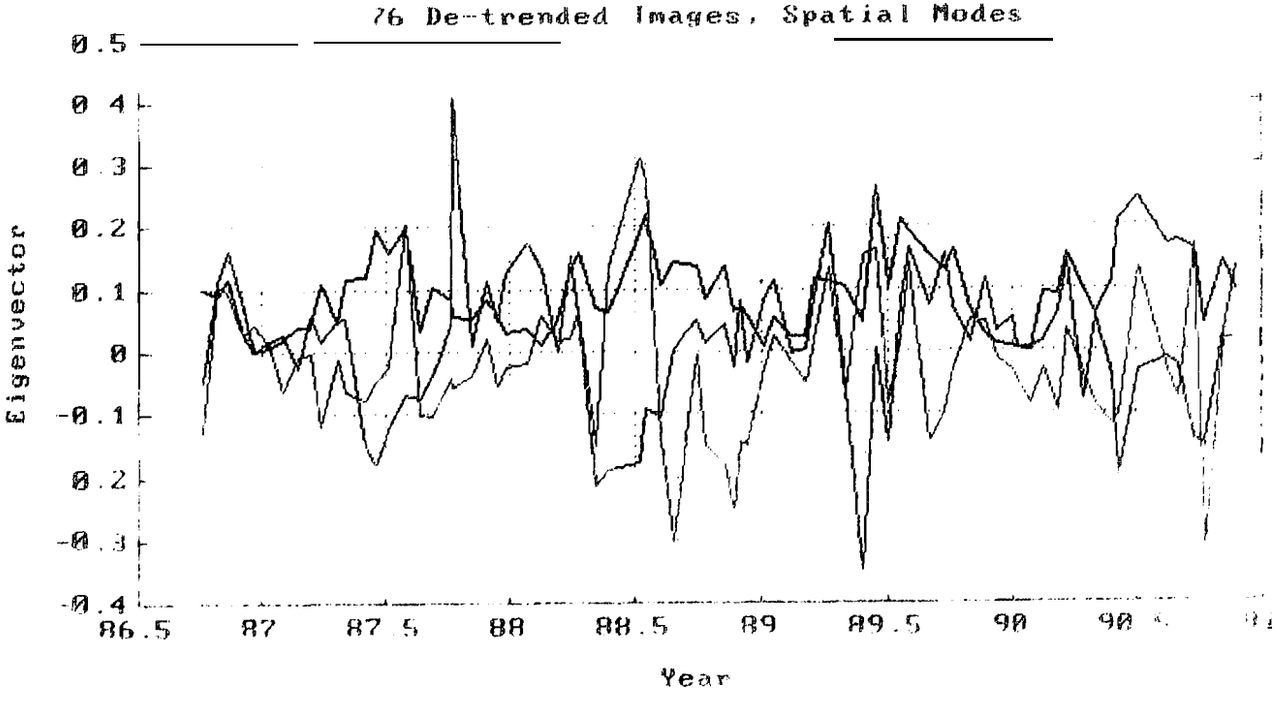

Figure 10. Time sequence of weights of modes 1, 2, and 3, for all 76 images in selected sst data set.

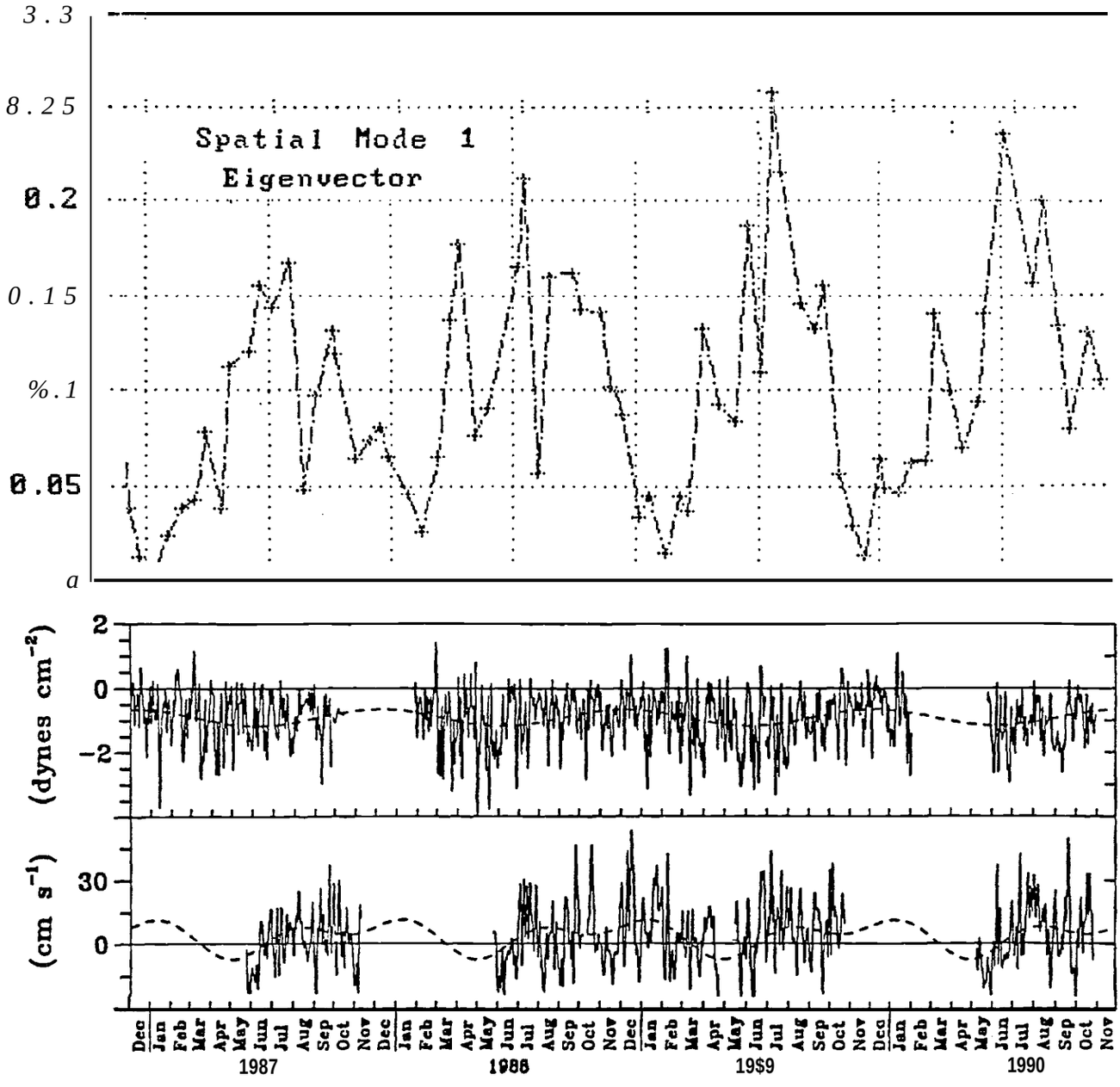

Figure **11.** Time sequence of mode 1 weights co-plotted with wind stress and 12 m depth current time series (repeated from Figure 2).

6. TEMPORAL AND SPATIAL CHANGES IN THE CONCENTRATION OF HYDROCARBONS AND TRACE METALS IN THE VICINITY OF AN OFFSHORE OIL PRODUCTION PLATFORM

MARGARETE STEINHAUER

Consultant
145 Abrams Hill, Duxbury, Massachusetts 02332, USA

ERIC CRECELIUS

Battelle Pacific Northwest Laboratory, Marine Research Laboratory
439 West Sequim Bay Road, Sequim, Washington 98382, USA

&

WILLIAM STEINHAUER

Battelle Ocean Sciences, Marine Chemistry Department
397 Washington Street, Duxbury, Massachusetts 02332, USA

INTRODUCTION

The California Outer Continental Shelf (OCS) Phase II Monitoring Program (CAMP) was designed and conducted to monitor potential short- and long-term environmental changes resulting from oil and gas development activities off the coast of Southern California. The 4-year multidisciplinary study, conducted between October 1986 and October 1991, was sponsored by the Minerals Management Service (MMS) of the Department of the Interior and focused on (1) detecting physical, chemical, and biological changes around oil and gas platforms and (2) determining whether observed changes could be attributed to drilling-related activities or to natural processes.

One element of the monitoring program was conducted near Chevron's Platform Hidalgo, a high-energy hard-bottom (rocky-substrate) region located off Point Arguello in the western reaches of the Santa Barbara Channel in southern California. The sampling design consisted of an array of nine stations at varying distances (0.5 km in the nearfield to ≈6 km in the farfield) from the platform (Fig. 1). Because the strategy of the sampling design was to monitor drilling-related effects on hard-bottom benthic communities, monitoring dose-response gradients was limited by the geographic distribution of the hard substrate. Drilling of the first well at Platform Hidalgo began in November 1987 and drilling activities at the platform continued until January 1989. Over the 4-year field program, samples were collected before, during, and after drilling operations at this platform. During the period of study, drilling activities were also being conducted at three additional platforms (Hermosa, Harvest, and Irene) in the vicinity of the study area. Figure 2 illustrates the location of the CAMP study areas, platforms in the immediate region, and CAMP sample collection surveys in relation to drilling/discharge periods at all four platforms.

A second component of CAMP included a 3-year monitoring study at a site proposed for the location of Platform Julius. Environmental concerns about onshore facilities associated with the proposed Platform Julius have delayed its installation. Therefore, because the platform has not been installed, all data collected from the Platform Julius site represented predrilling background conditions and were used for comparison with data from the Platform Hidalgo site. The proposed Platform Julius site is located on the continental shelf approximately 30 km northwest of Platform Hidalgo (see Fig. 2), and is in an area not likely to be affected by discharges from other platforms or by anthropogenic contaminants.

A comprehensive 3-year report of the overall monitoring program has been published (Steinhauer & Imamura, 1990). The background environmental conditions of both the Platform Hidalgo and Platform Julius monitoring areas have been described by Hyland *et al.* (1990) and Hyland *et al.* (Chapter 9). This paper discusses the hydrocarbon and trace metal chemistry of sediments at the Platform Hidalgo site, and examines natural variability and the effects of drilling operations on changes in sediment chemistry. Results of other elements of the study are discussed by Brewer *et al.* (in press), Coats (Chapter 8), Hardin *et al.* (Chapter 7), Hyland *et al.* (Chapter 9), Montagna (in press), Parr *et al.* (Chapter 3), Savoie *et al.* (Chapter 4), and Steinhauer *et al.* (Chapter 2).

METHODS

As shown in Fig. 2, three sampling surveys were conducted to collect predrilling background data from the Platform Hidalgo site and to examine annual seasonal variability in chemical parameters. Surface sediments were sampled during several cruises: October 1986 (CAMP l-l), May 1987 (CAMP 1-3), and October 1987 (CAMP 2-3). Although sediment traps were deployed at all stations in October 1986, prior to drilling the first well at Platform Hidalgo, fouling prevented recovery of the traps from all but two stations (PH-I and PH-U) in May 1987 (CAMP 1-3). During the period of drilling activities at Platform Hidalgo (November 1987 through January 1989), sediment traps, deployed in January 1988 and May 1988, were sampled in May 1988 (CAMP 2-5) and October 1988 (CAMP 3-l), respective y. Surface sediments were also collected during the October 1988 survey. Four additional sampling surveys, conducted in May 1989 (CAMP 3-4), October 1989 (CAMP 4-l), May 1990 (CAMP 4-2), and October 1990 (CAMP 5-1) were conducted to collect postdrilling and seasonal-variability data. Surface sediments were collected during all four postdrilling surveys; sediment traps were sampled in May 1989, October 1989, and retrieved in October 1990, at the end of the field program.

Paired samples for chemical and sedimentological analyses were collected from each station sampled during the 4-year field program. Analyses were performed on surface (O-2 cm) sediments, material collected in sediment traps, and samples of drilling muds and cuttings. In addition, samples of oil from a production well, the Isla Vista seep, and representative tar balls were analyzed for hydrocarbon content and composition.

Sample Collection

A Kynar®-coated 0.1 -m^2 modified vanVeen grab sampler was used to collect surface sediments from soft-bottom substrate adjacent to hard-bottom rock features at each station during each sampling survey. The O- to 2-cm surface sediment of three replicate grab samples was subsampled for hydrocarbon, trace metal, total organic carbon (TOC), and sediment grain-size analyses. Sediment samples for hydrocarbon and trace metal analysis were frozen (-20 “C) in solvent-rinsed glass containers. The three rep] icate subsamples, collected at each station for each type of analysis, were

pooled prior to laboratory analysis. Chemical and sedimentological analyses were conducted on the pooled replicate sediment samples from each station.

Material collected in sediment traps was used to estimate sediment flux and to determine chemical dose of drilling-related contaminants. Three replicate time-integrated (= 5-6 months) samples were obtained from cylindrical sediment-trap arrays deployed 1 m above the seabed at each Platform Hidalgo station and from a station near Platform Harvest, a production site approximately 3 km southeast of Platform Hidalgo (Fig. 1). Material collected in the traps was preserved in the field with sodium azide. Immediately after retrieval, sediment-trap samples were frozen at -20 'C until analysis. Chemical and sedimentological analyses were conducted on each replicate sample from each station.

Five wells at Platform Hidalgo were sampled for drilling muds and drill cuttings at depths between 400 and 4000 m. At each well, duplicate samples of drilling muds were obtained from four depth intervals: near-surface (= 500-550 m), midwell (= 800-1000 m), near-bottom (= 2300-3300 m), and bottom (= 2600-4000 m). Drill cuttings from a shale shaker were collected in duplicate from the near-surface (=400 m), midwell (= 1200-1800 m), and bottom (= 2400-3700 m) of each well. Aliquots of samples collected at the same depth from all five wells were pooled before analysis. Drill cuttings were also obtained from a desilter at the midwell depth of some wells and aliquots of these samples were also pooled prior to analysis. All samples of drilling muds and cuttings were collected in plastic containers and frozen at -20 'C until analysis.

Oil samples from a production well were obtained from MMS. Petroleum samples from the Isla Vista seep, located southeast of the Platform Hidalgo study area off Coal Oil Point near Santa Barbara, were provided by Dr. Robert Spies of Applied Marine Sciences, Inc., Livermore, CA. Tar balls and fragments, removed from surface sediments obtained from the study area, were collected for anal ysis.

Quality Assurance/Quality Control (QA/QC)

The hydrocarbon and trace metals analytical program for this study was conducted under a rigorous laboratory-wide QA program (Steinhauer & Steinhauer, 1990; Crecelius, 1990). Internal QC included initial and ongoing determinations of analytical precision and accuracy through analysis of

control materials. Approximate y 15% of all analyses were QC samples and included method blanks, spiked matrix blanks, standard reference materials, certified reference materials, and duplicates.

Analysis of Grain Size and Total Organic Carbon (TOC)

Sediment grain size was analyzed by using sieve and pipette methods described by Plumb (1981). Sediment particles $>62\ \mu m$ in diameter were separated into eight size classes by mechanical wet sieving through nested sieves. Silt and clay particles ($<62\ \mu m$) were fractionated by pipette analysis based on Stokes' Law correlating settling velocity with particle size.

Concentrations of TOC in surface sediments were determined with a LECO carbon analyzer according to the methods of Bandy & Kolpack (1963) and Van Andel (1964). Measured concentrations of total carbon and carbonate carbon were used to calculate TOC (Kinney *et al.*, 1990).

Analysis of Hydrocarbons

Samples were prepared for analysis of saturated and aromatic hydrocarbons by solvent extraction followed by column chromatography cleanup. From the pooled homogenized sample replicates, a 50-g (wet weight) subsample was extracted with 100 mL methanol to remove water. After centrifugation, the methanol was decanted and 10 μg each of the quantification internal standards (QIS), androstane and ortho-terphenyl, was added to the sample. Samples were extracted three times with dichloromethane (DCM)/methanol (9: 1, v/v). The combined extracts were acidified with 100 mL 0.1 M HCl. After separation, the aqueous phase was back-extracted with DCM and the extract was combined with the original solvent extracts. The combined extracts were dried with anhydrous sodium sulfate and concentrated by Kuderna-Danish (K-D) techniques to ≈ 4 mL. Sulfur was removed from the concentrated extract with 0.5 g activated copper. The DCM extract was exchanged for hexane and concentrated to ≈ 4 mL with a stream of nitrogen gas. Total extractable lipid was determined gravimetrically to ensure that the amount of extract applied to the chromatography column contained no more than 50 mg lipid. A silica gel/alumina (11:1, w/w) column was charged with the extract, and the F_1 saturate and F_2 aromatic hydrocarbon fractions were eluted with 18 mL hexane and 21 mL DCM/acetone (1/1, v/v), respectively. The eluates were combined and concentrated to 10 mL by K-D techniques, and further reduced to 500 μL by nitrogen gas evaporation. For samples of tar

balls, concentrations of saturated and aromatic hydrocarbons were also determined gravimetrically by separately weighing the F_1 and F_2 fractions. Prior to analysis, 10 μg of each recovery internal standard (RIS), cholestane and chrysene-d 12, was added to the extract.

Extracts were anal yzed for saturated and aromatic hydrocarbons by coupled gas chromatography/mass spectrometry (GC/MS) using a Hewlett-Packard model 5970 GC/MSD and companion computer-based data system. Specific operating conditions of the GC/MS system, and identification and quantification of analytes are described by Steinhauer & Steinhauer (1990). The saturated hydrocarbon compounds determined for this study included the straight-chain hydrocarbons, n-C_{10} to n-C_{34}, and the branched-chain hydrocarbons, pristane and phytane. Saturated hydrocarbons were quantified relative to their response to 5-α-androstane, a pentacyclic sterane. Polynuclear aromatic hydrocarbon (PAH) compounds included (1) the parent compound and alkylated homologs of naphthalene, fluorene, phenanthrene, and dibenzothiophene, and (2) fluoranthene, pyrene, benz[*a*]anthracene, chrysene, benzo[*b*]fluoranthene, benzo[*k*]fluoranthene, benzo[*a*]pyrene, benzo[e]pyrene, and perylene. The PAH compounds were quantified relative to their response to ortho-terphenye. The concentration of total resolved (i.e., GC/MS peaks) plus unresolved (chromatographic "hump") saturated and aromatic hydrocarbons is referred to as total hydrocarbons (THC; see Table 1).

Analysis of Trace Metals

Surface sediments, material collected in sediment traps, and drilling muds and cuttings were also analyzed for 11 trace metals, including barium. Samples were freeze-dried and blended. Surface sediments were additionally ground in a ceramic ball mill and drill cuttings were sieved through a 1.5-mm-mesh screen to remove large particles.

For sediments anal yzed by energydispersive x-ray fluorescence (XRF), a 0.5-g aliquot of ground sediment was pressed into a 2-cm-dia pellet (Nielson & Sanders, 1983). For analysis by atomic absorption spectrometry, a O. 2-g aliquot of sediment was digested with $HNO_3/HClO_4/HF$ in a Teflon bomb. Drilling muds and cuttings, and material collected in sediment traps were digested using microwave techniques modified from Nakashima et *al.* (1988).

Arsenic, barium, chromium, copper, nickel, lead, vanadium, and zinc in surface sediments were analyzed by XRF. Cadmium and silver were analyzed by Zeeman graphite-furnace atomic absorption spectrometry (ZGFAA) with a matrix modifier of ammonium phosphate (Bloom, 1983). In drilling muds and cuttings and in material collected in sediment traps, silver, cadmium, nickel, lead, and vanadium were analyzed by ZGFAA; copper, chromium, and zinc were analyzed by flame atomic absorption spectrometry. Neutron activation was used to analyze barium in drilling muds and cuttings and in material collected in sediment traps. Mercury was analyzed by cold-vapor atomic absorption spectrometry similar to the method described by Bloom & Crecelius (1983).

Analysis of Data

Data for individual hydrocarbon analytes and trace metals, acquired from instruments, were electronically transferred as ASCII files to a Digital Equipment Corporation VAX™ 11/750 computer for data reduction and for storage in a permanent database. The data set for each survey was reduced and summary statistics were calculated. Hydrocarbon data were reduced to selected diagnostic parameters and ratios (see Table 1). Reduced data were transferred to spreadsheet software to produce tables and graphics.

One-way analyses of variance (ANOVA) were conducted to determine statistically significant temporal and spatial trends, and patterns in the concentrations of chemical parameters. Both hydrocarbon and trace-metal data sets were analyzed by identical statistical routines because chemical analyses for both were performed on the same samples (i.e., splits of each replicate collected). ANOVAs were conducted using the general linear-model procedure in Statistical Analysis System (1985). A value of $\alpha = 0.05$ was selected.

Power analyses, using two-tailed t-test comparisons, were performed according to procedures described by Green (1989) and are described more thoroughly by Hyland *et al.* (Chapter 9). Percent detectable change was examined at a sample size (n) of three and at $\beta = 0.20$ ($\alpha = 0.05$).

RESULTS/DISCUSSION

Characterization of Surface Sediments

Surface sediments adjacent to most hard-bottom substrates in the study area were generally characterized by a high percentage (72% ± 9%) of fine material (<62 pm), At three stations (PH-K, PH-N, and PH-R) along an offshore transect southwest of Platform Hidalgo, grain size was consistent y coarser, averaging only 36% ± 6% fine material. Figure 3 illustrates the mean percent tine sediment and the ranges measured over all surveys at individual stations. Over time, grain size varied by approximately 20% at all stations except at the farfield stations PH-U and PH-W, where fine material varied by 40%.

Concentrations of TOC in study area sediments varied narrowly at individual stations, and ranged between 3.0 and 13.7 mg/g dry sediment (Fig. 3). Averaged over all stations and sampling times, the TOC concentration was 8.8 mg/g dry sediment. Overall, TOC concentrations were generally within ranges reported by SAIC (1986) for sediments in the same offshore region. As shown in Fig. 3, particularly at stations PH-K, PH-N, and PH-R, TOC was weakly correlated (r = 0.53 at α = 0.05) with the sediment fine fraction.

Hydrocarbon Chemistry

Saturated Hydrocarbons

The GC/MS-determined total hydrocarbon (THC) concentrations in surface sediments around Platform Hidalgo are shown in Fig. 4. At individual stations, the temporal mean THC concentrations ranged between 24 and 180 μg/g dry sediment and averaged 69 ± 13 μg/g over all stations and sampling surveys (n = 62). The range and grand mean for Platform Hidalgo sediment THC concentrations are very similar to the 3-year (n = 137) range (22-193 μg/g) and grand mean (62 ± 48 μg/g) measured at the proposed Platform Julius control site (Steinhauer & Steinhauer, 1990), and are also within the range reported by SAIC (1986) for sediments from the same offshore region and by Reed *et al.* (1977) for the basins of the southern California borderland.

Concentration ranges for THC were similar in sediments from both nearfield and farfield stations, Normalizing THC concentrations to the fine sediment fraction did not reduce spatial variability that

may have been attributed to a difference in sediment grain size. Instead, normalizing THC concentrations to the fine sediment fraction increased the variability in THC concentrations by a factor of ≈ 1.5-4 over THC concentrations that were not normalized. Pearson's correlation coefficients revealed that THC was not highly correlated (r = 0.36 at α = 0.05) to the fine sediment fraction or to TOC concentrations (r = 0.26 at α = 0.05). These results suggest that hydrocarbons in surface sediments of the study area are not specifically y associated with silt/clay particles or with TOC. The occurrence of discrete small tar particles originating from natural seepage would be consistent with our results.

Examination of the hydrocarbon data over time (Fig. 5a) shows that THC concentrations increased two- to three-fold in sediments from all stations, including the farfield control stations PH-U and PH-W, sampled in October 1988 (during drilling). Although this short-term area-wide increase in THC concentrations may appear to reflect low-level input related to drilling activities at Platform Hidalgo, it more likely represents variability related to natural input (e.g., seep-related materials) to the region.

Several features of the GC/MS total-ion and extracted-ion (m/z 57) chromatograms of the sediment extracts revealed evidence of petroleum input throughout the study area. The largest component of the THC concentration was consistently the unresolved complex mixture (UCM). The UCM, which is an elaborate mixture of branched, cyclic, and partially degraded hydrocarbons that cannot be individually identified by the chromatography techniques employed, generally reflects a petroleum input (Barrington & Tripp, 1977; Reed et *al.*, 1977; Wakeham & Barrington, 1980; Kennicutt *et* al., 1987;) and is a feature of most weathered oils (Barrington et al., 1973; Barrington & Meyers, 1977; Reed *et al., 1977).* Generally, UCM comprised 50% or more of the THC concentration of the sediments from all Platform Hidalgo stations and, in samples collected during October 1988, accounted for 80% or more of the THC (Fig. 5b). A large UCM component is not an unusual feature of sediments from the southern California offshore environment and is characteristic of sediments from a large region of the Southern California Bight (Reed & Kaplan, 1977; Reed *et al.*, 1977; Simoneit & Kaplan, 1980), and from the Santa Maria Basin and western Santa Barbara Channel (SAIC, 1986). In the region of the Isla Vista marine oil seep, Stuermer *et al.* (1982) reported that the UCM was a dominant feature of not only the seep oil, but also of the sediment near the seep as well as sediment from a control station ≈ 1 mile from the seep.

Total resolved alkane (n-C_{10} through n-C_{34}) concentrations, which reflect both biogenic and petrogenic input to the sediments, varied between 0.44 and 2.8 μg/g dry sediment, a relative] y small proportion of the THC concentration (1-3%, except May 1987 samples that averaged 10%; Fig. 5c). Based on analyses performed by Reed and Kaplan (1977), the n-alkane component of seep oils from offshore Santa Barbara represents only 2-3 % of the total hexane extract; the branched and cyclic hydrocarbons, manifested as UCM, account for > 95% of the total extract. Seep-related petroleum components of the sediments, therefore, can account for part of the elevated THC concentrations observed in the October 1988 samples, but contribute less significant y to the total resolved alkane concentrations (i.e., the concentrations of total alkanes in the October 1988 sediments were not elevated relative to THC; see Fig. 5c).

Chromatograms of sediment extracts also revealed that the n-alkanes were typically characterized by odd-carbon dominance in the n-C_{25} to n-C_{31} range ('Fig. 6) and that the most abundant alkane was n-C_{29} or, in several samples, n-C_{31}. These features are typical of sediments receiving saturated hydrocarbon input derived primarily from terrestrial plants (Wakeham & Barrington, 1980). The odd/even preference index (OEPI; Barrington & Tripp, 1977), which measures the ratio of odd- to even-carbon alkanes in the n-C_{25} to n-C_{31} range, varied between *3* and 30 for all samples analyzed, and was largest in samples collected during the postdrilling October 1990 survey. The ratio of odd- to even-carbon n-al kanes is close to 1 in most petroleum samples (0.8 in the production oil analyzed as part of this program) and increases as biogenic hydrocarbons become the dominant components.

The concentrations of low-molecular-weight alkanes in the n-C_{10} to n-C_{20} range were typically very low (c 0.03 μg/g), suggesting little evidence of fresh petroleum in the sediments. In several samples, n-C_{15} was relatively prominent. As discussed by Blumer *et al.* (1970), this alkane commonly is associated with some marine plant species. Concentrations of the isoprenoid hydrocarbons, pristane and phytane, which are primarily biogenic and petrogenic in origin, respectively, were remarkably similar for all samples analyzed (n = 62), and ranged from 0.03 to 0.13 μg/g dry sediment. Over all sampling surveys and stations, pristane/phytane ratios ranged narrowly between 0.9 and 1.5, and were most frequently near 1, suggesting evidence of some petroleum in the sediments. For the production oil and tar ball sample, this ratio was 0.75 and 0.80, respectively. The composition of the Isla Vista seep oil was much more enriched in phytane than either the production oil or the tar ball samples, and resulted in a pristane/phytane ratio of 0.29.

The saturated hydrocarbon distributions of the sediment samples collected for this study appear to result from a blend of petrogenic sources (e.g., large UCM; phytane) and biogenically derived plant waxes (e.g., n-C_{25}, n-C_{27}, n-C_{29}, and n-C_{31}). These features can be considered representative of the natural characteristics of sediments from the southern California OCS (Reed & Kaplan, 1977; Reed et al., 1977; Simoneit & Kaplan, 1980; SAIC, 1986).

Because of the uniformly large UCM component of sediments from both the Platform Hidalgo site and the proposed Platform Julius control site (Steinhauer & Steinhauer, 1990), it is probable that sediments in a large region of the Santa Maria Basin and western Santa Barbara Channel are exposed to chronic low-level petroleum input emanating from oil seeps in the region. During the CAMP study, many small tar balls and tar fragments were found in many sediment samples collected for macroinfaunal analysis and for mineralogical analysis. The fragments observed in the sediment samples collected for this program varied in appearance from relatively fresh petroleum to extremely weathered tar chips (Kinney et al., 1990). Barrington & Tripp (1977) suggest that a significant UCM in otherwise unpolluted sediments may be explained by a tar particle flux to the sediments from the overlaying water column. As discussed by Kinney *et al.* (1990), poleward transport of tar particles by the California countercurrent from offshore seep areas is consistent with sediment mineralogical trends observed in study area sediments.

Aromatic Hydrocarbons

Total resolved polynuclear aromatic hydrocarbon (ΣPAH) concentrations in surface sediments ranged between 0.01 and 0.2 μg/g and typically comprised only O. 1-0.3% of the THC. Figure 7 presents the concentrations of ΣPAH in surface sediments collected from all Platform Hidalgo stations during the seven sampling surveys. Except at three stations sampled in October 1986, PAHs were consistently detected at very low concentrations before, during, and after drilling at Platform Hidalgo. Sediments collected from stations PH-J, PH-K, and PH-R during the predrilling October 1986 survey revealed relatively higher (by a factor of 2-10) concentrations of PAHs than were detected at all other locations sampled in October 1986 and at all stations sampled during and after drilling.

Inspect ion of the PAH composition of all samples collected revealed that the dominant aromatic hydrocarbon occurring in the sediments was nearly always perylene, which ranged in concentration between 0.007 and 0.22 μg/g. It has been suggested that perylene, a 5-ring PAH, is formed from

biologically derived precursors under reducing conditions and is commonly detected in marine sediments (Wakeham, 1977; Wakeham *et al.*, 1980; Louda & Baker, 1984). Other individual PAHs frequently detected at trace levels (0.001-0.01 μg/g) in the Platform Hidalgo sediments were fluoranthene, pyrene, benz[*a*]anthracene, chrysene, benzo[*b*]fluoranthene, benzo[a]pyrene, and benzo[e]pyrene. These 4- and 5-ring PAHs, which usually accounted for the largest component (60-100%) of the ΣPAH concentration of most sediments, are ubiquitous compounds that can be derived from incomplete combustion of organic matter (Lee *et al.*, 1977), and are transported from land to offshore sediments by aerial deposition or surface runoff (NRC, 1985).

Graphic display of the relative abundance and distributions of the parent and alkylated homologs of the 2- and 3-ring PAHs, combined with the relative abundance of the 4- and 5-ring PAHs, is a useful tool for assessing the composition of the PAHs and for detecting petroleum-sourced signals (Youngblood & Blumer, 1975; Blumer, 1976). Figure 8 illustrates the alkyl homolog distributions of PAHs in sediments from stations PH-J, PH-K, and PH-R (October 1986), which revealed slightly elevated EPAH concentrations (see Fig. 7). Alkyl homolog distributions for station PH-J and PH-R sediments are nearly indistinguishable and show (1) parent and alkylated naphthalene compounds, (2) unsubstituted dibenzothiophene, (3) various combustion-sourced 4- and 5-ring PAHs, and (4) unsubstituted phenanthrene. The composition of the PAHs in the sediments at these two stations implies a mixture of petroleum (e.g., presence of alkylated PAHs) and combustion-derived (e.g., presence of dealkylated or parent PAHs) hydrocarbons. The presence of naphthalenes and, in particular, alkylated dibenzothiophenes suggests a petroleum input; the 4- and 5-ring combustion-derived PAHs, which accounted for nearly one-half of the absolute concentration of ΣPAH at these stations, were present as background constituents at similar levels in most sediments.

At station PH-K, however, the alkyl homolog distribution revealed a distinct and dominant petroleum signal, even though the absolute concentration of ΣPAH in the sediments was about three times lower than the concentrations detected at stations PH-J and PH-R (see Fig. 7). 'he PAH composition of station PH-K sediments was dominated by alkylated phenanthrenes and dibenzothiophenes; an absence of the more volatile naphthalene compounds suggests that the petroleum was not particularly fresh. Although phenanthrenes may be derived from petroleum, formed by chemically or biologically mediated processes, or result from combustion of fossil fuels, the presence of alkylated phenanthrenes observed in this sample usually suggests a petroleum source (Youngblood & Blumer, 1975; NRC,

1985). Additional evidence of a petroleum source is the presence of the parent and alkylated dibenzothiophene compounds. It is also significant to note that the sediment ΣPAH concentration at station PH-K was not dominated by perylene or by the 4- and 5-ring combustion PAHs, which together accounted for on] y 10% of the total PAH concentration in this sample.

Because stations PH-J, PH-K, and PH-R were sampled prior to initiation of drilling activities at Platform Hidalgo, the small but readily detectable input of petrogenic hydrocarbons may be associated with platform siting and predrilling activities at Hidalgo or with drilling activities at other platforms in the area (see Fig. 2). However, because a concomitant barium signal was not observed in these predrilling samples (see discussion below), it is unlikely that the petroleum hydrocarbons originated from drilling-related discharges. A more plausible source of the petroleum signal is the natural oil seeps that characterize the offshore southern California region (Wilkinson, 1972; Spies & Davis, 1979). Analyses of samples collected during active drilling at Platform Hidalgo did not reveal sediment PAH concentrations as high as those detected at stations PH-J, PH-K, and PH-R prior to drilling. Occasional and irregular petroleum signals, particularly if not accompanied by an increase in barium, suggest that the origin is probably not a point-source (e.g., a drilling platform) but, alternatively, related to a less-predictable phenomenon such as transport of seep-related petroleum material. Chemical characterization of sediments in the Platform Hidalgo monitoring area must consider natural petroleum inputs, such as those originating from seeps, part of the predrilling background conditions.

Tmce Metal Chemistry

The station-averaged and time-averaged mean concentrations of trace metals in surface sediments, collected during seven surveys between October 1986 and October 1990, are presented in Tables 2 and 3, respectively. The within-station variance for all metals was approximately 15%, estimated from the standard deviation of seven field replicates collected over the 4-year study. Except barium, none of the metals was elevated in concentration during the period of drilling at Platform Hidalgo (October 1988 samples) and the concentrations of metals generally reflected average concentrations in crustal rocks. For comparison, the grand mean concentrations of metals in sediments from the proposed site for Platform Julius (redrilling control area) are included in both tables.

The concentrations of all metals (except barium) measured in sediments from Platform Hidalgo were similar to the concentrations reported for sediments from the proposed Platform Julius site, implying that the metals represent natural background concentrations for this offshore region. Other investigators have reported similar concentrations of trace metals in southern California coastal sediments (Bruland et *al.*, 1974; Chow & Earl, 1979; Katz & Kaplan, 1981; Hershelman *et al.*, 1983; and SAIC, 1986).

The only elements that showed some correlation with the silt/clay sediment fraction were nickel, copper, and lead (r = 0.86; 0.77, and 0.63 at α = 0.05, respectively); these elements were also slightly lower in concentration (see Table 3) at the three stations (PH-K, PH-N, and PH-R) characterized by sandier sediments. Chromium, which was negatively correlated (r = -0.49 at α = 0.05) with the fine sediment fraction, probably occurs as sand-sized particles of chromite minerals (SAIC, 1986). None of the metals correlated well with TOC ($r \approx$ -0.47 to 0.54).

Barium, which is a major constituent of drilling muds, was the only element that changed significantly over the 4-year study. Figure 9 illustrates the mean barium concentrations and ranges in surface sediments from five nearfield stations (PH-I, PH-J, PH-K, PH-N, and PH-R) located along a northeast-to-southwest transect through Platform Hidalgo. Between October 1986 and October 1988, the mean barium concentration at these five stations increased by 200-300 μg/g; a two-way ANOVA indicated that this trend was significant at α = 0.001. Peak barium concentrations in sediments from the five nearfield stations were detected in samples obtained during October 1988, while Platform Hidalgo was being drilled. The gradual decline to near-background concentrations ($\approx$ 700 μg/g) of barium between May 1989 and October 1990 was significant at α = 0.1. Natural sources of barium that contribute to the background concentration include riverine transport of barite minerals that occur as outcrops in the drainage basin of the Santa Ynez River, just north of Point Arguello (SAIC, 1986).

Barium concentrations in sediments from the background station (PH-W), located 6 km northwest of Platform Hidalgo, did not change significantly during the 4-year sampling period, indicating that station PH-W is outside the area of detectable change. The increase in sediment barium concentrations observed at the nearfield stations is due to barite in the drilling mud discharges. As illustrated in Fig. 2, between October 1986 and October 1988, drilling fluids were being discharged at four platforms, three of which are located within 7 km of the five transect stations. Platform Hidalgo

began discharging barite in January 1988. Both Platform Harvest and Platform Hermosa, located 3.3 and 7 km southeast of Platform Hidalgo, respectively, discharged barite throughout most of 1987 and 1988. Platform Irene, located 13 km north of Platform Hidalgo, discharged relatively minor amounts of barite.

Characterization of Sediment-Trap Material

Hydrocarbon Chemistry

Saturated Hydrocarbons

Sediment-trap samples were collected 1 m from the bottom in replicate traps deployed at nine Platform Hidalgo stations and at one location near Platform Harvest. Only the first set of traps, deployed in October 1986 and retrieved in May 1987, collected sediment prior to drilling the first well at Platform Hidalgo. Because most traps in the first deployment were lost, predrilling data were available only for stations PH-I and PH-U. After the traps were redesigned, subsequent retrievals were more successful and represented a majority of the platform stations.

To illustrate temporal changes in the concentrations of THC in sediment-trap material, station-averaged THC concentrate ions are presented in Fig. 10. Mean THC concentrations, which, overall, were 2-4 times higher in the trapped material than in surface sediments, ranged between 69 and 526 μg/g dry sediment, The lowest concentrations were detected in the two predrilling samples collected between October 1986 and May 1987, and in samples collected from all stations between October 1989 and May 1990, after cessation of drilling. The highest mean THC concentration and the broadest concentration range were both measured in trap samples collected between May and October 1988, a period when Platform Hidalgo and at least two other platforms were discharging drilling fluids (see Fig. 2). The distribution of THC among stations for the May-October 1988 samples reveals that the highest concentrations were found in sediment-trap material collected from stations PHAR (526 μg/g), PH-W (475 μg/g), PH-R (442 μg/g), PH-U (397 μg/g), and PH-N (341 μg/g). These increases in THC concentrations, however, were unusual because they were not accompanied by increases in PAHs during the same period and because the two farfield control stations (PH-U and PH-W) had among the highest THC concentrations. For these reasons, it is unlikely that the short-term increases in THC observed in sediment-trap samples collected between May and October 1988 can be attributed to platform discharges.

As found in the surface sediment samples, UCM was also the major component of THC (= 30-80%) in most sediment-trap samples. Total alkanes generally comprised 1-5% of the THC and exhibited the plant-wax pattern of odd-carbon dominance between n-C_{25} and n-C_{31}, with maxima at n-C_{29}. Other important saturated hydrocarbons in many samples included n-C_{15}, n-C_{17}, and n-Cm Because these components were not part of the characteristic petroleum hydrocarbon pattern, their presence was probably due to marine biogenic input that is often distinguished by odd-carbon preference in the n-C_{15} to n-C_{21} range (Clark & Blumer, 1967; Blumer *et al.*, 1970; NRC, 1985).

Concentrations of pristane were disproportionately higher (5- to 25-fold) in sediment-trap samples than in surface sediments and, therefore, resulted in much larger pristane/phytane ratios. This ratio, which was near unity in most surface sediments, averaged 4.8 in trapped sediments and, in many samples, was much larger, Although present in varying concentrations in petroleum products, pristane is a dominant isoprenoid hydrocarbon in marine plankton and is primarily biogenic in origin (Blumer *et al.*, 1963; NRC, 1985). Because plankton are more likely to accumulate in sediment traps than in bottom sediments, higher ratios of pristane/phytane in the sediment-trap samples may not be unusual.

Aromatic Hydrocarbons

Concentrations of ΣPAHs in sediment-trap material varied over time and station location by a factor of about 100, ranging from below detection limit to 1.1 μg/g. However, although the high end of the concentration range was due to just several samples, there were no spatial or temporal trends associated with these few samples. For example, the highest ΣPAH concentrations were associated with two samples (stations PH-I and PH-U) collected between October 1986 and May 1987, before drilling at Platform Hidalgo was initiated.

In general, GC/MS chromatograms revealed that individual PAHs were either not detected or were detected only in trace amounts (= 0.00143.05 μg/g) and, overall, were negligible constituents of the sediment-trap material. As found in surface sediments, the dominant PAH in all but several samples was perylene. Concentrations of perylene were highest (0.238 and 0.314 μg/g) in the two predrilling samples from stations PH-I and PH-U, and for all other samples, generally ranged between 0.01 and 0.05 μg/g. Unsubstituted naphthalene and phenanthrene were detected only at trace levels (0.001-0.03 and 0.001-0.08 μg/g, respectively) in several samples collected between May 1987 and October 1988 when three platforms were drilling. "Although naphthalenes and phenanthrenes are

common aromatic components of crude oil, their alkylated (substituted) homologs are more indicative of petroleum sources than are the unsubstituted parent compounds. Therefore, the presence of individual naphthalene and phenanthrene components in these samples was probably not related to a petroleum input. Most of the PAHs (except perylene) measured in the sediment-trap samples were combustion hydrocarbons (i, e., 4- and 5-ring PAHs) probably originating from terrestrial runoff or atmospheric fallout. Concentrations of individual 4- and 5-ring PAHs ranged between detection limit values (< 0.001 μg/g) and 0.010 μg/g.

Several samples revealed low-level PAH contamination. These samples included (1) two predrilling samples from stations PH-I and PH-U retrieved in May 1987, (2) a sample from station PHAR collected during drilling and retrieved in October 1988, (3) a postdrilling sample from station PH-I retrieved in May 1989, and (4) a postdrilling sample from station PH-F retrieved in October 1989. Examination of the PAH homolog patterns indicated that a small petroleum signal, evidenced by alkylated naphthalenes, phenanthrenes, and dibenzothiophenes, was indeed present in these samples. However, because barium concentrations, in all but the Platform Harvest (station PHAR) October 1988 sample, were near background levels (=700 μg/g), the petroleum signal was probably due to seep petroleum associated with particles rather than to drilling discharges.

The chemical composition of the Platform Harvest sample collected during drilling was more likely drilling-related because both a distinct petroleum hydrocarbon signal and a significant increase in the barium concentration were detected, The PAH alkyl homolog distribution for the sample from station PHAR, located approximately 0.6 km northwest of Platform Harvest, is shown in Fig. 11. Alkylated naphthalenes (0.28 μg/g), phenanthrenes (O. 17 μg/g), and dibenzothiophenes (0.04 μg/g) were significant components of the ΣPAH, and together accounted for ≈80% of the ΣPAH concentration. The pyrogenic hydrocarbons (4- and 5-ring compounds) and perylene, although present in this sample, accounted for c 20 % of the ΣPAH concentration.

Trace Metal Chemistry

None of the metals, except barium, showed drilling-related enrichment in the sediment-trap material. However, because material collected in the sediment traps was primarily <62 μm in diameter (fine fraction), the concentrations of most metals were slightly higher in sediment-trap samples than in bottom sediments. Chromium was the only element higher in concentration in surface sediments

(grand mean: 124 μg/g) than in the sediment-trap material (grand mean: 96 μg/g). Because chromium probably occurs in mineral form associated with larger grain-sized material, it occurs at lower concentrations in the finer particles collected by sediment traps.

Figure 12 illustrates mean barium concentrations of sediment-trap samples collected during drilling at Platform Hidalgo and after drilling had ceased. Predrilling data were not included in this figure because on] y two traps were retrieved from the study area before the first well at Platform Hidalgo was drilled and also because three other platforms, within 13 km of Platform Hidalgo, were drilling between October 1986 and October 1987. Figure 12 shows that the mean concentrations of barium during drilling ranged between 1809 and 2723 μg/g, and increased 2- to 3-fold at all near- and mid-field stations while drilling was occurring. At the farfield stations (PH-U and PH-W), barium increased only 1.5-fold during the same period. Postdrilling barium concentrations showed little spatial variability, and ranged between 749 and 959 μg/g sediment-trap material. Because the concentrations of barium measured in sediment-trap samples collected during all three postdrilling surveys were similar, and because these concentrations approximated predrilling concentrations of barium in surface sediments, the 749-959 μg/g barium range can be considered representative of background concentrations in sediment-trap samples (i.e., predrilling conditions).

Characterization of Source Materials

Production Oil, Seep Oil, and Tar Balls

To obtain information on the composition of materials that may serve as sources of hydrocarbons to the Platform Hidalgo area sediments, samples of a production oil, seep oil, and various macroscopic tar particles were analyzed chemically. Tar materials, obtained opportunistically from infaunal sediment samples, were grouped into three types based on physical properties. The physical appearance of the tar materials suggested that the collected particles had been weathered to different degrees. Table 4 includes a description of the tar materials analyzed, the gravimetrically determined saturated and aromatic hydrocarbon content, and GC/MS-determined concentrations of aromatic hydrocarbons. For reference, some data on the production and seep oils are included in Table 4.

Tar particles and the seep oil were characterized by a high percentage (96-98%) of UCM and low absolute concentrations of alkanes, both features that result from weathering of the source oil

(Barrington et al., 1973). Gravimetrically determined saturated and aromatic hydrocarbon concentrations increased consistently from the visually most-weathered tar balls to the potential source oil (production oil). Analysis of the tar materials and seep oil did not reveal a similar trend, suggesting that the gravimetrically determined saturated and aromatic hydrocarbons were components of the UCM (i .e., polycyclic alkanes and partially aromatized polycyclic compounds) rather than targeted analytes. The alkane and PAH signatures of the tar samples were highly weathered and did not resemble those of the seep or production oils. When detected, the concentrations of individual hydrocarbons in the tar particles were in the low ppm range. A depletion of n-alkanes in the tar samples is characteristic of material from shallow water-washed oil reservoirs (i. e., potential seeps; Stuermer *et al.*, 1984).

Drilling Discharges

Chemical analysis of drilling muds and drill cuttings, obtained at several depth intervals from five wells at Platform Hidalgo, are summarized in Tables 5 and 6, respectively. Petroleum hydrocarbons, in concentrations ranging between 2 and 1000 times background sediment concentrations, were found in samples of drilling muds and drill cuttings collected at all well depths (see Tables 5 and 6). Concentrations of THC in drilling muds, and concentrations of THC and PAHs in both drilling muds and cuttings increased with well depth. Both the saturated and aromatic hydrocarbon compositions of the near-bottom drilling muds and drill cuttings closely resemble the composition of the production oil collected from a well near the study area, Figure 13 illustrates the relative concentrations of individual saturated and aromatic hydrocarbons in the three sample types. The saturated hydrocarbon distribution was very similar in the samples of mud, cuttings, and production oil (Fig. 13a). The PAH distribution (Fig. 13b) illustrates that the C_2 and C3 alkyl-substituted members in each homologous series generally were quantitatively more significant than their corresponding parent compounds and were dominant components of the aromatic hydrocarbon fraction. It is noteworthy that the 4- and 5-ring PAHs were negligible components of the aromatic hydrocarbon composition of all three source materials.

Hydrocarbons found in the drilling discharges can originate either from (1) lubrication oil added to drilling-mud formulations or (2) crude oil from the geologic formation being drilled. Because inventories of discharges from Platform Hidalgo revealed no evidence of refined oil in the drilling fluids (see Steinhauer *et al.*, Chapter 2), in addition to the compositional similarity to the production

oil, the petroleum hydrocarbons measured in the drilling fluids probably originate in the petroleum-bearing strata cut during drilling.

s shown in Table 5, only barium and zinc were significantly higher in drilling muds than in surface sediments surrounding Platform Hidalgo. Barium, in the form of barite (barium sulfate), is used as a weighting agent in drilling muds. Barite concentrations in drilling muds vary with the depth of the well being drilled, but can be as high as 2 kg/L in the muds (Neff *et al.*, 1987), In the drill cuttings (Table 6), concentrations of all metals, except chromium and mercury, were elevated relative to the surface sediments. Although lead and zinc may be derived from pipe-thread compound (pipe dope) used to lubricate the threads of drill pipes, the higher concentrations of most other metals (except barium) in the drill cuttings are unusual and may reflect mineral enrichment from the rock strata being drilled or contamination from metal filings abraded from the drill bit.

Effects of Drilling-Related Discharges on the Geochemical Environment

The ability to detect drilling-related changes in the concentrations of chemical parameters in sediment-trap samples or in surface sediments is a function of (1) the concentrations of contaminants in drilling discharges relative to background concentrations and the expected dilution of the drilling discharges in the environment, (2) the statistical power to detect change based on the observed variability of each contaminant, and (3) the chemical or physical transformation (e.g., volubility) of each contaminant during the transport process. A description of the power analyses used for CAMP is presented by Hyland *et al.* (Chapter 9).

As discussed above, the only chemical parameter that showed a significant drilling-related increase in either trapped sediments or surface sediments near Platform Hidalgo was barium. In comparison to predrilling concentrations in surface sediments or postdrilling concentrations in surface and trapped sediments, barium was enriched by 200-300% in sediment-trap samples and by 10-40% in surface sediments at nearfield stations during drilling. The highest relative enrichment in sediment-trap samples was detected at station PH-J (May-October 1988 sample) where peakdrilling barium concentrations were 2809 μg/g, compared to postdrilling concentrations of 703 μg/g. The highest relative concentration in surface sediments was also found at station PH-J where peakdrilling barium concentrations were 1135 μg/g, compared to predrilling concentrations of 798 μg/g. No other contaminants were significantly elevated in either surface or trapped sediments from station PH-J during the May-October 1988 sample collection period.

Drilling-related increases in the concentrations of other contaminants in trapped sediments or in surface sediments can be estimated from the concentrations of barium in the drilling mud and the enrichment of barium in the sediments during peak drilling discharges (Tables 7 and 8, respectively). Coats (in preparation) has determined that discharged drilling mud accounts for 1.97 % of the suspended sediment flux at station PH-J and suggested that this factor be used to determine barium enrichment in the May-October 1988 samples. Given this small fraction of the total suspended material derived from the drilling muds and the negligible difference between the concentrations of most contaminants in the drilling muds and background trapped sediments, the predicted increase of most inorganic contaminants is small (2% or less; see Table 7) and below the statistical power to detect change.

For the trapped sediments, the predicted increase in concentrations of the aromatic hydrocarbon parameters (ΣPAH and naphthalenes) is greater than the increase observed for barium, and is also greater than the abilit y to detect change, based on the power analyses (see Table 7). The inability to detect a strong aromatic hydrocarbon signal in trapped sediments suggests that the fate of aromatic hydrocarbons is different from that of barium. The high concentrations of naphthalenes in drilling muds relative to trapped sediments also account for most (72%) of the ΣPAH enrichment. Because naphthalenes are relatively soluble in water, preferential weathering through dissolution can reduce their concentrations in particulate matter in the water column or in the traps during the 6-month period of deployment. In addition, although the traps were fixed with sodium azide, microbial degradation of low-molecular-weight PAHs may have occurred during the 6-month period of deployment.

Barium enrichment in the May-October 1988 surface sediments at station PH-J can be accounted for if drilling muds comprise 0,32 % of the surface (O-2 cm) sediment (Table 8). The smaller barium signal in surface sediments as compared to trapped sediments represents the dilution of drilling mud in the surface layer, and potential resuspension and transport of barium out of the station area. The small drilling-mud signal will not significantly increase the concentrations of the inorganic contaminants. The calculated relative increase for the hydrocarbon parameters in surface sediments is far less than expected from drill ing-mud dilution because surface sediments at station PH-J have relatively elevated background concentrations of hydrocarbons and large, variabilities associated with individual analytes.

As shown in Table 8, the predicted increase in hydrocarbon analytes in surface sediments is below the power to detect change.

Given the low drilling-mud signal in sediment-trap material and in surface sediments at station PH-J, and the measured variability in chemical parameters, it is unlikely that the amounts of drilling mud discharged at Platform Hidalgo have significantly altered the inorganic geochemistry in the mid- to far-field region (beyond 1 km from the platform). Within 1.5 years after drilling in the Arguello Field ended, barium in trapped sediments dropped to predrilling concentrations. In surface sediments, the barium signal decreased gradually from peak concentrations observed during drilling but, at the end of the CAMP study in October 1990, was still approximately 20% higher than predrilling concentrations measured in October 1986. Mixing of barium into deeper sediments may explain, in part, the decrease in barium concentrations in surface sediments during the postdrilling period. However, barium also could be lost through resuspension of the surface layer and transport out of the study area. Detailed examination of barium concentrations with sediment depth could aid in understanding the fate of barium in the surface sediments around drilling platforms.

CONCLUSIONS

Between October 1986 and October 1990, petroleum hydrocarbons and metals (except barium) in surface sediments were in the general range of concentrations reported by other investigators for southern California coastal sediments (Bruland *et* al., 1974; Simoneit & Kaplan, 1979; Chow & Earl, 1979; Katz & Kaplan, 1981; Hershel man et *al.,* 1983; SAIC, 1986). Therefore, it is reasonable to conclude that the concentrations of contaminants (except barium) measured during this study represent background conditions and do not reflect anthropogenic input associated with drilling in the Arguello Field. Hydrocarbon concentrations in sediments from the study area were occasionally elevated. Such random increases in concentrations are not necessarily related to drilling activities but, instead, appear to be influenced by tar particles emanating from various natural seeps identified in a large region off the coast of southern California. In characterizing hydrocarbon concentrations of sediments from regions of known seeps, occasional petroleum hydrocarbon signals, such as those detected in our study, should be considered in determinations of background or predrilling concentrations.

Barium, the only chemical parameter for which a statistically significant increase was found during the period of drilling at Platform Hidalgo (November 1987 to January 1989), appears to be the most sensitive indicator of drilling activities. In trapped sediments, concentrations of barium showed a statistically significant enrichment during the period of drilling activities in the Arguello Field. Within 1.5 years after cessation of drilling at Platform Hidalgo, concentrations of barium (749-959 μg/g) in the sediment-trap material represented background. However, at the end of the CAMP Phase-Ii study, or approximately 1.5 years after cessation of drilling at Platform Hidalgo, barium concentrate ions in surface sediments were still slightly higher than background concentrations measured before drilling began.

ACKNOWLEDGMENTS

This was study was supported by the U.S. Department of the Interior, Minerals Management Service, Pacific OCS Office, under Contract No. 14-12-0001-30262 to Battelle Memorial Institute. The authors are grateful to Dr. Donald Boesch, Dr. Fred Weiss, Dr. Fred Grassle, Dr. Robert Spies, and Dr. Jerry Neff for critical review of the manuscript. Statistical analyses were designed by Dr. Roger Green. Ms. Ellie Baptiste provided database support and conducted statistical analyses, and Ms. Deirdre Dahlen assisted with graphics. We thank the Marine Chemistry Laboratory teams at Battelle Ocean Sciences, Duxbury, Massachusetts, and Battelle Marine Research Laboratory, Sequim, Washington. for the hydrocarbon and trace metal analytical chemistry.

REFERENCES

Bandy, O.L. & R. L. Kolpack. 1963. Foraminiferal and sedimentological trends in Tertiary section of Tecolote Tunnel, California. *Micropaleontol. 9:117-170.*

Bloom, N.S. 1983. Determination of silver in marine sediments by Zeeman corrected graphite furnace atomic absorption spectroscopy. *At. Spectrosc.* 4:204-207.

Bloom, N.S. & E.A. Crecelius. 1984. Determination of silver in sea water by coprecipitation with cobalt pyrrolidinedithicarbamate and Zeeman graphite-furnace atomic absorption spectrometry. *Anal. Chim. Acts. 156:139-145.*

Blumer, M. 1976. Polycyclic aromatic compounds in nature. *Sci. Am.* 234:34-45.

Blumer, M., M. Mullin, & R. Guillard. 1970. A polyunsaturated hydrocarbon (3,6,9,12,15,18-heneicosahexaene) in the marine food web. *Mar. Biol.* 6:226-235.

Blumer, M., M.M. Mullin, & D.W. Thomas. 1963. Pristane in zooplankton. *Science* 140:974.

Brewer, G. D., J. Hyland, & D.D. Hardin. In press. Effects of oil drilling on deep-water reefs offshore California. *Am. Fish. Sot. Symp.* 11.

Bruland, K. W., K. Bertine, M. Koide, & E.D. Goldberg. 1974. History of metal pollution in Southern California coastal zone. *Environ. Sci. Technol.* 5:425-432.

Chow, T.J. & J. Earl. 1979. Trace Metal Distribution in Southern California OCS Benthic Sediments. Southern California Baseline Study, Benthic Year 2 Final Report, Volume 2 (SAI-77-917-LJ). Report to the U.S. Department of the Interior, Bureau of Land Management.

Clark, R., Jr. & M. Blumer. 1967. Distribution of n-paraffins in marine organisms and sediments. *Limnol. Oceanogr.* 12:79-87.

Crecelius. E. 1990. Chemical analysis of trace metals in sediments, pore waters, and animal tissues. In: Steinhauer, M. & E. Immura (Eds.), California OCS Phase II Monitoring Program: Year-Three Annual Report. Report prepared for the U.S. Department of the Interior, Minerals Management Service, Pacific OCS Region, Los Angeles, CA. Contract No. 14-12-0001-30262. Volume 1 (MMS 90-0055).

Barrington, J. W., J.M. Teal, J.G. Quinn, T. Wade, & K. Bums. 1973. Intercalibration of analyses of recently biosynthesized hydrocarbons and petroleum hydrocarbons in marine lipids. *Bull. Environ. Contain. Toxicol. 10(3):129-136.*

Farrington, J. W. & P.A. Meyers. 1975. Hydrocarbons in the marine environment. Pages 109-136 *In:* Eglinton, G. (Ed.), *Environ. Chem.*, Volume I. The Chemical Society, London, England, UK.

Barrington, J.W. & B.W. Tripp. 1977. Hydrocarbons in western North Atlantic surface sediments. *Geochim. Cosmochim. Acts 41:1627-1641.*

Green, R.H. t 989. *Sampling Design and Statistical Methods for Environmental Biologists.* John Wiley & Sons, New York, NY. 270 pp.

Hershelman, G. P., P. Szalay, & C. Ward. 1983. Metals in Surface Sediments from Point Dume to Point Hueneme. Biennial Report for the Years 1981-1982. Pages 259-265 *In:* Bascom, E.W. (Ed,), Coastal Water Research Project. Southern California Coastal Water Research Project, Long Beach, CA.

Hyland, J., D. Hard in, E. Crecelius, D. Drake, P. Montagna, & M. Steinhauer. 1990. Monitoring long-term effects of offshore oil and gas development along the southern California outer continental shelf and slope: Background environmental conditions in the Santa Maria Basin. *Oil & Chem. Pollut. 6:195-240.*

Hyland, J., E. Baptiste, J. Campbell, J. Kennedy, R. Kropp, & S. Williams. In press. Macroinfaunal communities of the Santa Maria Basin on the California outer continental shelf and slope. *Mar. Ecol. Progr. Ser.*

Katz, A., & I.R. Kaplan, 1981. Heavy metals behavior in coastal sediments of Southern California: A critical review and synthesis. *Mar. Chem.* 10:261-299.

Kennicutt, M. C.,II, J.L. Sericano, T.L. Wade, F. Alcazar, & J.M. Brooks. 1987. High Molecular weight hydrocarbons in Gulf of Mexico continental slope sediments. *Deep-Sea Res.* 34(3):403-424.

Kinney, P., D. Hardin, T. Parr, F. Newton, & R. Kolpack. 1990. Sedimentology. In: Steinhauer, M. & E. Immura (Eds.), California OCS Phase II Monitoring Program: Year-Three Annual Report. Report prepared for the U.S. Department of the Interior, Minerals Management Service, Pacific OCS Region, Los Angeles, CA. Contract No. 14-12-0001-30262. Volume I (MMS 90-0055).

Lee, M, L., G.P. Prado, J.B. Howard, & R.A. Hites. 1977. Source identification of urban airborne polycyclic aromatic hydrocarbons by gas chromatographic mass spectrometry and high resolution mass spectrometry. *Biomed. Mass Spec. 4:182-186.*

Louda, J. W. & E. W. Baker. 1984. Perylene occurrence, alkylation and possible sources in deep-ocean sediments. *Geochim. Cosmochim. Acts 48(5):1043-1058.*

Montagna, P. In press. Meiobenthic communities of the Santa Maria Basin on the California continental shelf. *Cont. Shelf Res.*

Nakashima, S., R.E. Sturgeon, S.N. Willie, & S.S. Berman. 1988. Acid digestion of marine samples for trace element anal ysis using microwave heating. *Analyst* 113:159-163.

NRC. 1985. *Oil in the Sea.* National Research Council, National Academy Press, Washington, DC, 601 pp.

Neff, J. M., N.N. Rabalais, & D.F. Boesch. 1987. Offshore oil and gas development activities potentially causing long-term environmental effects. Pages 149-173 *In*: Boesch, D.F. & N.N. Rabalais (Eds.), *Long-Term Effects of Offshore Oil and Gas Development.* Elsevier Applied Science Publishers, London, England, UK.

Nielson, K. K., & R.W. Sanders. 1983. Multielement analysis of unweighed biological and geological samples using backscatter and fundamental parameters. *Adv. X-ray Anal.* 26:385-390.

Plumb, R. H., Jr. 1981. Procedure for handling and chemical anal yses of sediment and water samples. Technical report EPA/CE-81-1. USACOE Waterways Experimental Station, Vicksburg, MS. 487 pp.

Reed, W.E. & I.R. Kaplan. 1977. The chemistry of marine petroleum seeps. *J. Geochem. Explor.* 7:255-293.

Reed, W. E., I.R. Kaplan, M, Sandstrom, & P. Mankiewicz. 1977. Petroleum and anthropogenic influence on the composition of sediments from the Southern California Bight. Pages 183-188 *In: Proceedings, 1977 Oil Spill Conference (Prevention, Behavior, Control, Cleanup).* American Petroleum Institute, Washington, DC.

SAIC. 1986. Science Applications International Corporation. Assessment of Long-Term Changes in Biological Communities of the Santa Maria Basin and Western Santa Barbara Channel - Phase I, Volume II Synthesis of Findings (MMS 86-9912). Report prepared for the U.S. Department of Interior, Minerals Management Service, Pacific OCS Region, Los Angeles, CA. Contract No. 14-12-0001-30032.

Simoneit, B.R.T & I.R. Kaplan. 1980. Triterpenoids as molecular indicators of paleoseepage in recent sediments of the Southern California Bight. *Mar. Environ. Res. 3:113-128.*

Spies, R.B. & P.H. Davis. 1979. The infaunal benthos of a natural oil seep in the Santa Barbara Channel. *Mar. Biol.* 50:227-237.

Steinhauer, M. & W. Steinhauer. 1990. Chemical analysis of hydrocarbons in sediments, pore water, and animal tissues. *In*: Steinhauer, M. & E. Imamura (Eds.), California OCS Phase II Monitoring Program: Year-Three Annual Report. Report prepared for the U,S. Department of the Interior, Minerals Management Service, Pacific OCS Region, Los Angeles, CA. Contract No. 14-12-0001-30262. Volume I (MMS 90-0055).

Steinhauer, M. & E. Imamura (Eds.). 1990. California OCS Phase II Monitoring Program: Year-Three Annual Report. Report prepared for the U.S. Department of the Interior, Minerals Management Service, Pacific OCS Region, Los Angeles, CA. Contract No. 14-12-0001-30262. Volume I (MMS 90-0055).

Stuermer, D. H., R.B. Spies, P.H. Davis, D.J. Ny, L.J. Morris, & S. Neal, 1982. The hydrocarbons in the Isla Vista marine seep environment. *Mar. Chem.* 11:413-426.

Van Andel, T.H. 1964. Recent marine sediments of the Gulf of California: Marine geology of the Gulf of California. Pages 216-310 In: *Amer. Assoc. Petrol. Geol. Mere. 3.*

Wakeham, S .G. 1977. Synchronous fluorescence spectroscopy and its application to indigenous and petroleum-derived hydrocarbons in lacustrine sediments. *Environ. Sci. Technol.* 11:272-276.

Wakeham, S.G. & J.W. Barrington. 1980. Hydrocarbons in contemporary aquatic sediments. Pages 3-32 *In:* Baker, R.A. (Ed.), *Contaminants and Sediments,* Volume 1. Ann Arbor Science Publishers, Ann Arbor, MI.

Wakeham, S. G., C. Schaffner, & W. Giger. 1980. Polycyclic aromatic hydrocarbons in recent lake sediments. II. Compounds derived from biogenic precursors during early diagenesis. *Geochim. Cosmochim. Acts* 44:415-429.

Wilkinson, E.D. 1972, California offshore oil and gas seeps. *In: 57th Annual Report of the State Oil and Gas Supervisor.* Resources Agency of California, Department of Conservation, Division of Oil and Gas. Publ. No. TR08.

Youngblood, W. W. & M. Blumer. 1975. Polycyclic aromatic hydrocarbons in the environment: Homologous series in soils and recent marine sediments. *Geochim. Cosmochim. Acts 39:1303-1314.*

Table 1. Hydrocarbon interpretive parameters.

Total Hydrocarbons **(THC)**	Quantifies the total resolved (i.e., GC/MS peaks) plus unresolved saturated and aromatic hydrocarbons (i.e., chromatographic "hump" or unresolved complex mixture, UCM).
Total **Alkanes**	Normal alkanes between C_{10} and C_{34}.
Pristane (PRIS)	A C_{19} isoprenoid alkane that, although present in petroleum, is primarily biogenic in origin, occurring in biota and in recent sediments as a degradation product of the phytol side chain of chlorophyll.
Phytane (PHYT)	A C_{20} isoprenoid alkane that is rarely biogenic but a common component of crude oil.
PRIS/PHYT	A diagnostic isoprenoid ratio useful in determining the relative contribution of petroleum inputs to the sediments, In sediments "uncontaminated" by petroleum, this ratio is usually much larger than 1.0 and typically ≈ 3 to 5. PRIS/PHYT is 0.78 for production oil from the Arguello Field and 0.87 for Isla Vista seep oil.
Unresolved Complex Material **(UCM)**	The base] ine-corrected unresolved "hump" or UCM under the resolved peaks of a chromatogram is usually a mixture of branched and ring-structured hydrocarbons that cannot be individual] y identified by gas chromatography. UCM is a feature of most weathered oils and generally implies the presence chronic inputs of petroleum (Reed et *al.,* 1977; Barrington *et* al., 1973).
Naphthalenes (N)	The sum of the naphthalene homologous series includes the unsubstituted 2-ring parent, naphthalene, and the alkyl-substituted homologs (Co-N + C_1-N + C_2-N + C_3-N + C_4-N). N compounds are commonly associated with unweathered petroleum and are rarely found in "clean" sediments at detectable levels.

Table 1. Hydrocarbon interpretive parameters. (continued)

Fluorenes (F)	The sum of the fluorene homologous series includes the unsubstituted 3-ring parent compound, fluorene, and the alkyl-substituted homologs (Co-F + C1-F + C2-F + C3-F).
Phenanthrenes (P)	The sum of the phenanthrene homologous series includes the unsubstituted 3-ring parent compound, phenanthrene, and the alkyl substituted homologs (Co-P + C 1-P + C2-P + C3-P + C4-P). P compounds have petroleum, combustion, and diagenetic sources but the presence of the more highly alkylated homologs is usually indicative of petroleum (Youngblood & Blumer, 1975).
Dibenzothiophenes (D)	The sum of the dibenzothiophene homologous series includes the unsubstituted 3-ring sulfur-containing heterocyclic parent compound, dibenzothiophene, and the alkyl-substituted homologs (Co-D + C 1-D + C2-D + C3-D). D compounds are distinct components of many crude oils.
4-,5-PAH	The sum of the 4- and 5-ring polynuclear aromatic hydrocarbons (fluoranthene, pyrene, benz[*a*]anthracene, chrysene, benzofluoranthene, benzo[*a*]pyrene, benzo[e]pyrene, and perylene) includes primarily the high-molecular-weight pyrogenic compounds. Perylene is a common constituent of organic-rich sediments and may also be formed through natural chemical transformation processes. The other 4-and 5-ring aromatics in this group are produced from the combustion of fossil or wood fuels on land, and subsequent y transported and deposited offshore.
ΣPAH	The sum of the 2-to 5-ring polynuclear aromatic hydrocarbons (N + F + P + D + 4-,5 -PAH) includes those of petrogenic, pyrogenic, and diagenetic origin. When used in conjunction with the 4-,5-PAH parameter, the relative contribution of petrogenic and pyrogenic sources can be determined.

Table 2, Mean concentrations (μg/g dry weight) of trace metals in surface sediments from Platform Hidalgo shown by sampling date, Concentrations shown for each sampling survey are means for all stations. Percent fine sediment is included for reference.

	n	Ag	As	Ba	Cd	Cr	Cu	Hg	Ni	Pb	V	Zn	%Fines
Ott 86	27	0.13	8.3	752	0.56	127	16	0.066	42	15	69	70	69
May 87	24	0.14	8.6	811	0.59	117	17	0.099	42	14	55	77	57
Ott 87	9	0.15	8.4	859	0.51	118	16	0.075	39	14	40	73	61
May 88	9	0.10	9.1	965	0.59	117	16	0.085	42	14	53	72	62
Ott 88	9	0.08	9.0	930	0.54	125	16	0.072	44	14	52	71	62
Ott 89	9	0.08	7.5	926	0.50	120	15	0.053	43	15	62	70	57
Ott 90	9	0.09	7.9	862	0.66	126	16	0.057	40	14	54	70	58
Mean	96	0.11	8.4	872	0.56	121	16	0.072	42	14	55	72	61

Table 3. Mean concentrations (μg/g dry weight) of trace metals in surface sediments from Platform **Hidalgo** shown by station. Concentrations shown for each station are **means** for all samples collected over time. Grand mean concentrate ions in surface sediments from Platform Julius and mean percent tine sediment are included for reference.

	n	Ag	As	Ba	Cd	Cr	Cu	Hg	Ni	Pb	V	Zn	%Fines
PH-E	11	0.13	6.2	1020	0.58	110	18	0.087	48	16	60	71	76
PH-F	11	0.13	6.4	820	0.52	110	18	0.076	50	15	78	72	80
PH-I	11	0.14	6.2	900	0.55	110	19	0.079	49	16	58	72	79
PH-J	11	0.13	6.2	930	0.56	110	18	0.073	48	15	55	69	72
PH-K	11	0.09	15	700	0.43	140	14	0.055	30	12	54	89	39
PH-N	11	0.09	15	680	0.43	140	13	0.057	29	12	49	86	29
PH-R	11	0.10	6.7	880	0.87	120	13	0.062	34	14	47	59	40
PH-U	11	0.13	6.3	810	0.57	100	18	0.076	48	15	67	69	74
PH-W	8	0.09	7.3	830	0.61	180	12	0,068	38	16	48	59	54
Mean	96	0.11	8.4	841	0.57	124	15	0.070	42	15	57	72	60
Platform Julius		0.09	5.9	740	0.45	80	15	0.078	39	15	57	64	82

Table 4. Summary of hydrocarbon analyses of tar materials collected in CAMP study-area sediments. Data for production oil and **Isla** Vista seep oil are included for comparison.

	Saturated Hydrocarbons[a] (%)	Aromatic Hydrocarbons[a] (%)	U C M[b] (%)	Total **Alkanes** (μg/g)	Total **N**[c] (μg/g)	Total **F**[d] (μg/g)	Total **P**[e] (μg/g)	Total **D**[f] (μg/g)
Type 111 Tar Ball: Brown crumbly aggregates of small weathered particles	2	3	98	77	0	0	1	0
Type II Tar Ball: Exterior slightly weathered; interior soft and **taffy-like;** most samples this type	3	14	96	133	1	0	33	0
Type I Tar Ball: Soft tar throughout; exterior smooth, not crumbly or weathered	5	19	96	113	1	2	14	0
Isla Vista Seep **Oil**	10	18	88	288	5,656	1,110	1,280	933
Production **Oil**	19	19	39	39,200	8,323	766	958	875

Table 4. (Continued)

"Percent of sample dry weight (gravimetrically determined)
[b]Unresolved complex material (UCM) as percent of total hydrocarbons (THC)
[c]Naphthalene + alkylated naphthalenes
[d]Fluorene + alkylated fluorenes
[e]Phenanthrene + alkylated phenanthrenes
'Dibenzothiophene + alkylated dibenzothiophenes

Table 5. Concentrations of hydrocarbons and trace metals (μg/g dry weight) in composite samples of drilling muds collected from Platform Hidalgo. Mean concentrations in surface sediments from Platform Hidalgo are included for comparison.

	Near-Surface	Mid-Well	Near-Bottom	Bottom	Composite Average[a]	Surface Sediments[b]
THC[c]	159	137	268	*988*	390	23-180
ΣPAH[d]	0.87	8.0	39	*51*	25	< DL[e]-1.5
Naphthalenes[f]	0.27	5.4	28	*39*	18	< DL-0.38
Fluorenes[f]	< DL	0.38	2.0	4.1	1.6	< DL-0.01
Phenanthrenes[f]	0.34	0.94	5.3	4.5	2.8	< DL-0.23
Dibenzothiophenes[f]	0.03	0.71	2.9	3.9	1.9	< DL-0.20
Ag	0.19	0.36	0.31	0.23	0.28	0.05-0.18
As	8.95	4.41	5.28	6.74	6.34	4.4-18
Ba	24,742	49,083	178,900	178,405	107,782	495-1,181
Cd	0.84	1.24	1.40	1.33	1.20	0.32-1.0
Cr	82	126	96	37	85	71-229
Cu	26	38	28	27	30	9-23
Hg	0.08	0.10	0.15	0.18	0.13	0.03-0.06
Ni	49	51	40	22	41	19-55
Pb	20	3.2	2.3	51	19	8-28
V	78	99	69	38	71	27-125
Zn	126	138	182	714	290	53-95

[a]Average for all depths
[b]4-year range for surface sediments from Platform Hidalgo
[c]Total resolved + unresolved hydrocarbons
[d]Total 2- to 5-ring PAH target compounds
[e]DL: method detection limit
[f]Parent compound + alkylated homologies

Table 6. Concentrations of hydrocarbons and trace metals (μg/g dry weight) in composite samples of drill cuttings collected from Platform Hidalgo. Mean concentrations in surface sediments from Platform Hidalgo are included for comparison.

	Surface	Mid-Well	Bottom	Composite Average[a]	Surface Sediments[b]
THC[c]	600	95	526	407	23-180
ΣPAH[d]	2.3	12	121	45	< DL[e]-1.5
Naphthalenes[f]	1.2	8.9	96	35	< DL-0.38
Fluorenes[f]	< DL	0.35	8.2	2.8	< DL-0.01
Phenanthrenes[f]	0.79	0.64	9.3	3.6	< DL-0.23
Dibenzothiophenes[f]	< DL	0.40	8.1	2.8	< DL-O.20
Ag	0.20	0.86	0.66	0.57	0.05-0.18
As	9.5	9.4	11	10	4,4-18
Ba	2547	3355	9697	5200	495-1181
Cd	1.37	2.56	2.95	2.29	0.32-1.0
Cr	106	209	140	152	71-229
Cu	43	60	41	48	9-23
Hg	0.09	0.12	0.09	0.10	0.03-0.56
Ni	53	83	64	67	19-55
Pb	5559	25	193	1926	8-28
v	71	122	122	105	27-125
Zn	2871	179	988	1346	53-95

[a] Average for all depths
[b] 4-year range for surface sediments from Platform Hidalgo
[c] Total resolved + unresolved hydrocarbons
[d] Total 2- to 5-ring PAH target compounds
[e] DL: method detection limit
[f] Parent compound + alkylated homologies

Table 7. Maximum predicted contaminant concentrations (μg/g dry weight) in trapped sediments at the nearfield station PH-J. Predicted concentrations are based on a 1.97 % drilling-mud-derived fraction of total suspended sediments.

	Background[a] Concentration (μg/g)	Concentration in Muds[b] (μg/g)	Enrichment Ratio[c]	Predicted Concentration[d] (μg/g)	Predicted Increase (%)	Detectable Change[e] (%)
Ag	0.14	0.28	2.0	0.14	2.2	±20
As	6.5	6.3	1.0	6.5	0.0	±30
Ba	703	107,782	153	2,809[f]	3oo[f]	±4
Cd	0.72	1.2	1.7	0.73	1.2	*13
Cr	99	85	0.9	98	-0.3	±22
Cu	21	30	1.4	21	0.9	±12
Hg	0.07	0.13	1.7	0.08	1.4	±57
Ni	48	41	0.8	48	-0.4	±11
Pb	14	19	1.4	14	0.7	±19
v	81	71	0.9	80	-0.2	±36
Zn	71	290	4.1	76	6.0	±6
THc	80	388	4.8	86	7.5	±48
ΣPAH	0.05	25	543	0.54	1,070	±32
Naph	0.01	18	18,000	0.36	35,900	±155

'Average postdrilling concentration at station PH-J
[b]Average depth-integrated concentration
'Ratio of contaminant concentrations in drilling muds to background concentrations at station PH-J
'Based on observed barium concentration in background trapped sediments, drilling muds, and trapped sediments collected during peak drilling discharge (October 1988)
[e]$n = 3; \beta = 0.2$
'Measured concentrations

Table 8. Maximum predicted contaminant concentrations (μg/g) in surface sediments at the nearfield station PH-J. Predicted concentrations are based on a 0.32% drilling-mud-derived fraction of surface sediments.

	Background* Concentration (μg/g)	Concentration in Muds[b] (μg/g)	Enrichment Ratio[c]	Predicted Concentration[d] (Jig/g)	Predicted Increase (%)	Detectable Change[e] (%)
Ag	0.15	0.28	1.9	0.15	0.0	±20
As	6.0	6.3	1.1	6.0	0.0	±30
Ba	798	107,782	135	1,135[f]	42[f]	±9
Cd	0.55	1.2	2.2	0.55	0.0	±25
Cr	112	85	0.8	112	0.0	±25
Cu	19	30	1.6	19	0.0	±21
Hg	0.06	0.13	2.3	0.06	0.0	±53
Ni	48	41	0.9	48	0.0	±13
Pb	16	19	1.2	16	0.0	±34
v	63	71	1.1	63	0.0	±42
Zn	65	290	4.5	66	1.1	±6
THc	51	388	7.5	53	2.1	±19
ΣPAH	1.5	25	17	1.5	5.0	±56
Naph	0.38	18	48	0.43	15	±40

'Average predrilling concentration at station PH-J
[b]Average depth-integrated concentration
'Ratio of contaminant concentrations in drilling muds to background concentrations at station PH-J
'Based on barium concentrations measured in background surface sediments, drilling muds, and surface sediments collected during peak drilling discharge (October 1988)
[e]$n = 3; \beta = 0.2$
'Measured concentrations

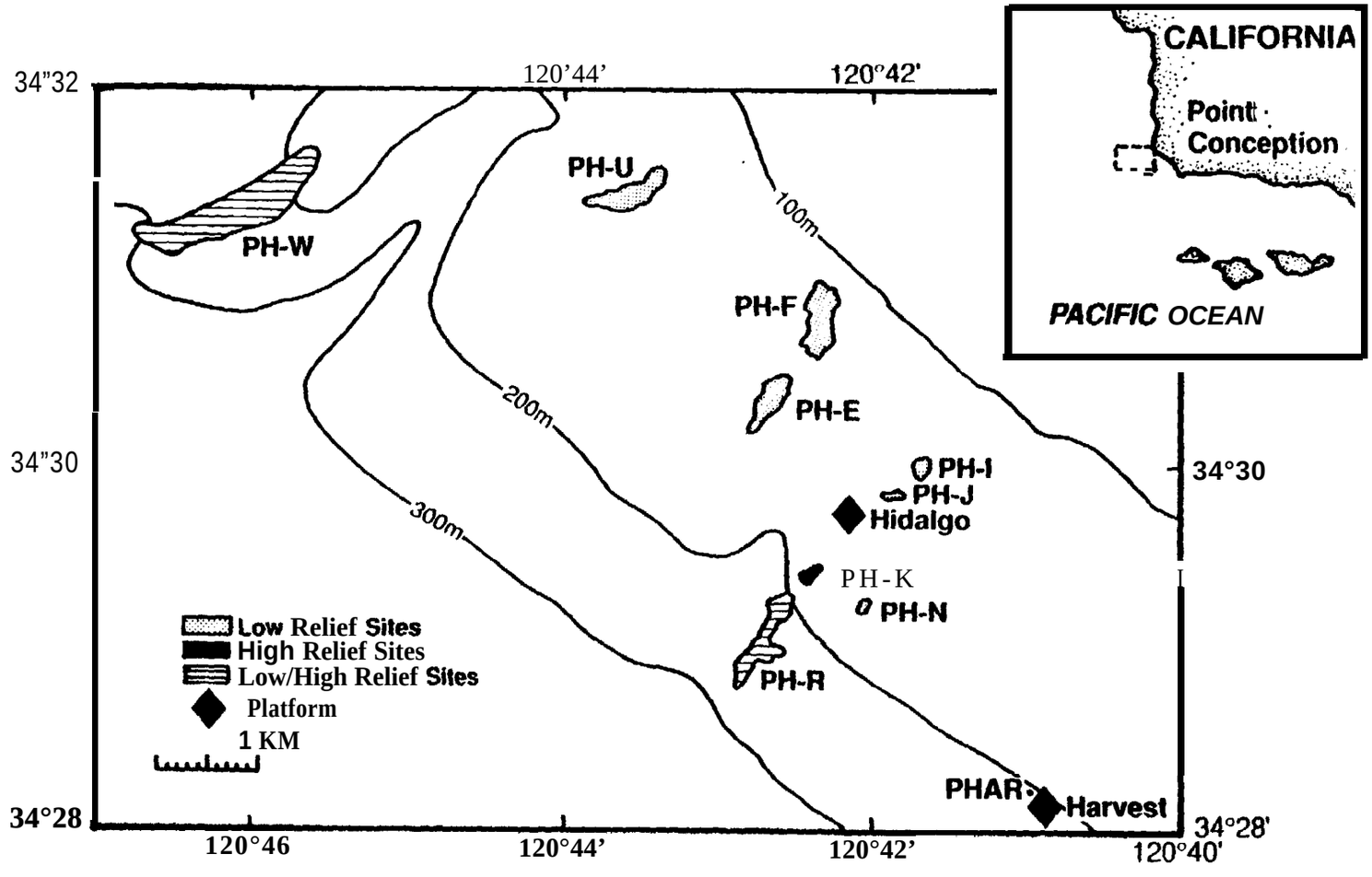

Figure 1. Locations of hard-bottom sampling stations in the Platform Hidalgo study area. Stations PH-I, PI-I-J, PH-K, PH-N, and PH-R are nearfield; Stations Pi-i-E and PH-F are midfield; Stations PH-U and PH-W are farfield.

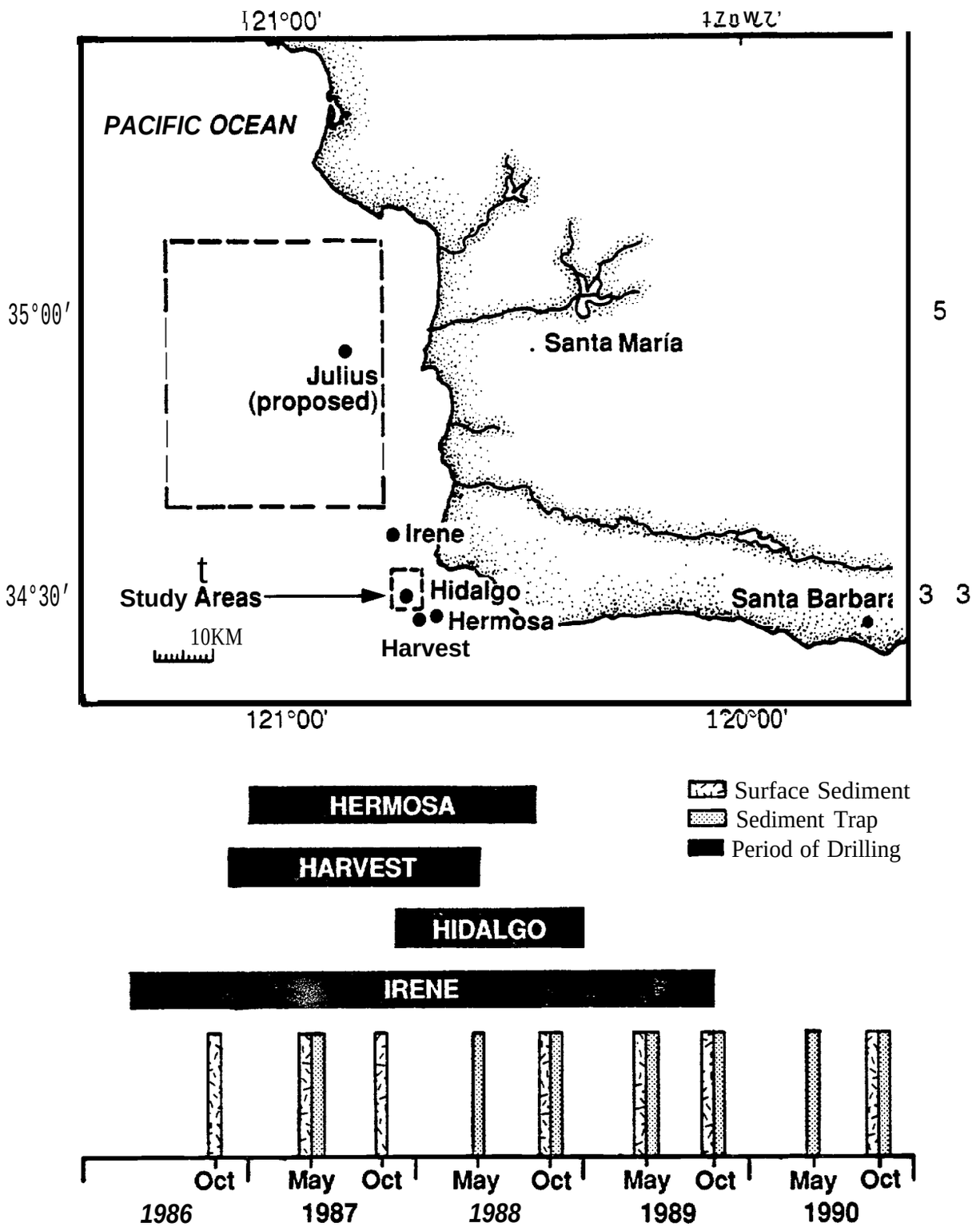

Figure 2. Location of Platform Hidalgo study area and the proposed site for Platform Julius (top). Types of samples collected and drilling periods at platforms in the Arguello Field are shown in relation to sampling times (bottom).

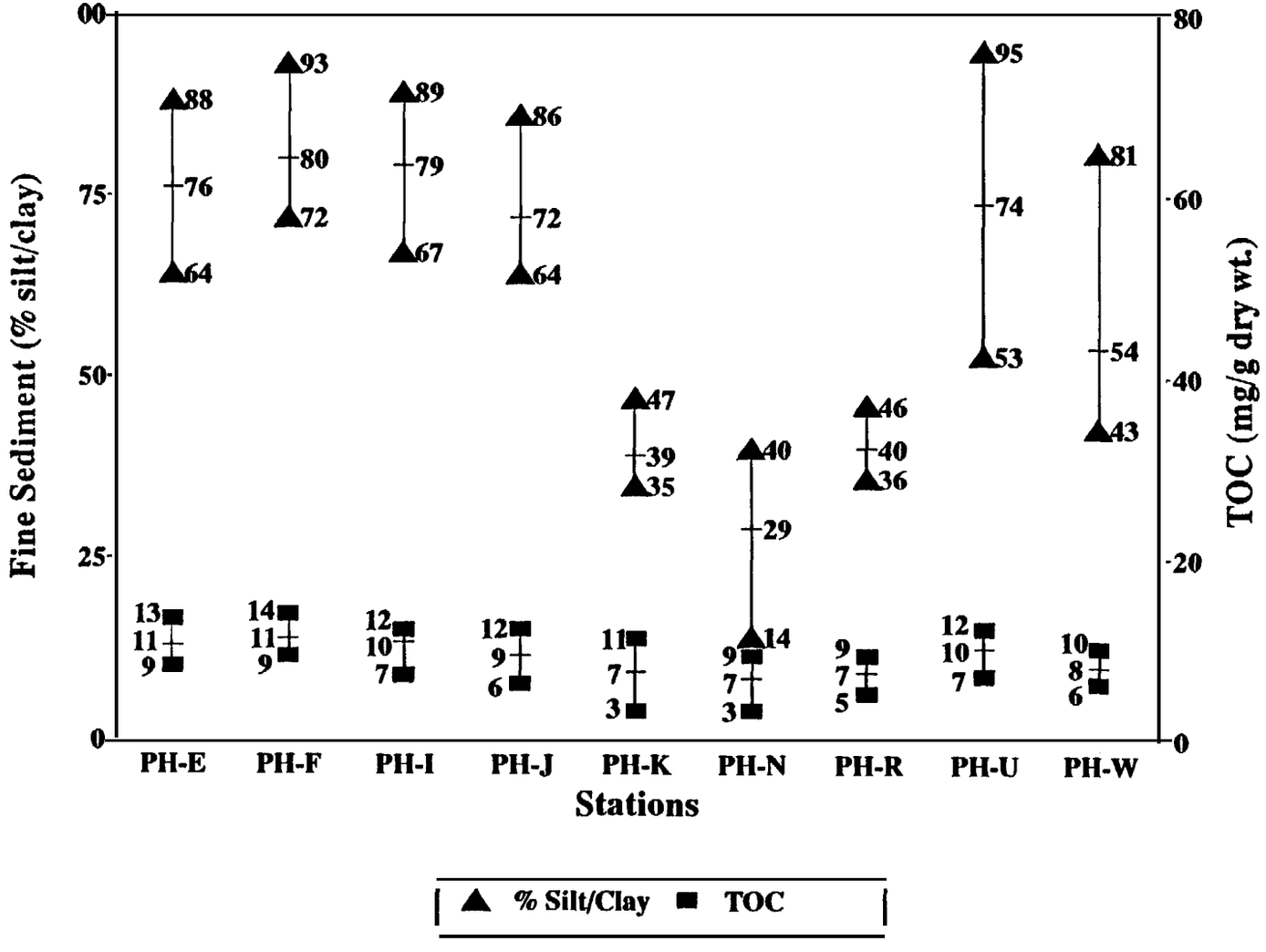

Figure 3. Spatial variation of fine sediment (% silt/clay; triangles) and total organic carbon (TOC) concentrations (mg/g dry weight; squares) in surface sediments from Platform Hidalgo stations. Percent fines and ranges, and TOC concentrations and ranges shown for individual stations are means for all samples collected over time.

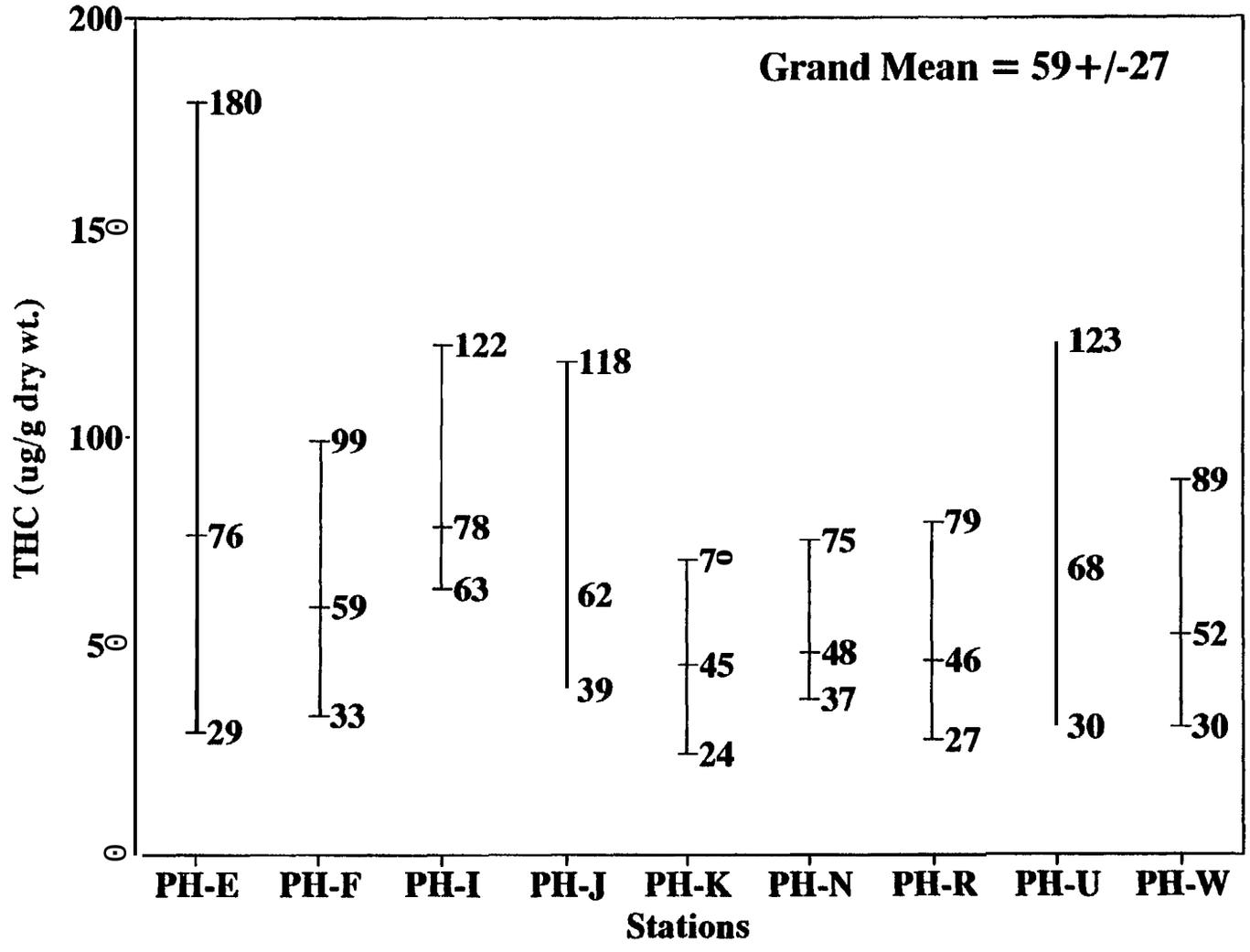

Figure 4. Spatial variation of total hydrocarbon (THC) concentrations (μg/g dry weight) in surface sediments from each Platform Hidalgo station. THC concentrations and ranges shown for individual stations are means for all samples collected over time.

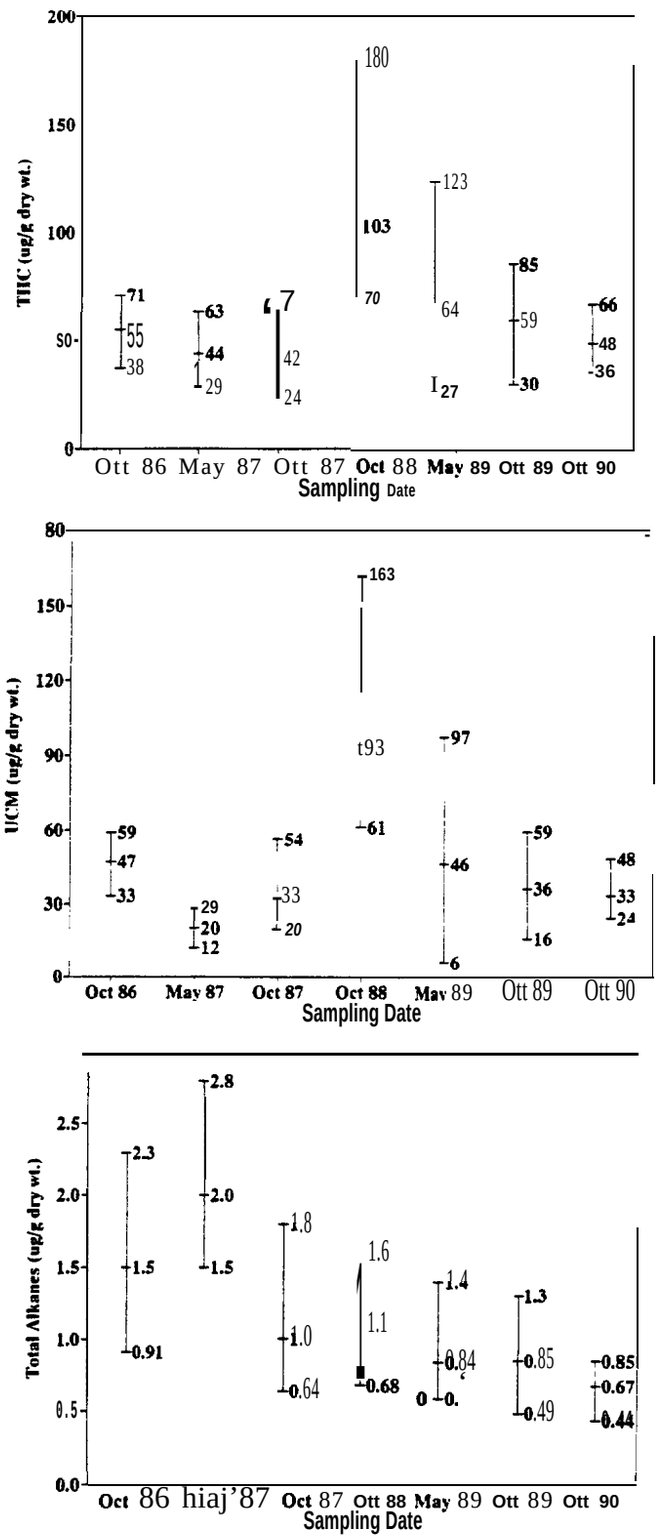

Figure 5. Temporal variation in total hydrocarbon **(THC)** concentrations (a); unresolved complex mixture **(UCM)** concentrations (b); and total **alkane** concentrations (c) in surface sediments near Platform **Hidalgo**. Concentrations and ranges shown for each sampling survey are means for all stations.

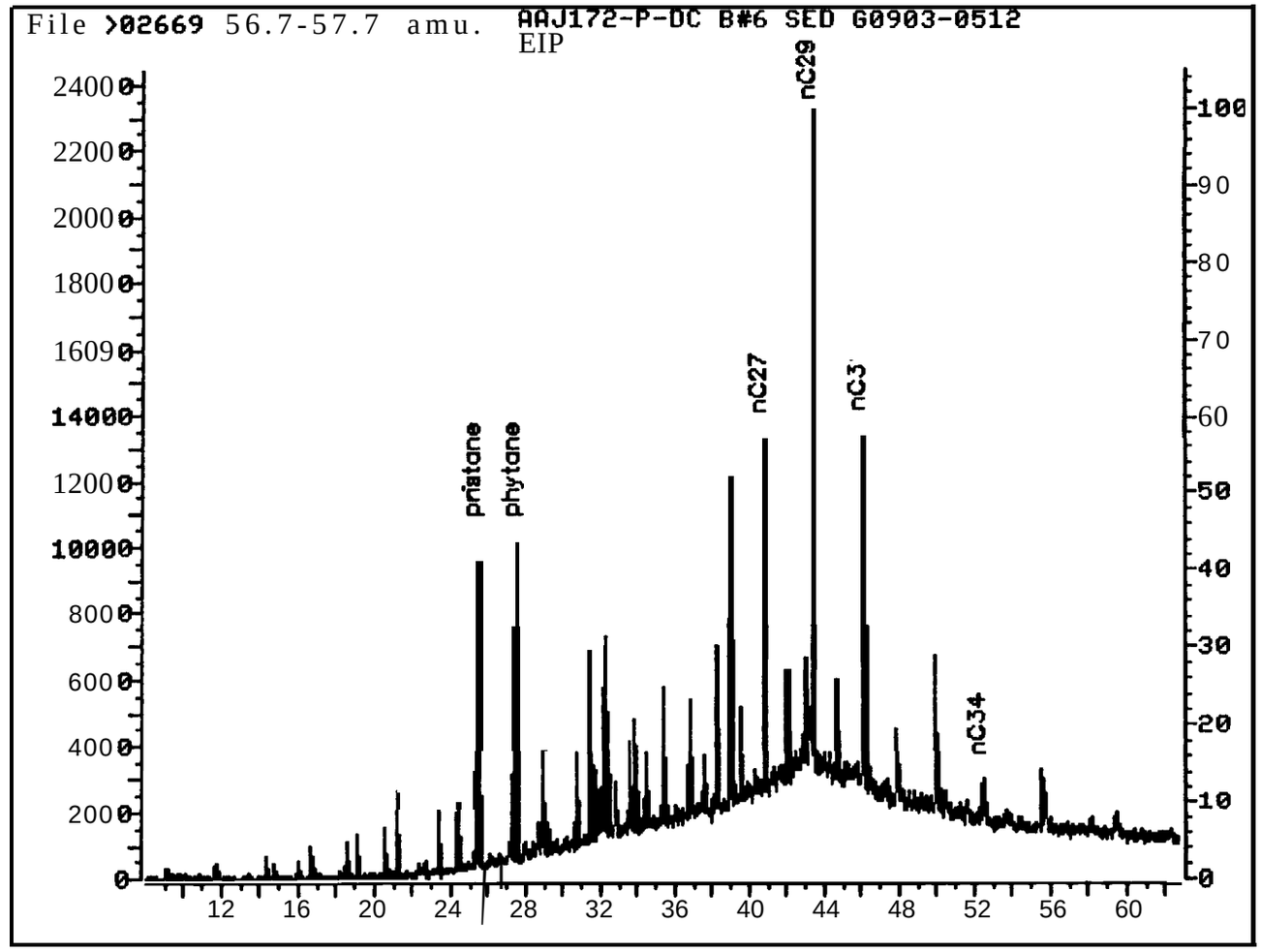

Figure 6. **GC/MS** extracted-ion (m/z 57) profile from station PH-E (October 1988) surface sediment. **Chromatogram** illustrates (1) **odd-carbon** dominance between **n-C_{25} and n-C_{31}** range; (2) near-equal **concentrations of pristane and phytane;** and (3) large unresolved complex mixture **(UCM). These features are typical of** most surface sediments collected in the study area.

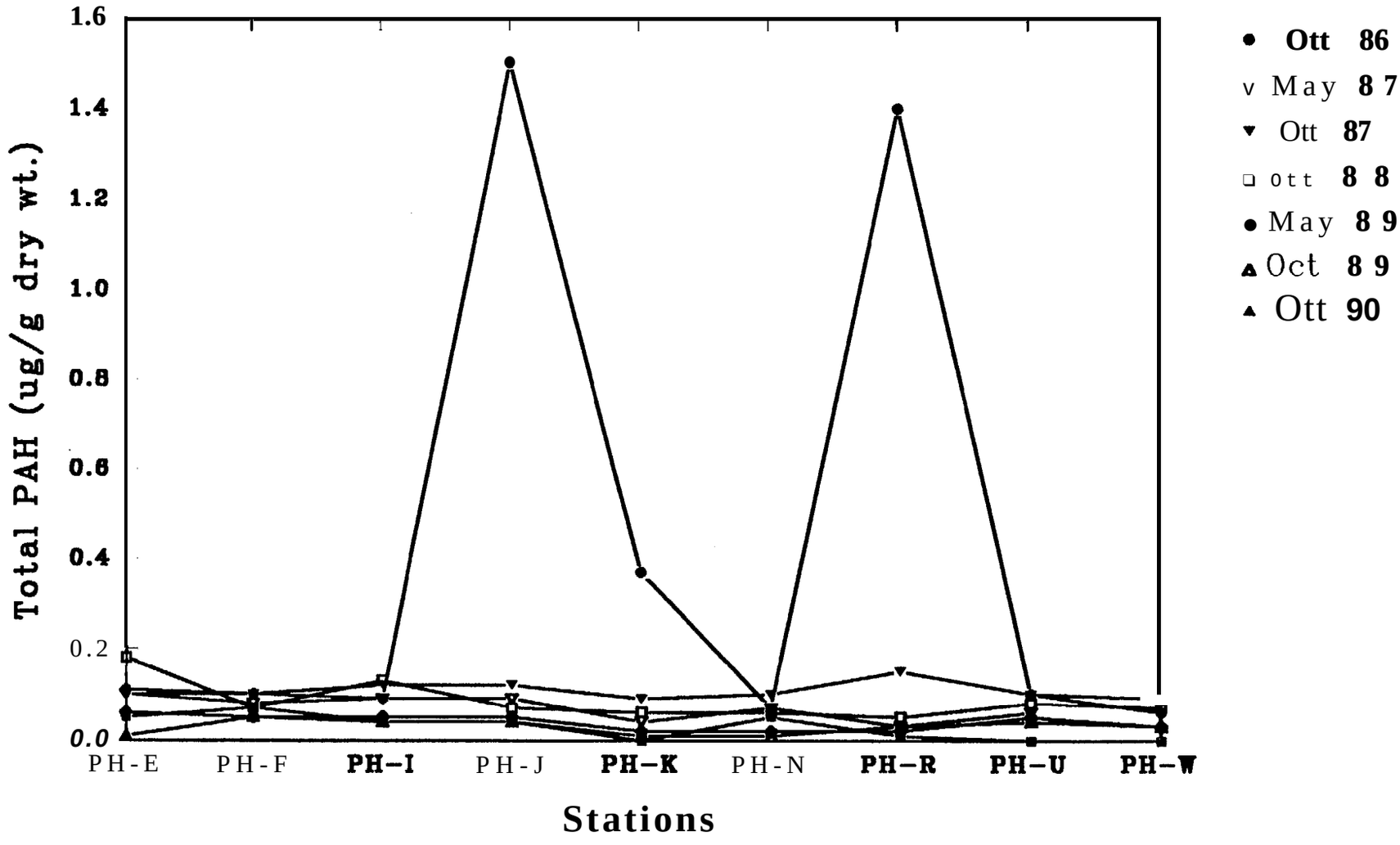

Figure 7. Total resolved polynuclear aromatic hydrocarbon (ΣPAH) concentrations (μg/g dry weight) in surface sediments from all Platform Hidalgo stations sampled during all surveys.

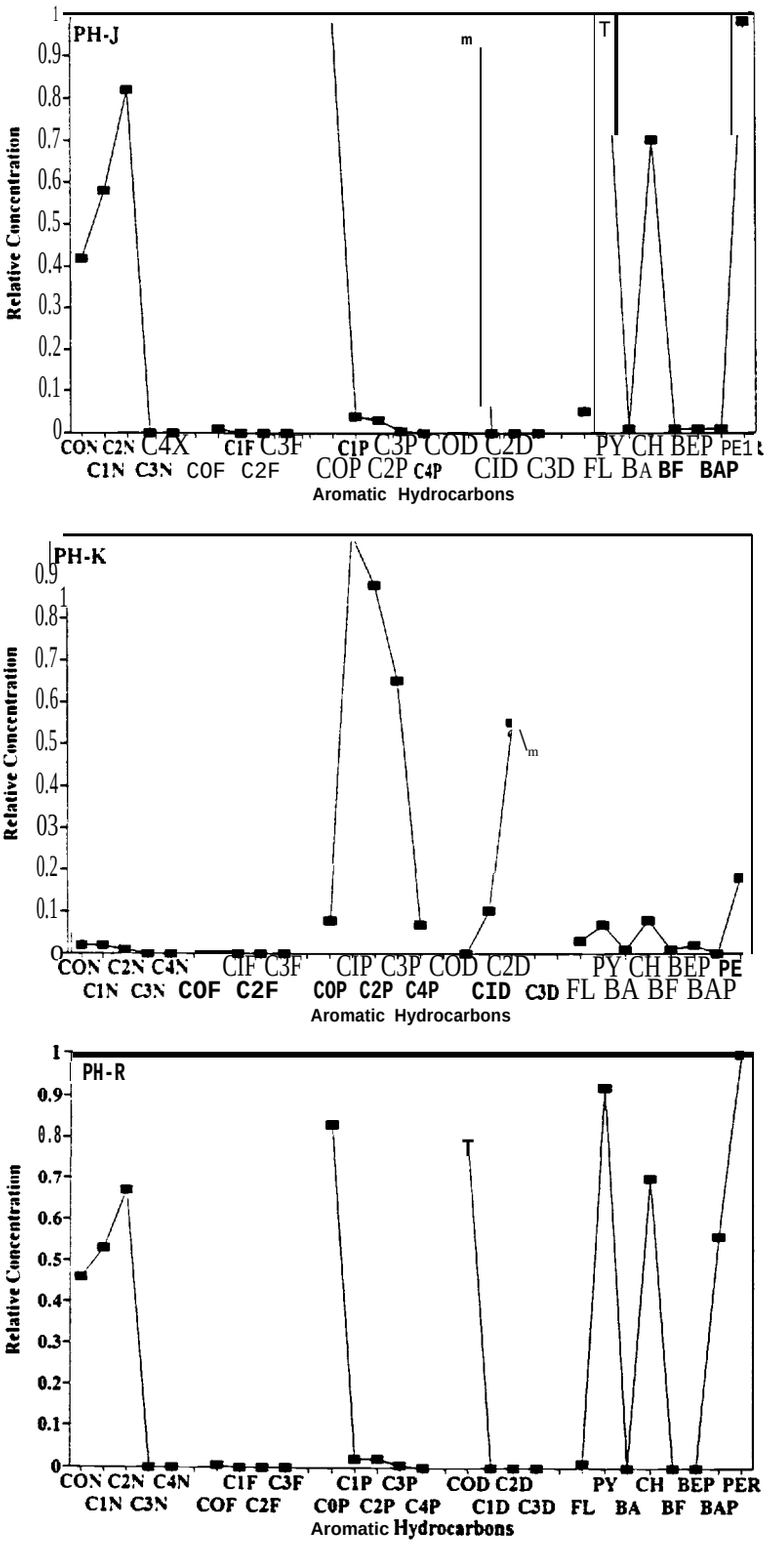

Figure 8. **Alkyl homologue** distributions of **polynuclear** aromatic hydrocarbons **(PAHs)** in surface sediments from Platform **Hidalgo** 'stations **PH-J**, PH-K, **and** PH-R sampled in October 1986. CON - C4N are **naphthalene** and **alkylated homologs;** COF - C3F are **fluorene** and **alkylated homologs;** COP - C4P are phenanthrene and **alkylated homologs;** COD - **C3D** are **fluorene** and **alkylated homologs;** FL = **fluoranthene; PY** = pyrene; **BA** = **benz[*a*]anthracene;** CH = **chrysene;** BF = **benzofluoranthenes;** BEp = benzo[e]pyrene; BAP = **benzo[*a*]pyrene;** PER = **perylene.**

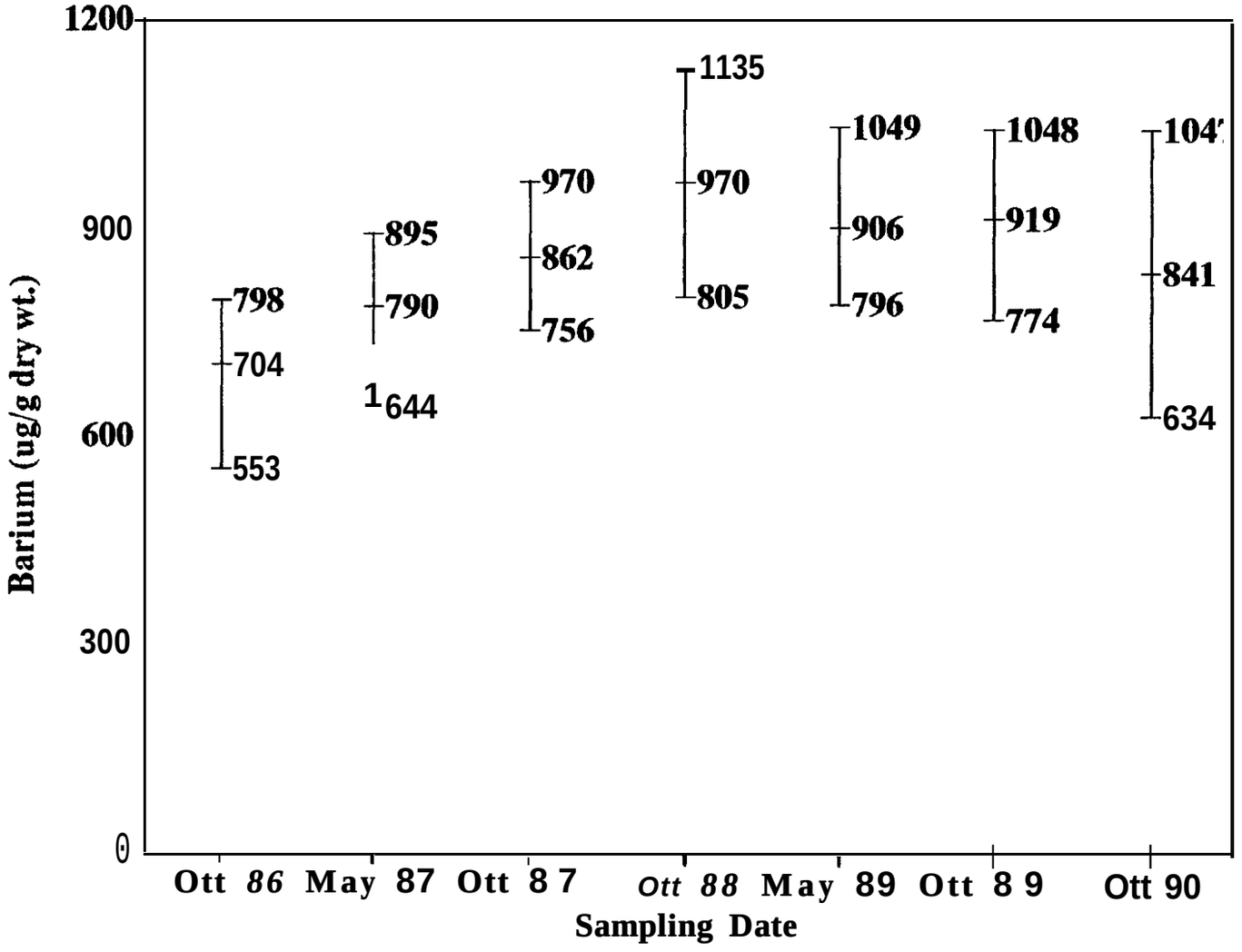

Figure 9. Temporal variation in barium concentrations (**μg/g** dry weight) in surface sediments from five nearfield stations along a northeast-south west transect through Platform **Hidalgo.** Concentrations and ranges shown for each sampling survey are means for all five stations **(PH-I,** PH-J, PH-K, PH-N, and **PH-R).**

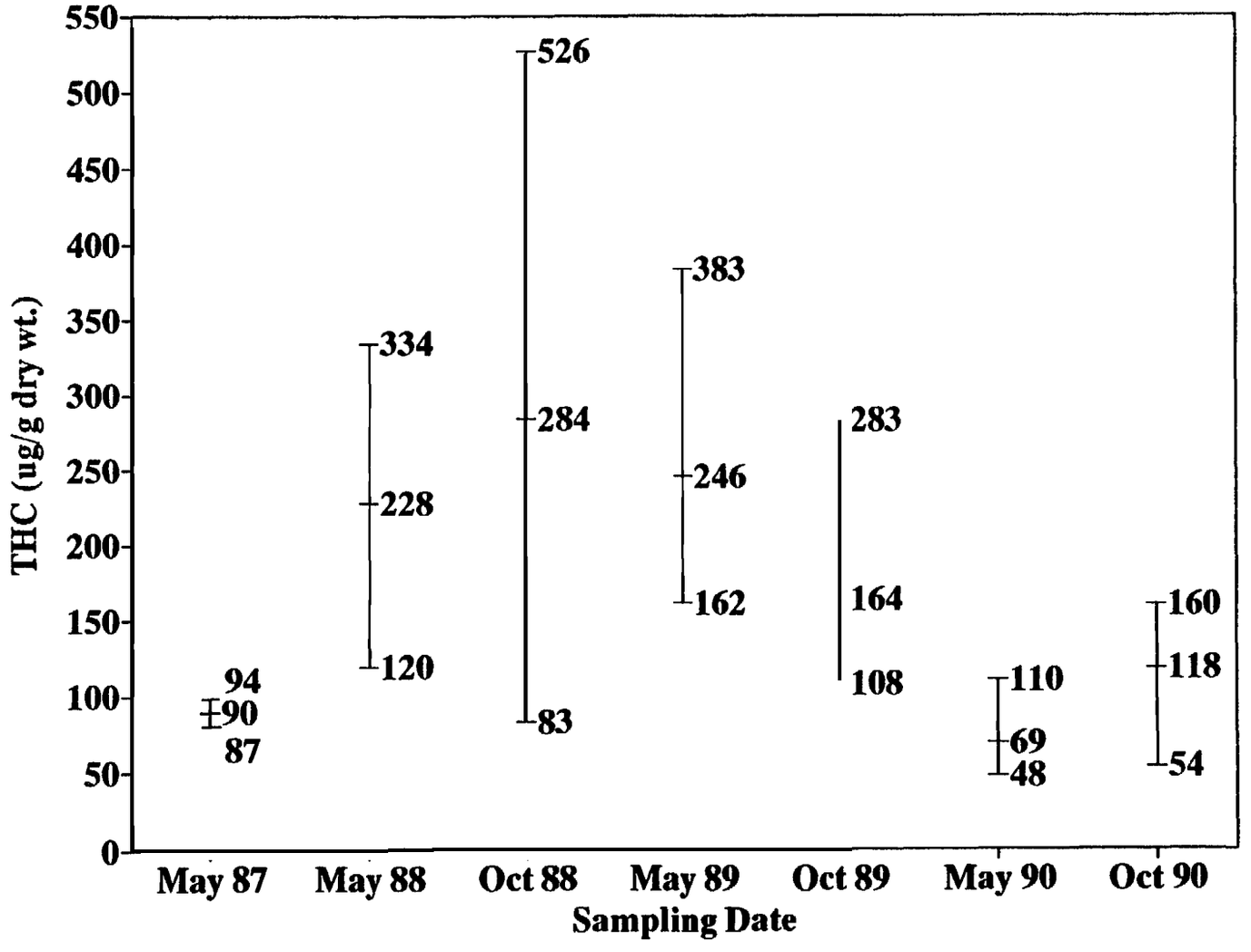

Figure 10. Temporal variation in total hydrocarbon (THC) concentrations (μg/g dry weight) in trapped sediments from Platform H algo stations. Concentrations and ranges shown for each sampling survey are means for all stations.

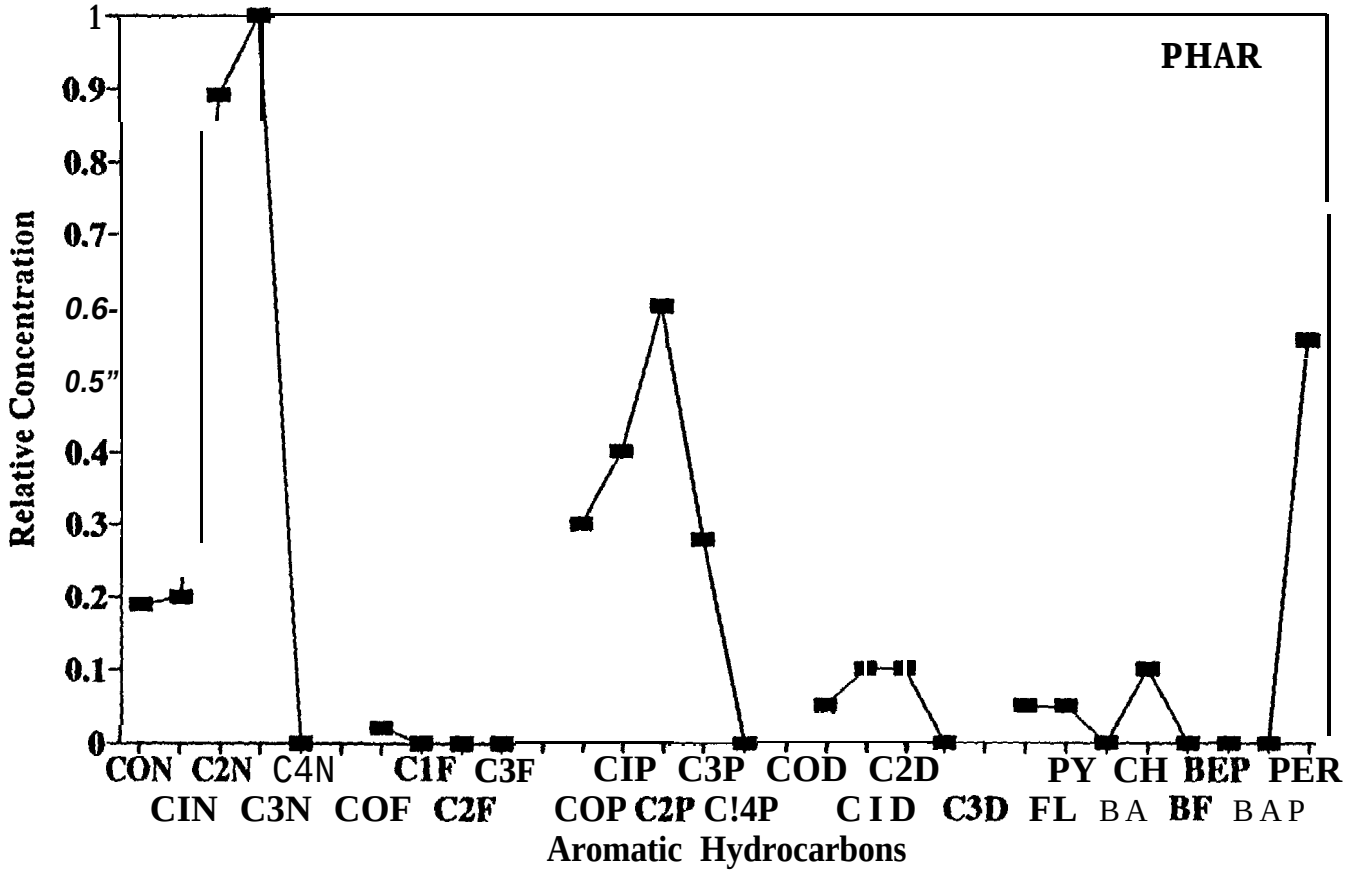

Figure 11. Alkyl homolog distributions of polynuclear aromatic hydrocarbons (PAHs) in trapped sediments collected from station PHAR, near Platform Harvest, during October 1988. CON - C4N are naphthalene and alkylated homologs; COF - C3F are fluorene and alkylated homologs; COP - C4P are phenanthrene and alkylated homologs; COD - C3D are fluorene and alkylated homologs; FL = fluoranthene; PY = pyrene; BA = benz[*a*]anthracene; CH = chrysene; BF = benzofluoranthenes; BEP = benzo[*e*]pyrene; BAP = benzo[*a*]pyrene; PER = perylene.

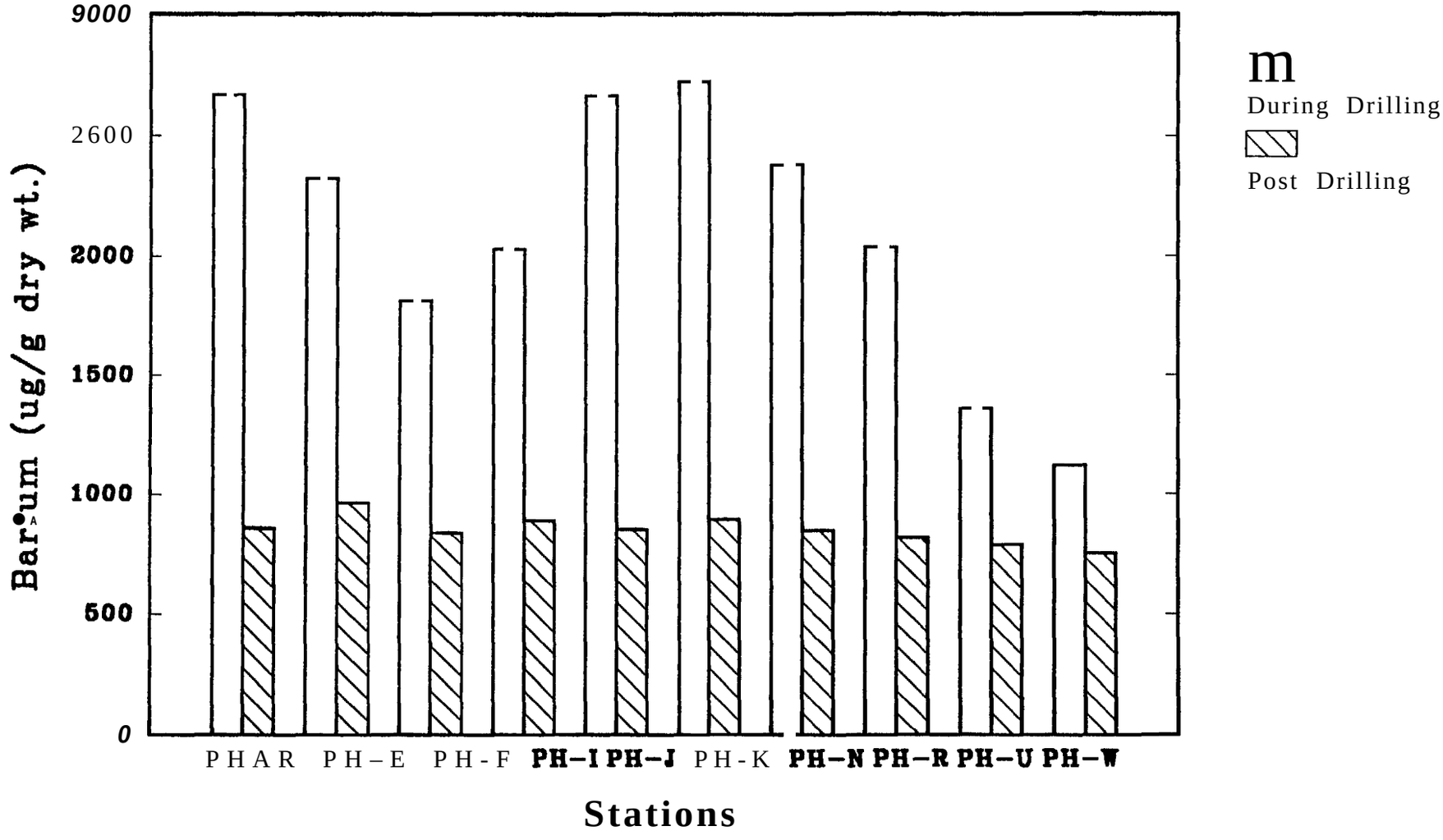

Figure 12. Mean barium concentrations (**μg/g** dry weight) in trapped sediments collected from **all** Platform Hidalgo stations sampled during periods **of drilling and after** drilling stopped. Duringdrilling data aremean concentrations fortiree sets of replicate trap samples collected October 1987-May 1988, May 1988-October 1988, and October 1988-May 1989. Postdrilling data are mean concentrations for four sets of replicate samples collected May 1989-October 1989, October 1989-May 1990, and May 1990-October 1990.

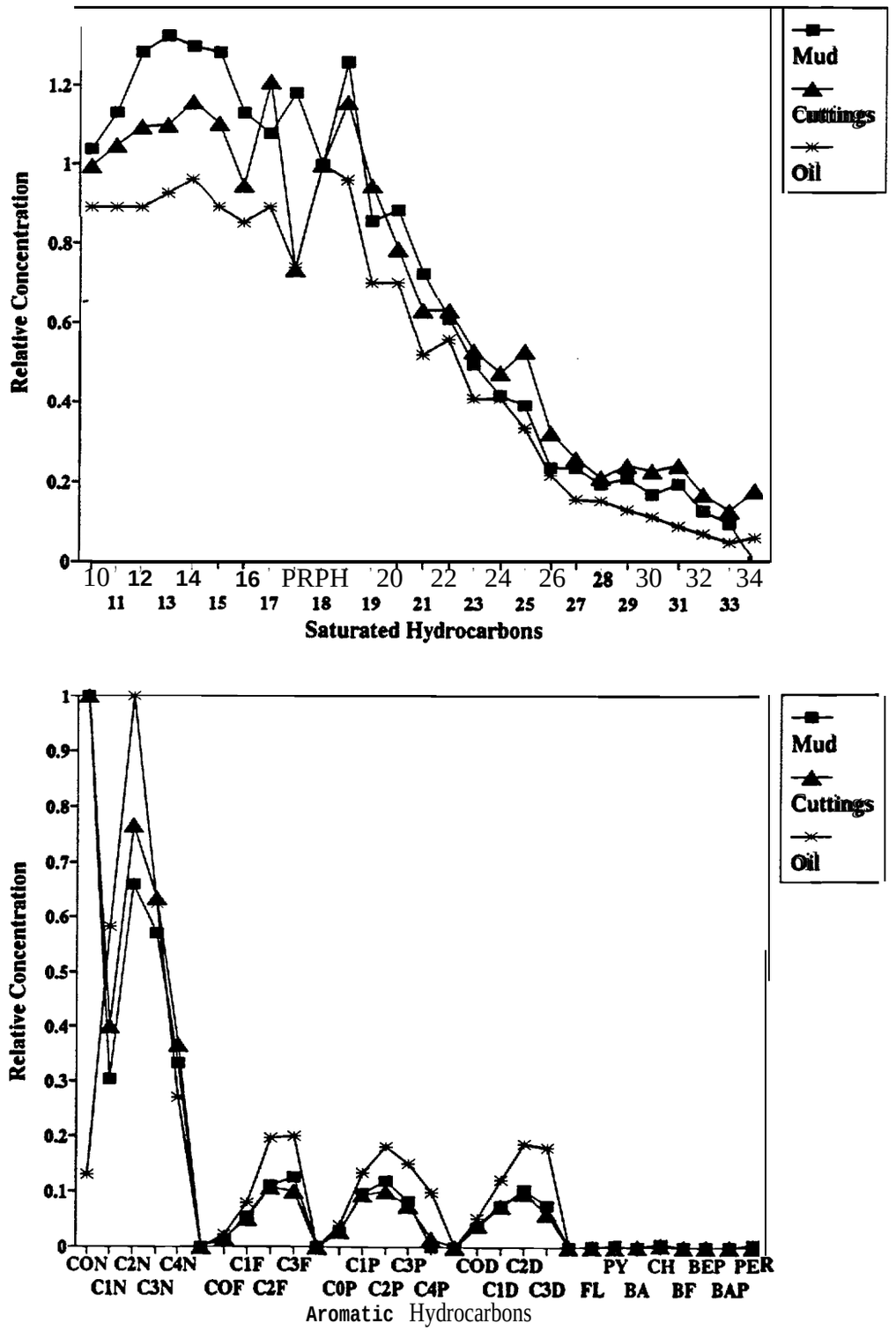

Figure 13. Comparison of saturated hydrocarbon distributions (a) in near-bottom drilling muds, near-bottom drill cuttings, and production oil; polynuclear aromatic hydrocarbon (PAH) homolog distributions (b) for all three samples. Normal alkanes are displayed by carbon number; PR is pristane; PH is phytane; CON - C4N are naphthalene and alkylated homologs; COF - C3F are fluorene and alkylated homologs; COP - C4P are phenanthrene and alkylated homologs; COD - C3D are fluorene and alkylated homologs; FL = fluoranthene; PY = pyrene; BA = benz[*a*]anthracene; CH = chrysene; BF = benzofluoranthenes; BEP = benzo[e]pyrene; BAP = benzo[*a*]pyrene; PER = perylene.

7. SPATIAL VARIATION IN HARD-BOTTOM EPIFAUNA IN THE SANTA MARIA BASIN, CALIFORNIA: THE IMPORTANCE OF PHYSICAL FACTORS

DANE D. HARDIN, JONATHON TOAL, TERENCE PARR,
PETER WILDE, AND KATHLEEN DORSEY

Kinnetic Laboratories, Inc.
307 Washington Street, Santa Cruz, California 95060

INTRODUCTION

Rocky intertidal and shallow subtidal habitats have been extensively studied, and there are numerous physical and biological factors known to affect their community composition. For example, community composition has been ascribed to larval settlement (Caffey, 1985; Connell, 1985; Davis, 1987), competition and predation (Bak et *al.*, 1982; Kay and Keough, 1981; Sebens, 1985, 1986), grazing (Witman, 1985, 1987; Miller, 1982), temperature (Glynn and D'Croz, 1990; Scheer, 1984), water currents (Barry and Dayton, 1986, 1988; Dayton et *al.*, 1982; Peattie and Hoare, 1981; Sebens, 1984), turbidity (Dodge and Vaisnys, 1977; Hong and Sasekumar, 1981; Hudson, 1981; Loya, 1976), and ultraviolet light (Jokiel, 1980). The rich ecological literature of rocky intertidal and shallow subtidal habitats is partly due to the ease of viewing and manipulating these habitats, and the steep gradients in physical factors which are present.

Until recently, ecologists have not had the instruments to investigate deeper hard-bottom habitats, which are inaccessible by SCUBA diving. Generally, deeper habitats have been assumed to vary less over time and space than shallower habitats, Observations have indicated deeper hard-bottom communities vary according to depth (Carney and Carey, 1976; Hecker *et al.*, 1983; Rowe and Menzies, 1969; Vinogradova, 1962), and a number of studies have suggested the importance of hydrodynamic processes in structuring these communities (Genin *et al.*, 1986; Messing et *al.*, 1990; Mullineaux, 1988, 1989). Nevertheless, few generalizations can be drawn, because of the paucity of quantitative 'investigations. Studies of deep hard-bottom communities are still generally limited to describing organism distributions, so that testable hypotheses can be formulated concerning the factors that affect those distributions.

The Santa Maria Basin, along the southern California shelf and slope, is the site of a multidisciplinary study to determine the effects of discharges from petroleum platforms on the benthic environment (Hyland *et aZ.*, 1990; Hyland *et al.*, Chapter 9). Hard-bottom communities have been emphasized, because of assumptions concerning their sensitivity to disturbance, and their importance as nursery areas for commercially valuable species. Few changes in species abundances have been related to the discharges (Hyland *et al.*, Chapter 9), so the 4-year set of data can be used to describe the natural spatial distribution of organisms in the study area.

The Santa Maria Basin has previously been the site of several qualitative surveys of hard-bottom communities related to petroleum exploration (Dames & Moore, 1982, 1983; Nekton, 1981; Nekton and Kinnetic Laboratories, 1983; SAIC, 1986). These surveys were important for describing the visibly dominant species in the area, and for proposing factors which may affect their distributions. Nevertheless, we are not aware of previous quantitative studies over the broad range of time and space covered by the present study, either in the Santa Maria Basin or elsewhere in outer continental shelf and slope environments.

METHODS

The study area is approximately 20 km west of Point Conception, near the western end of the Santa Barbara Channel (Figure 1). Oceanographic processes in the area are very complex due to the confluence of the westward flow along the northern shore of the Santa Barbara Channel with the southward flow of the California Current (Savoie *et al.*, Chapter 4). It is the site of substantial upwelling. Isobaths are oriented northwest-to-southeast, and bottom currents generally flow parallel to the isobaths, although current-meter records contain a strong cross-shelf tidal component (Savoie *et al.*, Chapter 4).

A reconnaissance was conducted in October 1986 of areas near Platform Hidalgo which had been indicated as hard-bottom habitat by previous geophysical surveys. Nine rocky reefs were chosen as sampling stations that were (1) at various distances from Platform Hidalgo, (2) across a range of depths, and (3) representative of two types of habitat (Figure 1 and Table 1). Low-relief habitat was defined as rocks 0.2-0.5 m in vertical relief, and high-relief habitat was defined as rocks > 1.0 m in vertical relief. High-relief habitat was found only below approximately 160 m water depth.

Sampling was conducted in October 1986, July 1987, November 1987, October 1988, May 1989, October 1989, and October 1990. The epifaunal assemblages at the hard-bottom stations were sampled photographically with a remotely operated vehicle (ROV). The ROV was equipped with a video camera, a 70-mm still camera, a strobe light, two split-beam lasers, and a five-function manipulator. The ship's position was determined with an accuracy of $\pm$ 3 m using range data from a series of transponders located at surveyed sites on shore. These data were interfaced with an acoustic navigation system on the ROV, which enabled a position accuracy for the ROV of c 5 m.

The primary sampling device for the hard-bottom assemblages was the 70-mm still camera. The coincidence of the parallel lines of laser images, as seen on the video monitor, indicated the proper distance and angle of incidence between the camera and the seabed (Caimi et *al.*, 1987). Photographs were taken from a distance of 1.4 m, so that the area sampled was 1 m^2. The mounts for the photographs provide a clear opening of 60 mm on a side, such that approximately 0.73m^2 was effectively sampled in each replicate.

Sampling methods at low-relief and high-relief stations differed slightly. Sampling at low-relief stations was accomplished by directing the ROV on a random heading with the cameras pointing down toward the bottom. Because the seabed in these areas is characterized by patchy hard bottom surrounded by soft bottom, all suitable rocks that occurred every 5-10s were photographed until five to 10 samples had been obtained (depending upon the density of rocks in the area). Another heading was then taken and the process was repeated. At high-relief stations, the ROV took a random heading with the cameras pointed toward the front of the vehicle. When suitable habitat was encountered, the ROV was maneuvered around, and up and down the rock feature, taking nonoverlapping photographs. After a rock feature was sampled, the ROV was directed on another random heading until the next suitable feature was located. The process was then repeated. The ROV position was recorded for every 10th photographic sample, to ensure that the same area of each reef was sampled on successive sampling periods.

Approximately 80 photographic samples were taken at each station to allow 60 samples per station to be analyzed. Some samples were rejected for having too little relief and some were rejected for having less than 30% cover of rock. In all, 3587 photographic samples were analyzed, representing seven samplings of 11 stations.

Epifaunal specimens were collected and identified to aid in the analysis of the photographs. The manipulator on the ROV was used to obtain rocks and to bring them to the surface. The rocks were labeled, placed into buffered 10% formalin, and taken ashore to the laboratory. The epifauna were subsequent y removed and identified.

Ancillary measurements were made at each station for later use as correlates in the statistical analyses. The compass heading of the ROV was recorded for each photograph in high-relief habitat to determine if species distributions vary according to their orientation on high-relief rocks. Sediment traps were also deployed at each station (Parr *et al.*, Chapter 3), and the sediment flux data are used to determine whether organism abundances vary according to concentrations of suspended sediments.

Photographic samples were analyzed by a random point-contact method. Although this method may be inferior to *in situ* methods of quantifying abundances in multilayered assemblages (Foster et *al.*, 1991), the inaccessibility of these deep habitats, and the absence of layering, justifies its use in this case. Each photograph was projected, at life size, onto a screen upon which 50 points were randomly distributed. The species or substrate type under each point was noted, and the numbers of individuals of solitary species were counted. Some types of sponges are very consistent in size and were also counted. In addition, all species that showed in a photograph were recorded, regardless of whether they had been contacted by a random point. These species were assigned a default percent cover of 0.5 for calculations of similarity. Default percent-cover values were not added into the total abundances for each taxonomic group.

The percent cover of a species that was contacted by the random points was estimated by dividing the number of contacts by the total number of points. Because this study is focusing on hard-bottom habitat, and because some points fell on deep shadow and could not be read, the denominator in the percent-cover calculations was reduced by the number of dots contacting sediment or shadow. Similarly, the counts of individual organisms were normalized to the visible amount of rock in each photograph by dividing them by the percentage of visible-rock points.

Many of the taxa (e.g., sponges, hydroids, anthozoans, polychaetes, and ectoprocts) observed in the photographs were given descriptive names only, which were assigned to specific morphological forms that could be consistent y distinguished from other forms. Such "speciation" of taxa can, however, result

in either overestimation or underestimation of the abundance of the correct species. Converse] y, because some descriptive taxa may contain several species that cannot be distinguished from one another, an underestimate of the species richness of the group would result.

Several procedures were performed to determine the factors affecting spatial variation in the hard-bottom epifaunal assemblages. Descriptive as well as parametric statistical methods were used. Initially, the affinities among the assemblages at each station and among species were estimated using the Bray-Curtis Similarity Index (Bray and Curtis, 1957). The values from these comparisons were clustered using an unweighed pair-group method (Swam, 1978). The trends suggested by the similarity comparisons were evaluated using analysis of variance (ANOVA).

The ANOVAs were performed to determine the effects of depth and relief on the abundance of each of the 15 most abundant taxa in each of low-relief and high-relief habitats. Because some taxa are present on both lists, a total of 22 taxa were tested. Stations were pooled into two depth categories: shallow (105 to 119 m) and deep (160 to 212 m). Stations were also categorized as being either low-relief or high-relief. There are significant differences in epifaunal abundances among stations within depth and relief categories, preventing the use of each random photographic sample as an independent replicate. Therefore, unreplicated two-way ANOVAs (time x depth and time x relief) were used, in which the mean of all photographic samples within each time x depth or time x relief combination was used as the unrepl icated value in each cell. The two-way interaction effects were pooled to provide an estimate of error variance. All tests based upon densities of organisms were run on data transformed by the square root transformation, and all tests based upon percent cover were run on data transformed by the arc sine transformation (Sokal and Rohlf, 1969). Species that failed Bartlett's test for homogeneity of variances were tested with a nonparametric two-way A NOVA. Because our sampling design is unbalanced (Table 1), two separate two-way ANOVAs were run. These included (1) for effects of depth, in low-relief habitat, and (2) for effects of relief, at deep stations.

Correlation coefficients (Pearson product-moment) were calculated to determine the relationships between physical and biological measurements. Correlations were determined among the 22 common taxa to ascertain whether interspecific interactions might be influencing their abundances and distributions.

The spatial variation of species abundances on high-relief rocks was evaluated with a one-way A NOVA. The percent cover of each of the 22 common taxa was tested in high-relief habitat for differences among eight orientation categories (N, NE, E, SE, S, SW, W, and NW). The reciprocal of the ROV heading, at the time each photograph was taken, was used to determine the orientation for each sample.

RESULTS

A rich epifaunal assemblage inhabits rocky areas near Platform Hidalgo in the Santa Maria Basin. Over seven sampling periods, there were 263 taxa observed at eight low-relief stations and 222 taxa observed at three high-relief stations. Total organismal cover on rocks averages approximate y 97.5 %. Much of this cover consists of a turf composed of komokoiacea forarniniferans and hydroids. This turf varies in average percent cover from 59.5 at station PH-R(H) to 87.1 at station PH-I(L), covering most of the unsedimented rock surfaces which are not occupied by megafauna.

No other taxon dominates the percent-cover estimates within the study area (Table 2). The 15 most abundant taxa in low-relief habitat total approximate y 19.3 % cover, whereas the 15 most abundant taxa in high-relief habitat total approximate] y 26.6% cover. Although no taxon dominates, seven are common in both low-relief and high-relief habitat. The group of unidentified ophiuroids, the crinoid *Florometra serratissima*, *the* anemone *Metridium giganteum* (formerl y *M. senile; see* Fautin et *al.*, 1989), the group of unidentified sabell ids, the solitary urochordate (ascidian) *Pyura haustor*, *the* white encrusting sponge, and the group of unidentified galatheid crabs are all among the 15 most abundant taxa in both types of habitat. Conversely, the solitary corals *Paracyathus stearnsii* and *Caryophyllia* sp(p)., the soft coral *Lophogorgia chilensis*, *the* unidentified terebellid polychaetes, the ectoproct *Cellaria* sp(p)., the ophiuroid *Ophiacantha diplasia*, and the solitary ascidian *Halocynthia hilgendorfi igaboja* are among the 15 most abundant taxa only in low-relief habitat. Similarly, the shelf sponge, four anemones (*Amphianthus californicus*, *Stomphia didemon*, *the* tan zoanthid, and the anemone with white disc and purple tentacles), the solitary coral *Desmophyllum cristagalli*, and the colonial coral *Lophelia prolifera* are among the most abundant taxa only in high-relief habitat.

Despite the lack of dominance by any one taxon, the 22 taxa comprising the 15 most abundant in each relief category consist mostly of anthozoans. Ten of these 22 taxa are anthozoans that cover 4.2% of the low-relief rock surfaces and 13.5% of the high-relief rock surfaces. Three of these 22 taxa are poriferans, which contribute 1.3% and 3.3% cover on low-relief and high-relief rocks, respectively,

There are two ophiuroid taxa that cover 6.9% and 3.5% of low-relief and high-relief rocks, respective] y. Two polychaete taxa cover 1.9% of low-relief rocks and 2,4% of high-relief rocks. Two urochordates cover 1.2 % of low-relief rocks and 0.9% of high-relief rocks. The one decapod taxon covers 0.6% and 1.7% of low-relief and high-relief rocks, respective y; the one ectoproct taxon covers 0.5 % of low-relief rocks; and the one crinoid taxon covers 2.7% and 1.3% of low-relief and high-relief rocks, respective] y.

The epifaunal distributions contribute to station similarities that cluster according to depth and relief (Figure 2). Cluster 1 is composed exclusively of shallow low-relief stations. The high similarity between stations PH-F(L) and PH-U(L) are attributable to high densities of the solitary coral ***Balanophyllia elegans***. Cluster 2 consists of all the deep stations, with smaller clustered pairs comprised of the shallowest two deep stations, PH-N(L) and PH-K(H), and pairs of deeper low-relief stations and high-relief stations.

The ANOVAs also indicate that abundances of the 22 common taxa generally vary according to either depth or habitat relief (Table 3). Nevertheless, no difference between depths was found for ***Lophogorgia chilensis, Metridium giganteum, Florometra serratissima, Ophiacantha diplasia***, *the* unidentified ophiuroids, ***Halocynthia hilgendorfi igaboja***, and ***Pyura haustor***. Similarly, no habitat relief preference is displayed by the anemone with white disc and purple tentacles, *L. chilensis*, *P. stearnsii*, *the* unidentified sabellids, *Cellaria* sp(p)., *F. serratissima*, *O. diplasia*, *the* unidentified ophiuroids, and *Pyura haustor*. Only *Caryophyllia* sp(p)., *Paracyathus stearnsii*, *Cellaria* sp(p)., and the combined cover of all taxa (including the foraminifera-hydroid turf) are highest at shallow stations. The abundances of 12 taxa and total suspension feeders, and the total number of taxa are highest at deep stations. Highest abundances are found in low-relief habitat only for *Caryophyllia* sp(p)., the unidentified terebellids, *H. hilgendorfi igaboja*, and total abundance of all taxa. There are significantly higher abundances for 10 taxa and total suspension feeders, as well as higher numbers of taxa at high-relief stations.

The ANOVA results enable the definition of eight categories of taxa, based upon variations in abundances according to depth and habitat relief [Figure 3(a-h)]. *Paracyathus stearnsii* and *Cellaria* sp(p). are most abundant at shallow stations and do not vary according to depth, whereas the anemone with white disc and purple tentacles and the unidentified sabellids are most abundant at deep stations, regardless of habitat relief [Figure 3(a, b)]. *Caryophyllia* sp(p). is most abundant in shallow low-relief habitat, and the unidentified terebellids are most abundant in deep low-relief habitat [Figure 3(c, d)]. *Halocynthia*

hilgendorfi igaboja is most abundant in low-relief habitat, without regard for depth, and *Metridium giganteum* is most abundant in high-relief habitat, without regard for depth [Figure 3(e, f)]. Nine taxa are significant y more abundant at deep stations with high-relief habitat [Figure 3(g)], and five taxa do not vary according to depth or habitat relief [Figure 3(h)].

Therefore, clusters of similarities among taxa, based upon their mean percent cover at each station and time (Figure 4), can be defined in terms of the depth and habitat differences determined by the ANOVA. Cluster 1 contains taxa that do not vary according to depth or habitat relief. Cluster 2 consists of all the taxa that are most abundant in low-relief habitat, without regard to depth, along with others that are widespread, but that may or may not vary according to depth or habitat relief. Cluster 3 contains ord y species with greatest abundances at deep stations, some of which are also most abundant in high- relief habitat. Cluster 4 contains two taxa that are almost exclusively restricted to deep stations with high-relief habitat.

Correlations among the 22 common taxa (Table 4) also suggest that the clusters of taxa similarities are due to abundance differences related to habitat variation, and not to obligate associations among taxa. Although these correlations are very low, many are highly significant due to the large number photographic samples analyzed. Seven of the 10 most positive correlations include at least one taxon that prefers deep high-relief habitat. Among these, numbers 1,2,5,6, and 9 are between taxa, both of which are most abundant in deep high-relief habitat. Conversely, only positive correlations 4 and 8 are between taxa that either have no depth or habitat preference, or that prefer shallow or low-relief habitat. The remaining positive interspecific correlation (number 3) is between taxa that are most abundant at deep stations, without regard to habitat relief.

The 10 most negative interspecific correlations probably also reflect abundance differences related to habitat variation, although antagonistic effects cannot be ruled out. Seven of the most negative correlations are between taxa, one of which is most abundant at shallow stations, with or without regard to habitat relief, and the other of which is most abundant at deep stations, with or without regard to habitat relief. Among these, numbers 2, 3, 7, and 10 are between *Paracyathus stearnsii* and one of several taxa which are most abundant in deep high-relief habitat. None of the most negative correlations are between taxa with the same pattern of distribution among depths and habitat reliefs.

The consistently positive correlations between taxa that are most abundant in deep high-relief habitat, and the consistently negative correlations between these taxa and those that are most abundant in shallow habitat suggest that these two groups have very different habitat requirements. Moreover, the requirements of the deep high-relief taxa appear to be especially strong, applying to many (41'%) of the 22 most common taxa.

The distributions of the nine deep high-relief taxa are apparently not related to differences in the abundances of predators. There were onl y four significant correlations between mean abundances of deep high-relief taxa and predator groups; there were positive correlations between gastropod and the shelf sponge (r = 0.692), the tan encrusting sponge (r = 0.676), the white encrusting sponge (r = 0.714), and the unidentified galatheids (r = 0.640). Positive correlations suggest that the high abundances of sponges and galatheids in deep high-relief habitat are not due to this habitat providing a refuge from predation. None of the other correlations between any of the deep high-relief taxa and the separate or combined mean abundances of gastropod, asteroids, or rock fishes was significant.

The strong habitat association displayed by the nine deep high-relief taxa may be related to the physical attributes of deep high-relief habitat. Parr *et al.* (Chapter 3) report a strong negative correlation between water depth and sediment flux, based upon sediment-trap measurements made at the nine reefs comprising our 11 stations. The effects of depth and sediment flux may be confounding, because depth can affect sediment flux through the attenuation of orbital water velocities caused by surface waves, and through the generally stronger currents at shallower depths (Savoie *et al.*, Chapter 4). Nevertheless, the combined abundance of the nine deep high-relief taxa is more strongly correlated with sediment flux [Figure 5(a), log-log comparison, r = -0.988] than it is with depth [Figure 5(b), log-log comparison, r = 0.869].

The orientation of several taxa on high-relief rocks may also be related to physical factors. The abundances of eight taxa display significant abundance differences among eight categories of orientation on high-relief rocks (Table 5). The anemone with white disc and purple tentacles, *Desmophyllum cristagalli*, and *Lophelia prolifera* are al l significant y more abundant on the northwest, north, or northeast sides of high-relief rocks than they are on the east sides of rocks. Conversely, the abundances of *Caryophyllia* sp(p)., *Lophogorgia chilensis*, *Florometra serratissima*, *Ophiacantha diplasia*, and *Halocynthia hilgendorfi igaboja* are significant] y greater on the east or south sides of high-relief rocks than they are on the north or northeast sides.

The reciprocal nature of these two orientation patterns is apparent (Figure 6). Moreover, the habitat distributions of these two groups of taxa are distinct. The taxa which have higher abundances on the northwest, north, or northeast sides of high-relief rocks are characteristic of either deep high-relief habitat (*Desmophyllum cristagalli* and *Lophelia prolifera*), or deep stations without regard to habitat relief (the white and purple anemone) (Table 3). The taxa with highest abundances on the east or south sides of high-relief rocks are characteristic of either shallow low-relief habitat [*Caryophyllia* sp(p).], or low-relief habitat (*Halocynthia hilgendorfi igaboja*), or do not vary according to habitat (*Lophogorgia chilensis*, *Florometra serratissima*, and *Ophiacantha diplasia*) (Table 3).

Current meter records from the study site (Savoie *et al.*, Chapter 4) indicate that strong and weak currents do not have the same frequency of occurrence in all directions, and that strong and weak currents are each usually directed toward a different side of high-relief rocks (Figure 7). Although currents > 50 cm/s (strong currents) account for only 0.2 % of all current records, they represent 8.2% of the kinetic energy in currents (current speed squared). Converse] y, currents <20 cm/s (weak currents) represent 78.6% of all current records, but provide onl y 41.1 % of the kinetic energy in currents.

The orientation of some taxa on high-relief rocks is correlated with current energy. Although correlations between the combined percent cover of the three northwest-northeast taxa (Figure 6) and the kinetic energy represented by strong currents are marginally not significant ($r = 0.683$, $p = 0.07$), *Lophelia prolifera is* significantly correlated with the energy in strong currents ($r = 0.764$). The combined percent cover of these three taxa are negatively correlated with weak currents, although not significantly ($r = -0.332$). The combined percent cover of the east and south taxa (Figure 6) are negatively correlated ($r = -0.381$) with strong currents and positively correlated ($r = 0.539$) with weak currents, although neither correlation was significant. Among the east and south tax a, only *Ophiacantha diplasia is* nearly significant] y correlated with the kinetic energy in weak currents ($r = 0.677$, $p = 0.07$). Therefore, the deep high-relief taxa that vary according to their orientation on high-relief rocks tend face into strong currents, and the low-relief and shallow low-relief taxa that vary according to their orientation on high-relief rocks tend to face into weak currents.

DISCUSSION

We have described a rich epifauna in hard-bottom habitats of the Santa Maria Basin. Many of these organisms are distributed according to depth and habitat, with the effects of habitat occurring over gradients of as little as 1 to 2 m. Because most of the most common taxa are suspension feeders it is reasonable to seek explanations for the observed distribution patterns through factors that might affect this mode of feeding.

The combined percent cover of suspension feeders was significantly greater in deep high-relief habitat (T'able 3). Moreover, among the 22 common taxa, all of those with highest abundances in deep high-relief habitat, except for the unidentified galatheids, are suspension feeders. The five anthozoans are passive suspension feeders that capture small food items as the water sweeps past their tentacles. The three sponges are active suspension feeders that capture food items from water which is pumped through the animals by ciliary action. In either mode of suspension feeding, decreased feeding efficiency can be assumed when the concentration of inorganic sediments increases in the water, relative to the concentration of food items. We know of no behavioral or morphological adaptations possessed by these eight taxa which would allow them to effectively exclude high concentrations of suspended sediments from their feeding apparatus.

Most of the nine taxa that were most abundant at either shallow stations, or in shallow low-relief habitat, or in low-relief habitat, or which did not vary according to depth or habitat relief, are also assumed to be suspension feeders (except for the ophiuroids). Nevertheless, in this group of taxa, *Cellaria* sp(p)., *Halocynthia hilgendorfi igaboja*, and *Pyura haustor* are able to either withdraw their feeding appendages into an enclosed space or close their incurrent and excurrent siphons for short periods of time to exclude high concentrations of suspended sediments. Two others of these taxa, *Lophogorgia chilensis* and *Florometra serratissima*, grow to be more than 30 cm tall, thus extending their feeding apparatus above the highest concentrations of suspended sediment near the bottom. Therefore, many of the suspension feeders that frequent] y occur in low-relief habitat may have ways of mitigating the effects of suspended sediments, although this topic requires further investigation.

High abundances of suspension feeders have previously been reported in locations that are elevated from the surrounding seabed (Genin et *al.*, 1986; Mullineaux, 1989; Pequegnat, 1964). In particular, *Lophelia prolifera* has been observed high on the up-current edge of high-relief features along the western edge

of Little Bahama Bank (Messing *et* al., 1990). It has often been assumed that the increased abundances of suspension feeders on high-relief rocks are related to the acceleration of currents as water is forced up and over the rocks. Acceleration of currents over high-relief rocks would increase the flux of both larvae and food items in these areas. The assumed effects of current flow and food flux upon suspension feeders has been supported by studies relating the distribution of benthic fauna to current patterns in McMurdo Sound, Antartica (Barry and Dayton, 1986, 1988; Dayton *et al.*, 1982).

The significant correlation between *Lophelia prolifera* on high-relief rocks and strong currents > 50 cm/s also indicates the importance of strong currents for at least some deep high-relief taxa in the Santa Maria Basin. Nevertheless, it is unlikely that the distribution of such large organisms (colonies may exceed 2 m in width) depends sole] y on events that occur less than 0.2% of the time. Moreover, there is evidence suggesting that near-bottom current speeds are greater at shallower depths in our study area. Unpublished data from current meters placed on sediment traps (Parr *et a/.*, Chapter 3), within 1 m of the seabed, show that the frequency of current speeds > 40 cm/s was 5.6% at a depth of 170 m from May to October 1988, whereas the frequency of currents > 40 cm/s was 11.8% at a depth of 118 m from May to October 1989. Although this higher frequency of fast currents at the shallower depth may have been due to temporal variation in current speeds, examination of records from a current meter that was moored near the seabed at 126 m during both periods indicates that maximum current speeds were actually lower from May to October 1989. The increased frequency of faster currents at shallower depths suggests that if suspension feeders, particularly the deep high-relief taxa, are responding solely to current speed, they should be more abundant at shallower depths. Therefore, while the importance of current speed and food flux to suspension feeders is undeniable, other considerations are necessary to explain the distributions of deep high-relief taxa in our study area.

There are clear gradients in the concentrations of suspended sediments in our study area that are related to depth and habitat relief (Parr *et al.*, Chapter 3). Mean fluxes of suspended sediments within 1 m of the seabed ranged from 44.62 to 58.34 g/m^2/day at our shallow stations (105-119 m) and from 27.03 to 31.75 g/m^2/day at our deep stations (160-212 m) over 18 months. Estimates of sediment flux 2 m off the seabed (using the intermediate wave model run from Glenn and Grant, 1987) ranged from 16.22 to 19.42 g/m^2/day for deep high-relief stations. These spatial patterns in suspended sediment closel y parallel those for the abundances of deep high-relief taxa [Figure 5(a)].

We suggest that suspended sediments and sedimentation are important factors associated with the spatial patterns of hard-bottom epifaunal assemblages in the Santa Maria Basin. *De facto, those* taxa that are most abundant at shallow stations, those that are most abundant in low-relief habitat, those whose abundances do not vary according to depth or habitat, and especially those that are most abundant in shallow low-relief habitat must be tolerant of sedimentation and high suspended sediment concentrations. Conversely, we propose that those taxa that prefer deep stations, and especially those that prefer deep high-relief habitat, may be relatively intolerant of sedimentation and high suspended sediment concentrations. If the positive influence of current speeds and food flux on suspension feeders is accepted, along with the probable negative influences of suspended sediments, it is likely that the rich assemblages that characterize high-relief habitat from 160 to 212 m in the Santa Maria Basin are associated with a balance between these two factors. Whether these distribution patterns arise as the result of selective larval settlement or over a long period as the result of competition, predation, growth, or mortality remains to be determined.

ACKNOWLEDGMENTS

Many people participated in this study and we gratefully acknowledge their important contributions, Study design and statistical approach were formulated by the authors, with generous assistance from Bob Spies, Bob Camey, and Roger Green. Special assistance in the field was provided by Jim Campbell, Janet Kennedy, and Jay Shrake. The laser ranging device for the ROV was provided by Frank Caimi and Bob Tust ing of Harbor Branch Oceanographic Institution. Taxonomic expertise was provided by Karen Green, John Ljubenkov, and Jay Shrake. Computerized data analyses were performed with assistance from Wei Chen and Keith Kutchins. Word processing was performed by Kathryn Long and Vicky O'Brien. This work was performed under a contract to Kinnetic Laboratories from Battelle Ocean Sciences, with funding provided by the U.S. Department of Interior Minerals Management Service (MMS) through contract number 14-12-0001-30262. Dr. Gary Brewer of MMS has ably directed the multidisciplinary program, of which this study was a part.

LITERATURE CITED

Bak, R. P.M., R.M. Termaat, and R. Dekker. 1982. Complexity of coral interactions: Influence of time, location of interaction and epifauna. Mar. Biol. 69:215-222.

Barry, J. P., and P.K. Dayton. 1986. Oceanographic influences on marine benthic communities in McMurdo Sound, Antarctica. Antarctic J. 21(5): 180-182.

Barry, J. P., and P.K. Dayton. 1988. Current patterns in McMurdo Sound, Antarctica and their relationship to local biotic communities. Polar. Biol. 8:367-376.

Bray, J. R., and J.T. Curtis. 1957. An ordination of the upland forest communities of southern Wisconsin. Ecol. Monogr. 27:325-349.

Caffey, H.M. 1985. Spatial and temporal variation in settlement and recruitment of intertidal barnacles. Ecol. Monogr. 55(3):313-332.

Caimi, F. M., R.F. Tusting, and D.D. Hardin. 1987. Laser-aided quantitative sampling of the seabed. 1234-1238 in proceedings of Oceans '87.

Carney, R. S., and A .G. Carey. 1976. Distribution patterns of holothurians on the northeastern Pacific (Oregon, U. S. A.) continental shelf, slope, and abyssal plain. Thalassia Jugosl. 12(1):67-74.

Come]], J.H. 1985. The consequences of variation in initial settlement vs. post-settlement mortality in rocky intertidal communities. J. Exp. Mar. Biol. Ecol. 93:11-45.

Dames & Moore. 1982. Site-specific marine biological survey, lease P-0446, P-0447, P-0450, P-0451 and P-0452 southern Santa Maria Basin area. Unpublished report to Chevron U. S. A., Inc. Dames & Moore, Los Angeles, California.

.

Dames & Moore. 1983. Site-specific marine biological survey, Chevron Platform Hermosa Project, western Santa Barbara Channel. Unpublished report to Chevron U. S. A., Inc. Dames & Moore, Los Angeles, California.

Davis, A.R. 1987. Variation in recruitment of the subtidal colonial ascidian *Podoclavella cylindrical* (Quoy & Gaimard): the role of substratum choice and early survival. J. Exp. Mar. Biol. Ecol. 106:57-71.

Dayton, P. K., W .A. Newman, and J. Oliver. 1982. The vertical zonation of the deep-sea Antarctic acorn barnacle, *Bathylasma corolliforme* (Hock): Experimental transplants from the shelf into shallow water. J. Biogeogr. 9:95-109.

Dodge, R. E., and J.R. Vaisnys. 1977. Coral populations and growth patterns: Responses to sedimentation and turbidity associated with dredging. J. Mar. Res. 35(4):715-730.

Fautin, D. G., A. Bucklin, and C. Hand. 1989. Systematic of sea anemones belonging to genus *Metridium* (Coelenterata: Actinaria), with a description of M. *giganteum* new species. Wasmann J. Biol. 47(1-2):77-85.

Foster, M. S., C. Harrold, and D.D. Hard in. 1991. Point vs. photo quadrat estimates of the cover of sessile marine organisms. J. Exp. Mar. Biol. Ecol. 146:193-203.

Genin, A., P.K. Dayton, P.F. Lonsdale, and F.N. Spiess. 1986. Corals on seamount peaks provide evidence of current acceleration over deep-sea topography. Nature 322:59-61.

Glenn, S. M., and W.D. Grant. 1987. A suspended sediment stratification correction for combined wave and current flows. J. Geophys. Res. 92:8244-8264.

Glynn, P. W., and L. D'Croz. 1990. Experimental evidence for high temperature stress as the cause of El Niño-coincident coral mortality. Coral Reefs 8:181-191.

Hecker, B., D.T. Logan, F.E. Gandarillas, and P.R. Gibson. 1983. Megafaunal assemblages in Lydonia Canyon, Baltimore Canyon, and selected slope areas. Vol. III, Chapter 1. Canyon and slope processes study. Prepared by Larnont-Doherty Geological Observatory of Columbia University, Palisades, New York, U.S.A. for U.S. Department of the Interior Minerals Management Service. Contract No. 14-12-0001-29178.

Hong, G. A-, and A. Sasekumar. 1981. The community structure of the fringing coral reef, Cape Rachado, Malaya. Attol Res. Bull. 244:1-11.

Hudson, J.H. 1981. Growth rates in *Monastrea annularis*: A record of environmental change in Key Largo Coral Reef Marine Sanctuary, Florida. Bull. Mar. Sci. 31(2):444-459.

Hyland, J., D. Hardin, E. Crecelius, D. Drake, P. Montagna, and M. Steinhauer. 1990. Monitoring long-term effects of offshore oil and gas development along the southern California outer continental shelf and slope: Background environmental condition in the Santa Maria Basin. Oil Chem. Pollut. 6:195-240.

Jokiel, P.L. 1980. Solar ultraviolet radiation and coral reef epifauna. Science 207:1069-1071.

Kay, A. M., and M .J. Keough. *1981.* Occupation of patches in the epifaunal communities on pier pilings and the bivalve *Pinna bicolor* at Edithburgh, South Australia. Oecologia 48:123-130.

Loya, Y. 1976. Effects of water turbidity and sedimentation on the community structure of Puerto Rican corals. Bull. Mar. Sci. 26(4):450-466.

Messing, C. G., A .C. Neumann, and J .C. Lang. 1990. Biozonation of deep-water lithoherms and associated hardgrounds in the northeastern Straits of Florida. Palaios 5:15-33.

Miller, A.C. 1982. Effects of differential fish grazing on the community structure of an intertidal reef flat at Enewetak Atoll, Marshal Islands. Pac. Sci. 36(4):467-482.

Mullineaux, L.S. 1988. The role of settlement in structuring a hard-substratum community in the deep sea. J. Exp. Mar. Biol. Ecol. 120:247-261.

Mullineaux, L.S. 1989. Vertical distributions of the epifauna on manganese nodules: Implications for settlement and feeding. Limnol. Oceanogr. 34(7):1247-1262

Nekton, Inc. 1981. A biological survey of a hard-bottom feature, Santa Maria Basin, California. Unpublished report to ARCO Oil and Gas Company.

Nekton and Kinnetic Laboratories. 1983. Site-specific faunal characterization survey for Platform Harvest, OCS lease P-0315, Point Conception, California. Unpublished report to Texaco U.S.A. Kinnetic Laboratories, Inc., Santa Cruz, California.

Peattie, M. E., and R. Hoare. 1981. The sublittoral ecology of the Menai Strait. II. The sponge *Halichondria panicea* (Pallas) and its associated fauna. Est. Coast. Shelf Sci. 13:621-635.

Pequegnat, W.E. 1964. The epifauna of a California siltstone reef. Ecology 45:272-283.

Rowe, G. T., and R.J. Menzies. 1969. Zonation of large benthic invertebrates in the deep-sea off the Carolinas. Deep Sea Res. 16:531-537.

SAIC. Science Applications International Corporation. 1986. Assessment of long-term changes in biological communities of the Santa Maria Basin and western Santa Barbara Channel - Phase I. Volume II, Synthesis of findings. Report to the U.S. Department of the Interior Minerals Management Service, Contract No. 14-12-0001-30032. (MMS 86-9912)

Scheer, G. 1984. The distribution of reef-corals in the Indian Ocean with a historical review of its investigation. Deep Sea Res. 31(6-8):885-900.

Sebens, K.P. 1984. Water flow and coral colony size: Interhabitat comparisons of the octocoral *Alcyonium siderium*. Proc. Natl. Acad. Sci. USA. 81:5473-5477.

Sebens, K.P. 1985. Community ecology of vertical rock walls in the Gulf of Maine, U. S. A.: Small-scale processes and alternative community states. Chapter XXIII, pp. 346-371 in Moore, P. G., and R. Seed, (Eds.) *The* Ecology *of Rocky Coasts*. Hodder and Stoughton Educational, Sevenoaks, Kent, England, U.K.

Sebens, K.P. 1986. Spatial relationships among encrusting marine organisms in the New England subtidal zone. Ecol. Monogr. 56(1):73-96.

Sokal, R. R., and F.J. Rohlf. 1969. *Biometry*. W.H. Freeman and Co., San Francisco, CA, U.S.A. 776 pp.

Swartz, R.C. 1978. Techniques for sampling and analyzing the macrobenthos. U.S. Department of Commerce. National Technical Information Service, PB-281 631. Corvallis Environmental Research Laboratory, Corvallis, Oregon.

Vinogradova, N.G. 1962. Vertical zonation in the distribution of the deep-sea benthic fauna of the ocean. Deep Sea Res. 8:245-250.

Witman, J.D. 1985. Refuges, biological disturbance, and rocky subtidal community structure in New England. Ecol. Monogr. 55(4):421-445.

Witman, J.D. 1987. Subtidal coexistence: Storms, grazing, mutualism, and the zonation of kelps and mussels. Ecol. Monogr. 57(2):167-187.

Table 1. Stations sampled for abundances of hard-bottom epifauna near Platform Hidalgo.

Station	Depth (m)	Depth Category[a]	Habitat Relief[b]
PH-E(L)	119	Shallow	Low
PH-F(L)	105	Shallow	Low
PH-I(L)	109	Shallow	Low
PH-J(L)	117	Shallow	Low
PH-K(H)	160	Deep	High
PH-N(L)	166	Deep	Low
PH-R(L)	212	Deep	Low
PH-R(H)	212	Deep	High
PH-U(L)	113	Shallow	Low
PH-W(L)	195	Deep	Low
PH-W(H)	195	Deep	High

[a]Shallow: 105-l 19 m. Deep: 160- 212 m.
[b]Low-relief: 0.2-0.5 m. High-relief: > 1.0 m

Table 2. The 15 most abundant hard-bottom taxa in low-relief (0.2-0.5 m) and high-relief (> 1.0 m) habitat near Platform Hidalgo. Percent cover averaged over all stations in each relief category and over seven sampling periods from October 1986 through October 1990.

Taxa	Taxon Group	Mean Percent Cover	Standard Deviation	Percent Frequency of Occurrence
Low Relief				
Ophiuroidea, unidentified	Ophiuroidea	5.8	6.4	99.8
Florometra serratissima	Crinoidea	2.7	7.3	26.5
Paracyathus stearnsii	Anthozoa	1.5	2.4	75.2
Metridium giganteum	Anthozoa	1.2	4.9	14.2
Sabellidae, unidentified	Polychaeta	1.1	2.6	51.6
Ophiacantha diplasia	Ophiuroidea	1.1	2.3	51.0
Caryophyllia sp(p).	Anthozoa	1.0	1.5	91.3
Pyura haustor	Urochordata	0.8	1.5	67.5
Terebellidae, unidentified	Pol ychaeta	0.8	1.7	55.4
Sponge, white encrusting	Porifera	0.7	1.1	84.9
Galatheidae, unidentified	Decapoda	0.6	1.2	61.8
Sponge, tan encrusting	Porifera	0.6	1.0	70.2
Cellaria sp(p).	Ectoprocta	0.5	1.0	59.4
Lophogorgia chilensis	Anthozoa	0.5	1.0	64.7
Halocynthia hilgendorfi igaboja	Urochordata	0.4	1.0	46.7
High Relief				
Amphianthus californicus	Anthozoa	4.6	5.2	97.9
Ophiuroidea, unidentified	Ophiuroidea	3.5	4.0	99.6
Sabellidae, unidentified	Pol ychaeta	2.4	3.2	93.2
Desmophyllum cristagalli	Anthozoa	2.1	3.4	75.9
Galatheidae, unidentified	Decapoda	1.7	2.0	97.6
Metridium giganteum	Anthozoa	1.7	4.7	28.2
Lophelia californica	Anthozoa	1.6	5.9	23.1
Sponge, white encrusting	Porifera	1.5	2.0	96.5
Stomphia didemon	Anthozoa	1.4	3.1	38,4
Florometra serratissima	Crinoidea	1.3	5.3	14.6
Anemone, tan zoanthid	Anthozoa	1.1	2.8	66.2
Sponge, shelf	Porifera	1.0	2.7	34.6
Anemone, white disc, purple tentacles	Anthozoa	1.0	1.7	65.1
Pyura haustor	Urochordata	0.9	1.6	75.7
Sponge, tan encrusting	Porifera	0.8	1.4	76.1

Table 3. Results of A NOVA for effects of depth at low-relief stations, and effects of relief at deep stations.

Taxa	Depth		Relief	
	P	Result[a]	*P*	Result[a]
Sponge, shelf cover	<0.0001	D	0.0005[b]	H
Sponge, tan encrusting cover	0.0327	D	0.0022[b]	H
Sponge, white encrusting cover	<O. 0001[b]	D	<0.0001	H
Amphianthus californicus counts	< O. 0001[b]	D	<0.0001	H
Anemone, tan zoanthid cover	<O. 0001[b]	D	0.0100	H
Anemone, white disc and purple tentacles counts	< O. 0001[b]	D	*0.3672*	
Caryophyllia sp(p). counts	<0.0001	s	*0.0027*	L
Desmophyllum cristagalli counts	< O. 0001[b]	D	<O. 0001[b]	H
Lophelia prolifera cover	<0.0001	D	<O. 0001[b]	H
Lophogorgia chilensis cover	0.3455		0.6962[b]	
Metridium giganteum counts	0.1709		0.0014	H
Paracyathus stearnsii counts	<0.0001	s	0.4600	
Stomphia didemon counts	<O. 0001[b]	D	0.0004	H
Sabellidae, unidentified counts	<0.0001	D	0.6403[b]	
Terebellidae, unidentified counts	<O. 0001[b]	D	<0.0001	L
Galatheidae, unidentified counts	<0.0001	D	<0.0001	H
Cellaria sp(p). cover	<0.0001	s	0.0678[b]	
Florometra serratissima counts	0.3837		0.1153	-
Ophiacantha diplasia counts	0.2600		0.0972	
Ophiuroidea, unidentified counts	0.6822		0.0541	
Halocynthia hilgendorfi igaboja counts	0. 1532[b]		0.0413	L
Pyura haustor counts	o.0657[b]		0.8253	
Total Suspension Feeders cover	<O. 0001[b]	D	<0.0001	H
Total Abundance cover	<0.0001	s	0.0016	L
Total Number of Species	<0. 0001[b]	D	<0,0001	H

[a]S: Highest abundance occurred at shallow stations (105-119 m).
D: Highest abundance occurred at deep stations (160-212 m).
L: Highest abundance occurred in low-relief habitat (0.2-0.5 m).
H: Highest abundance occurred in high-relief habitat (> 1.0 m).

[b]Nonparametric A NOVA used because of failure to pass Bartlett's test for homogeneity of variances.

Table 4. The 10 strongest positive and 10 strongest negative interspecific correlations (Pearson product-moment) for hard-bottom epifauna near Platform Hidalgo. Correlations are based upon replicate values across seven times and 11 stations. All correlations are significant (p c 0,0001).

	Taxa	*r*
1	*Desmophyllum cristagalli* to *Amphianthus californicus*	*0.389*
2	*Desmophyllum cristagalli* to *Lophelia prolifera*	0.307
3	Anemone (white disc and purple tentacles) to Sabellids	0.256
4	Unidentified ophiuroids to *Ophiacantha diplasia*	0.245
5	*Amphianthus californicus* to Galatheids	0.221
6	*Desmophyllum cristagalli* to Galatheids	0.212
7	*Desmophyllum cristagalli* to Anemone (white disc and purple tentacles)	0.208
8	*Paracyathus stearnsii* to *Caryophyllia* sp(p).	0.195
9	*Amphianthus californicus* to White encrusting sponge	0.170
10	*Amphianthus californicus* to Anemone (white disc and purple tentacles)	0.163
1	*Paracyathus stearnsii* to Sabellids	*-0.205*
2	*Paracyathus stearnsii* to *Amphianthus californicus*	-0.191
3	*Paracyathus stearnsii* to Galatheids	-0.178
4	*Paracyathus stearnsii* to Anemone (white disc and purple tentacles)	-0.160
5	Galatheids to Unidentified ophiuroids	-0.154
6	*Amphianthus californicus* to Unidentified ophiuroids	-0.151
7	*Paracyathus stearnsii* to *Desmophyllum cristagalli*	-0.136
8	*Desmophyllum cristagalli* to Unidentified ophiuroids	-0.127
9	*Caryophyllia* sp(p). to Sabellids	-0.116
10	*Paracyathus stearnsii* to *Stomphia didemon*	-0.115

Table 5. Results of ANOVA for abundance differences among orientation categories (N, NE, E, SE, S, SW, W, NW) on high-relief rocks. Taxa tested are the 15 most abundant in each of low-relief and high-relief habitat, listed phylogenetically.

Taxa	ANOVA *P*	Duncans[a]
Sponge, shelf cover	0.5611	E N NW W S S W S E N E
Sponge, tan encrusting cover	0.4357	NE W S SW N E NW SE
Sponge, white encrusting cover	0.8186	NW WE N S N E S W S E
Amphianthus californicus counts	0.1205	N W N S E S W N E E S W
Anemone, tan zoanthid cover	0.8595	E W S E N S N E S W N E
Anemone, white disc and purple tentacles counts	0.0055	N N W S W N E S E S W E
Caryophyllia sp(p). counts	0.0282	S S W S E E W N E N W N
Desmophyllum cristagalli counts	0.0109	NW NE NW SW SSEE
Lophelia prolifera cover	0.0163	N N E S W S E N W E S W
Lophogorgia chilensis cover	**0.0001**	E S SW W N E N S E N W
Metridium giganteum counts	0.1528	E SW S W NE SE N NW
Paracyathus stearnsii counts	0.2022	W E S S W N S E N E N W
Stomphia didemon counts	0.0590	N N E S E N W S W W S E
Sabellidae, unidentified counts	0.9194	NE NW NW SE SSWE
Terebellidae, unidentified counts	0.3619	W N E S W S S E N E N E
Galatheidae, unidentified counts	0.1528	N W W S S E N E S W N E
Cellaria sp(p). cover	0.5557	E S E W S W S N N W N E
Florometra serratissima counts	0.0039	E S W S N W W S E N N E
Ophiacantha diplasia counts	***0.0220***	E N E S S W W S E N W N
Ophiuroidea, unidentified counts	0.1510	E S SW W N E S E N W N
HaloCynthia hilgendorfi igaboja counts	0.0035	E S E S S W W N N E N W
Pyura haustor counts	0.8019	NW NE N S E W S W E S
Total Suspension Feeders cover		
Total Abundance cover	0.7507	SE SE SW NNEWNW
Total Number of Species	0,8125	E S W N W S N E SE W N

[a]Duncans Multiple Range Test; categories underlined by a common line are not significantly different; highest mean on left, lowest mean on right.

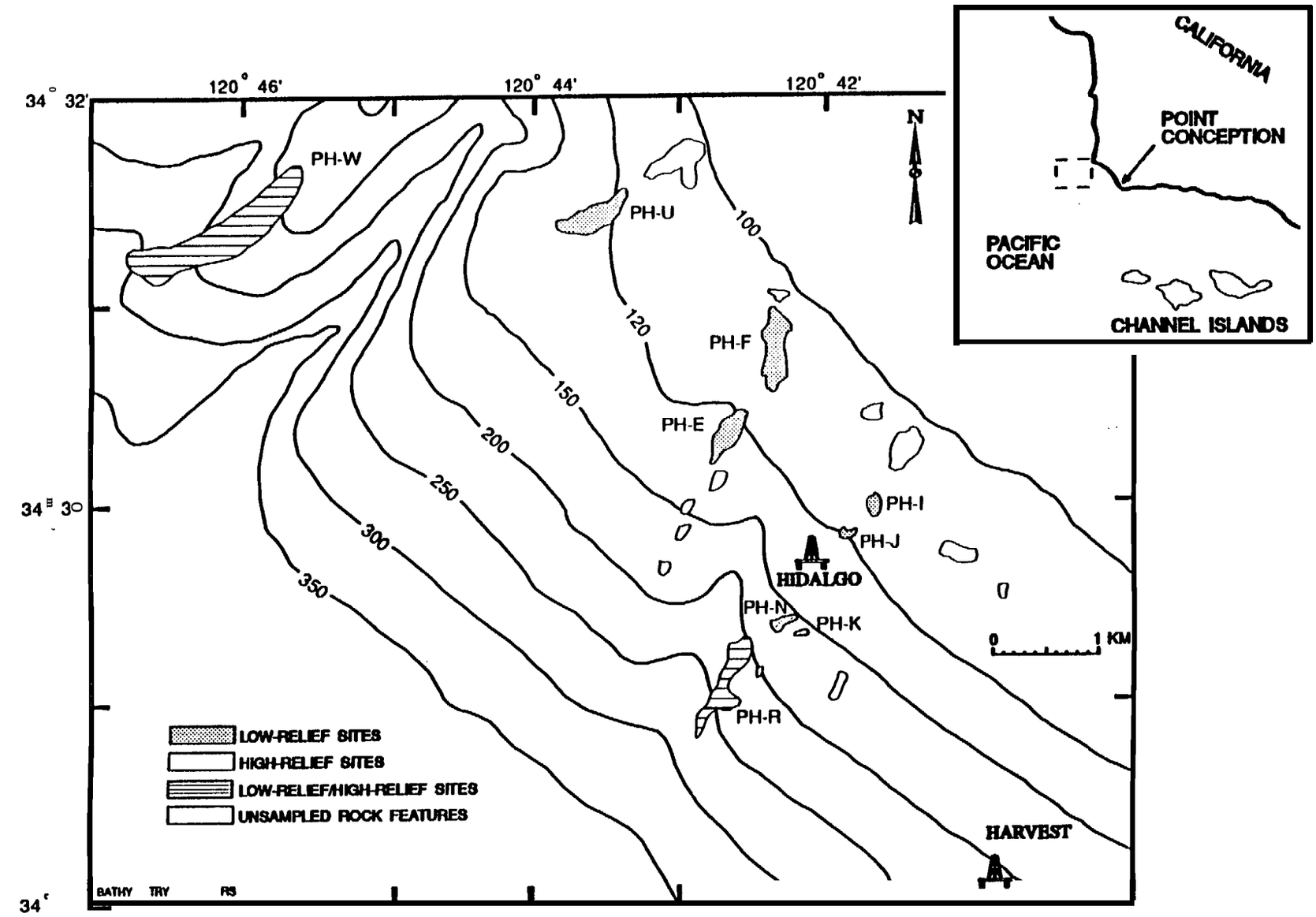

Figure 1. Hard-bottom features sampled in the Santa Maria Basin, near Point Conception, California.

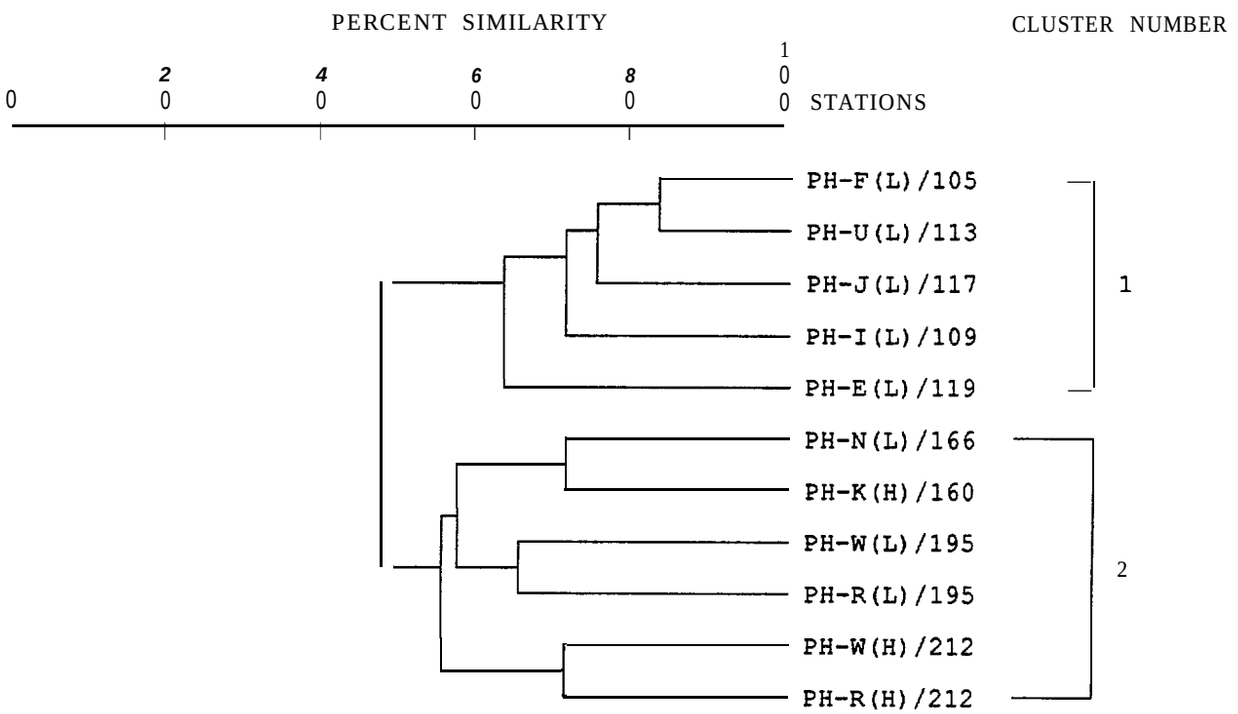

Figure 2. Clusters of similarities (Bray and Curtis, 1957) between hard-bottom stations in the Santa Maria Basin, based on comparisons of mean abundances over seven sampling periods from October 1986 to October 1990. Low(L) and high(H) habitat relief (L = 0.2-0.5m, H = > 1.0 m) and depth in meters are indicated for each station.

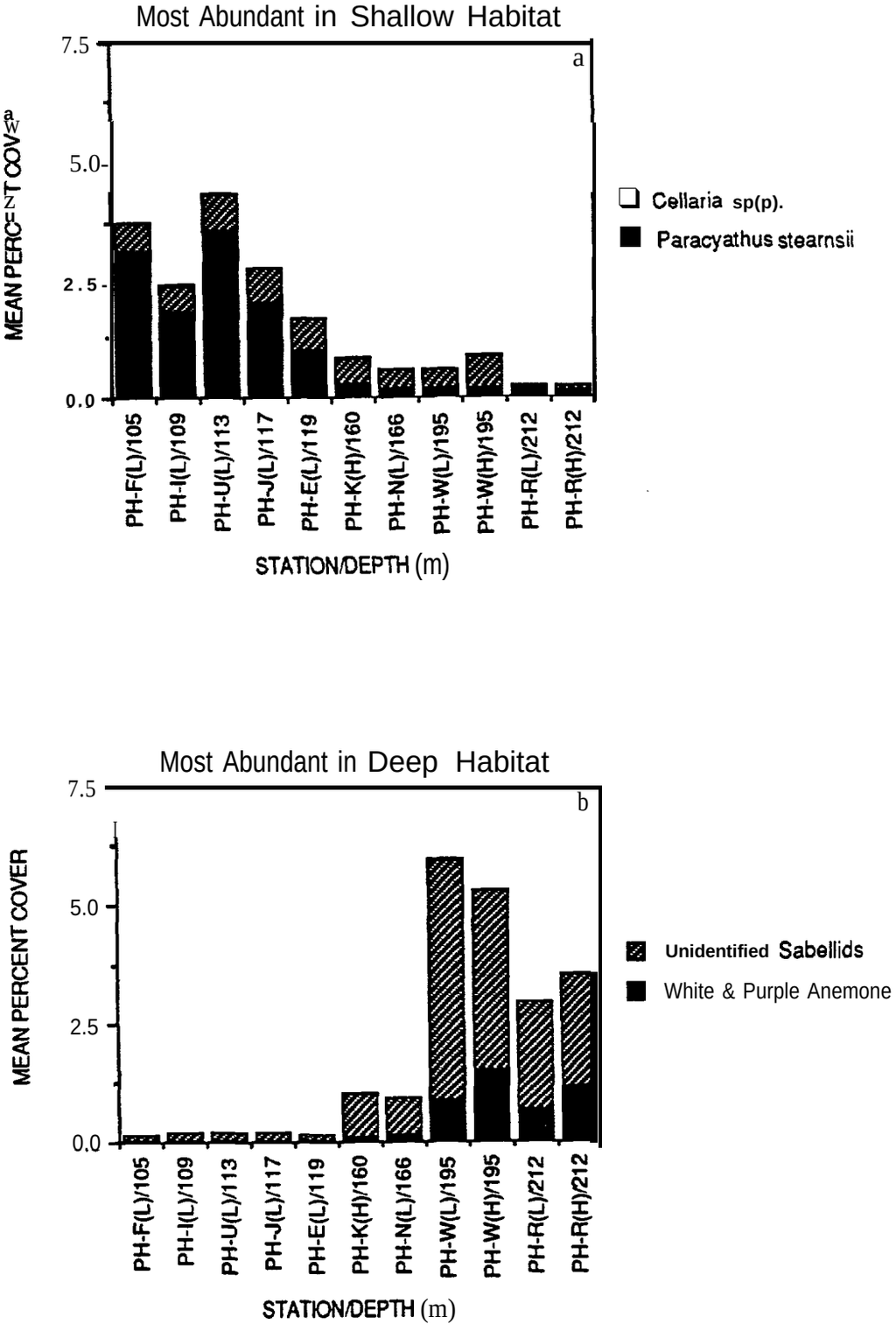

Figure 3. Combined mean abundances for 22 common hard-bottom taxa from 11 stations in the Santa Maria Basin. Taxa are combined according to the A NOVA results shown in Table 3. Means are over seven sampling periods from October 1986 to October 1990. Low(L) and high(H) habitat relief (L = 0.2-0.5 m, H = > 1.(3 m) and depth in meters are indicated for each station.

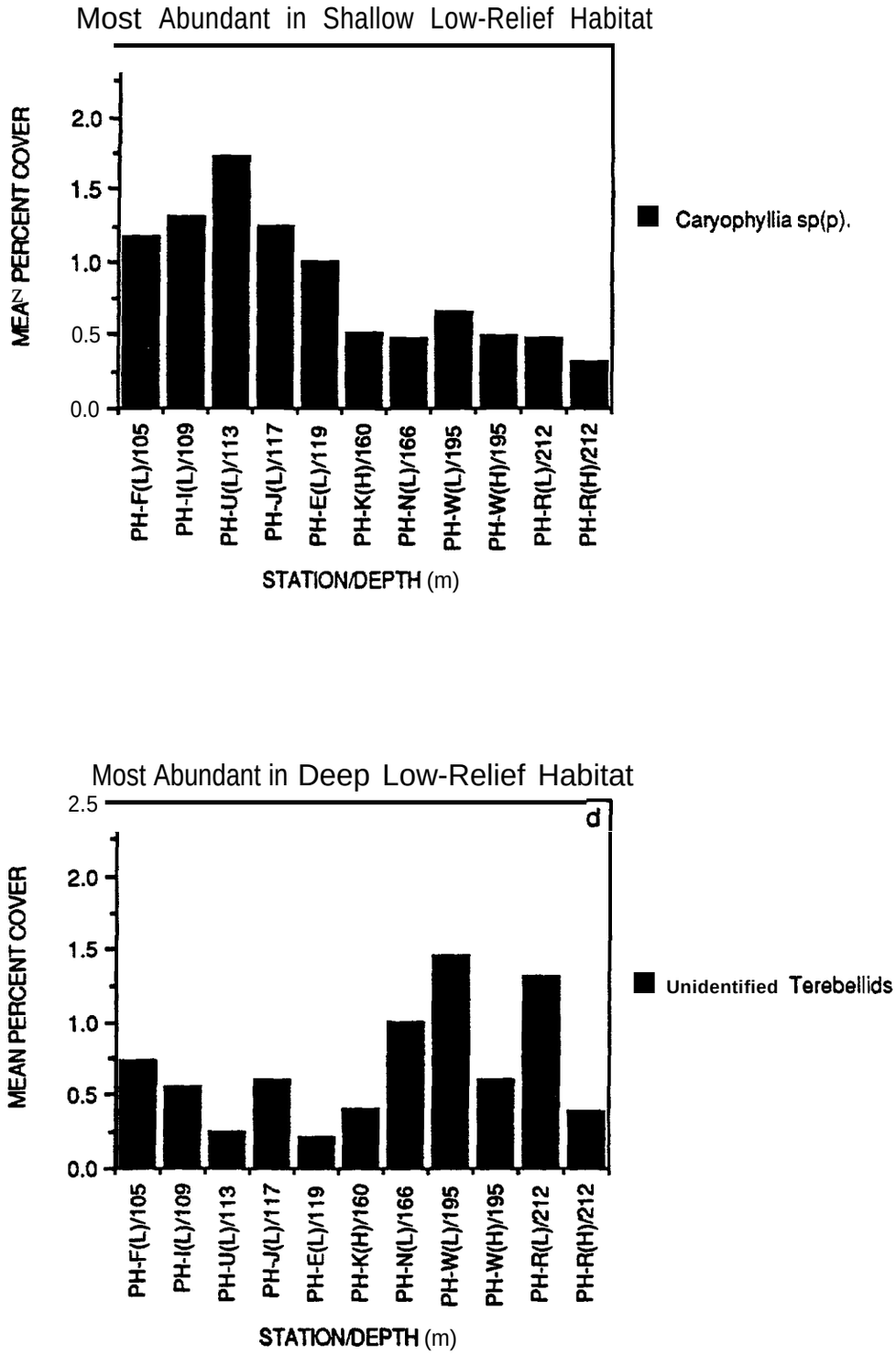

Figure 3. Combined mean abundances for 22 common hard-bottom taxa from 11 stations in the Santa Maria Basin. Taxa are combined according to the ANOVA results shown in Table 3, Means are over seven sampling periods from October 1986 to October 1990. Low(L) and high(H) habitat relief (L = 0.2-0.5 m, H = >1.0 m) and depth in meters are indicated for each station. (continued)

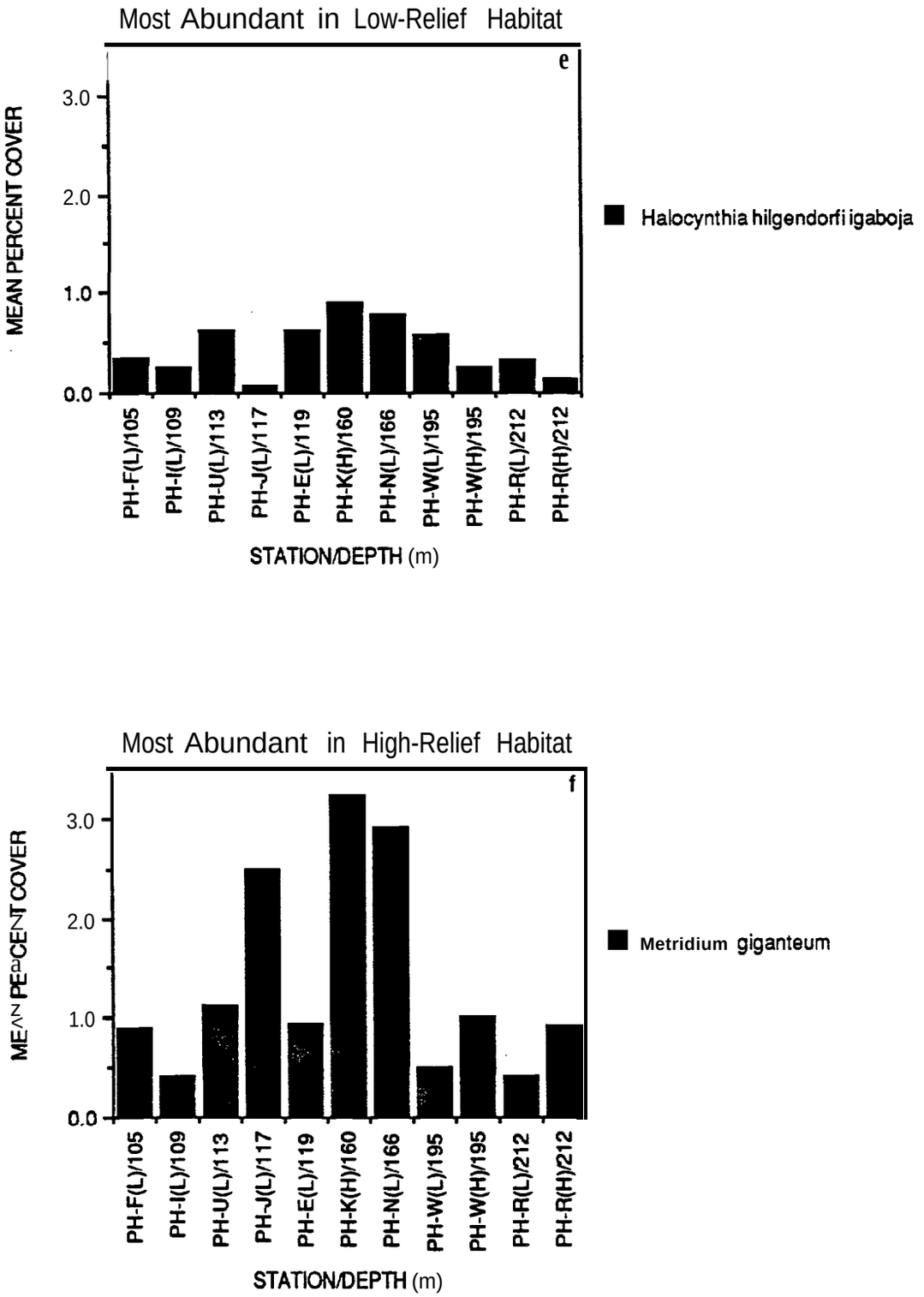

Figure 3. Combined mean abundances for 22 common hard-bottom taxa from 11 stations in the Santa Maria Basin. Taxa are combined according to the ANOVA results shown in Table 3. Means are over seven sampling periods from October 1986 to October 1990. Low(L) and high(H) habitat relief (L = 0.2-0.5 m, H = >1.0 m) and depth in meters are indicated for each station. (continued)

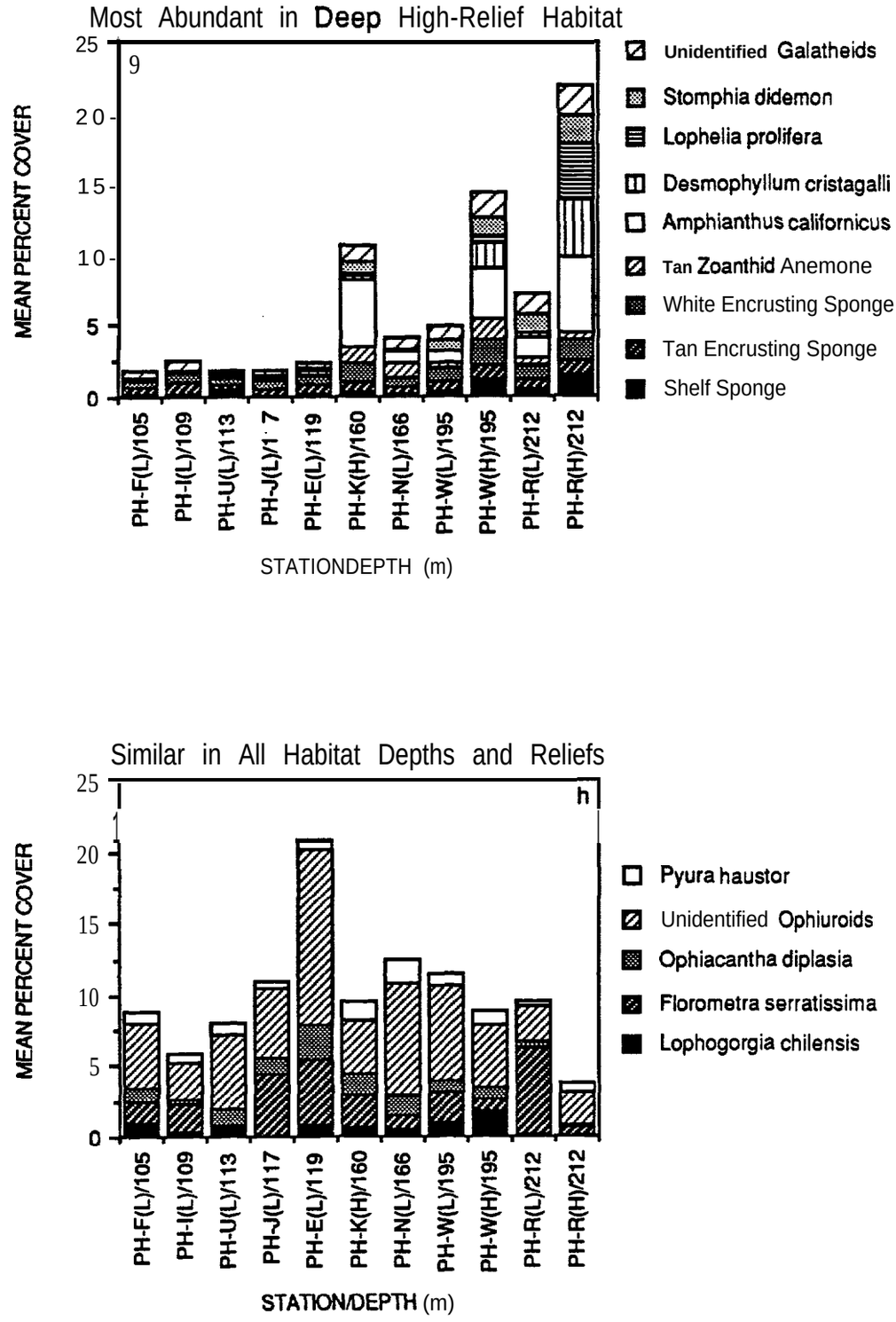

Figure 3. Combined mean abundances for 22 common hard-bottom taxa from 1 1 stations in the Santa Maria Basin. Taxa are combined according to the ANOVA results shown in Table 3. Means are over seven sampling periods from October 1986 to October 1990. Low(L) and high(H) habitat relief (L = 0.2-0.5 m, H = >1.0 m) and depth in meters are indicated for each station. (continued)

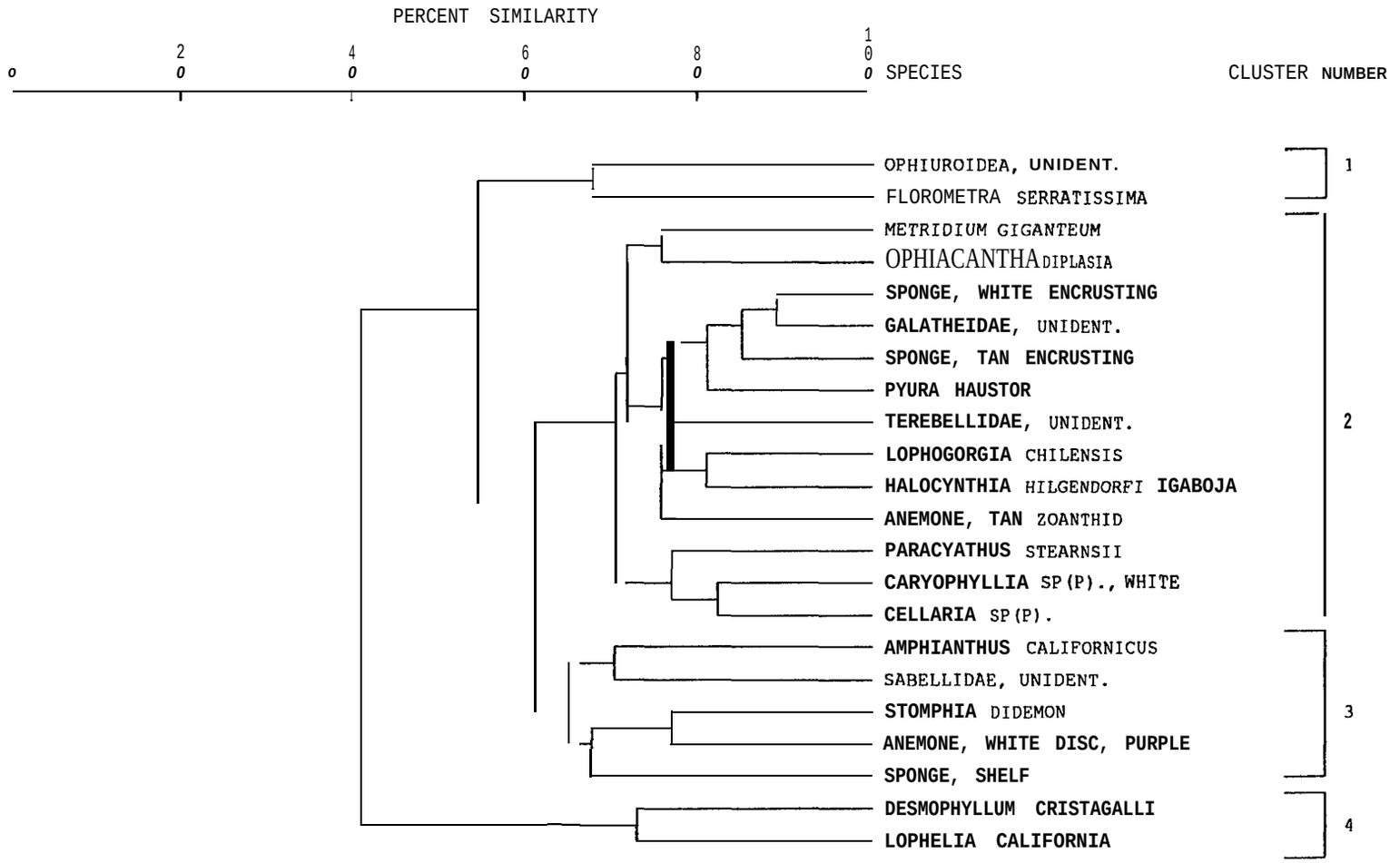

Figure 4. Clusters of similarities (Bray and Curtis 1957) between hard-bottom taxa over 11 stations in the Santa Maria Basin, based on comparisons of mean abundances over seven sampling periods from October 1986 to October 1990.

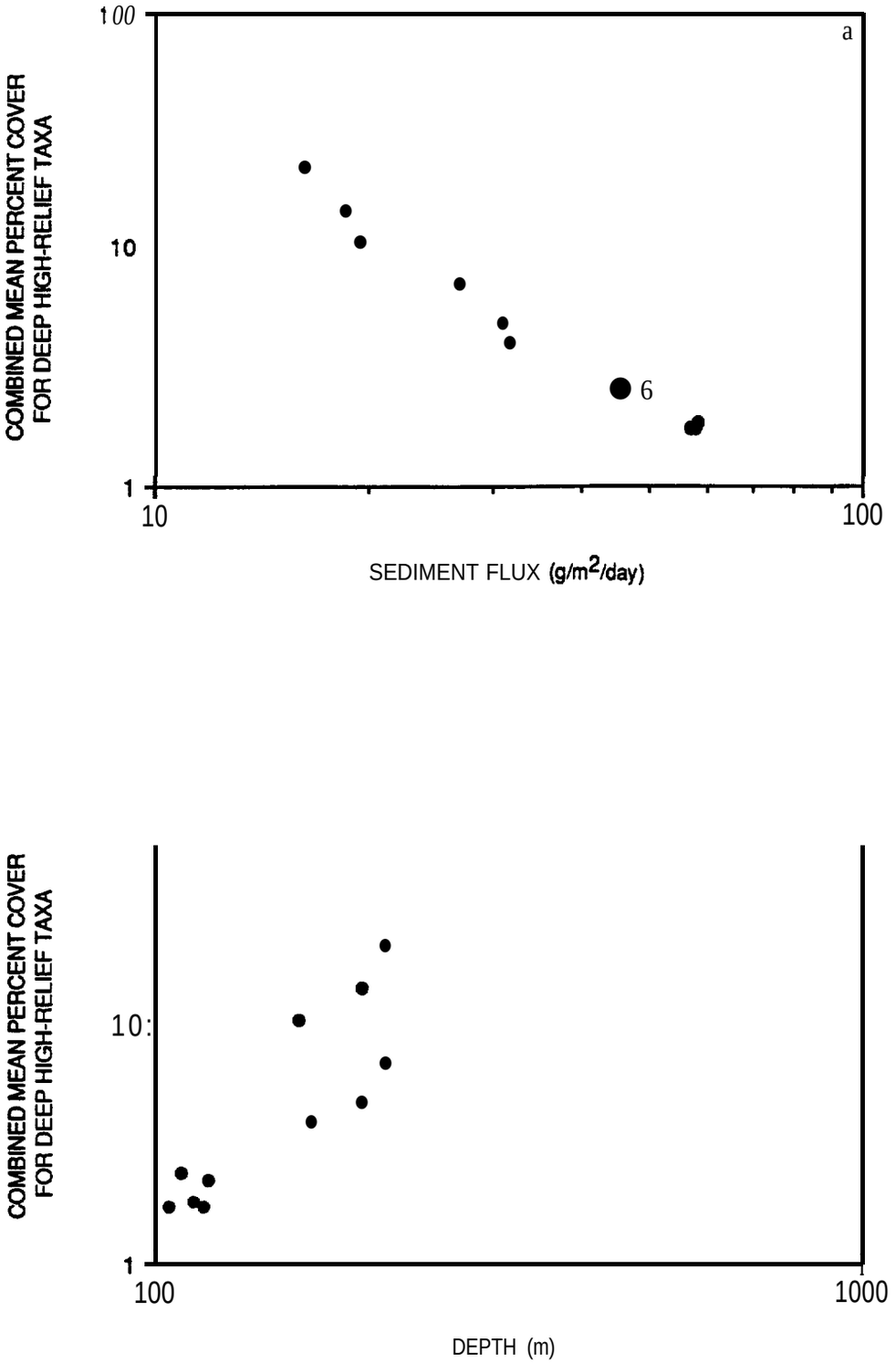

Figure 5. *Log-log* plots of combined mean abundances for nine taxa with highest abundances in deep high-relief habitat in the Santa Maria Basin versus sediment flux and depth at 11 stations. Sediment flux was measured over 18 months with sediment traps 1 m from the seabed at low-relief (0.2-0.5 m) stations, represented by the eight points farthest to the right in Figure 5(a). Sediment flux for high-relief (> 1.0 m) stations, represented the three points farthest to the left in Figure 5(a), was estimated using the intermediate wave model run of Glenn and Grant (1987).

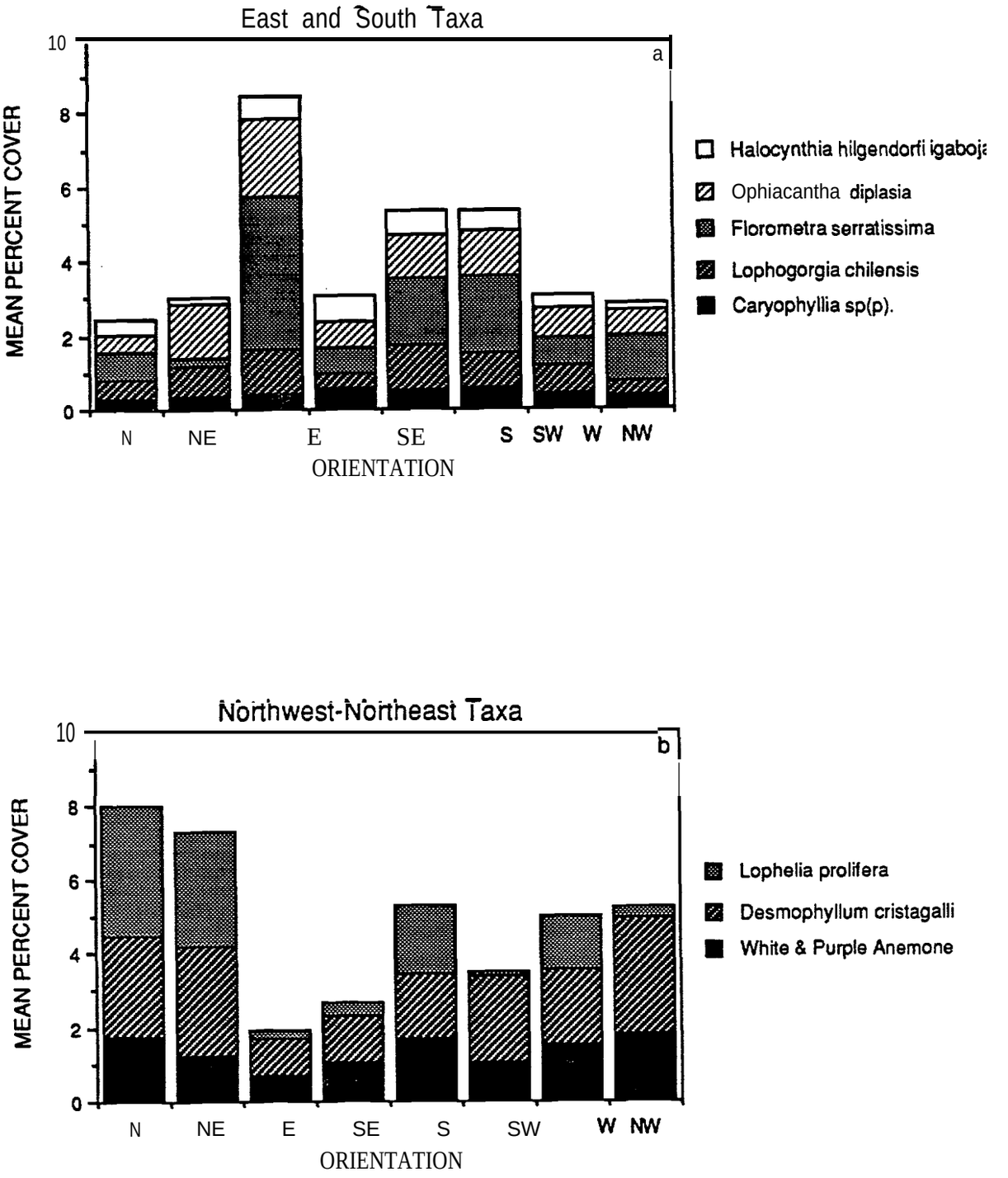

Figure *6.* Combined mean abundances for hard-bottom taxa with highest abundances on the east or south sides of high-relief (>1.0 m) rocks or on the northwest-northeast sides of high-relief rocks. Abundances are means from three high-relief stations, 160-212 m deep, sampled during seven sampling periods from October 1986 to October 1990.

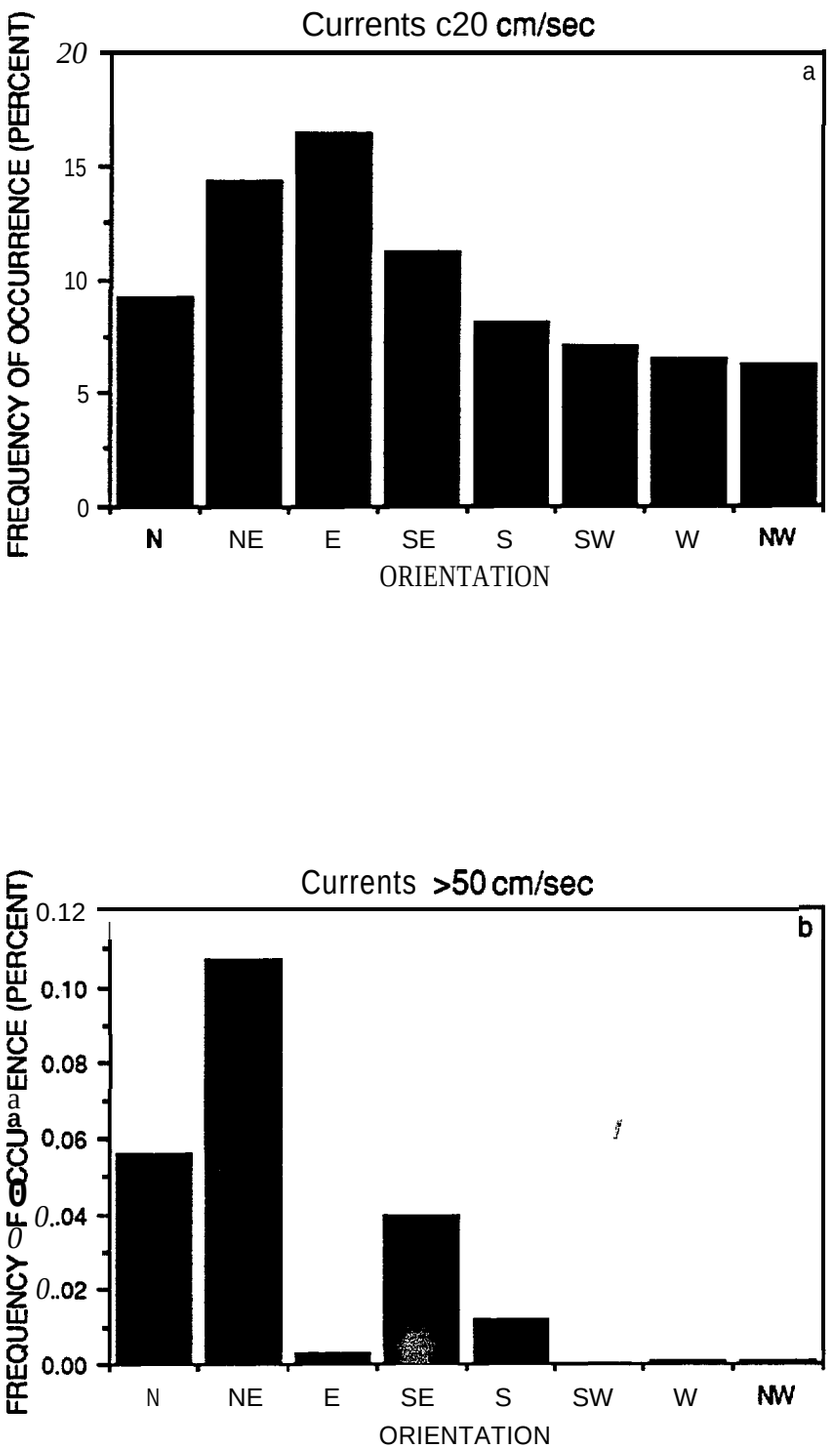

Figure 7. The frequency of occurrence of weak (**<20** cm/s) and strong (> 50 cm/s) currents directed toward eight orientations on high-relief rocks. Data were obtained from a current meter moored near the seabed at *126* m near Platform **Hidalgo** in the Santa Maria Basin from October 1986 to October, 1990 (**Savoie** et *al.*, manuscript in preparation).

8. DEPOSITION OF DRILLING PARTICULATE OFF POINT CONCEPTION, CALIFORNIA

DOUGLAS A. COATS

Marine Research Specialists
3639 E. Harbor Blvd., Suite 208, Ventura, CA **93001**

INTRODUCTION

A five-year interdisciplinary study was initiated in 1986 to investigate environmental consequences of offshore petroleum production in the southern Santa Maria Basin (Hyland et al., 1990). This study, entitled the California Outer Continental Shelf Phase II Monitoring Program (hereinafter CAMP), included sampling near rock features between Points Conception and Arguello (refer to Figure 1). Physical, chemical and biological changes around these sampling sites were investigated for their relation to drilling activities on three adjacent petroleum production platforms. Thus, attention focussed on potential impacts to hard-substrate epibiota from exposure to over 40,000 m^3 of drilling fluid that was discharged from the three platforms during the first two years of monitoring. Demonstration of a relationship between drilling activity and biological change required an accurate estimate of the exposure of specific hard-substrate features to drilling waste. These dose estimates were derived largely from anal ysis of solids collected in thirteen sediment trap arrays located around the northernmost platform (Platform Hidalgo in Figure 2). In the investigation described here, platform mass emissions were directly associated with time series of material trapped near the biological sampling sites.

Suspension feeders comprised a significant portion of the epifaunal assemblages that were monitored as part of the hard-substrate field investigation. Consequently, the quantity and quality of solids suspended in the water column immediately above the seafloor was thought to be a potentially influential factor on organism abundance (Hardin et al., Chapter 7). Material accumulated in sediment traps was used to quantify the amount and type of particulate impinging on the hard-substrate habitats selected for biological survey. Because trap openings were located 1 m above the seafloor (Parr et al., Chapter 3), they captured a mix of particles suspended within the benthic boundary layer. Particulate deposited in the traps included anthropogenic (drilling-related) solids, ambient particles settl ing out from the upper water column, surficial sed iments resuspended locally, and resuspended sediments transported horizontal y by benthic boundary-layer flow. Because resuspended particles were also trapped, the measured flux

does not necessarily reflect net seafloor accretion. Nevertheless, it more appropriately represented the exposure of benthic epibiota to near-bottom suspended particulate.

Moreover, spatial and temporal differences among trap measurements were probably more reliable than the absolute flux computed from a single deployment of a sediment trap. The ability of sediment-trap designs to accurately measure actual downward particulate flux, has been investigated theoretically (e.g., Hargrave and Burns, 1979) and experimentally (e.g., Gardner, 1980; Butman, 1986). These investigations clearly demonstrated that trapping efficiency is a function of the geometry of the trap, including its shape, aspect ratio (height to diameter), use of baffling, and the nature of the ambient flow regime, specifically the level of turbulence. While the trap configurations used in CAMP corresponded to efficient designs discussed by Butman (1986), their ability to accurate] y measure absolute flux levels under the specific flow regimes experienced in the field remains somewhat uncertain. To mitigate potential temporal and spatial sampling biases, CAMP deployed sediment traps that, for the most part, were of identical design. Thus, resulting depositional patterns were suitable for evaluating the relative exposure of biological communities located on different hard-substrate features.

Most past field investigations into the fate of drilling wastes have focussed on the distribution of drilling solids in surficial sediments close (<0.5 km) to short-term exploration wells (e.g., O'Reilly et al., 1989, Boothe and Presley, 1989; Jenkins et al., 1989; and Neff et al., 1989a). Others have concentrated on drill cuttings that were deposited immediate] y below platforms (Zingula and Larson, 1977; de Margerie, 1989). In contrast, this investigation centered on the lighter fraction of drilling fluid that was carried by ambient currents and initially deposited at mid- and far-field distances (beyond 0.5 and 1.0 km from the source, respective y). As in these past studies, this investigation uses the presence of elevated barium concentrations as the primary means for determining the presence of drilling-derived solids.

Drilling fluids, or synonymously, drilling muds used on the three platforms consisted of mixtures of natural clays, polymers, and weighting agents suspended in a water base. Barium, in the form of barite (barium sulfate) was the primary weighting agent. Because of its high density (4.50 g cm-'), barite was effective at containing reservoir pressures and as well-depth increased, greater amounts of barite were added as a fine powder to accommodate increasing well-bore pressures. This fine-grained barium constituted up to 18% of the solids in the spent drilling fluid discharged into the ocean. During and after drilling, elevated barium concentrations were detected in both trapped and surficial sediments surrounding Platform Hidalgo (Steinhauer et al., Chapter 6).

Barium was selected because of its relative enrichment in drilling fluid and its properties as a conservative tracer of drilling solids; not because of any potential toxicity to marine life, In contrast to oil-based drilling fluids that exhibit clear environmental effects (Davies et al., 1989), the majority of constituents in water-based drilling fluid, including barite, are not toxic most marine organisms (National Research Council, 1983). As with other metals present in drilling fluid discharged by the three platforms, barium's low aqueous volubility limits bioavailability (Neff et at., 1989b). Furthermore, other metals including iron, lead, zinc, mercury, arsenic, chromium, cadmium, nickel, and copper had concentrations closer to ambient environmental levels (Steinhauer et al., Chapter 6) making their use as a tracer untenable. In discharged drilling fluid, barium was 150 times more concentrated than in natural sediments allowing detection of relative] y small fractions of drilling particulate in samples at mid and far-field distances from platforms, Also, because of its low seawater volubility, it behaves as a conservative tracer for mass balance computations. Finally, because barite is a fine clay-sized material, it is more likely to be maintained in suspension and transported into the far-field along with other drilling-mud fines.

In this study, cumulative drilling-particle flux, estimated from barium enrichment in sediments trapped over four- to six-month intervals, were compared with estimates derived from trajectories of daily drilling-fluid discharges. Spatial patterns of cumulative drilling particle flux, covering these same intervals, were estimated from trajectory computations which convolved daily mass -emission data from Platforms Hidalgo, Harvest, and Hermosa, with current velocities measured concurrent] y near Platform Hidalgo. The trajectory computations were not applied prognostically, as had been the case with more robust models which predict the detailed dynamics of individual plumes of discharged material over short times (Continental Shelf Associates, 1985; O'Reilly et al., 1989). Instead, the diagnostic trajectory computation established a direct l ink between multi-year time series of platform discharges, the ambient flow field, and gross spatial patterns of trapped material. Results lent credence to site-specific estimates of the exposure of benthic organisms to drilling fluid as determined from sediment traps. Further, they added insight into the origin and fate of drilling-derived particulate at distances beyond 0.5 km from the surrounding production platforms.

Trajectory Computation

Processes that determine the ultimate fate of drilling-derived particulate in the marine environment include initial plume dynamics, passive current transport, wave-current resuspension, chemical weathering, bioturbat ion, burial, and biological uptake (National Research Council, 1983). Immediate] y after discharge, only those processes associated with the dynamics of the plume dominate the distribution of drilling particulate. These initial dynamic processes within the plume rapidly mix and dilute

suspended particulate in addition to depositing most of the drill cuttings and much of the accreted drill ing particulate in the near-field, within about 0.5 km of platforms (Continental Shelf Associates, 1985). The lighter particulate material, remaining in the water column, is then passively advected by ambient currents and deposited over greater distances. After deposition, longer-term processes, such as resuspension, serve to further disperse drilling particles. Resuspension also exposes benthic epibiota to low concentrations of drilling particles over extended periods. This study focussed on the process of passive current transport, which initially distributes the particulate over wide areas and exposes epibiota to brief episodes of high drilling-particle flux. As described below, it was this initial deposition that resulted in significantly enriched barium signatures in sediment traps located at distances beyond 0.5 km from the Platform Hidalgo.

The numerical computation of initial deposition employed here was based on the trajectory of drilling-fluid discharges as they settle and impinge on the benthos. Similar particle tracking anal yses have been employed to evaluate other aspects of pollutant dispersion in the ocean (van Dam, 1982). Recently, Fry and Butman (in press) used a comparable approach to estimate depositional patterns resulting from disposal at the 106-mile dump site off the Atlantic coast. Although trajectory computations, in general, neglect initial plume dynamics and oceanic turbulence, they are capable of generating gross temporal and spatial patterns consistent with direct observations of particulate flux. These computations indicate that, over the long-term, far-field depositional patterns are primarily controlled by the general circulation and geometry of the sources of discharge.

The schematic shown in Figure 3, illustrates the relationship among the principal parameters applied in the drilling-mud trajectory computation. For each of the three platforms, an hourly mass emission of particulate was computed from discharge volumes reported on daily log sheets by the mud engineer. This drilling-fluid discharge volume exhibited a substantial daily variation as indicated by the time series (Figure 4). The large daily variation in discharge, convolved with the short-term temporal variability in currents (Figure 5c), resulted in a relatively stochastic trajectories for individual plumes. Only when these trajectories were examined over several months did stable patterns emerge.

The particulate mass remaining in the water column at mid-field distances (<0.5 km) was assumed to be approximate y 80% of the original mass emission at the end of the discharge pipe. The coarse-fraction of particulate were assumed to be deposited in the near field during an initial phase of convective descent and dynamic collapse as described by the Offshore Operators Committee model (Continental Shelf Associates, 1985). The depth of the plume of material remaining suspended at the

edge of this zone of initial dilution was determined by the shunt depth on each of the platforms (Table 1). Differences in the shunt depth of the discharge pipe resulted in different settling distances for plumes generated by each platform.

The rate at which the plume of material settled was one of the most sensitive deposition parameters in this analysis and that of Fry and Butman (in press). However, Fry and Butman's computation of sewage-sludge trajectories, benefited from the results of a number of laboratory studies on the settling rates of sewage particulate. In contrast, settling velocity for drilling mud is difficult to precisely determine since flocculation processes strongly affect finer particulate and these processes are not easy to predict theoretically or reproduce in the laboratory. Nevertheless, research in this area is progressing and preliminary estimates of settling rates for fine -grained floes (Lick, 1989) compare with the 0.06 cm s^{-1} mean settling velocity assumed for this analysis. Moreover, the purpose of this diagnostic trajectory computation was to interpret observations of sediment trap flux not to predict them. Thus, the mean settling velocity was selected because it provided measurable particulate accumulations within the 400 km^2 anal ysis grid. Specifically, the majority of material with a slightly lower settling rate (<0.04 cm s-') remained in the water column for periods greater than three days and was transported out of the study area before impinging on the seafloor. A consequence of this *a posteriori* approach to parameter selection was a diagnostic computation of deposition that was not necessarily y suitable for prognostic modeling of absolute flux levels, but provided insight into temporal and spatial patterns of variability in flux. For example, results cannot be generalized to predict the depositional flux of drilling discharges from platforms in other regions where there are differences in flow regimes, mud properties and source geometries that are not explicitly modeled here.

Variation in settling velocity about the mean was included to empirically account for a range of particulate sizes. This was parameterized with a vertical distribution in the concentration of particulate. As indicated in Figure 3 the particulate mass associated with each hourly discharge was spread over depth as a Gaussian distribution. This allowed continuous deposition of particulate along the plume path. At a given position along the plume trajectory, the fraction of particulate adjacent to the seafloor were deposited within the underlying 1-km^2 grid cell. The amount of deposition within the cell depended upon the vertical spread in particulate and their mean depth as the plume settled with time. The vertical spread was assumed to span three standard deviations from the centroid of the distribution to the seafloor. Initially, this meant that the plume was effectively suspended well off the seafloor and the first deposits constituted less than 1 % of the total mass in the plume. As the particulate plume settled through the water column, increasingly larger fractions of material adjacent to the seafloor were accumulated within

the grid cells until the distribution center was deposited. Thereafter, decreasing fractions were deposited within grid cells along the plume trajectory. The flux of drilling-derived particulate within an individual grid cell was determined from

$$Flux = \sum_{Platforms} \sum_{\substack{Hourly \\ Discharges}} \frac{M \cdot F(\Delta t) \cdot \delta(\vec{x}_{cell}, \vec{x}_{plume})}{A \cdot T} \quad (1)$$

where $\delta = 1$ indicated that the plume at $\vec{x}_{plume}$ was within the limits of the grid cell at $\vec{x}_{cell}$, otherwise $\delta = 0$; A was the area of the grid cell (1 km^2); T was the total duration of the sediment trap deployment; M was the total particle mass in the plume; and $F(\Delta t)$ was the fraction of mass adjacent to the seafloor Δt hours after discharge or,

$$F(\Delta t) = \frac{1}{\sqrt{2\pi}} \exp\left[-\frac{9}{2}\left(1-\frac{2\Delta t}{t}\right)^2\right]; \quad \text{“A”} \quad (2)$$

where t was the settling time from shunt to seafloor in hours,

To a great extent, the amount of material accumulated within a particular grid cell was determined by the frequency with which plumes encountered that region (viz. $\delta = 1$). Thus, the long-term pattern of drilling particle flux was largely dictated by the location of the platforms and the ambient flow field which controlled the plume trajectories. The movement of plumes was determined with an approach reminiscent of progressive vector diagrams. The plume displacement relative to a platform was determined by temporal integration of current velocity. However, progressive vector diagrams are usually determined from a velocity time series recorded by a single current meter. Here, the vertical structure of the velocity field was included to account for depth differences in flow as the plume centroid settled through the water column. The velocity field at the depth of the plume centroid was determined by interpolation of velocity measured at three depths on the mooring near Platform Hidalgo (Figure SC).

Regional Circulation

To a large extent, fluctuations in mid-depth current flow at subtidal frequencies (<1 day^{-1}) dictated plume trajectories and depositional patterns. Particulate were released at depth (Table 1) and the discharge plumes required two to three days to transit the remaining 100 to 150 m of water column at an assumed mean settling rate of 50 m day^{-1} (0.06 cm s^{-1}). During the four- to six–month sediment trap deployments, nearly continuous hourly emissions from each of the three platforms were tracked until deposition. Consequently, the trajectory computation emphasized a climatological summary of subtidal

current statistics and depositional patterns reflected the relative likelihood of plume impingement on a specific epifaunal community. This differed from an assessment of the detailed short term behavior of an individual bulk discharge. Similarly, it differed from long-term fate assessments which include resuspension processes and therefore, it was not necessarily synonymous with drilling-particulate distribution in surficial sediments. Nevertheless, patterns of initial deposition were more representative of sediment-trap measurements which integrate the initial depositional flux over an extended time.

The subtidal current flow strongly influenced the initial depositional flow patterns determined in this stud y. The long-term current meter records employed in the trajectory computations exhibited features that were observed in other studies in the region but departed from the results of investigations along other sections of the California coast. One reason for the differences could be that the wind and current fields near Point Conception were complicated by the nearly right-angle change in coastline trend (Figure 1). For example, the degree of coupling between the surface flow field and along-shore wind was not as strong as along other sections of the central California coast (Chelton et al., 1988). Also, winds near Point Conception did not exhibit the strong diurnal variability evident in orographical y influenced winds to the south, in the Santa Barbara Channel (Caldwell et al., 1986).

Three flow regimes were identified in the current meter records of CAMP (Savoie et al., Chapter 4). First, intermittent upwell ing was driven by local along-shore wind stress. These upwelling events were superimposed on a sustained poleward -directed coastal jet that dominated flow field throughout much of the year. Lastly, intermittent events of across-shelf and equatorward flow were superimposed on the seasonal flow by propagating meso - scale features such as transient eddies and offshore jets. Time series that illustrate some of these flow regimes are shown in Figure 5. Along-shore components are shown since winds and currents were strongly polarized along local isobaths between Points Conception and Arguello (Figure 1). Here, poleward along-shore flow (v) refers to the component directed toward 324"T which is parallel to local isobaths and within 10 of the principal direction of local wind stress. Also, the principal current direction throughout the water column was within 10° of this direction. Defined analogously, onshore directed across-shelf flow (u) refers to 54°T.

All time series in Figure 5, exhibit statistically significant annual cycles. In late 1987, a consistent departure from the annual harmonic is evident in the temperature field (Figure 5a). These anomalously high temperatures may have been related to a mild El Niño - Southern Oscillation that induced global climate variations in the fall of 1987 (Kousky and Leetmaa, in press). Shorter-duration surface temperature fluctuations, lasting from 2 to 5 days, were superimposed on annual variations and were

significantly correlated with local wind stress. An increased equatorward wind stress preceded drops in sea surface temperature by about one day. These fluctuations reflected recurrent upwelling events that were often evident as cold-water plumes extending offshore from the upwelling center located between Points Conception and Arguello (Bernstein et al., Chapter 5). This upwelling center was the subject of the first major field program in the region entitled the Organization of Persistent Upwelling Structures (OPUS) (Atkinson et al., 1986).

Throughout CAMP, wind stress (Figure 5b) was directed equatorward except for brief poleward events, primarily associated with winter storms. The strongly equatorward mean wind opposed the largely poleward current velocities (Figure 5c). During the summer of 1984, a similar poleward flow, opposing mean wind stress, was observed extending far to the north along the continental shelf in a prior field program designated the Central California Coastal Circulation Study (CCCCS) (Chelton et al., 1988). From the south, poleward -directed outflow from the Santa Barbara Channel has also been observed in acoustic doppler velocity profiles collected during OPUS in 1983 (Barth and Brink, 1987). Climatological maps of geostrophic velocity suggested that a poleward surface current over the continental slope, designated the Davidson current, reverses in the spring in response to increased equatorward wind stress (Hickey, 1979). While surface currents recorded in CAMP (Figure 5c) also exhibit a brief spring reversal in conjunction with strengthening equatorward winds, currents at mid-depth (54 m) and at the seafloor (126 m) do not exhibit a clear seasonal reversal although they do weaken around the same time. As described below, the sustained northwestward flow at depth was present throughout the periods of active drill ing on the three platforms and it strong] y influenced the depositional pattern of drilling particulate.

A final component of low-frequency coastal flow that affected the distribution of particulate was externally driven meso - scale eddies that are advected through the region by the mean flow. These meso-scale features drove much of the across-shelf exchange at subtidal frequencies and were responsible for the large fraction of rotational energy recorded by the moored current meter at Point Conception (Savoie et al., Chapter 4). Because this single mooring provided the onl y data to determine trajectories, the computation of depositional patterns inherently assumed lateral uniformity in flow. Clearly, because of the presence of meso-scale variability at subtidal frequencies, flow defined by drogued-drifter tracks would have been preferable for determining plume trajectories.

Time-lagged correlations quantify differences in the behavior of passively -adverted particles, for example, drifters moving with fluid parcels within a Lagrangian reference frame, and Eulerian

measurements from moored current meters. Davis (1985) found a significantly shorter velocity time scale for Lagrangian measurements collected within 20 km of the northern California coast during the Coastal Ocean Dynamics Experiment (CODE). Davis ascribed shorter, one to three day, Lagrangian time scales (Figure 6a) to the rapid changes that drifters experienced as they were swept through the field of relatively slow- moving but vigorous eddies and jets. In contrast, over longer intervals of four to six days, moored instruments reflected motions within the individual slowly-propagating eddies. Figure 6a also shows that across-shelf (u) motions in CODE had shorter time scales than the along-shelf (v) fluctuations. This result is in keeping with along-shelf polarization in subtidal velocities and with correlations determined for the CAMP study region (Figure 6b). Eulerian time scales determined from the mooring near Platform Hidalgo were somewhat shorter than those determined in CODE, and were closer to Lagrangian time scales determined from drifters released near Point Conception during CCCCS (Chelton, 1987). This suggests that Eulerian eddy-field statistics in the two regions differ and trajectory errors from fixed - mooring computations in the CAMP region were lower. Furthermore, since the duration of trajectories fell within two days, the differences in along-shelf time scales were smaller than the four day differences in along-shelf decorrelation times between the two-day Lagrangian and six-day Eulerian zero-crossings in CAMP.

Sediment Trap Flux

The majority of sediment traps were located near rock features that were selected for biological study during CAMP (Figure 2). Because their primary purpose was to establish estimates of the site-specific exposure of biological assemblages to contaminants contained in drilling muds, a suite of hydrocarbon and trace metal analyses were performed on the trapped sediments and surficial sediments collected near the sediment trap arrays (Steinhauer et al., in review). The dry weight concentration of barium in trapped sediments exhibited the largest signature of drilling particulates, although surficial sediment concentrations also revealed temporal variation consistent with drilling activities. Although the sediment trap collections were sufficient to determine drilling particulate dose, the source (resuspension or direct plume impingement) of elevated barium concentrations was not immediately clear from their limited temporal and spatial distribution. The computations described below, were used to estimate the flux of drilling-particulates into the traps and the fraction that arose from plume encounters.

Sediment trap deployment intervals were nominally six months although some were a few months less. Three, in particular, cover most of the one-year period of drilling at Platform Hidalgo (Figure 4). The majority of the thirteen sediment traps were located near Platform Hidalgo because this was where the rock structures were located and because it was thought that discharge from this platform would dominate

the local distribution of drilling particulate. The total particulate flux into the traps was determined from the mass of material in the trap normalized by the area of the opening and duration of deployment. The fraction of drilling-derived particulate in this total flux was found by computing the difference between barium concentrations in the trapped material and background levels. Background levels in surficial sediments rarely exceed 0.8 mg g^{-1} dry weight but were positive] y correlated with fine- grained sediment fraction (Steinhauer et al., in review). This grain-size dependence was consistent with findings in other regions (e.g. Erickson et al., 1989). Compared to ambient sediments, the barium concentration was much larger in drilling mud, increasing from around 25 mg g^{-1} in mud discharged from shallow wells to 180 mg g-' when mud from the deepest wells was discharged (Steinhauer et al., in review). The large-grained drill cuttings and any mud adhering to them was not included in this analysis since they were initially deposited near the platforms and would not reach the closest sediment traps, 0.5 km from Platform Hidalgo. This was consistent with past investigations where the maximum depositional range in drill cuttings was on the order of 200 m (de Margerie, 1989).

To reconcile barium concentrations in surficial and trapped sediments with platform discharges, the mass balance of sediment-trap material was described both in terms of the total particulate flux and the flux of barium. From these two conservation equations, the total drilling-derived particulate flux deposited by plumes impinging on the sediment traps was determined from measured quantities. The first equation partitioned the flux of total particulate (F_{Trap}) into the flux from direct impingement of drilling-mud plumes (F_{Plume}) and the depositional flux from resuspension processes and ambient fallout from the water column ($F_{Sediment}$).

$$F_{Trap} = F_{Plume} + F_{Sediment} \tag{3}$$

A second equation governed the flux of barium into the trap.

$$F_{Trap}C_{Trap} = F_{Plume}C_{Plume} + F_{Sediment}C_{Sediment} \tag{4}$$

where C_{Trap} was the barium concentration in the sediment trap measured on a dry-weight basis. The barium concentration in the plume (C_{Plume}) was taken to be equal to the dry weight concentration of barium in drilling muds on the platform averaged over all well depths (- 108 mg g-l). The sediment barium concentrate ion ($C_{Sediment}$) was determined from grab samples of surficial sediments collected during

each sediment-trap recovery cruise. Eliminating the unknown resuspension flux ($F_{Sediment}$) between (1) and (2), the plume deposition was given by,

$$F_{Plume} = F_{Trap}\left|\frac{C_{Trap} - C_{Sediment}}{C_{Plume} - C_{Sediment}}\right| \quad (5)$$

The term within the brackets estimated the fraction of trapped sediments that arose from direct impingement of the plume, The initial depositional flux of drilling-derived particulate, computed from (5), were tabulated for edch of the three sediment-trap deployments during drilling on Platform Hidalgo. The weight fraction of total

particulate contributed by direct plume impingement is shown in parenthesis in Table 2. In evaluating (5), the estimated barium concentration in surficial sediments ($C_{Sediment}$) was decreased slightly to account for post-drilling differences between surficial and trapped sediments. In post-drilling deployments, the barium concentration in surficial sediments was found to be consistently 0.2 mg g-' higher than the concentration in the adjacent sediment traps. However, in the absence of drilling, C_{Trap} should equal $C_{Sediment}$ for F_{Plume} to vanish. A consistent offset in barium concentration within sediment traps could have arisen, for instance, from preferential resuspension of fine-grained natural particulate relative to heavier drilling- mud aggregates remaining below the 1-m high trap openings. Adjustment of $C_{Sediment}$ in (5) resulted in a change of less than 10% in estimated drilling-derived particulate flux. This change was on the order of uncertainty resulting from variation about average $C_{Sediment}$ estimates determined from replicate samples.

Replicate samples were obtained from the array of three individual sediment traps that were deployed at each of the thirteen sediment-trap sites. While the parameters in (5) were estimated from averages of these three rep] icate samples, a measure of pure error was provided by variance about these means. Usually, the standard error among replicates was relative] y low, below 10 percent for both total flux and barium concentration, However, parametric uncertainty was compounded in (5), resulting in standard errors of approximate el y 15 percent for F_{Plume} values near 400 mg m^{-2} day-l. Thus, for the first two deployments in Table 2, apparent differences in drilling-derived particulate fluxes among mid-field sediment traps were not stat ist i call y significant at the 95 percent confidence level. The larger differences between mid-field and far-field flux were, however, significant.

RESULTS

The daily discharge rate of drilling mud was discontinuous and day-to-day extremes in drilling particulate flux into the surrounding waters was evident in time series of discharge volumes (Figure 4). These discharge time series were digitized from mud engineer's reports that were filed each day drilling was conducted on a platform. An example of the extreme variations was evident at the beginning of April 1988, when a large bulk discharge from Platform Herrnosa, approaching 400 m^3, was preceded and followed by days without discharge. The subsurface current flow that disperses these bulk discharges exhibited similar levels of daily variability with reversals in direction occurring frequently over the span of a few days (Figure 5c). This temporal complexity in bulk discharge and prevailing flow would make it difficult to generalize depositional patterns determined from short-term analyses. Instead, cumulative patterns of deposition, representing the dispersion of numerous bulk discharges, were computed for time spans of four months or longer.

Four time spans of drilling-mud discharge were investigated. The first encompassed the two years of nearly continuous drilling that occurred from February 1987 through January 1989. During this time, at least one of the three platforms was actively drilling. The three other time spans corresponded to sediment-trap deployment periods and were subsets of this two-year cumulative analysis (Figure 4). Over the two-year drilling period, Table 3 shows that discharge volumes for Platforms Harvest and Hermosa were comparable. In contrast, Platform Hidalgo's total discharge of approximately 8,000 m^3 represented only half of the total volume discharged by either of the other platforms. With a drilling duration equivalent to Platform Harvest, Platform Hidalgo averaged a 50 percent lower discharge rate. This reduced rate was a consequence of the fewer (seven) development wells that were drilled on Platform Hidalgo as compared to thirteen for Platform Hermosa and nineteen for Platform Harvest.

The three sediment -trap deployments encompassed different combinations of overlap for drilling on three platforms (Figure 4). During the first deployment, from January through May 1988, all three platforms were drill ing. During the second deployment, from May through October 1988, drilling activities on Platform ceased and only the two most widely separated platforms were discharging. Finally, only Platform Hidalgo discharged drilling fluid during the final deployment period from October 1988 through May 1989. The flux of drilling particulate, arising from direct impingement of drilling-mud plumes rather than resuspension. was computed for these three sediment-trap deployment periods using the approach described in the previous section (Table 2). At all sediment trap stations (Figure 2), peak levels of the direct flux arising from drilling-derived particulate represented less than 2 percent of total particulate collected in the sediment traps. This indicated that drilling-mud plumes rarely impinged on

mid -field sites and that the vast majority of total particulate flux, averaging over 25 g m^{-2} day^{-1}, originated from other sources. Resuspension of surficial sediment was the most likely source for this large total flux rate, since regional flux from ambient fallout of detrital and terrigenous material from the water column has been reported to be much smaller, ranging from 0.6 to 2.5 g m^{-2} day^{-1} (Jackson et al., 1989).

Although weak spatial patterns in drilling-derived particulate were evident (.Table 2), the most obvious trend was temporal. The flux of drilling particles into sediment traps located near Platform Hidalgo declined significantly over the three deployment intervals despite the relatively constant discharge of drilling mud from Platform Hidalgo (Figure 7). On the other hand, the decline in total discharge volume from the three platforms over the three successive deployment intervals compared with declines in average drilling-derived particulate flux at mid-field distances from Platform Hidalgo (0.5 - 1.0 km). This suggests that the two platforms to the southeast deposited significant amounts of particulate near Platform Hidalgo and generated particulate fluxes comparable to that of Platform Hidalgo itself. Although Platform H idalgo was much closer to the sediment traps, Platforms Harvest and Hermosa discharged greater volumes of mud when they were actively drilling.

Further evidence for the significant influence of these remote platforms resulted from the relative lack of any strong relationship between distance from Platform Hidalgo and drilling particulate flux into traps. While flux consistent] y declined in each successive deployment (Table 2), there was no clear pattern of deposition around Platform Hidalgo. The only exceptions to the temporal decline were at Stations W and E. The slight increase in flux at Station E, between the first and second deployments, was not significant but the subsequent decrease of over 200 mg m^{-2} day^{-1} in the last deployment was statistically significant at the 95 percent confidence level. Station W, on the other hand, exhibited uniformly low deposition rates throughout all deployments. Station W is the most distant station from Platform Hidalgo (Figure 2), and is even farther removed from the other two platforms. This suggests that the small flux of drilling particles at Station W was primarily due to discharge from Platform Hidalgo. While significant amounts of drilling mud discharged from Platforms Harvest and Hermosa, was transported over 6.8 km and deposited near Platform Hidalgo, little of the material traveled as far as Station W.

Thus, sediment trap -data indicated that significant amounts of drilling-derived particulate were carried over distances of as much as 6.8 km, which was the separation between the most distant platforms. However, because of the location of sediment traps, the actual depositional pattern associated with transport from Platforms Harvest and Hermosa remained unclear. Because sediment-trap locations were

selected primarily for their proximity to the rock features where hard-substrate epibiota were monitored, spatial sampl ing was biased to the northwest of Platform Hidalgo, and away from the other platforms. This spatial bias prevented immediate resolution of issues concerning whether material discharged from platforms was deposited in radially-symmetric patterns or if plumes were transported along a preferential direction. Mass-balance suggested that simple radial spreading could not account for the significant contributions made by distant platforms to drilling particle flux near Platform Hidalgo. For example, if drilling muds were distributed uniformly over a 6-km radius around Platform Herrnosa, a moderate increase in deposit ional flux of 100 mg m^{-2} day^{-1} would require daily discharge volumes exceeding -7,800 m^3. Since bulk discharge volumes were more than an order of magnitude smaller, it was more likel y that preferential transport toward Platform Hidalgo resulted in the high measured flux.

Numerical computations of plume transport supported this finding. Cumulative deposition over the entire two - year drilling period (Figure 8) was clearly asymmetric and skewed toward the northwest. The major axis of cumulative flux was oriented approximately parallel to the local bathymetry of the continental shelf and peak depositional flux was centered near Platform Hidalgo. This distribution resulted from the combined effect of along-isobath polarization of ambient currents and the along-shelf alignment of the three platforms. To a large extent, plume trajectories were controlled by the mid-depth current vectors that spanned the deployment periods (Figure 9). For much of the time, current vectors were directed to the northwest. The resulting joint probability of occurrence for current velocity (Figure 10) was also elongated parallel to the northwest trend of isobaths. This velocity histogram quantified the scatter of observations of current speed and direction at subtidal frequencies. Peaks corresponded to frequently occurring velocity observations near a mean (maximum likelihood) velocity of 7 cm S-l directed to the northwest. Current speeds of 7 cm s^{-1} were associated with northwest-flow about three times more often than offshore flows of similar magnitude. This 7 cm s^{-1} mean current was capable of transporting material about 6 km in one day.

Depositional patterns determined for each of the three sediment-trap deployments exhibited similar along-shelf alignments (Figures 11 through 13). During the first deployment (Figure 11), individual depositional patterns from each of the three platforms were elongated toward the northwest and overlapped, producing a high particulate flux near Platform Hidalgo. The amplitude of depositional rates computed from the trajectory computations did not precisely match the site- specific flux estimates determined from trapped sediments and posted on Figure 11. This was due in part to the inherent uncertainty in estimating the fraction of drilling-derived particulate in the sediment traps. Similarl y, the accuracy of trajectory computations was limited by uncertainty in the input data such as settling

velocity or the specification of Lagrangian flow from a single current-meter mooring. Differences in absolute flux estimates arising from limitations in both approaches suggested that only interpretation of gross climatological features in depositional patterns was warranted. Nevertheless, the depositional patterns computed from plume trajectories only marginally over-predicted a sediment-trap peak flux that exceeded 500 mg m^{-2} day^{-1} at mid-field (-0.5 km) distances from Platform Hidalgo. Furthermore, both captured the trend toward lower values, below 100 mg m^{-2} day^{-1}, to the northwest near Station W.

Similar correspondence was shown for the second deployment interval (Figure 12). Without drilling at Platform Harvest, a lower overall peak flux was evident near Platform Hidalgo. Nevertheless, contours were still elongated to the southeast toward Platform Harvest, reflecting the influence of continued drilling at Platform Hermosa, farther to the southeast. This accounted for the relatively high drilling-derived particulate flux observed in sediment traps at Station HAR during the second deployment (Table 2) even though no discharge occurred there during that deployment.

DePositional patterns during the last deployment (Figure 13) differed significant y from other patterns. Specifically, they exhibited a more limited dispersion to the southeast and a lower overall peak flux near Platform Hidalgo. Nevertheless, prevailing currents still carried the majority of drilling mud to the northwest of Platform H idalgo; a finding supported by sediment trap observations posted on Figure 13. Also, the relative] y small number of plume trajectories extending to the southeast was consistent with the low flux observed in the sediment traps at Station HAR.

CONCLUSIONS

The magnitude, areal extent and temporal decline in drilling-mud deposition determined from trajectory computations, was consistent with observations of elevated barium concentrations in sediment traps, Thus, the excess barium concentrations that were detected near the rock features used for biological monitoring, can be ascribed to drilling-mud emissions from three production platforms in the region. However, this site- specific depositional flux of drilling muds represented less than 2 percent of total particulate flux into sediment traps. The majority of suspended material originated from other processes, particularly resuspension and transport of ambient surficial sediments.

The observed decline in drilling particulate flux near Platform Hidalgo was reconciled with its continuous constant-volume discharge by considering discharges from the platforms located some distance to the southeast. Trajectory computations indicated drill ing- mud plumes are preferential] y transported to the northwest over distances as much as 6.8 km, which was the maximum separation between platforms.

Consequently, when all three platforms were drilling, the elevated flux of platform-derived particulate near Platform Hidalgo (> 500 mg m^{-2} day-]), were a direct result of discharge from relatively distant sources. Furthermore, this relatively-high flux was not uniformly distributed but was centered near Platform Hidalgo on] y because of alignment between prevailing currents and the along-shelf configuration of platform locations, Specifically, the along-isobath polarization in poleward flow resulted in overlapping depositional patterns from the three platforms which produced regions of high local flux in the northwest quadrant.

The estimates of drilling-derived particulate flux reported here, integrated deposition from many individual drill ing-mud plumes discharged over several months. Thus, they did not reflect the short-term, more acute exposure caused by an individual drilling-mud plume impinging on hard-substrate epifaunal communities, Nevertheless, they provided a useful measure of dose for correlating with observed long-term biological change since they accurately reflected the cumulative relative likelihood of plume impingement on a particular rock feature.

REFERENCES

Atkinson, L. P., K.H. Brink, R.E. Davis, B.H. Jones, T. Paluszkiewicz, and D.W. Stuart. 1986. *Mesoscale hydrographic variability in the vicinity of Points Conception and Arguello during April-May 1983: The OPUS 1983 Experiment.* J. Geophys. Res., 91 (Cl 1), 12899-12918.

Barth, J. A. and K .H, Brink. 1987. *Shipboard acoustic doppler profiler velocity observations near Point Conception: Spring 1983.* J. Geophys. Res., 92(C4), 3925-3943.

Boothe, P.N. and B.J. Presley. 1989. *Trends in sediment trace element concentrations around six petroleum drilling platforms in the northwestern Gulf of Mexico.* Drilling Wastes. F.R. Engelhardt, J.P. Ray and A.H. Gillam, eds. Elsevier Applied Science, New York, pp. 3-22.

Butman, C. A. 1986. *Sediment trap biases in turbulent flows: Results from a laboratory flume study.* J. Mar. Res., 44, 645-693.

Cal dwell, P. C., D. W. Stuart, and K.H. Brink. 1986. *Mesoscale wind variability near Point Conception, California during Spring 1983.* J. Clim. Appl. Met., 25, 1241-1254.

Chelton, D.B. 1987. *Central California coastal circulation study drifter observations: February, July, October 1984 and January 1985.* Data Report 130, Reference 87-06, College of Oceanography, Oregon State University, Corvallis, Oregon. Prepared for the Minerals Management Service, U.S. Department of the Interior under Contract No. 14-12-0001-30020.

Chelton, D. B., A. Bratkovich, R.L. Bernstein, and P.M. Kosro. 1988. *Poleward flow off central California during the spring and summer of 1981 and 1984.* J. Geophys. Res., 93(C9), 10604-10620.

Continental Shelf Associates, Inc. 1985. *Assessment of the long-term fate and effective methods of mitigation of California Outer Continental Shelf platform particulate discharges.* Report prepared for the U.S. Department of the Interior, Minerals Management Service, Pacific OCS Region, Los Angeles, CA. Contract No. 14-12-0001-30056. Volume I (MMS 85-0033).

Davies, J. M., D.R. Bedborough, R. A. A,. Blackman, J.M. Addy, J.F. Appelbee, W.C. Grogan, J.G. Parker and A. Whitehead. 1989. *Environmental effect of oil-based mud drilling in the North Seas.* Drilling Wastes. F.R. Engelhardt, J.P. Ray and A.H. Gillam, eds. Elsevier Applied Science, New York, pp. 59-90.

Davis, R.E. 1985. *Drifter observations of coastal surface currents during CODE: The statistical and dynamical views.* J. Geophys. Res., 90(C3), 4756-4772.

de Margerie, S. 1989. *Modeling drill cuttings discharges.* Drilling Wastes. F.R. Engelhardt, J.P. Ray and A.H. Gillam, eds. Elsevier Applied Science, New York, pp. 627-646.

Erickson, P., B. Fowler and D.J. Thomas. 1989. *The fate of oil-based drilling muds at two artificial island sites in the Beaufort Sea.* Drilling Wastes. F.R. Engelhardt, J .P. Ray and A .H. Gil lam, eds. Elsevier Applied Science, New York, pp. 23-58.

Fry, V. A., and B. Butman. (In press). *Estimates of the seafloor area impacted by sewage sludge dumped at the 106-mile Site in the Mid-Atlantic Bight.* Mar. Environ. Res.

Gardner, W.D. 1980. *Sediment trap dynamics and calibration: a laboratory evaluation.* J. Mar. Res., 38, 17-39.

Hard in, D. D., J. Teal. T. Parr, P. Wilde and K. Dorsey. (In review). *Spatial variation in hard-bottom epifauna in the Santa Maria Basin, California: The importance of physical factors.* Mar. Environ. Res.

Hargrave, B. T., and N.M. Burns. 1979. *Assessment of sediment trap collection efficiency.* Limnol. Oceangr., 24(6), 1124-1136.

Hickey, B.M. 1979. *The California Current System - hypotheses and facts.* Prog. Ocean., 8, 191-279.

H yland, J., D. Hard in, E. Crecelius, D. Drake, P. Montagna, and M. Steinhauer. 1990. *Monitoring long-term effects of offshore oil and gas development along the southern California outer continental shelf and slope: background environmental conditions in the Santa Maria Basin. Oi l* Chem. Poll., 6, 195-240.

Jackson, G. A., F. Azam, A.F. Carlucci, R.W. Eppley, P.M. Williams, B. Finney, C. Huh, L.F. Small, D.S. Gorsline, B. Hickey, R.A. Jahnke, I.R. Kaplan, M.I. Venkatesan, M.R. Landry, and K.M. Wong. 1989. *Elemental cycling and fluxes off southern California.* Eos, Trans., Amer. Geophys. Union, 70(10), pp. 146-155.

Jenkins, K. D., S. Howe, B.M. Sanders, and C. Norwood. 1989. *Sediment deposition, biological accumulation and subcellular distribution of barium following the drilling of an exploratory well.* Drilling Wastes. F.R. Engelhardt, J.P. Ray and A.H. Gillam, eds. Elsevier Applied Science, New York, pp. 587-608.

Kousky, V. E., and A. Leetmaa. (In press). *The* 1986-87 *Pacific warm episode: Evolution of oceanic and atmospheric anomaly fields.* **J. Clim.**

Lick, W. 1989. ***Discharge*** *and sediment* ***transport*** *modeling.* In: Fourth Information Transfer Meeting Conference Proceedings. Report prepared for the U.S. Department of the Interior, Minerals Management Service, Pacific OCS Region, Los Angeles, CA. Contract No. 14-12-0001-30327. (MMS 89-0069).

National Research Council. 1983. *Drilling Discharges in the Marine Environment.* National Academy Press, Washington, DC., 180 pp.

Neff, J.M., M.H. Bothner, N.]. Maciolek, and J.F. Grassle. 1989a. ***Impacts*** *of exploratory drilling for* ***oil*** *and gas on* ***the benthic*** *environment of* ***Georges*** *Bank.* Mar. Environ. Res., 27, 77-114.

Neff, J. M., R.E. Hill man, and J.J. Waugh. 1989b. ***Bioaccumulation*** *of trace* ***metals from*** *drilling mud* ***barite*** *by* ***benthic*** *marine animals.* **Drilling** Wastes. F.R. Engelhardt, J.P. Ray and A.H. Gillam, eds. Elsevier Applied Science, New York, pp. 461-479.

O'Reilly, J. E., T.C. Sauer, R.C. Ayers, M.G. Brandsma, and R. Meek. 1989. ***Field*** *verification of the* ***OOC Mud*** *Discharge Mode/.* Drilling Wastes. F.R. Engelhardt, J.P. Ray and A.H. Gillam, eds. Elsevier Applied Science, New York, pp. 647-666.

van Dam, G.C. 1982. ***Models*** *of Dispersion.* In: Pollutant Transport and Transfer in the Sea. G. Kullenberg, Ed. Vol. 1. CRC Press, Boca Raton, Fla., Chapter 2.

Zingula, R.P. and D.W. Larson. 1977. *Fate of* ***drill*** *cuttings in the marine environment.* Ninth Annual Offshore Technology Conference. Paper 3040, pp. 553-556.

Table 1. Depth parameters used in the trajectory computation.

Parameter	Current Meter Mooring'	Platform Hidalgo	Platform Harvest	Platform Hermosa
Seafloor Depth (m)	131	131	204	183
Shunt Depth **(mab[2])**		97	113	149
Bottom Current Meter **(mab)**	6			
Mid-depth Current Meter **(mab)**	78			
Surface Current Meter **(mab)**	111			

'Mooring located adjacent to Platform Hidalgo.
[2]mab: meters above the bottom.

Table 2. Estimated flux (mg m^{-2} day^{-1}) of drilling Particles deposited in sediment traps by direct impingement of drilling-mud plumes. The fraction (in percent) of total particulate flux contributed by direct impingement of drilling-mud plumes is shown in parenthesis.

Station	Distance to Platform Hidalgo (km)	Jan. 1988 through May 1988 (Deployment 1)		May 1988 through Oct. 1988 (Deployment 2)		Oct. 1988 through May 1989 (Deployment 3)		Mean
Far Field								
W	6.4	74	(0.4%)	107	(0.5%)	69	(0.3%)	83
u	3.8	ND[1]		189	(0.6%)	129	(0.3%)	159
HAR	3.02	ND		379	(1.6%)	34	(0.1%)	207
S3	2.3	ND		98	(0.4%)	16	(0.1%)	57
F	2.1	ND		246	(0.8?6)	201	(0.5%)	224
S2	1.9	ND		196	(0.3%)	84	(0.4%)	140
S1	1.9	ND		216	(0.7%)	104	(0.3%)	160
E	1.2	317	(1.1%)	404	(1.4%)	170	(0.5%)	297
R	1.1	396	(1.6%)	174	(0.8%)	91	(0.4%)	220
Mid-Field								
N	.9	506	(1.7%)	311	(1.3%)	69	(0.2%)	295
I	.8	374	(1.1%)	344	(1.2%)	230	(0.5%)	316
K	.6	419	(1.8%)	ND		78	(0.3%)	249
J	.5	503	(1.6%)	449	(1.9%)	146	(0.4%)	366
Mid-Field Mean		451		368		131		

[1]ND: No data available.
[2]0.6 km from Platform Harvest (See Figure 2).

Table 3. Total volume (m^3) of drilling muds and cuttings discharged by the three production platforms on the continental shelf off Point Conception.

		Discharge Volume (m^3)			
Activity	Time-Span	Hidalgo	Harvest	Hermosa	Combined
Platform Drilling	Feb 1987- Jan 1989	7,772	16,432	17,176	41,380
First Deployment	Jan 1988- May 1988	2,382	6,193	3,742	12,317
Second Deployment	May 1988- Ott 1988	1,648	*0*	3,375	5,023
Third Deployment	Ott 1988- May 1989	2,064	*0*	*0*	2,064

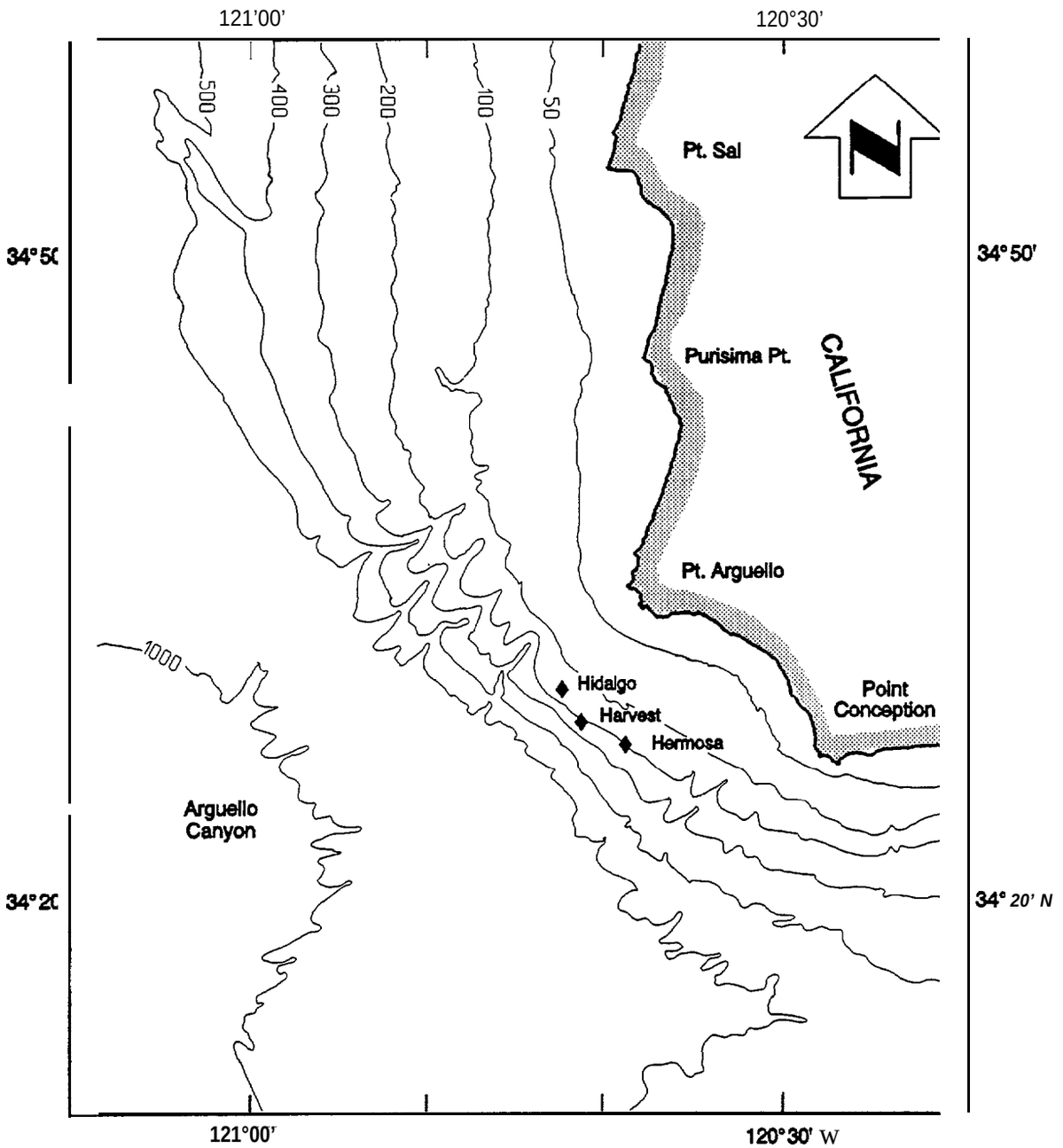

Figure 1. The CAMP region and bathymetry in meters. The three petroleum production platforms lie approximately 12 km offshore of Point Conception.

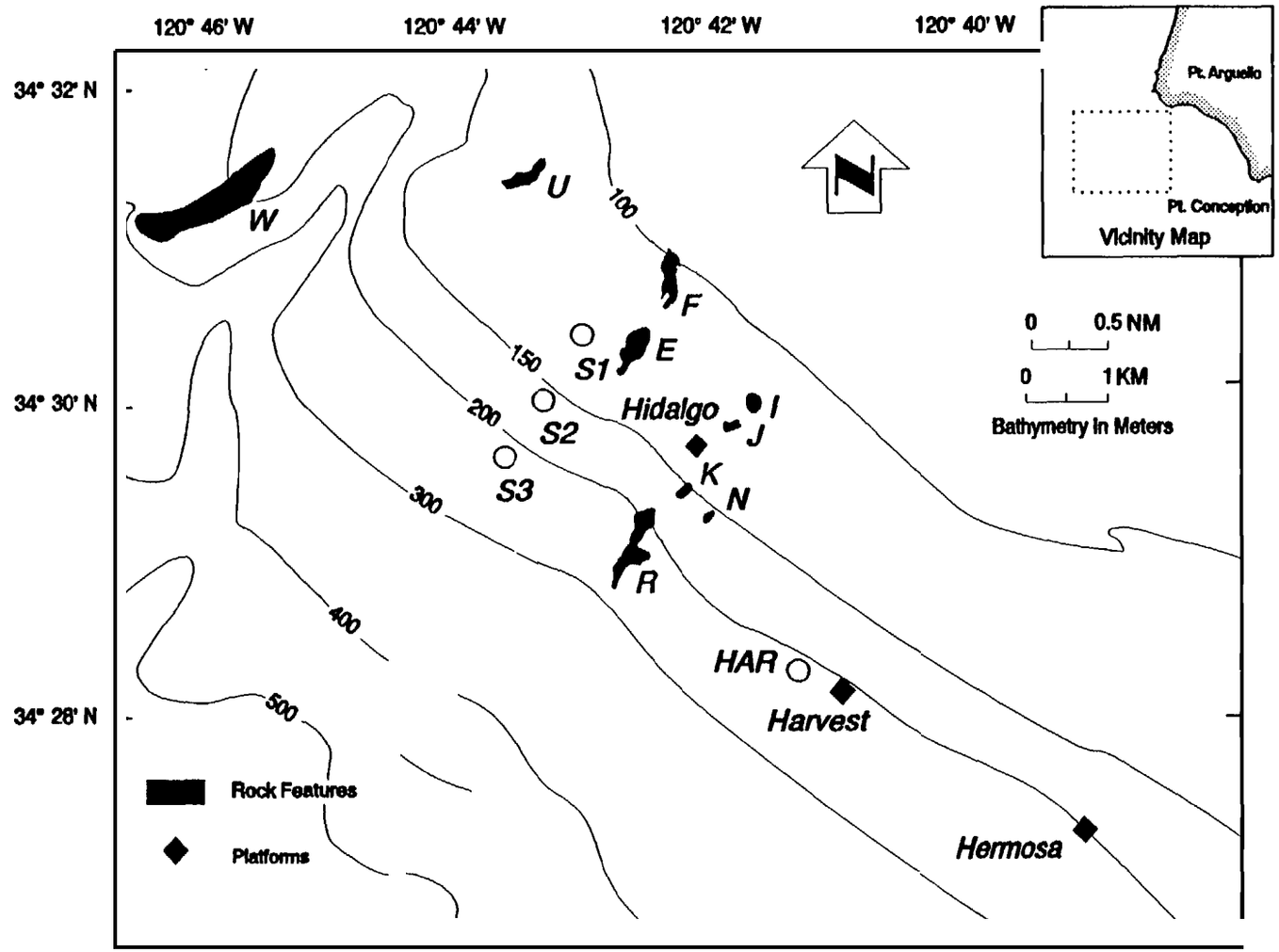

Figure 2. Local bathymetry and sediment-trap station locations in the vicinity of the production platforms. Nine sediment traps (***W***, ***U***, ***F***, ***E***, ***I***, ***K***, ***N*** and ***R***) are located near rock features. The four ancillary stations (***S1***, ***S2***, ***S3***, and ***HAR***) are indicated by circles.

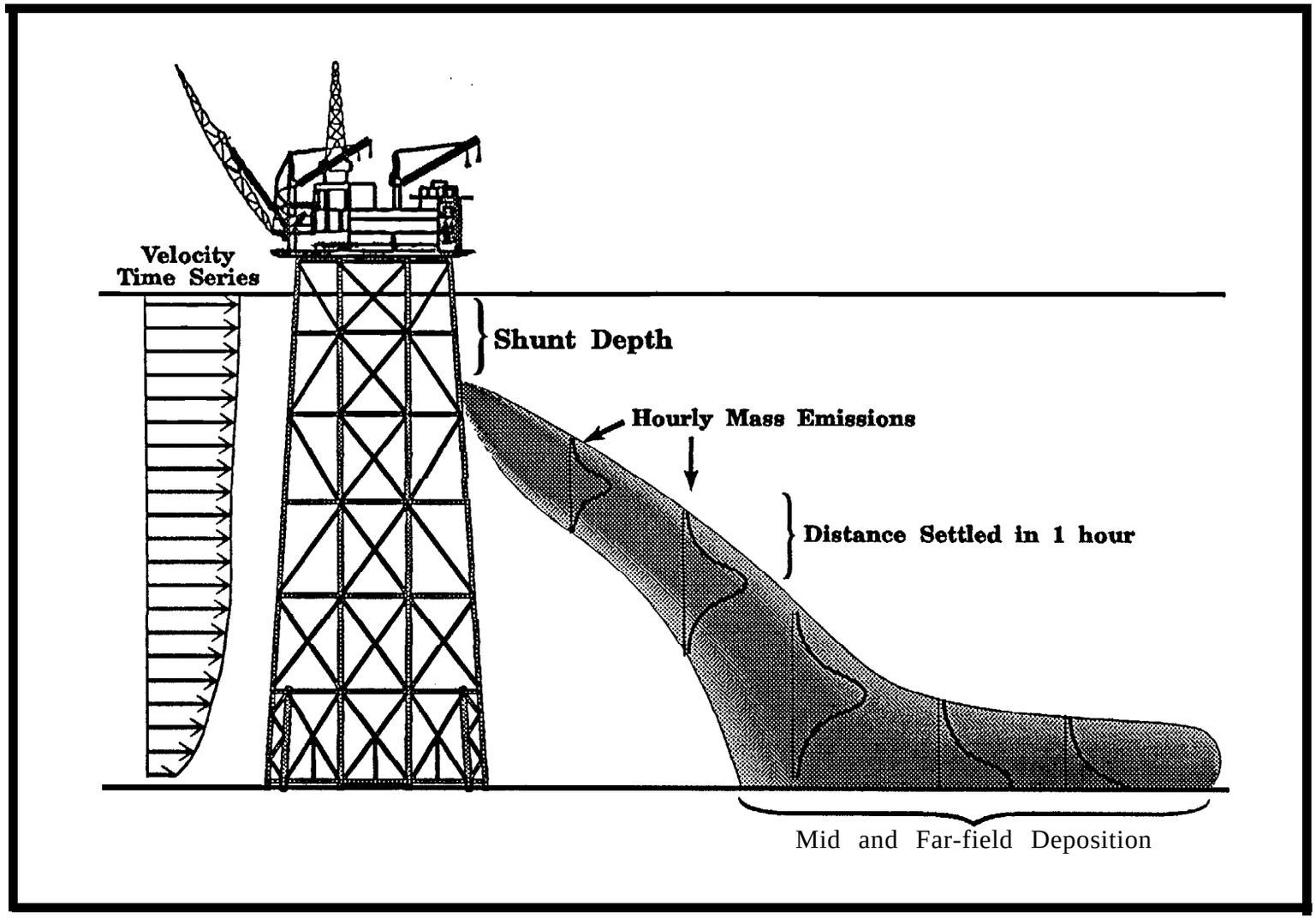

Figure 3. Schematic of the relation among parameters in the trajectory computation.

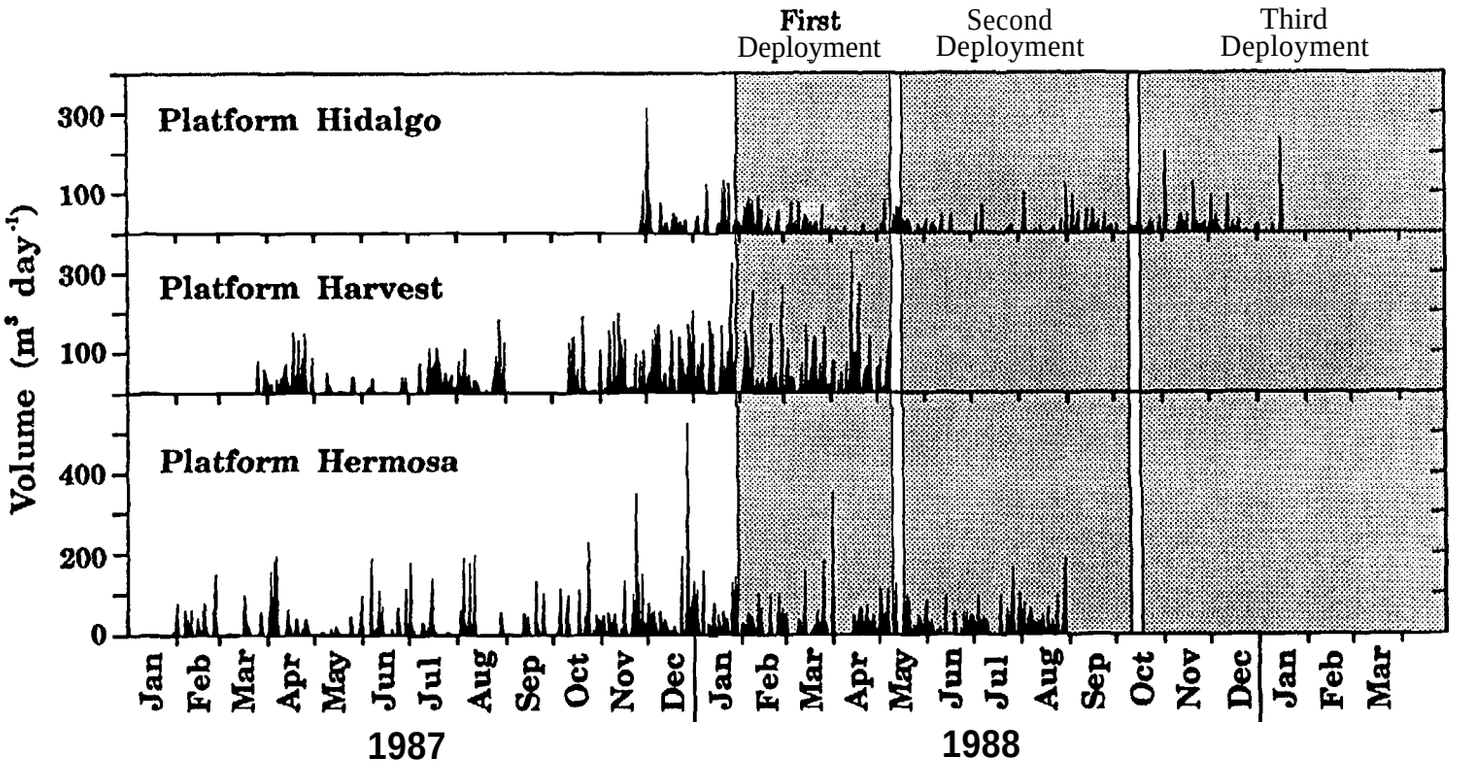

Figure 4. Time series of the volume of drilling mud discharged on a daily basis from the three production platforms off Point Conception. Also shown are the time spans of the three sediment trap deployments that covered periods of active drilling.

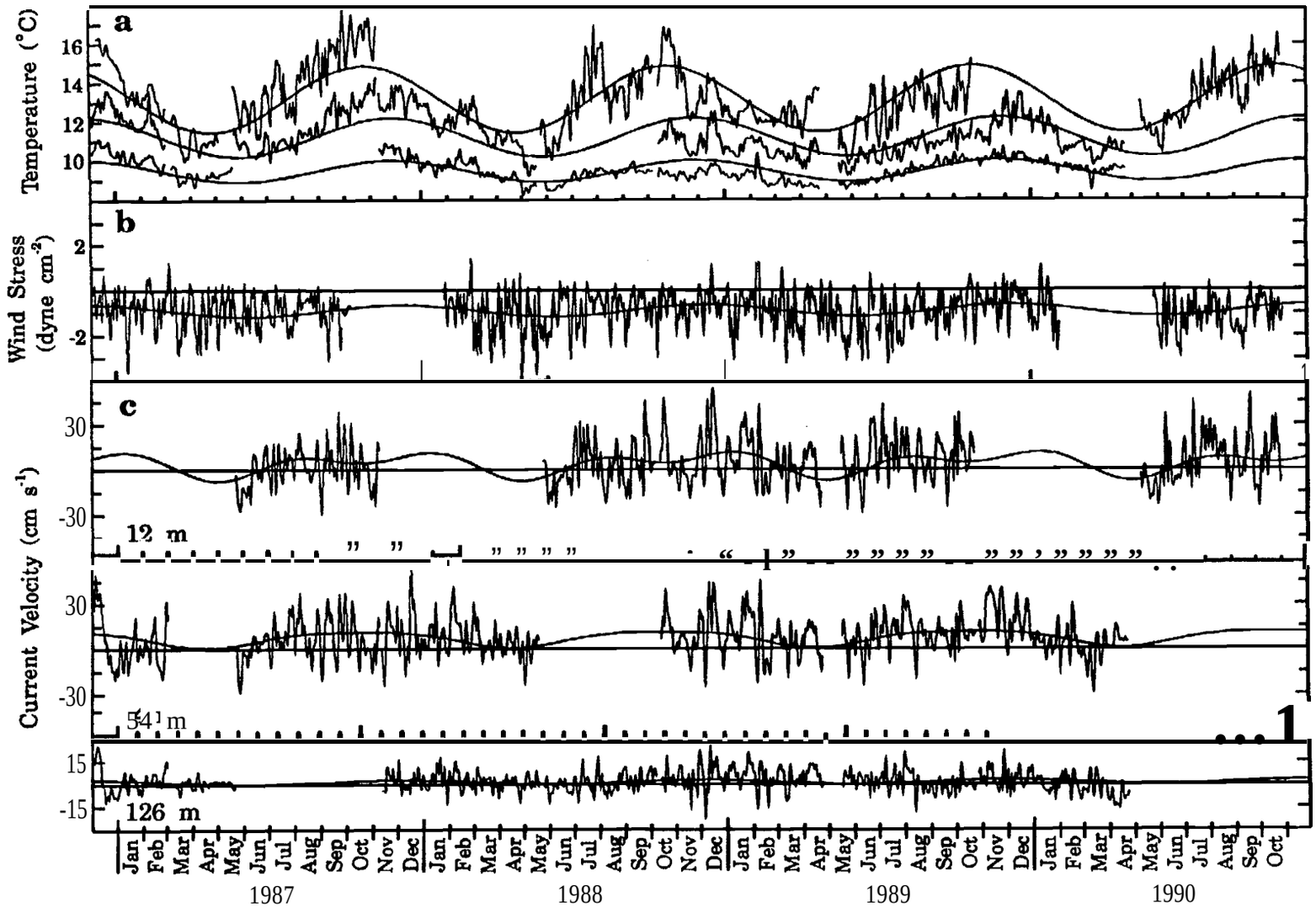

Figure 5. Time series **of** a) temperature measured at three depths (21, 54 and 126 **m) on the** current meter mooring located near Platform **Hidalgo;** b) the along-shore (324°T) component **of** wind stress computed from anemometer measurements on NDBC buoy 46023 off Point Concept ion; and c) the along-shore component of current velocity recorded by moored current meters at three depths near Platform **Hidalgo.**

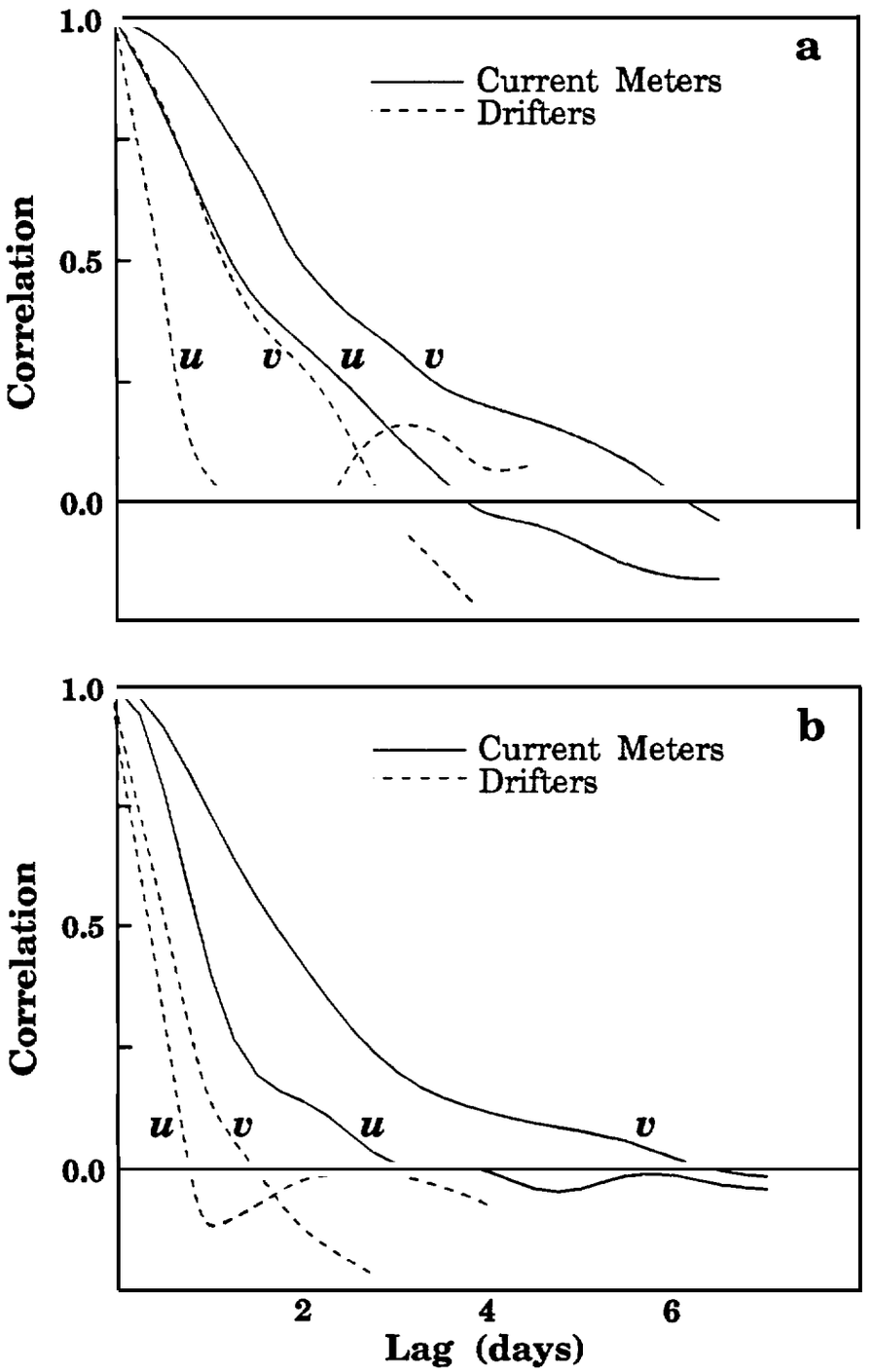

Figure 6. Time-lagged correlation of velocity from near-surface moored current meters (solid) and from surface drifters (dashed) on the continental shelf a) in the CODE region (from Davis, 1985) and b) in the CAMP region. Principal components of velocity are directed along (v) and across (u) the orientation of the continental shelves in each location.

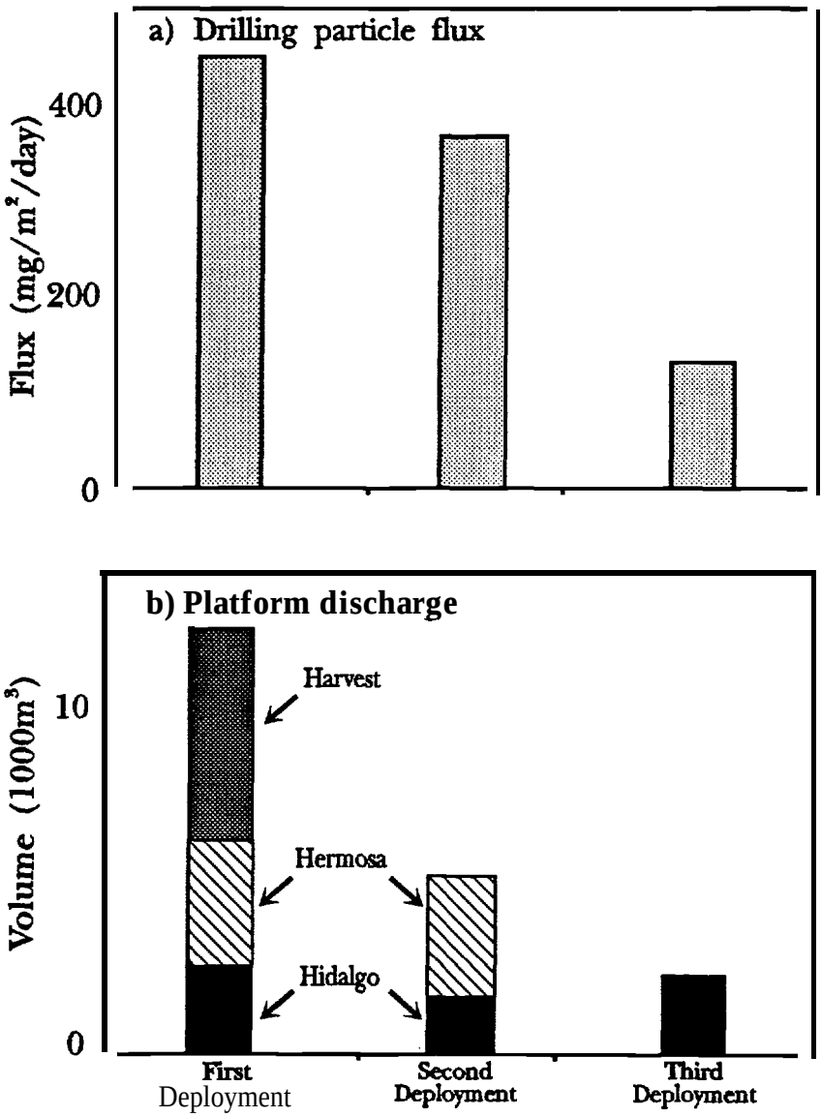

Figure 7. Comparison of a) drilling particle flux into sediment traps at mid-field distances during three separate deployments and b) total volume of drilling muds discharged over the same deployment intervals.

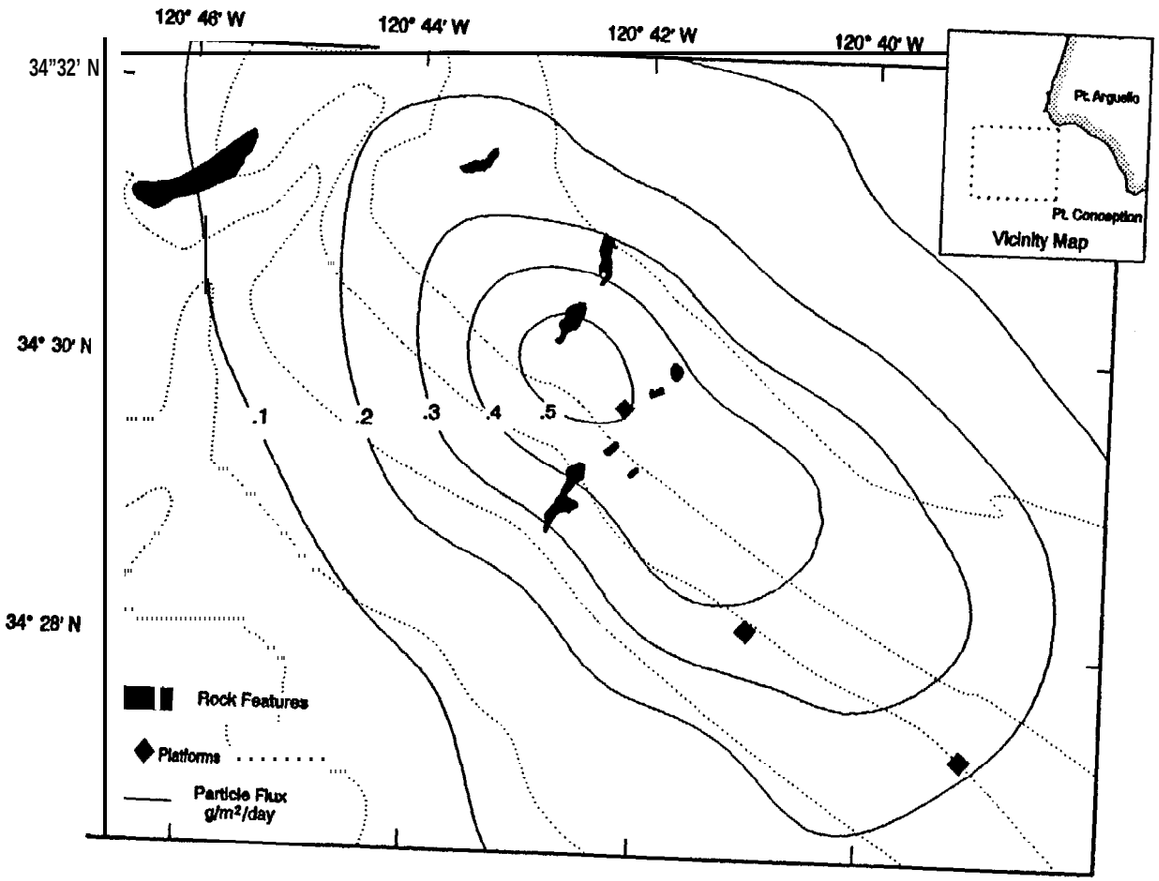

Figure 8. Estimated drilling particle flux due to the initial deposition of daily discharges of drilling mud from the three production platforms indicated by diamonds. Depositional patterns were determined from plume-trajectory computations for the two-year drilling period spanning February 1987 through January 1989.

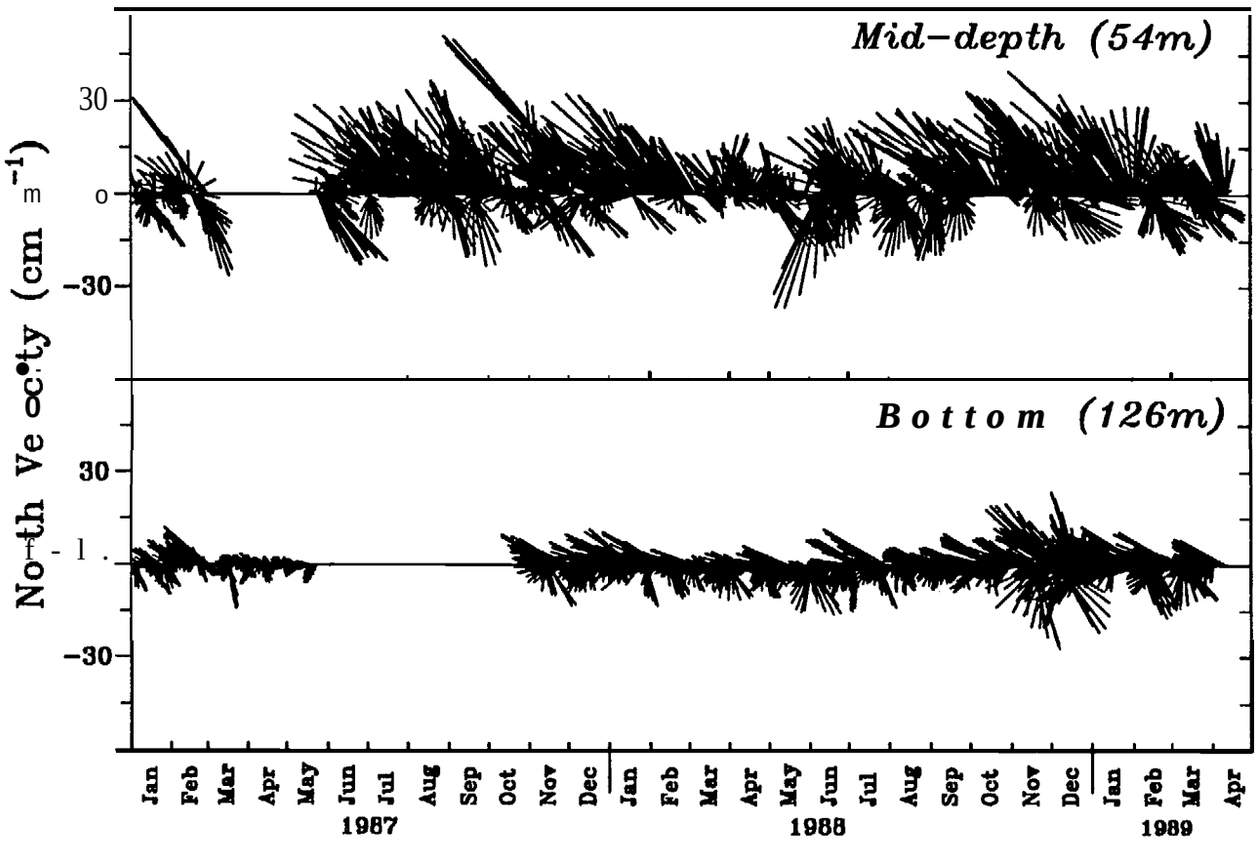

Figure 9. Time series of subsurface current velocity vectors covering the entire two-year drilling period.

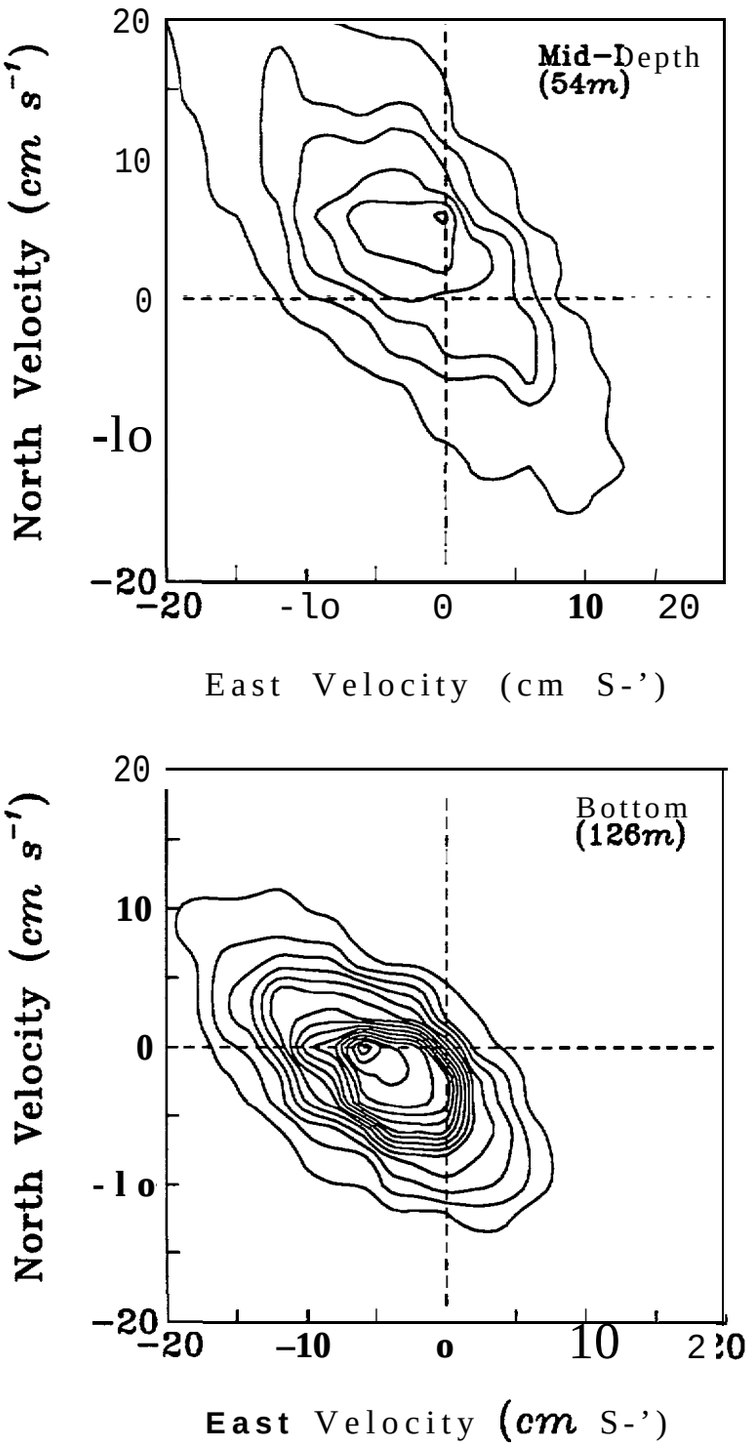

Figure 10. Joint probability of occurrence for current velocity determined from the moored current meters. The contour interval is 0.05% where the amp] itude represents the probability of observing a particular value of north and east velocity-within a square, 1 cm s-1 on a side.

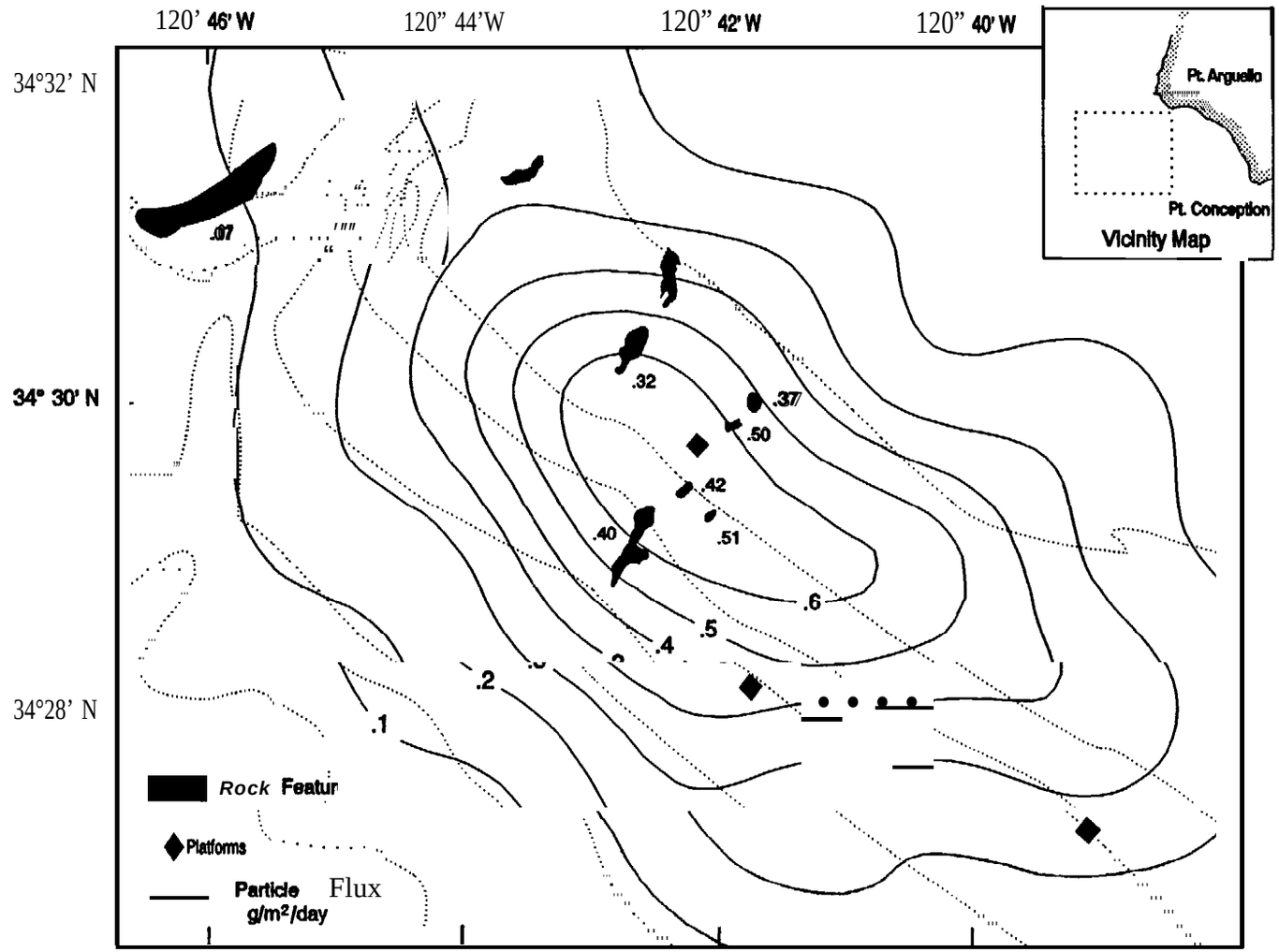

Figure 11. Estimated drilling particle flux due to the initial deposition of daily discharges of drilling mud from the three production platforms indicated by diamonds. Depositional patterns are determined from plume-trajectory computations for the first deployment of the sediment traps spanning January through May 1988. Posted number-s indicate the estimated flux determined from sediment traps.

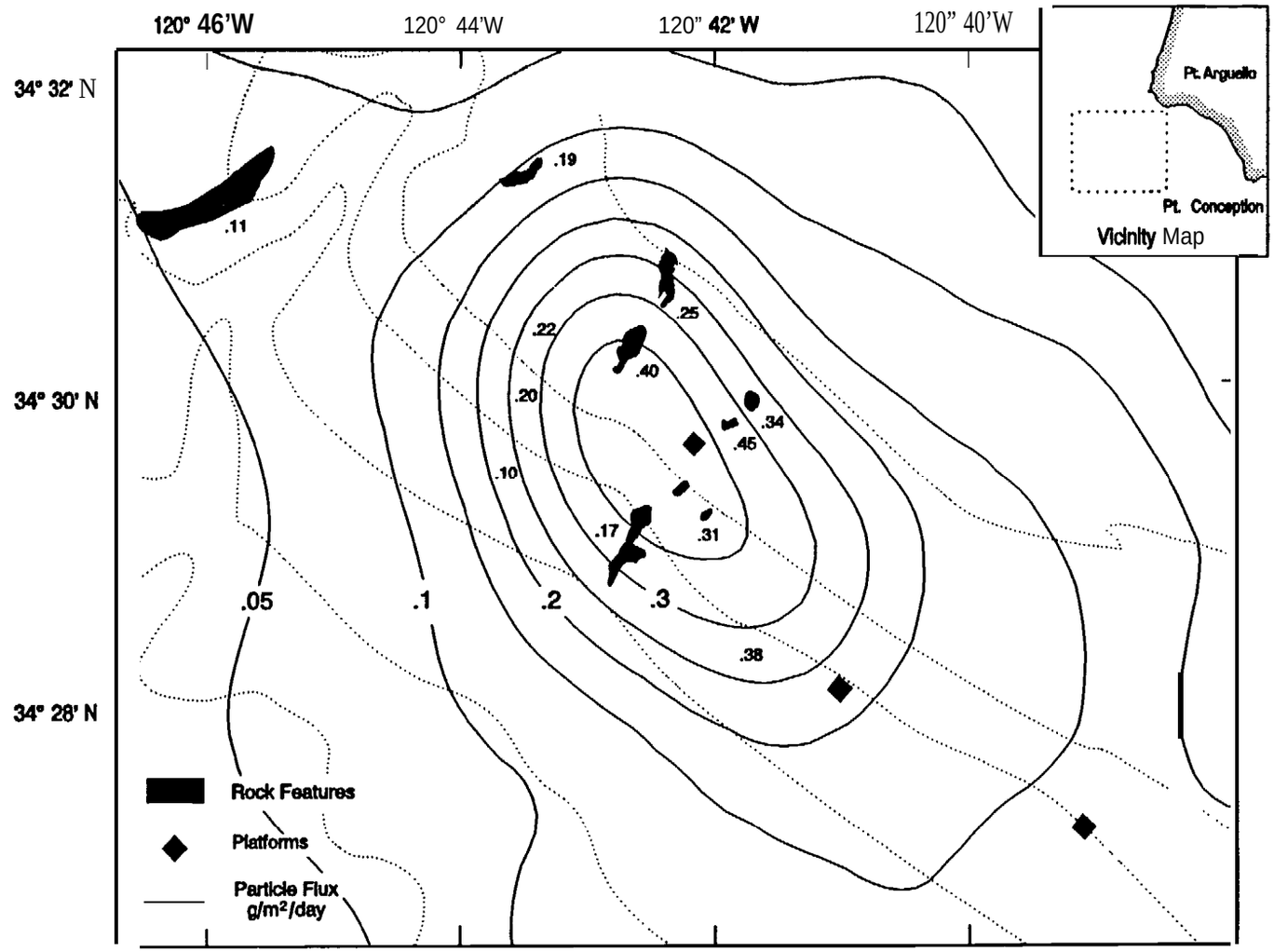

Figure 12. Estimated drilling particle flux due to the initial deposition of daily discharges of drilling mud from the southernmost and northernmost product ion platforms. Depositional patterns are determined from plume-trajectory computations for the second deployment of the sediment traps spanning May through October 1988. Posted numbers indicate the estimated flux determined from sediment traps.

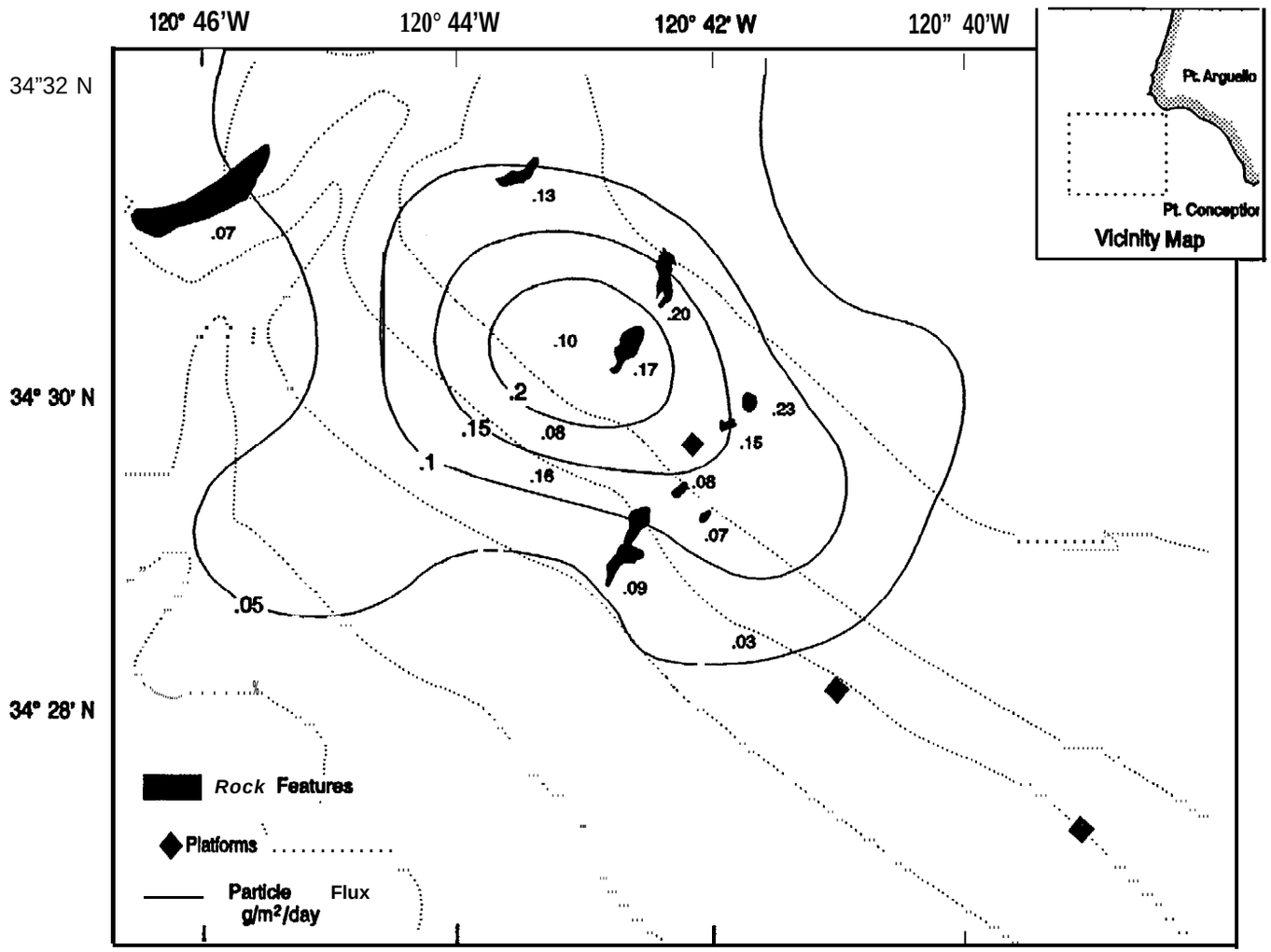

Figure 13. Estimated drilling particle flux due to the initial deposition of daily discharges of drilling mud from the northernmost production platform. Depositional patterns are determined from plume-trajectory computations for the third deployment of the sediment traps spanning October 1988 through May 1989. Posted numbers indicate the estimated flux determined from sediment traps.

9. ENVIRONMENTAL IMPACT OF OFFSHORE OIL DEVELOPMENT ON THE OUTER CONTINENTAL SHELF AND SLOPE OFF POINT ARGUELLO, CALIFORNIA

JEFFREY HYLAND

Marine Science Institute
University of California, Santa Barbara, California, 93106-6150

DANE HARDIN

Kinnetic Laboratories, Inc.
307 Washington Street, Santa Cruz, California 95060

MARGARETE STEINHAUER

Consultant
145 Abrams Hill, Duxbury, Massachusetts 02332

DOUG COATS

Marine Research Specialists
3639 E. Harbor Boulevard, Suite 208, Ventura, California 93001

ROGER GREEN

University of Western Ontario, Department of Zoology
London, Ontario N6A 5B7, Canada

JERRY NEFF

Arthur D. Little, Inc.
20 Acorn Park, Cambridge, Massachusetts 02140-2390

INTRODUCTION

The California outer continental shelf and slope just north of Point Conception is an oceanographically complex, productive region with seasonal occurrences of strong coastal upwelling (Brink *et al.*, 1984;

Savoie *et al.*, Chapter 4) and associated increases in new primary production (Dugdale and Wilkerson, 1989). Hyland *et al.* (in press) and Montagna (in press) have shown that this area supports abundant and diverse assemblages of soft-bottom macrofauna and meiofauna, respectively, comparable to other regions of known, high biological productivity, such as the North Sea. Patches of exposed rock, common between Point Arguello and Point Conception, support rich assemblages of hard-bottom epifauna as well (Hardin *et al.*, Chapter 7). This area is also believed to contain commercially significant deposits of hydrocarbons (Rintoul, 1985).

Concern over long-term environmental impacts that could result from developing the oil resources of this region led to the initiation of a comprehensive, four-year monitoring study focused on assessing potential impacts on the benthos (Hyland *et al.*, 1990; Brewer *et al.*, 1991). This study, referred to as the Phase II California Outer Continental Shelf Monitoring Program (CAMP), had two broad objectives: (1) to detect and measure potential long-term (or short-term) chemical, physical, and biological changes around oil development/production platforms in the Santa Maria Basin; and (2) to determine whether observed changes were attributable to platform-related activities or to natural processes. Hyland *et al.* (1990) described the overall design of CAMP and provided a summary of background chemical, physical, and biological features of the benthic environment, including patterns of natural spatial and temporal variability, based on the first two years of sampling, The present paper reports on the apparent effects of actual drilling events on hard-bottom epifaunal assemblages in the Platform Hidalgo area, based on the final four years of monitoring, and discusses the ability to detect changes in the benthic environment (soft and hard-bottom substrates) related to future activities.

The Study Area

The study was conducted off the southern California coast between Point Conception (34°28'N) and Point San Luis (35°06'N), at water depths of 90 to 565 m (Fig. 1). This area represents the southern offshore portion of the Santa Maria Basin, a geologic structure bounded on the northeast by Franciscan basement rocks elevated by coastal faults, and on the southwest by the Santa Lucia Bank, a topographic high which rises to about 500 m (see McCulloch *et al.*, 1982). Measuring approximately 40 km x 230 km (McCulloch *et al.*, 1982), the Santa Maria Basin encompasses a majority of the continental margin between Point Conception and Monterey, including an onshore component between the Santa Ynez and San Rafael Mountains.

The continental shelf is oriented along a northwest-to-southeast axis between Point Conception and Point Arguello and along a north-to-south axis between Point Arguello and Point San Luis. The shelf extends seaward to a depth of about 110 m and varies in width from about 4 km in the Point Conception area to about 20 km between Point Arguello and Point San Luis (Uchupi and Emery, 1963). In the Point Arguello area, the slope rapidly drops to a depth of about 1000 m and is incised by the Arguello Canyon; northward, the slope is less steep and is interrupted by the Santa Lucia Bank (Uchupi and Emery, 1963). Eastward of the bank is a sea valley (Station R-7, Figure 1) which acts as a depositional sink for fine-grained sediments (Hyland et *al.*, 1990).

Data from instrumented moorings deployed during CAMP suggest that low-frequency surface and mid-depth currents generally flow parallel to the coastline, in both upcoast and downcoast directions, whereas the bottom flow veers offshore due to leftward Ekman turning in the bottom boundary layer of the poleward mean current (Hyland *et al*,, 1990; Savoie *et a).*, Chapter 4). Records of currents from all three depths, however, reveal a strong cross-shelf component due to higher-frequency tidal influences, particularly near the bottom (Hyland *et al.*, 1990; Savoie *et al.*, Chapter 4). Because of such influences, patterns of ocean circulation, when examined at any given point in time, are much more complex than the mean circulation derived from time-averaged data. The local flow field, for example, may consist of a variety of transient phenomena, including eddies, swirls, filaments, meanders, and narrow jets. Such features have been detected in satellite images (Bernstein *et al.*, 1977), and are thought to be responsible for significant cross-shelf transport of heat, nutrients, and pollutants (Mooers and Robinson, 1984). In addition, less frequent interannual variations (e.g., El Niño/ Southern Oscillations) can obscure the generalized circulation pattern, although no major El Niño events were observed during the study period (Savoie *et al.*, Chapter 4). Such variations must be taken into consideration when assessing the transport path of materials discharged at given points in time from offshore platforms in the region.

Natural oil seeps have not been cataloged for the waters north of Point Conception but it is likely that they exist in numbers large enough to be a principal source of background hydrocarbons to the sediments. During the first year of CAMP, macroscopic tar particles were observed in bottom sediments throughout the study region (Steinhauer *et al.*, Chapter 6). Additional evidence has been provided by local reports of fouled fishing gear and oil sl icks washed onto beaches. For comparison, Wilkinson (1972) cataloged approximately 20 oil and gas seeps along the coast south of the study area, between Point Conception and Coal Oil Point. Allen *et al.* (1970) estimated that seeps in the Coal Oil Point area alone introduce daily

about 7600-11,400 liters of oil into surrounding waters of the Santa Barbara Channel. In spite of this natural source, results of CAMP hydrocarbon monitoring (Steinhauer and Steinhauer, 1990) indicate th at mean concentrations of hydrocarbons in sediments among various regional sampling sites (21 $\mu g/g$ at shallowest stations to 112 $\mu g/g$ at deepest stations, and typically less than 50 $\mu g/g$) are generally low and characteristic of background fine-grained sediments along the west coast of the United States.

There are four offshore platforms in the study area: Platforms Harvest, Hermosa, Hidalgo, and Irene (Fig. 1). Platform Hidalgo was selected during CAMP as a site for monitoring potential impacts of drilling on hard-bottom fauna. A fifth platform (Julius), which was scheduled to be installed in July to August 1987, was selected as a site for monitoring drilling-related impacts on soft-bottom infauna; however, because of scheduling delays this platform was not installed within the time-frame of the study. Since drilling began in April 1986, a total of 1.51×10^7 kg of drilling muds was discharged from the four offshore platforms in the overall study region (Table 1). Platforms Hidalgo, Harvest, and Hermosa, which are closest to the hard-bottom monitoring sites and are included in mud-deposition modeling herein, released a total of 1.12×10^7 kg of drilling muds between November 1986 (first well on Harvest) and January 1989 (last well on Hidalgo). Barite accounted for 5.73×10^6 kg (46%) of the total mud solids discharged from these three platforms. There was no production during the study, nor any development drilling after January 1989 through the end of the study, at any of these three platforms.

METHODS

The station design consisted of a series of 10 regional stations and two arrays of additional site-specific stations located in the vicinity of either actual or planned oil development/ production platforms (Fig. 1). Regional stations consisted of three cross-shelf transects of three stations each (encompassing water depths of 90 to 410 m) and an additional station (R-7) located in the sea valley 50 km west of Point Sal. Regional stations were established to examine natural oceanographic features and processes, and to monitor potential drilling-related impacts, over a broad area including different bathymetric zones. All regional stations were soft-bottom sites. One of the two site-specific sampling arrays also was located in an area containing predominantly unconsolidated substrates. This array, located about 15 km offshore of Point Sal, consisted of 18 stations centered around Regional Station PJ-1, the proposed site for Platform Julius (Fig. 1). Most of these stations were closely spaced within 2 km of the proposed platform site and arranged in a semi-radial pattern to allow detection of nearfield impacts in a number of possible directions. However, there was a greater concentration of stations, particularly those outside

the 2-km ring, along the axis parallel to local isobaths, based on the assumption that long-term mean current flow and pollutant transport would be in an along-shelf direction. Typically, three replicate samples were collected from each regional and Platform Julius station, These samples were obtained with a Hessler-Sandia, 0.25-m^2 box corer partitioned into a series of subcores to allow synoptic measurement of the following variables: macrofauna, meiofauna, hydrocarbons, trace metals, total organic carbon, and grain size.

Sampling at regional stations and at the Platform Julius array was conducted during October 1986; January, May, and October 1987; January, May, and October 1988; and May 1989. Typically, the 10 regional stations (inclusive of PJ-1) and 18 additional Platform Julius stations were sampled on the first three cruises. All regional stations were sampled on remaining cruises, except Station R-7 in May 1988. Because of delays in the installation of Platform Julius, the number of stations sampled around the planned platform site was reduced to three (PJ-1 and two others) on the October 1987 cruise, and final] y to one station (PJ- 1) beginning with the May 1988 cruise. With news of indefinite delays in the installation of Platform Julius, all sampling of the soft-bottom benthos was discontinued after May 1989. Thus all data from these stations represent pre-drilling conditions. Because the present paper focuses on platform impacts, treatment of the soft-bottom benthos will be limited to assessing the ability to detect possible changes related to future discharges, based on results of power analysis.

The second site-specific sampling array was located off Point Arguello at Platform Hidalgo (Fig. 1 and 2). Monitoring at this site focused on rock substrates inhabited by hard-bottom epifaunal assemblages. Nine stations were established at various depths and distances from the platform so that a range of possible doses of drilling materials would be represented. Also, epifaunal assemblages both on "high-relief' substrates (vertical relief greater than approximately 1 m) and on "low-relief' substrates (0.2 -0.5 m) were monitored to compare their relative sensitivities to potential impacts.

Hard-bottom stations were sampled during October 1986, May and October 1987, October 1988, May and October 1989, and October 1990. Drill ing at Platform Hidalgo began in November 1987 and ended in January 1989 (Table 1). Thus the first three sampling periods represent pre-drilling conditions and the last four periods represent conditions after the initiation of drilling. Sixty random 70-mm photographs (each representing a surface area of 0.75 m^2) were taken from a remotely operated vehicle (ROV) during each sampling period at each of the nine hard-bottom sites and examined for variations in the densities

and percent cover of all visible epifaunal species. Further details on methods for collection and analysis of epifaunal samples are given in Hardin *et al.* (Chapter 7).

Near each of the nine hard-bottom stations, three replicate samples of surficial sediment (O -2 cm) were collected with a 0.1 -m*, modified van Veen grab sampler and analyzed for h ydrocarbons and trace metals. Total hydrocarbon content (THC) and concentrations of targeted saturated and two- to five-ring polynuclear aromatic hydrocarbons (PAHs) were measured by gas chromatography coupled with mass spectrometry (GC/MS). Concentrations of 11 trace metals (arsenic, barium, cadmium, chromium, copper, lead, mercury, nickel, silver, vanadium, and zinc) were measured by either energy dispersive X-ray fluorescence or Zeeman graphite-furnace atomic absorption spectrometry. Further details on methods for chemical analyses are given in Steinhauer *et al.* (Chapter 6).

Three replicate sediment traps were deployed for six-month periods 1 m off the bottom near each of the nine hard-bottom photosurvey sites and at a site (PHAR) 500 m northwest of Platform Harvest (Fig. 2). Sediments collected in these traps were analyzed for trace metals, hydrocarbons, and relative particle flux. Successful trap deployments were made during January - May 1988, May - October 1988, October 1988 - May 1989, May - October 1989, October 1989- May 1990, and May - October 1990. Excess barium concentrations in the traps were used to compute fluxes of platformderived particles to the seafloor. Fluxes estimated from the traps were compared to those derived from trajectory modeling of platform discharges, based on mud-discharge records supplied by the platform operators and water-current data obtained from an instrumented mooring deployed 1 km northwest of Platform Hidalgo (Fig. 2). The moored instrumentation - which consisted of three vector-averaging current meters (near-surface, mid-depth, near-bottom), each equipped with conductivity and temperature sensors and a bottom pressure recorder - made continuous measurements of currents, pressure/sea-surface elevations, temperature, and conductivity. Data from the current meters were stored internally and telemetered to shore each day via ARGOS satellite link.

The ability to detect statistically significant changes in the environment was assessed through power analysis performed on 17 chemical and biological response variables from both soft-bottom and hard-bottom sites. The analyses were conducted using formulae based on Taylor's Power Law for a

two-group contrast (t-test comparison between two sample means) on a given variable. The procedures used are described by Green (1989). These analyses provide measures of the amount of detectable change in the various response variables as functions of the degree of power, alpha level, and sample size.

RESULTS AND DISCUSSION

Estimated Fluxes of Drilling Particles to the Seafloor

Fig. 3 provides a time-series record of drilling muds discharged from Platform Hidalgo and Platforms Harvest and Hermosa, located 3-7 km away. Discharge volumes for these platforms vary considerably from zero to over 500 m^3 in a single day. Each platform record reveals a number of intermittently spaced discharge peaks.

Concurrent drilling at all three platforms occurred over a five-month period between November 1987 and May 1988, which coincides with a period (January - May 1988) when sediment traps were deployed. Trap deployments prior to January 1988 were unsuccessful (except for traps retrieved at Stations PH-I and PH-U in May 1987). Five additional trap deployments took place after May 1988. The May - October 1988 deployment coincides with a period when Platforms Hidalgo and Hermosa (but not Harvest) were drilling. The October 1988- May 1989 deployment coincides with a period when only Platform Hidalgo was drilling. The three remaining trap deployments (May - October 1989, October 1989- May 1990, May - October 1990) represent post-drilling periods for all three platforms.

Drilling-mud depositional fluxes for each sediment-trap location and deployment period are given in Table 2. These values were calculated from excess concentrations of barium in the traps relative to background concentrations, determined separately for each station by selecting the lowest mean value (averaged over replicates) among the various deployment periods. For all sites, the lowest level that was recorded represented one of the last two post-drilling deployments, which took place a year or more after cessation of drilling. Concentrations of barium in suspended sediments were consistently low during these post-drilling periods and approximated pre-drilling concentrations in surface sediments. This background value was subtracted from the barium concentration in each sediment trap for all other deployment times to determine the excess concentration of barium derived from drilling sources. The excess concentration of barium in each trap was then multiplied by the sediment flux measured by that trap (i. e., weight of trapped material normalized per unit area and time) to determine the flux of barium ($mg/m^2/day$).

Because the average concentration of barium in drilling muds was 1 g barium/10 g dry weight mud (Table 5), the barium flux in each trap was multiplied by a factor of ten to estimate the flux of total drilling-derived particles.

Mean fluxes averaged over the three deployments during drilling were high at Stations PH-E, PH-J, PH-I, PH-N, PH-K, and PHAR (251 -377 mg/m^2/day); moderate at Stations PH-F and PH-R (215 -234 mg/m^2/day); and low at Stations PH-U and PH-W (89 - 172 mg/m^2/day). Mean fluxes averaged over all post-drilling deployments were consistently low (1 -24 mg/m^2/day) at all stations. The high fluxes at Stations PH-E and PHAR during drilling suggest a depositional pattern that follows the notthwest/southeast trend of the bathymetry and direction of mean current flow.

The mean flux averaged over all traps was highest (384 mg/m^2/day) for the deployment ending in May 1988, which coincides with the period of maximum mud discharge when drilling occurred concurrently at all three platforms. The mean flux decreased steadily over the next two deployments, to 303 mg/m^2/day by October 1988 and 132 mg/m^2/day by May 1989. Mean fluxes averaged over all stations for the three postdrilling deployment periods remained at low levels between 3-43 mg/m^2/day. Because the volume of drilling muds discharged from Platform Hidalgo did not decrease with time (Fig. 3), the steady decline in fluxes over the first three trap-deployment periods at sites around Platform Hidalgo reflects the influence of discharges from the other two platforms while they were drilling.

The amounts and patterns of initial deposition of drilling muds discharged from Platforms Hidalgo, Harvest, and Hermosa were also examined by plume-trajectory modeling. This approach is based on tracking a simulated plume of discharged particles as they are passively transported by ambient currents and allowed to settle through the water column to the seafloor. Simple trajectory models are recognized as effective methods for analyzing long-term continuous discharges under conditions of time-varying currents and discharge volumes (van Dam, 1982; CSA, 1985; Coats, Chapter 8). Fry and Butman (in press) have described a similar trajectory-modeling approach to predicting initial depositional patterns of sewage sludge on the seafloor.

The model used here combined daily discharge data from the three platforms with current velocities measured concurrently from an instrumented mooring deployed near Platform Hidalgo (Fig. 2). Results of the model are applicable at mid-field distances, between 0.5 and 10 km from Platform Hidalgo, and

can be compared directly to flux data obtained from the sediment traps deployed over similar distances. However, two limitations to recognize are: 1) the model predicts initial muddepositional patterns and does not account for subsequent resuspension of deposited material; and 2) depositional patterns predicted from the model are based on a number of plume-transports integrated over several months and thus do not represent conditions resulting from single discharge events.

The results of trajectory modeling of platform discharges between May and October 1988 are shown in Fig. 4(a). Predicted peak fluxes of 400- 5(KI mg/m^2/day within about 1.5 km of Platform Hidalgo match the fluxes computed from sediment-trap data. The model results also showed a ridge of high deposition oriented along the northwest-southeast axis and extending over all three platforms.

During the third sediment-trap deployment (October 1988- May 1989), drilling occurred only at Platform Hidalgo and ended there halfway through the deployment period (Fig. 3), Because of relatively intense bottom currents in the fall of 1988, the model results suggest that the small amount of muds discharged during this period was distributed over a broad area [Fig. 4(b)]. For example, a small accumulation of drilling mud was predicted near Platform Hermosa, 6.8 km to the southeast of Platform Hidalgo, even though there was no discharge at that site. Also, the results suggest that drilling mud was transported relatively far to the northwest, a prediction that is consistent with the small increase in flux observed at Station PH-U (Table 2).

The close agreement between sediment-trap data and modeling results suggests that the excess amounts of barium found in the traps can be attributed to drilling discharges and thereby provide an effective tracer of drilling-mud accumulations. Both indicate peak fluxes of drilling solids at Station PH-J, located about 500 m northeast of Platform Hidalgo. The estimated flux of drilling-derived particles at this station during May - October 1988 (464 mg/m^2/day based on sediment-trap data) represents 1.96% of the total suspended particles (23.7 g/m^2/day) collected in these same traps. This ratio of drilling-mud flux to flux of total suspended particles, which was the highest among all station/time combinations, is used below as a 'dilution factor" to establish the expected concentrations of various other drilling-mud constituents in ambient suspended sediments, based on their initial concentrations in source drilling muds.

Surficial sediments

Concentrations of trace metals and several hydrocarbon variables in surficial sediments (O-2 cm) from nearfield and farfield (control) stations are summarized in Table 3 according to drilling period. Mean concentrations (averaged over all stations and times) of analytes in sediments from the proposed Platform Julius site, 30 km north of Platform Hidalgo, have been included in Table 3 for comparison. Concentrations at Platform Julius stations represent pre-drilling conditions and are within concentration ranges typical of offshore sediments along the southern California coast (Bruland et *a/.,* 1974; Reed *et al.*, 1977; Katz and Kaplan, 1981; SAIC, 1986).

Table 3 reveals that mean THC concentrations increased about twofold in sediments from both nearfield and farfield stations between pre-drilling and during-drilling periods at Platform Hidalgo. However, there were no parallel increases in mean concentrations of total polynuclear aromatic hydrocarbons (ΣPAH) or of the naphthalene, phenanthrene, and dibenzothiophene homologous series. Instead, the mean ΣPAH concentrations in nearfield samples, collected before drilling was initiated, were four times higher than in samples collected during drilling or after drilling had ceased. These variations are most likely linked to natural petroleum inputs (e.g., seep-related material) rather than drilling activities. In most samples, *50%* or more of the THC concentration was due to the presence of an unresolved complex mixture (UCM; see Steinhauer *et al.,* Chapter 6). The presence of a UCM usually suggests a petroleum input (Barrington and Tripp, 1977; Reed *et al.,* 1977; Wakeham and Barrington, 1980; Kennicutt et *al.,* 1987) but is characteristic of weathered oils (Barrington *et al.,* 1973; Barrington and Meyers, 1975; Reed et *al.,* 1977) and a common component of sediments off southern California (Reed and Kaplan, 1977; Reed *et al.*, 1977; Simoneit and Kaplan, 1980; Stuermer *et al.,* 1982; SAIC, 1986).

GC/MS chromatograms of sediments (see Steinhauer *et al.,* Chapter 6) also revealed that normal (unbranched) alkanes were dominated by C29 and other odd-carbon members in the C25 to C31 range. This is a common feature of hydrocarbons derived from terrestrial plants (Wakeham and Barrington, 1980). Concentrations of lower-molecular-weight alkanes (n-C10 through n-C20) generally were very low, suggesting little evidence of fresh petroleum in surficial sediments.

Barium was the only analyte that displayed spatial and temporal trends that could be related to drilling activities. Pre-drilling concentrations of barium in surficial sediments around Platform Hidalgo were

similar to background concentrations at the planned Platform Julius site (Table 3). During drilling the mean barium concentration in sediments from the five nearfield stations increased by approximately 200 μg/g dry weight. A slight increase (83 μg/g) occurred during drilling at farfield stations as well. The mean barium concentrations in sediments averaged over the three post-drilling sampling periods declined substantially but were still approximately 100 μg/g higher than either the pre-drilling concentrations around Platform Hidalgo or the baseline concentrations in sediments from the Platform Julius control area.

Suspended sediments

Table 4 presents trace metal and hydrocarbon concentrations in suspended particles collected in sediment traps at high-, medium-, and low-flux stations during and after drilling at Platform Hidalgo. The station categories are based on the above estimates of drilling-mud fluxes computed from excess barium concentrations measured in the trap samples. Because sediment traps were recovered successful] y from only two stations (PH-I and PH-U) prior to drilling, pre-drilling concentrations of various chemical variables are not given.

Except for barium and THC, there was little variation in other chemical variables among the various stat ions or sampling intervals. The THC concentrations were higher during drilling than after drilling for all station categories, but these increases did not follow a pattern consistent with the estimated sediment flux: mean concentrations were highest at low-flux stations (411 μg/g, Table 4) and lowest at high-flux stations (182 μg/g). As with surficial sediments, these variations are probably not related to drilling discharges.

Mean concentrations of barium in suspended particles, however, followed a pattern consistent with both the timing of platform discharges and the proximity of stations to the discharge source. During drilling, mean concentrations were highest at high-flux (nearfield) stations and lowest at low-flux (farfield) stations (Table 4). After drilling ceased, mean concentrations were consistently low (771 -883 μg/g) among all stations and were within the range of background concentrations of barium in suspended particles (749 -959 μg/g; Steinhauer *et al.*, Chapter 6). The mean concentration of barium at high-flux stations during drilling (2397 μg/g) was about two to three times these levels. Barium was the only chemical variable that revealed a clear signal of drilling-related inputs to either suspended or surficial sediments.

Table 5 presents estimated peak concentrations of trace metals and hydrocarbons in the expected area of maximum drilling-mud flux, at nearfield Station PH-J. These values are presented as worse-case predictions of exposure levels in suspended particles, based on the 1.96% ratio of drilling-mud flux to flux of total suspended particles (see derivation above) and the measured concentrations of the various analytes in source drilling muds. Table 5 also lists the predicted percent increases in these analytes above background concentrations. Because concentrations of barium, zinc, and all three hydrocarbon variables in the drilling muds increased with increasing well depth (Steinhauer *et* al., Chapter 6), predicted concentrations in Table 5 are shown for two cases: (1) using depth-integrated mean concentrations of analytes in drilling muds collected from four well depths, and (2) using mean concentrations of analytes in drilling muds collected only from the bottoms of wells. The higher concentrations of hydrocarbons in drilling muds exposed to the bottoms of wells reveal their source in the oil-bearing rock strata.

Zinc and the three hydrocarbon variables were the only analytes other than barium with predicted percent increases above background concentrations greater than 8.0% (Table 5). Zinc could have increased by as much as 20%, if it is assumed that only muds from the bottoms of wells were discharged. However, the predicted concentrations of zinc in suspended particles (77 -85 μg/g) were still very low and within the range of concentrations (71 -94 μg/g) observed in individual samples of surficial sediments around Platform Hidalgo prior to drilling (Hyland *et al.*, 1990).

Similar] y, although the predicted percent increases in THC and ΣPAH were moderate to large (9.5 -24% for THC; 817-1667% for ΣPAH), their predicted peak concentrations in suspended particles (88 -99 μg/g for THC; 0.55 -1.1 μg/g for PAHs) were low, overlapping with concentrations found in samples removed from drilling influences. For example, Steinhauer and Steinhauer (1990) reported that mean concentrations of THC in surficial sediments among CAMP regional stations ranged from 21 μg/g at shallowest sites to 112 μg/g at deepest sites, and that mean concentrations of ΣPAHs in surficial sediments around Platform Hidalgo prior to drilling ranged from 0.026 to 1.48 μg/g among the various stat ions. Concentrations of naphthalenes in suspended particles were predicted to increase *35,000%* to 77,000% above background. Increases of these magnitudes would result in suspended-particle concentrations between 0.35 mg/g and 0.77 μg/g. However, because low-molecular-weight naphthalenes have a high volubility in water, preferential weathering through dissolution would be expected to reduce their concentrate ions in suspended material. The mean concentration of naphthalenes measured in suspended particles at high-flux stations during drilling was only 0.007 μg/g (Table 4).

The predicted maximum hydrocarbon concentrations in suspended particles at Platform Hidalgo were much lower than levels observed in sediments at a nearby oil-spill site, 19 km southeast of the CAMP study area, following the sinking of the freighter *Pac Baroness* (Hyland et *al.*, *1988).* Significant reductions in the abundances of infauna within 500 m of the wreck were linked to the elevated hydrocarbon levels, including average ΣPAH and naphthalene concentrations of 70 μg/g and 24 μg/g, respectively. The mean concentration of THC in the contaminated sediments, although not reported, was 309 μg/g (unpublished data from the authors).

Effects of Platform Discharges on Hard-Bottom Epifauna

Possible impacts of platform discharges on selected dominant hard-bottom epifauna were examined by ANOVA. A total of 22 cases resulted by combining the 15 most abundant taxa from each of low- and high-relief habitats. The abundances of each of these taxa, as well as the combined cover of all suspension feeders, the combined cover of all taxa, and the total number of species were tested with an unreplicated three-way ANOVA model (Sokal and Rohlf, 1969). Because the abundances of most of these fauna have been shown to vary in relation to depth and habitat relief (Hardin *et al.,* Chapter 7), and because high-relief habitat occurred only at the deeper stations (Table 6), two separate series of three-way ANOVAs were run. One tested the significance of differences among low-relief stations due to main effects of sampling time, relative dose of drilling solids, and depth. The other tested the significance of differences among deep stations due to main effects of sampling time, dose, and habitat relief. The class variable dose consisted of three levels (low, moderate, and high) corresponding to the three categories of drilling-solid flux computed from excess barium concentrations in sediment traps (Table 2). Sampling time consisted of seven levels: October 1986, July 1987, November 1987, October 1988, May 1989, October 1989, and October 1990. Depth consisted of two levels: shallow (105-119 m) and deep (160-212 m). Relief also consisted of two levels: low (0.2-0.5 m) and high (> 1.0 m). The distribution of stations among these various classes is shown in Table 6.

The value in each cell of the ANOVA is the mean of all photographic samples (i.e., 70-mm still images, each representing a bottom surface area of 0.75 m^2) from each corresponding combination of time x dose x depth, or time x dose x relief. The mean value for each of the seven time x highdose x shallow-depth combinations among low-relief stations is based on 180 photographs (60 per each of the three stations PH-J, PH-E, and PH-I). All remaining factorial combinations are represented by a single station (Table 6); thus the mean values for all corresponding cells are based on 60 photographs. Tests for differences

in abundances of organisms were run on square-root transformed data; tests for differences in the percent cover of organisms were run on arc-sine transformed data (Sokal and Rohlf, 1969).

An unreplicated ANOVA model was used because there were not enough natural reefs in the study area to replicate all factorial combinations of depth, relief, and dose (Table 6). Furthermore, because abundances of many of the taxa varied significantly among stations within each of the class variables depth and relief (Hard in *et al.*, Chapter 7), the various station means within these classes could not be used as independent replicate samples of the variable dose. The three-way interaction effects in these tests and all nonsignificant ($p > 0.05$) time/depth, time/relief, dose/depth, and dose/relief interactions were pooled to provide an estimate of error variance (Sokal and Rohlf, 1969). The main effects and time/dose interactions were tested against this pooled estimate of error variance.

Significant time/dose interactions, corresponding to contrasting patterns of temporal change among the different dose levels, were evaluated as possible drilling impacts. In an effort to determine whether there were any negative effects of drilling, this evaluation was limited to significant time/dose interactions in which: (1) the biological response variable showed a decline at highdose stations after drilling began in comparison to the before-drilling period, and (2) the correlation coefficient (r) between changes in the biological response variable and fluxes of drilling-mud particles was substantially negative.

Sabellid pol ychaetes and the white and purple anemone were the only low-relief taxa that displayed significant ($p \leq 0.05$) time/dose interactions (Table 7), and of the two only sabellids satisfied the above criteria for a possible negative drilling impact. Densities of the unidentified white and purple anemone at shallow low-relief stations [Fig. 5(a)] decreased after drilling began at all three dose levels, and the largest reduction occurred at the lowest level ($r = 0.933$). Moreover, densities of this anemone among deeper low-relief stations [Fig. 5(a)] increased after initiation of drilling at all three dose levels, although they showed the greatest increase at the lowest level ($r = \%.884$). In contrast, densities of sabellids at deep low-relief stations [Fig. 5(b)] decreased at the highdose level and increased at the moderate- and lowdose levels after drilling began ($r = -0.728$), indicating a possible negative effect of the drilling discharges. It should be noted, however, that the time/dose interaction for sabellids was only marginally significant in the time x dose x relief ANOVA at deep stations (Table 7). Furthermore, although this

group displayed a negative correlation between changes in density and fluxes of drilling-mud particles at shallow low-relief stations (r = -0.650), mean densities in this case actually increased slightly at the highdose level after drilling began.

Five taxa exhibited significant time/dose interactions in the time x dose x relief ANOVA at deep stations (Table 7), although two of these taxa did not satisfy the above criteria for a negative drilling effect. In fact, responses of the anemone *Amphianthus californicus* [Fig. 6(a)] suggest a possible enhancement effect. Densities of this anemone increased after drilling began by a percentage greater at the highdose level than at the moderatedose level, and were slightly reduced at the low-dose level in both deep, low-relief and deep, high-relief habitat (r = 0.998 and 0.901, respectively). Similarly, the significant time/dose interaction for the brittle star *Ophiacantha diplasia* [Fig. 6(e)] also did not seem to indicate a negative drilling effect. Although its correlation coefficients were negative (r = -0.894 and -0.848 in low- and high-relief, respectively), densities of this species increased substantially after initiation of drilling at all dose levels. In addition, densities of galatheid crabs in deep high-relief habitat showed proportionally greater increases at the highdose level than at the moderate-dose level, while showing a decrease at the low-dose level, after initiation of drilling [Fig. 6(c); r = 0.956]. This taxon, however, apparently did display a negative response to drill ing discharges at deep, high-relief stations (see below).

Time/dose interactions for the ahermatypic coral *Caryophyllia* sp(p). in both low- and high-relief habitat, as well as galatheid crabs and the ascidian *Halocynthia hilgendorfi igaboja* in low-relief habitat, suggest possible negative effects of the drilling discharges. Changes in mean densities of *Caryophyllia* sp(p). after drilling began were closely correlated with the flux of drilling-mud particles in both deep, low-relief and deep, high-relief habitat [Fig. 6(b); r = -1.000 and -0.928, respectively]. In both types of habitat, highest densities occurred at low-dose stations after drilling began, and lowest densities occurred at the highdose stations after drilling began. The negative relationship between changes in galatheid crab abundances and the fluxes of drilling-mud particles in deep, low-relief habitat [Fig. 6(c); r = -0.675] is less conclusive and largely a function of peak densities occurring at the highdose station before drilling began and at the moderatedose and lowdose stations after drilling began. Nevertheless, the lowest densities of these crabs occurred at the highdose station after the onset of drilling. Similarly, the negative relationship between abundance changes and fluxes of drilling-mud particles for *H. hilgendorfi igaboja* in deep low-relief habitat [Fig. 6(d); r = -0.612] may have been caused by unusually high pre-drilling densities at the highdose station, although an effect of drilling discharges cannot be ruled out.

Thus four of 22 taxa displayed significant ($p \leq 0.05$) time/dose interactions representing possible negative responses to the drilling-mud discharges. These four taxa were: (1) sabellids in deep low-relief habitat, (2) *Caryophyllia* sp(p). in deep low-relief and deep high-relief habitat, (3) galatheids in deep low-relief habitat, and (4) *Halocynthia hilgendorfi igaboja in* deep low-relief habitat. Sabellids, *Caryophyllia* sp(p)., and *H. hilgendorfi igaboja are* all sessile suspension feeders that obtain food particles as water passes over their tentacles or filtration apparatuses. Also, once their larvae settle onto suitable substrates and metamorphose, they are unable to escape adverse conditions. Given these biological characteristics, a possible pollution-response mechanism is proposed, namely that reductions in the densities of these fauna resulted from the physical effects of increased particle loading (e.g., disruption of feeding or respiration, or burial of settled larvae). Hardin *et al.* (Chapter 9) have shown that the natural distributions of hard-bottom epifauna are correlated with variations in the concentrations of suspended particles. While the estimated maximum flux of drilling-derived particles was only 1.96% of the flux of total suspended particles, based on time-integrated data from sediment traps at nearfield Station PH-J, it is possible that organisms near the platform were exposed to higher percentages of drilling-derived particles in intermittent pulses from individual discharges.

The variations in these fauna do not appear to be related to the chemical toxicity of drilling-mud constituents. As shown above, results of hydrocarbon and trace-metal monitoring suggest that organisms living even in the area of maximum drilling-mud deposition were not exposed to unusually high concentrations of any of the measured analytes other than barium. Barium concentrations in suspended particles at high-flux stations during drilling averaged 2397 mg/g, and were about two to three times higher than ambient levels. Virtually all the barium in drilling mud, however, is in the form of insoluble and biological] y inert barium sulfate. Because of the low volubility of barium in seawater (<50 µg/l), ionic barium is not considered toxic to marine organisms (National Research Council, 1983), although high concentrations (> 500 µg/l) of suspended barite in the water column may cause physical damage to marine organisms (Tagatz and Tobia, 1978; Carls and Rice, 1980). Jenkins *et al.* (1989) show that about 97% of the barium accumulated by the clam *Cyclocardia ventricosa* and the polychaete *Pectinaria californiensis* from sediments near a drilling platform off southern California was in an insoluble, granular form (presumably barium sulfate) in the gut and tissues. Therefore, it is unlikely that elevated concentrations of barium in suspended particles caused any toxic effects in hard-bottom epifauna.

Nekton, Inc. (1987) performed a similar study of the potential environmental effects of drilling discharges on hard-bottom epifauna following exploration drilling off southern California. Elevated concentrations of several metals, including barium, were observed in sediment traps and surficial sediments near the drilling site. The estimated average increase in barium concentration in sediments within about 500 m of the drilling site was 175 $\mu g/g$. Concentrations of barium in surficial sediments within 200 m of the site remained elevated above background for at least a year after drilling ceased. In contrast to the present study, abundances of hard-bottom epifauna, also based on random photoquadrat sampling, did not change significantly between pre-drilling and post-drilling surveys. The limited data collected on larval settlement on artificial hard substrates also did not indicate any significant changes attributable to the drilling discharges.

Kingston (1987) and Davies *et al*. (1989) have reviewed the effects on soft-bottom fauna of drilling discharges from platforms and drilling rigs in the United Kingdom sector of the North Sea, Adverse biological effects, limited to within about 500-1000 m of the installations, were found regardless of whether water-based, diesel-based, or low-toxicity (low-aromatic) oil-based muds had been used. The extent of these impacts, however, was substantially greater with oil-based than with water-based muds. It is believed that chemical toxicity of the oil was not the onl y factor responsible for biological changes. In the immediate vicinity of the platform, effects were due mainly to physical burial of the natural sediments by the discharges of cuttings. In addition, organic enrichment of the sediments from oil in the muds and cuttings, or from epifauna falling from submerged platform structures and accumulating on the bottom, is believed to have contributed to the development of anoxic conditions in the sediments. Similar effects due to discharges of cuttings from water-or oil-based drilling, with greater impacts resulting from oil-contaminated cuttings, have been observed around platforms in the Norwegian sector of the North Sea (Reiersen et *al.*, 1989). While the impact zone at most of these fields was within 500-1000 m, as reported for the British sector of the North Sea, at one field (Statfjord) a change in fauna was found out to 5000 m.

While some previous studies have demonstrated direct effects of offshore drilling on soft-bottom fauna, the present study is the first to document apparent effects on hard-bottom epifaunal assemblages. In both this and most past studies, adverse biological effects on the benthos, when observed, have been limited to within about 1 km of the discharge source. Also, in some cases these effects have been attributed to

causes other than (or in addition to) the chemical toxicity of oil. Results of the present study suggest that any biological effects due to the drilling muds were related to physical effects of the increased particle loading.

Ability to Detect Drilling-Related Impacts

The power (1- β) of 17 different response variables measured during CAMP was computed and the results are presented here as a basis for evaluating the ability to detect current and future drilling-related impacts in the area. Five chemical variables (THC, ΣPAHs, naphthalenes, barium, and chromium) were examined with respect to both the bard- and soft-bottom data sets. Levels of zinc in suspended particles collected in sediment traps at the hard-bottom sites were also examined. Eight additional biological variables were examined with respect to only the soft-bottom data set: four synthetic community-level variables (total macroinfaunal individuals, total number of macroinfaunal species, total harpacticoid copepod individuals, total number of harpacticoid species), the abundances of two individual species of macroinfauna (*Mediomastus ambiseta* and *Chloeia pinnata*), and the abundances of two meiofaunal species (the harpacticoid copepods *Cletodes smirnov* and *Zosime* sp. A). The remaining three variables are represented by the abundances of two hard-bottom taxa, the caryophyllid corals *Paracyathus stearnsii* and *Desmophyllum crista-galli*, and one community-level variable for hard-bottom taxa, numbers of species of suspension feeders. These particular variables were selected because they are common or sensitive measures of environmental impact, because they appear to be key ecological components, or because of the amount of variability that they displayed among sites or times during the CAMP study (e.g., variables both with large and small natural fluctuations were included).

All power analyses are based on power to detect a real difference between two means, each estimated by a set of n random replicate samples (see Green, 1989). Appropriate comparisons might be between two stations (e.g., nearfield versus farfield) at a given time or between two sampling times (e.g., pre-drilling versus post-drilling) at a given station. Power analysis requires an estimate of error variation that is stable and not dependent on the mean of the variable. A transformation of the raw data was necessary to achieve this condition for eight of the 13 variables examined with respect to the soft-bottom sampling regime. A square-root transformation was applied to the variable naphthalene, total harpacticoid individuals, *Zosime* sp. A, and *Cletodes smirnov*. A logarithmic transformation was applied to THC, chromium, and ΣPAH. A fourth-root transformation was applied to *Chloeia pinnata*. The remaining variables for the soft-bottom data set did not require a transformation. For the hard-bottom sampling

regime, no transformation of the raw data was necessary for any of the five chemical variables measured in grab samples or for any of the six chemical variables measured in sediment-trap samples. All three epifaunal variables required transformation: for *Paracyathus* a power = 0.3 transformation, and for both *Desmophyllum* and total suspension feeding species a cube-root transformation.

Tables *8* and *9* compare all variables in their power to detect change due to impact for the soft- and hard-bottom sampling arrays, respectively, For each variable, the detectable percentage increase and decrease relative to the initial pre-impact value is listed for three sample sizes, including the actual sample size used during the study. The larger hypothetical sample sizes could be achieved by pooling samples (e.g., among depths, transects, times). Detectable change in the different variables is presented for a power of 1- ß = 0.8. The soft-bottom array was never subjected to drilling, so the "initial pre-impact value" for each variable was calculated as the mean value of all data. For the hard-bottom array, this value was calculated as the mean of all the pre-drilling data.

The two soft-bottom variables for which small changes could be detected, based on actual sample sizes used in the field (i.e., n = 3 in the table), were barium and total number of macrofaunal species (Table 8). A change of 6.4% in barium concentration from an initial value of 735 µg/g could be detected 80% of the time using a sample size of n = *3*. Detection 95% of the time (a power of 0.95) would require a change of 8.2%. Based on the barium signals detected around Platform Hidalgo, such a change would be likely to occur if a platform were eventually installed in the proposed Platform Julius area and began drilling. A change of 16% in the number of macrofaunal species from an initial number of 118 could be detected 80% of the time using a sample size of n = 3. For a power of 0.95, a change of 21 % would be necessary. Four other soft-bottom variables (THC, chromium, Tot. Macrofaunal No., and *Mediomastus ambiseta*) showed moderate percent detectable changes, below 50%, at n = 3 and power of 0.80. Increasing the sample size to n = 9, for example by pooling three replicates each from three stations, would permit detection of moderate changes below 50% for all but three variables. Given these results, and the fact that concentrations of hydrocarbons and trace metals were, for the most part, uniformly low throughout the soil-bottom sampling regime, it is likely that impacts of discharges from future platform operations will be detectable, should any occur.

Detectable changes in hard-bottom variables (Table 9) are presented separately for the chemical variables, which were estimated from a sample size of n = *3* (whether grabs or sediment traps), and the biological

variables, which were estimated from 60 random photographic observations per each unreplicated reef. Results should be interpreted independently, because the type of "replication" used to estimate error variation is inherently different for the two cases. In fact, use of the 60 photographic observations for detecting biological changes in relation to a suspected effect could be criticized as overpowered pseudoreplication. However, if one wishes to contrast two reefs (or two times at a given reef), then nothing else is possible. For actual tests of the effects of dose, relief, depth and time among the nine reefs, from which our conclusions of biological impacts were drawn (see previous section), a different and more conservative approach (i.e., unreplicated multi-way ANOVA design) was used.

Among the chemical variables at hard-bottom sites, barium was again the one for which small changes could be detected with high power (9.3% in grabs and 4.1% in sediment traps, with n = 3 and a power of O. 8). These increases were well below the predicted percent increases of barium in suspended particles during drilling (i.e., 300- 497%, Table 5). In sediment traps, two other chemical variables offered high power to detect small changes, namely chromium (11% at n = 3) and zinc (6.3% at n = 3). Chromium in suspended particles, however, was not expected to have increased more than 0.7 - 1.7% above background concentrations following the platform discharges (Table 5). On the other hand, the predicted small increases in zinc of 8- 20% (Table 5) would be detectable with the present sample size of n = 3 and power of 0.80. Similarly, percent detectable changes in PAH and naphthalenes were well below their predicted percent increases in suspended particles following platform discharges. For most chemical variables at hard-bottom sites (both sediment-trap and grab samples) detection of moderate changes below 50% was possible.

Of the two epifaunal coral species examined, *Paracyathus stearnsii* provided greater power to detect change, although with both variables very small changes ($\leq$ 7.1% with $n = 60$) could be detected because of the large sample sizes used in the power analyses. Total number of suspension-feeding species also provided high power to detect small changes (14% with n = 60 and power of 0.8), although this power was lower compared to the abundances of the two individual epifaunal species or to total number of soft-bottom macrofaunal species (16% at the same power and a much lower $n = 3$).

Thus at a relatively high power of 0.80, small to moderate changes (below 50%) in six of the 13 soft-bottom variables (THC, barium, chromium, total macrofaunal individuals, total macrofaunal species, and *Mediomastus ambiseta*) and all but two hard-bottom variables (ΣPAH in grabs, and naphthalenes in

traps) could be detected with actual sample sizes used in the study. Increasing the sample sizes by pooling replicate samples from as few as three neighboring stations allowed detection of such changes in all but a few variables (soft-bottom: ΣPAH, C. *smirnov* and C. *pinnata*; hard-bottom: naphthalenes in traps). Consistent y, the smallest detectable changes were in barium concentrations. Large increases in concentrations of barium, ΣPAH and naphthalenes, and small to moderate increases in zinc and THC in suspended particles relative to background levels were expected to have occurred at stations nearest to Platform Hidalgo during periods of drilling discharges. These increases (with the exception of THC) were detectable in sediment traps at the actual sample size of $n = 3$ and power of $1 - \beta = 0.80$. Predicted peak concentrations of other analytes in the zone of maximum drilling-mud accumulation were near or at background levels.

The ability to detect drilling-related impacts in the present study was enhanced greatly by the synoptic and time-series sampling of the different biological and environmental variables, making it possible to link biological changes to detectable contaminant signals. We strongly recommend that this approach be continued in future related studies. In addition, a combination of manipulative field and laboratory experiments should be considered as a means of investigating the processes and mechanisms that may be responsible for these apparent impacts.

ACKNOWLEDGMENTS

This study was funded by the U.S. Department of Interior/Minerals Management Service (Pacific OCS Office, Camarillo, California 93010) under Contract No. 14-12-0001-30262 to Battelle Ocean Sciences. Dr. Gary Brewer, the MMS Project Technical Officer, provided a great deal of support throughout the course of study. Special appreciation is extended to the following individuals: William Steinhauer for his contributions as the final, overall Program Manager; Robert Spies and Robert Carney for input in the synthesis and interpretation of data; Eiji Imamura for his involvement as interim Program Manager and for his assistance with the acquisition and synthesis of drilling-mud data; Paul Boehm for establishing the initial sampling and analytical designs for chemical measurements; James Blake for his initial involvement in planning and directing macroinfaunal analyses; Eric Crecelius for providing trace-metal data; Patrick Kinney and Mark Savoie for providing physical oceanographic data; Paul Montagna for providing meiofaunal data; Terry Parr, Jay Shrake, and Jon Toal for their assistance with the collection and analysis of hard-bottom epifaunal data; James Campbell and Janet Kennedy for leading the field efforts for soft-bottom sampling; Hal Petersen, Tom Gulbransen, and John Hennessy for overall database

management; and Ellen Baptiste for helping to run power analyses. We also wish to acknowledge the importance of the contributions and sacrifices that the many others behind the scenes have made throughout the various phases of this ambitious, interdisciplinary program.

REFERENCES

Allen, A, A., R.S. Schlueter, and P.G. Mikolaj. (1970). Natural oil seepage at Coal Oil Point, Santa Barbara, California. *Science,* **170, 974-977.**

Bernstein, R. L., L. Breaker, and R. Whritner. (1977). California Current eddy formation: Ship, air and satellite results. *Science, 195, 353-359.*

Brewer, G. D., J. Hyland, and D.D. Hardin. (1991). Effects of oil drilling on deep-water reefs offshore California, *Amer. Fish. Sot. Symp.*, 11, 26-38.

Brink, K. H., D. W. Stuart, and J .C. Vanleer. (1984). Observations of the coastal upwelling region near 34°30 N off California: Spring 1981. *J. Phys. Oceanogr., 14, 378-391.*

Bruland, K. W., K. Bertine, M. Koide, and E.D. Goldberg. (1974). History of metal pollution in Southern California coastal zone. *Environ. Sci. Technol., 5,* 425-432.

Cads, M.G. and S.D. Rice. (1980). Toxicity of oil well drilling fluids to Alaskan larval shrimp and crabs. Research Unit 72. Final Report to the U.S. Department of the Interior, Bureau of Land Management, Outer Continental Shelf Environmental Assessment Program, Project No. R7120822, Washington, D. C., 29 pp.

CSA (Continental Shelf Associates, Inc.). (1985). Assessment of the long-term fate and effective methods of mitigation of California outer continental shelf platform particulate discharges. Report prepared for the U.S. Department of the Interior, Minerals Management Service, Pacific OCS Region, Los Angeles, CA. Contract No. 14-12-0001-30056. Vol. I (MMS 85-0033).

Davies, J. M., D.R. Bedborough, R.A.A. Blackman, J.M. Addy, J.F. Appelbee, W.C. Grogan, J.G. Parker and A. Whitehead. (1989). The environmental effect of oil-based mud drilling in the North Sea. In *Drilling Wastes,* eds. F.R. Engelhardt, J.P. Ray and A.H. Gil lam. Elsevier Applied Science Publishers, London, pp. 59-89.

Dugdale, R.C. and F.P. Wilkerson. (1989). New production in the upwelling center at Point Conception, California: Temporal and spatial patterns. *Deep-Sea Res.,* 36, 985-1007.

Barrington, J.W. and P.A. Meyers. (1975). Hydrocarbons in the marine environment. In *Environ. Chem.*, Vol. I, ed. G. Eglinton. The Chemical Society, London, pp. 109-136.

Barrington, J. W., J.M. Teal, J.G. Quinn, T. Wade, and K. Burns. (1973). Intercalibration of anal yses of recent] y biosynthesized hydrocarbons and petroleum hydrocarbons in marine 1 ipids. *Bull. Environ. Contam. Toxicol., 10(3), 129-136.*

Barrington, J .W. and B.W. Tripp. (1977). Hydrocarbons in western North Atlantic surface sediments. *Geochim. Cosmochim. Acts, 41, 1627-1641.*

Fry, V.A. and B. Butman. (In press). Estimates of the seafloor area impacted by dumping at the 106-mile deepwater municipal sewage sludge disposal site. *Mar.* Environ. *Res.*

Green, R.H. (1989). Power analysis and practical strategies for environmental monitoring. *Environ. Res., 50, 195-205.*

Hyland, J., E. Baptiste, J. Campbell, J. Kennedy, R. Kropp, and S. Williams. (In press). The infaunal benthos of the outer continental shelf and slope north of Point Conception, California. *Mar. Ecol. Prog. Ser.*

Hyland, J., D. Hardin, E. Crecelius, D. Drake, P. Montagna, and M. Steinhauer. (1990). Monitoring long-term effects of offshore oil and gas development along the southern California outer continental shelf and slope: background environmental conditions in the Santa Maria Basin. *Oil & Chem. Pollut. ,6, 195-240.*

Hyland, J., J. Kennedy, J. Campbell, S. Williams, P. Boehm, A. Uhler, and W. Steinhauer. (1988). Environmental effects of the *Pac Baroness* oil and copper spill. In *Proceedings of the 1989 Oil Spill Conference, San* Antonio, TX. API, EPA, and USCG, pp. 413-419.

Jenkins, K. D., S. Howe, B.M. Sanders, and C. Norwood. (1989). Sediment deposition, biological accumulation and subcellular distribution of barium following the drilling of an exploratory well. In *Drilling Wastes, eds.* F.R. Engelhardt, J.P. Ray, and A.H. Gillam. Elsevier Applied Science Publishers, London, pp. 587-608.

Katz, A. and I.R. Kaplan. (1981). Heavy metals behavior in coastal sediments of Southern California: A critical review and synthesis. *Mar. Chew.,* 10, *261-299.*

Kennicutt II, M. C., J.L. Sericano, T.L. Wade, F. Alcazar, and J.M. Brooks. (1987). High molecular weight hydrocarbons in Gulf of Mexico continental slope sediments. *Deep-Sea Res., 34(3), 403-424.*

Kingston, P.F. (1987). Field effects of platform discharges on benthic macrofauna. *Phil. Trans. Roy. Sot. London. B, 316, 545-565.*

McCulloch, D. S., S.H. Clarke, Jr., G.L. Dolton, M.E. Field, E.W. Scott and P.A. Utter. (1982). Geology, environmental hazards, and petroleum resources for 1982. OCS Lease Sale 73, offshore central and northern California. U.S. Geological Survey Open File Report 82-1OOO, 77 pp.

Montagna, P. (In press). Meiobenthic communities of the Santa Maria Basin on the California continental shelf. Cent. Shelf Res., 11.

Mooers, C.N.K. and A.R. Robinson. (1984). Turbulent jets and eddies in the California Current and inferred cross-shore transports. *Science, 223, 51-53.*

National Research Council, (1983). *Drilling Discharges in the Marine Environment.* National Academy Press, Washington, D. C., 180 pp.

Nekton, Inc. (1987). An ecological study of discharge drilling fluids in the western Santa Barbara Channel. Report to Texaco USA, Los Angeles, CA.

Reed, W. E., I.R. Kaplan, M. Sandstrom, and PJ. Mankiewicz. (1977). Petroleum and anthropogenic influence on the composition of sediments from the Southern California Bight. In *Proceedings, 1977 Oil Spill Conference (Prevention, Behavior, Control, Cleanup),* Washington, D.C. American Petroleum Institute, pp. 183-188.

Reed, W .E. and I.R. Kaplan. (1977). The chemistry of marine petroleum seeps. *J. Geochem. Explor.*, 7, 255-293.

Reiersen, L. O., J.S. Gray, K.H. Palmork and R. Lange. (1989). Monitoring in the vicinity of oil and gas platforms; results from the Norwegian sector of the North Sea and recommended methods for forthcoming surveillance. In *Drilling Wastes, eds.* F.R. Engelhardt, J.P. Ray and A.H. Gillam. Elsevier Applied Science Publishers, London, pp. 91-117.

Rintoul, B. (1985). Fifteen platforms planned off California. *Offshore,* 45(l), 60-61.

SAIC (Science Applications International Corporation). (1986). Assessment of Long-Term Changes in Biological Communities of the Santa Maria Basin and Western Santa Barbara Channel - Phase I, Volume 11 Synthesis of Findings 9MMS 86-9912). Report prepared for the U.S. Department of Interior, Minerals Management Service, Pacific OCS Region, Los Angeles, CA. Contract No. 14-12-0001-30032.

Simoneit, B.R.T. and I.R. Kaplan. (1980). Triterpenoids as molecular indicators of paleoseepage in recent sediments of the Southern California Bight. *Mar. Environ. Res., 3,* 113-128.

SokaI, R.R. and F.J. Rohlf. (1981). *Biometry.* Second Edition, W.H. Freeman and Company, New York, 859 pp.

Steinhauer, M. and W. Steinhauer. (1990). Chemical analysis of hydrocarbons in sediments, pore water, and animal tissues. Chapter 5. In *California OCS Phase II Monitoring Program: Year-Three Annual Report, eds.* M. Steinhauer and E. Imamura. Report prepared for the U.S. Department of the Interior, Minerals Management Service, Pacific OCS Region, Los Angeles, CA. Contract No. 14-12-0001-30262. Volume I (MMS 90-0055).

Stuermer, D. H., R.B. Spies, PJ.H. Davis, D.J. Ny, L.J. Morris, and S. Neal. (1982). The hydrocarbons in the Isla Vista marine seep environment. *Mar. Chem.*, 11, 413426.

Tagatz, M.E. and M. Tobia. (1978). Effect of barite ($BaSO_4$) on the development of estuarine communities. *Estuar. Cstl. Mar. Sci., 7, 401-407.*

Uchupi, E. and K.O. Emery. (1963). The continental slope between San Francisco, California and Cedros Island, Mexico. *Deep-Sea Res.,* **10(4), 397-447.**

van Dam, G.C. (1982). Models of Dispersion. Chapter 2. In *Pollutant Transport and Transfer in the Sea,* Vol. I, ed. G. Kullenberg. CRC Press, Boca Raton, FL.

Wakeham, S.G. and J.W. Farrington. (1980). Hydrocarbons in contemporary aquatic sediments. In *Contaminants and Sediments,* Volume I, ed. R.A. Baiter. Ann Arbor Science Publishers, Am Arbor, MI, pp. 3-32.

Wilkinson, E.D. (1972). California offshore oil and gas seeps. California Division of Oil and Gas Pub. No. TR-08, 11 pp.

Table 1. Summary of drilling activities

Platform	Drilling Period	No. Wells	Mud Discharged (kg)[a]	Mud Discharged (m')	Barite Discharged (kg)	Cuttings Discharged (m')
Harvest[b]	**11 /86** to 05/88	19	4,100,292	16,340	1,844,136	
Hermosa	01 /87 to 09/88	13	3,651,410	16,373	1,470,955	3,114
Hidalgo	11/87 to 01/89	7	3,473,402	7,963	1,805,000	2,294
Irene	04/86to **10/89**[c]	18	3,916,032	12,967	612,455	4,585

[a]Dry weight.
[b]Cuttings discharge data incomplete.
"Drilling (i.e., at well No. A-19) recommenced December ! 990, which was after the last sampling period for this study. Production has been continuous at Platform Irene since April 1987.

Table 2, Drilling-mud depositional fluxes ($mg/m^2/day$) computed from excess barium concentrations in sediment traps. Dashes indicate missing data. Zeros indicate background concentrate ions of barium

	During Drilling ,				Post Drilling			
	May 88	Ott 88	May 89	Mean	Ott 89	May 90	Ott 90	Mean
Low Flux								
PH-W	79	113	74	89		21	0	11
PH-U		198	147	172	58	0	9	22
Moderate Flux								
PH-R	399	179	68	215	39	0	2	14
PH-F		250	219	234	23	0	3	9
High Flux								
PHAR		421	81	251	45	0	14	20
PH-K	437		96	267	37	36	0	24
PH-E	331	417	180	310		8	0	4
PH-N	512	316	76	301		2	0	I
PH-I	407	369	237	338	48	0	3	[7
PH-J	523	464	I 45	377	54	6	0	20
Mean	384	303	132		43	7	3	

Table 3. Mean contaminant concentrations (μg/g) in surficial sediments collected from nearfield and farfield stations before drilling, during drilling, and after drilling at Platform Hidalgo. Grand mean concentrations in surficial sediments from the proposed Platform Julius control site are included for comparison.

	Pre-Drilling[a]		During-Drilling[b]		Post-Drilling[c]		Platform Julius
	Nearfield[d]	Farfield[e]	Nearfield[d]	Farfield[e]	Nearfield[d]	Farfield[e]	Mean (n = 137)
Silver	0.13	0.13	0.09	0.09	0.08	0.08	0.09
Arsenic	9.7	6.7	11	6.8	9.7	6.8	5.9
Cadmium	0.56	0.59	0.62	0.61	0.58	*0.58*	0.45
Chromium	124	131	120	127	123	139	80
Copper	15	16	16	14	15	15	15
Mercury	0.067	0.075	0.085	0.088	0.054	0.063	0.078
Nickel	40	44	*39*	42	40	43	39
L e a d	14	17	13	15	14	14	15
Vanadium	54	63	48	53	51	54	57
Zinc	75	66	76	63	74	63	64
Barium	764	789	970	872	888	853	740
THC[f]	49	**41**	*93*	93	50	67	62
ΣPAH[g]	0.29	*0.08*	*0.07*	0.08	0.03	0.02	0.12
Naph[h]	0.056	*0.010*	*0.014*	0.014	0.002	0,002	0.015
Fluor[i]	0	*0*	*0*	0	0	0	0.004
Phen[j]	0.060	*0.021*	*0.013*	0.010	0.005	0.004	0.029
DBT[k]	0.033	*0.001*	0.005	0	0	0	0.007

Table 3. (continued)

"October 1986, May 1987, and October 1987,

[b]May 1988, October 1988.

[c]May 1989, October 1989, October 1990.

'Stations PH-I, PH-J, PH-K, PH-N, and PH-R.

'Stations PH-U and PH-W.

'Total resolved and unresolved hydrocarbons.

[g]Total two- to five-ring target PAH compounds.

'Sum of naphthalene + alkylated homologous series.

'Sum of fluorene + alkylated homologous series.

hum of phenanthrene + alkylated homologous series.

'Sum of dibenzothiophene + alkylated homologous series.

Table 4. Average concentrations ($\mu g/g$ dry weight) of trace metals and hydrocarbons in suspended particles collected in sediment traps during and after drilling at Platform Hidalgo. The three station categories are based on estimates of drilling-mud fluxes computed from excess barium concentrations in traps relative to station background concentrations

	During-Drilling[a]			Post-Drilling[b]		
	High Flux[c]	Medium Flux[d]	Low Flux[e]	High Flux[c]	Medium Flux[d]	Low Flux[e]
Silver	0.18	0.18	0.17	0.16	0.16	0.15
Arsenic	4.3	4.4	4.2	6.4	6.0	6.7
Cadmium	0.65	0.69	0.71	0.71	0.68	0.67
Chromium	93	90	85	100	97	96
Copper	19	16	19	20	20	21
Mercury	0.069	0.075	0.055	0.080	0.069	0.075
Nickel	45	47	47	45	45	49
Lead	15	18	15	15	14	13
Vanadium	83	79	81	76	81	69
Zinc	81	82	83	79	78	79
Barium	2397	1923	1237	883	825	771
THC[f]	182	259	411	136	152	157
ΣPAH[g]	0.08	0.07	0.08	0.09	0.06	0.06
Naph[h]	0.007	0.009	0.022	0.015	0.019	0.009
Fluor[i]	0.004	0	0	0	0	0
Phen[j]	0.013	0.003	0.011	0.032	0.015	0.008
DBT[k]	0	0	0	0.005	0	0

Table 4. (continued)

[a]Traps deployed January - May 1988, May - October 1988, and October 1988- May 1989.

[b]Traps deployed May - October 1989, October 1989- May 1990, and May - October 1990.

[c]Stations PH-I, PH-J, PH-K, PH-N, and PH-E.

[d]Stations PH-F and PH-R.

[e]Stations PH-U and PH-W.

[f]Tot al resolved and unresolved hydrocarbons.

[g]Total two- to five-ring target PAH compounds.

[h]Sum of naphthalene + alkylated homologous series.

[i]Sum of fluorene + alkylated homologous series.

[j]Sum of phenanthrene + alkylated homologous series.

[k]Sum of dibenzothiophene + alkylated homologous series.

Table 5. Estimated peak concentrations ($\mu g/g$ dry weight) of trace metals and hydrocarbons in suspended particles at nearfield high-flux station PH-J based on model predictions of a 1.96'% ratio of maximum drilling-mud flux to total-suspended-particle flux

	Background Concentration' (A)	Concentration in Drilling Mud (B)		Predicted Peak Concentration[b] (c)		Predicted Percent Increase Above Background[e]	
		Average[c]	Bottom[d]	Average[c]	Bottom[d]	Average[C]	Bottom[d]
Silver	0.14	0.28	0.23	0.15	0.14	7.1	0
Arsenic	6.5	6.3	6.7	6.6	6.6	1.8	2.0
Cadmium	0.72	[.2	1.3	0.74	0.75	2.8	4.2
Chromium	99	85	37	101	100	1.7	0.7
Copper	21	30	27	22	21	2.8	2.5
Mercury	0.075	0.130	0.182	0.077	0.079	6.7	6.7
Nickel	48	41	22	49	48	1.7	0.9
Lead	14	19	51	14	15	2.6	7.1
Vanadium	81	71	38	82	82	1.7	0.9
Zinc	71	290	714	77	85	8.0	20
Barium	703	107,782	178,405	2815	4200	300	497
THC[f]	80	390	988	88	99	9.5	24
ΣPAH[g]	0.06	25	51	0.55	1.1	817[h]	1,667h
Naph[i]	0.001	18	39	0.35	0.77	34,900[h]	76,900[h]

Table 5. **(continued)**

'Mean concentration of replicate sediment-trap samples from station PH-J during the October 1990 **postdrilling** sampling period.

[b]**[Column** (b) x 0.0196] + column (A) = peak concentration within area of maximum drilling-mud flux.

'Composite average of surface, mid, and bottom well depths.

'Bottom well depth,

'[Column (C) - column **(A)]/[column** (A)] x 100 = percent increase.

[f] Total resolved and unresolved hydrocarbons.

[g]**Total** two- to five-ring target PAH compounds.

'Large increase results from extremely low background concentrations.

'Sum of **naphthalene** + **alkylated** homolog series.

Table 6. Station categories for A NOVAs of hard-bottom tax a. Each station was sampled seven times.

	High Dose		Moderate Dose		Low Dose	
	Low Relief	High Relief	Low Relief	High Relief	Low Relief	High Relief
Shallow Reefs	PPH-J PH-E PH-I	-	PH-F	-	PH-U	-
Deep Reefs	PH-N	PH-K	PH-R	PH-R	PH-W	PH-W

Table 7. Significance of time/dose interactions from three-way ANOVAS for effects of time, dose, and depth at low-relief stations, and effects of time, dose, and relief at deep stat ions

Taxa	p > a Low-Relief Stations	p > a Deep Stations
Sponge, shelf (cover)	0.5154'	*0.5988*
Sponge, tan encrusting (cover)	**0.9286**[a]	*0.9724*
Sponge, white encrusting (cover)	**0.2989**[a]	*0.6965*
Amphianthus californicus (counts)	0.0784'	*0.0184*
Anemone, tan **zoanthid** (cover)	0.4434'	*0.2352'*
Anemone, white disc and purple tentacles (counts)	**0.0057**[a]	**0.0781**[b]
Caryophyllia **sp(p).** (counts)	**0.0982**[a]	*0.0498*
Desmophyllum crista-galli (counts)	**0.0652**[a]	*0.8035*[b]
Lophelia prolifera (cover)	0.9572	**0.6136**[b]
Lophogorgia chilensis (cover)	**0.9346**[a]	**0.2555**[b]
Metridium *senile* (counts)	**0.8946**[a]	*0.2632*
paracyathus stearnsii (counts)	0.9941'	*0.4283*
Stomphia didemon (counts)	**0.1558**[a]	*0.0904*
Sabellidae, unident (counts)	**0.0013**[a]	**0.0510**[b]
Terebellidae, unident (counts)	**0.7878**[a]	**0.4159**[b]
Galatheidae, unident (counts)	**0.8003**[a]	*0.0386*[b]
Cellaria **sp(p).** (cover)	**0.7842**[a]	*0.3735*
Florometra serratissima (counts)	0.8810	*0.6835*[b]
Ophiacantha diplasia (counts)	0.9216	*0.0320*
Ophiuroidea, unident (counts)	0.9970	**0.0687**[b]
Halocynthia hilgendorfi igaboja (counts)	0.8581'	**0.0045**[b]
Pyura haustor (counts)	0.1250	*0.3532*[b]
Total Suspension Feeders (cover)	**0.6627**[a]	*O.* 1629b
Total Abundance (cover)	0.3749	0.0568
Total Number of Species	0.0822	0.0669[b]

'Dose/depth interaction was significant ($p \leq 0.05$).
[b]Dose/rel ief interaction was significant ($p \leq 0.05$).

Table 8. Detectable change for 13 soft-bottom variables for each of three sample sizes (n = 3, 6 and 9), given type I error probability $\alpha = 0.05$ (two-tailed) and type 11 error probability $\beta = 0.2$ (power: $1-\beta = 0.8$). Initial pre-impact value is based on the mean of all sampling periods

Variable	Initial Value	n = 3 Increase (%)	n = 3 Decrease (%)	n = 6 Increase (%)	n = 6 Decrease (%)	n = 9 Increase (%)	n = 9 Decrease (%)
THC	60.3 µg/g	+48	-33	+32	-24	+26	-21
Napthalene	0.015 µg/g	+89	-61	+60	-46	+48	-39
ΣPAH	0.121 µg/g	+ 193	-66	+95	-49	+70	-41
Barium	735 µg/g	+6.4	-6.4	+4.5	-4.5	+3.7	-3.7
Chromium	85.8 µg/g	+34	-26	+23	-19	+19	-16
Tot. Macro. No.	1160/m²	+37	-37	+26	-26	+21	-21
Tot. Macro Spp.	118	+16	-16	+12	-12	+9	-9
Tot. Harp. No.	27/m²	+101	-66	+68	-50	+54	-43
Tot. Harp. Spp.	12	+59	-59	+42	-42	+34	-34
Zosime sp. A	3.5/10 cm²	+188	-91	+123	-75	+97	-65
C. smirnov	3.6/10 cm²	+188	-91	+123	-74	+97	-64
C. pinnata	119/inn	+92	-54	+60	-41	+48	-35
M. ambiseta	174/m²	+40	-40	+29	-29	+24	-24

Note: Except for THC, Cr, and ΣPAH, the detectable change depends on the initial value used.

Table 9. Detectable change for 14 hard-bottom variables for each of three sample sizes (n = 3, 6 and 9 for the chemical variables; and n = 30, 60, and 120 for the epifaunal variables), given type 1 error probability a=0.05 (two-tailed) and type 11 error probability β = 0.2 (power: 1 - β = 0.8). Initial pre-impact value is based on the mean of all pre-drilling periods (October 1986, May 1987 and October 1987, except sediment-trap variables not samples in October 1987)

Variable	Initial Value	n=3 Increase (%)	n=3 Decrease (%)	n=6 Increase (%)	n=6 Decrease (%)	n=9 Increase (%)	n=9 Decrease (%)
Grabs:							
Barium	752 µg/g	+9.3	-9.3	+5.8	-5.8	+4.6	-4.6
Chromium	127 µg/g	+25	-25	+16	-16	+12	-12
THC	41.9 µg/g	+19	-19	+12	-12	+10	-lo
ΣPAH	0.108 µg/g	+56	-56	+35	-35	+27	-27
Napthalene	0.012 µg/g	+40	-40	+25	-25	+20	-20
Seal. Traps:							
Barium	707 µg/g	+4.1	-4.1	+2.5	-2.5	+2.0	-2.0
Chromium	109 µg/g	+11	-11	+6.5	-6.5	+5.1	-5.1
Zinc	80.2 µg/g	+6.3	-6.3	+3.9	-3.9	+3.1	-3.1
THC	93.4 µg/g	+48	-48	+30	-30	+24	-24
ΣPAH	0.055 µg/g	+32	-32	+20	-20	+16	-16
Napthalene	0.002 µg/g	+155	-155	+96	-96	+76	-76

Table 9. (continued)

Variable	Initial Value	n = 30 Increase (%)	n = 30 Decrease (%)	n = 60 Increase (%)	n = 60 Decrease (%)	n = 120 Increase (%)	n = 120 Decrease (%)
Epifauna:							
P. stearnsii	*11610.75* m^2	**+2.4**	**-2.4**	**+1.7**	**-1.7**	**+1.2**	**-1.2**
D. crista-galli	*13.210.75* m^2	+ 10.3	-9.6	**+7.1**	-6.8	+5.0	-4.8
Tot. Suspension-Feeding Spp.	18.310.75 m^2	+21	-18	+14	-13	+10	-9

Note: For all variables, the detectable change depends on the initial value used.

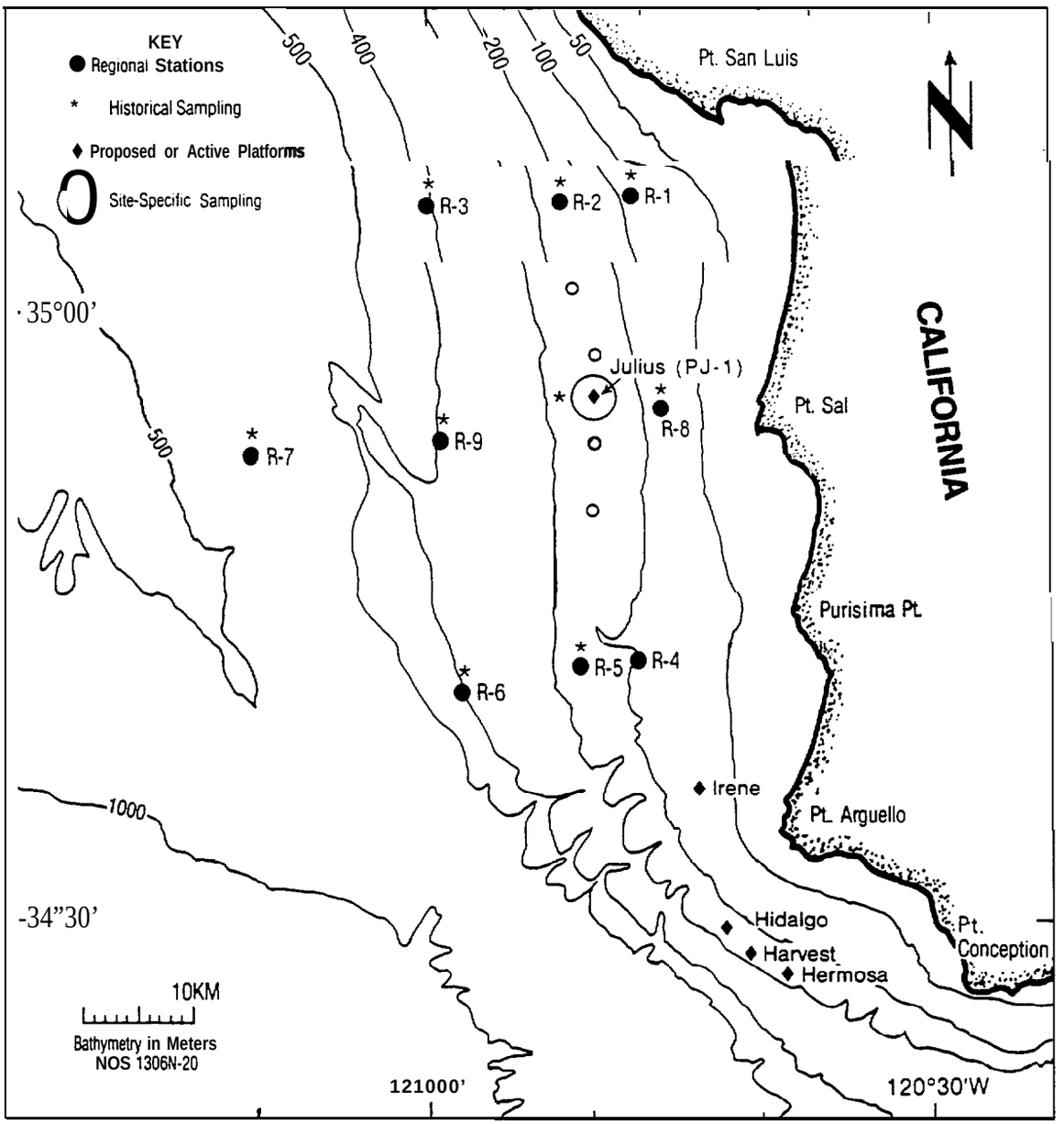

Figure 1. The study area,

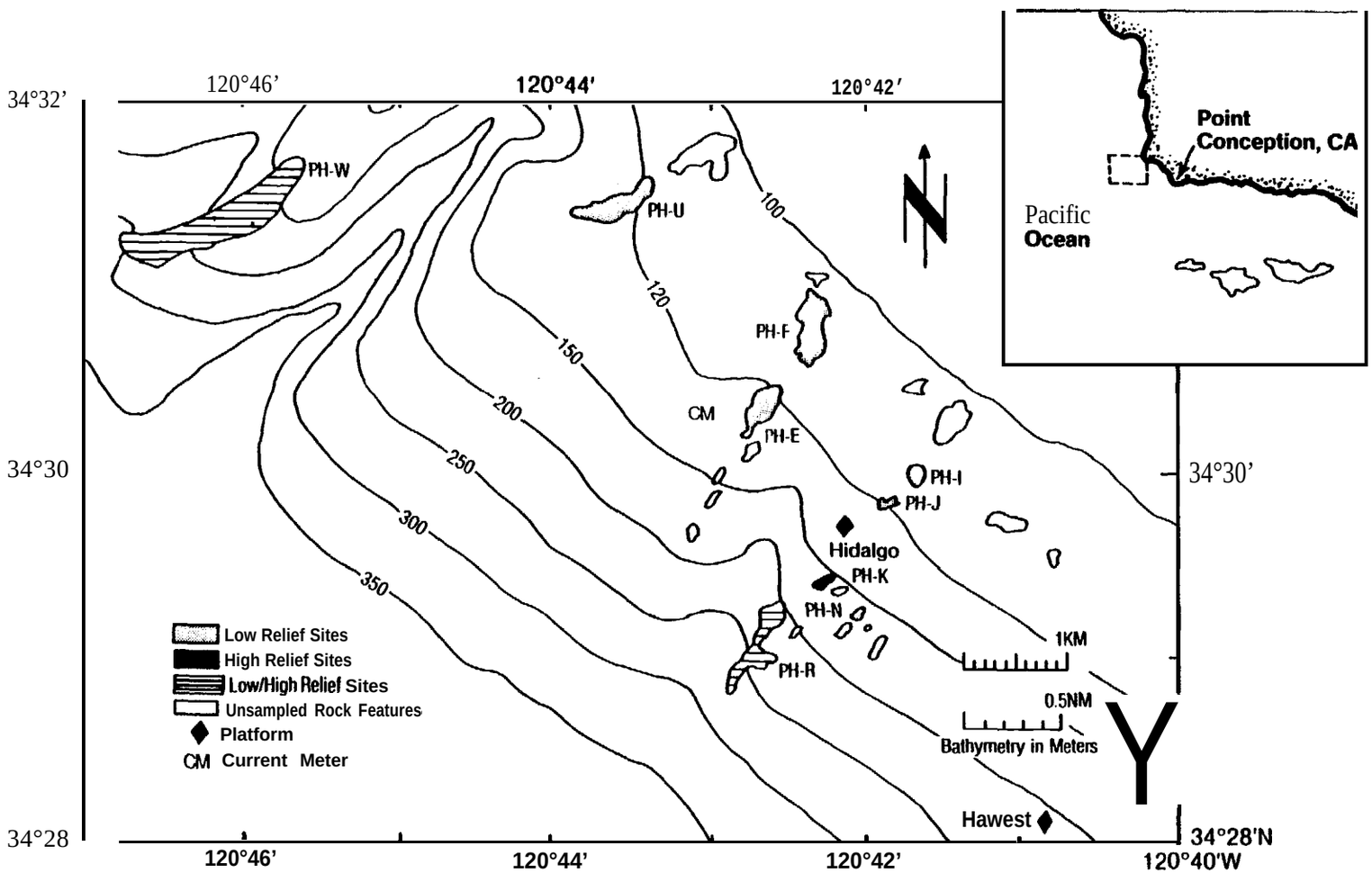

Figure 2. Hard-bottom sampling sites. Sediment traps were located within 50-100 m of each hard-bottom photosurvey site and at an additional site approximate y 500 m NW of Platform Harvest.

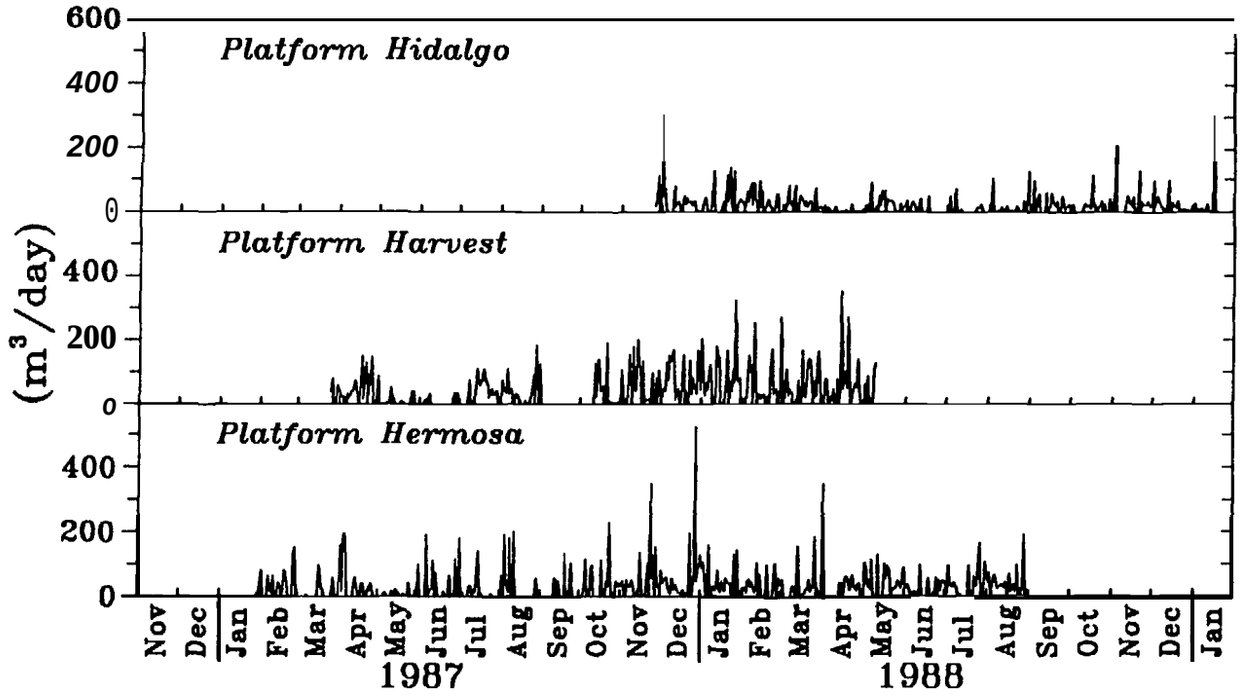

Figure 3. **Daily drilling-mud** volumes discharged from development/production platforms in the hard-bottom sampling area.

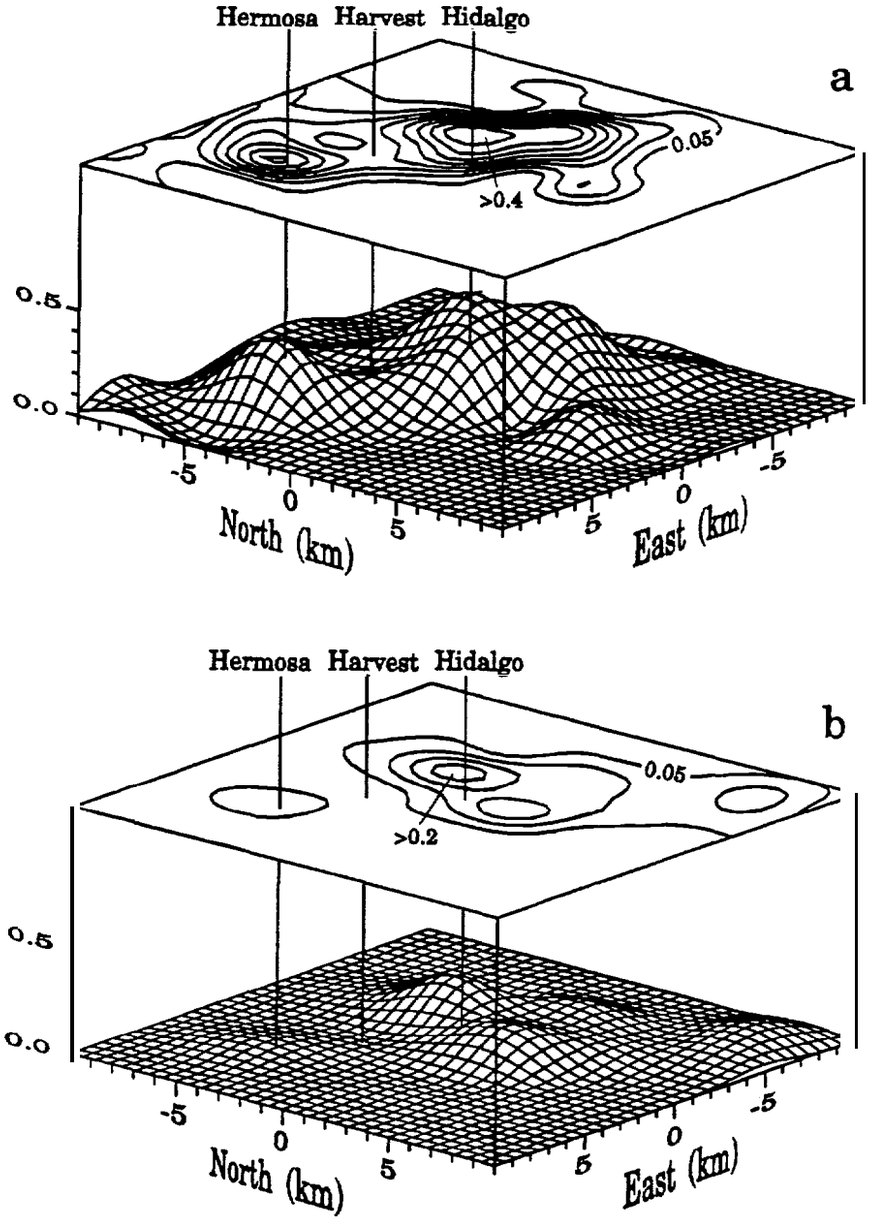

Figure 4. Depositional patterns of drilling-mud solids as viewed by an observer looking offshore, toward the southwest. Contour interval = 0.05 **g/m²/day**. a = May 21- October 12, 1988; b = October 12, 1988- May 17, 1989.

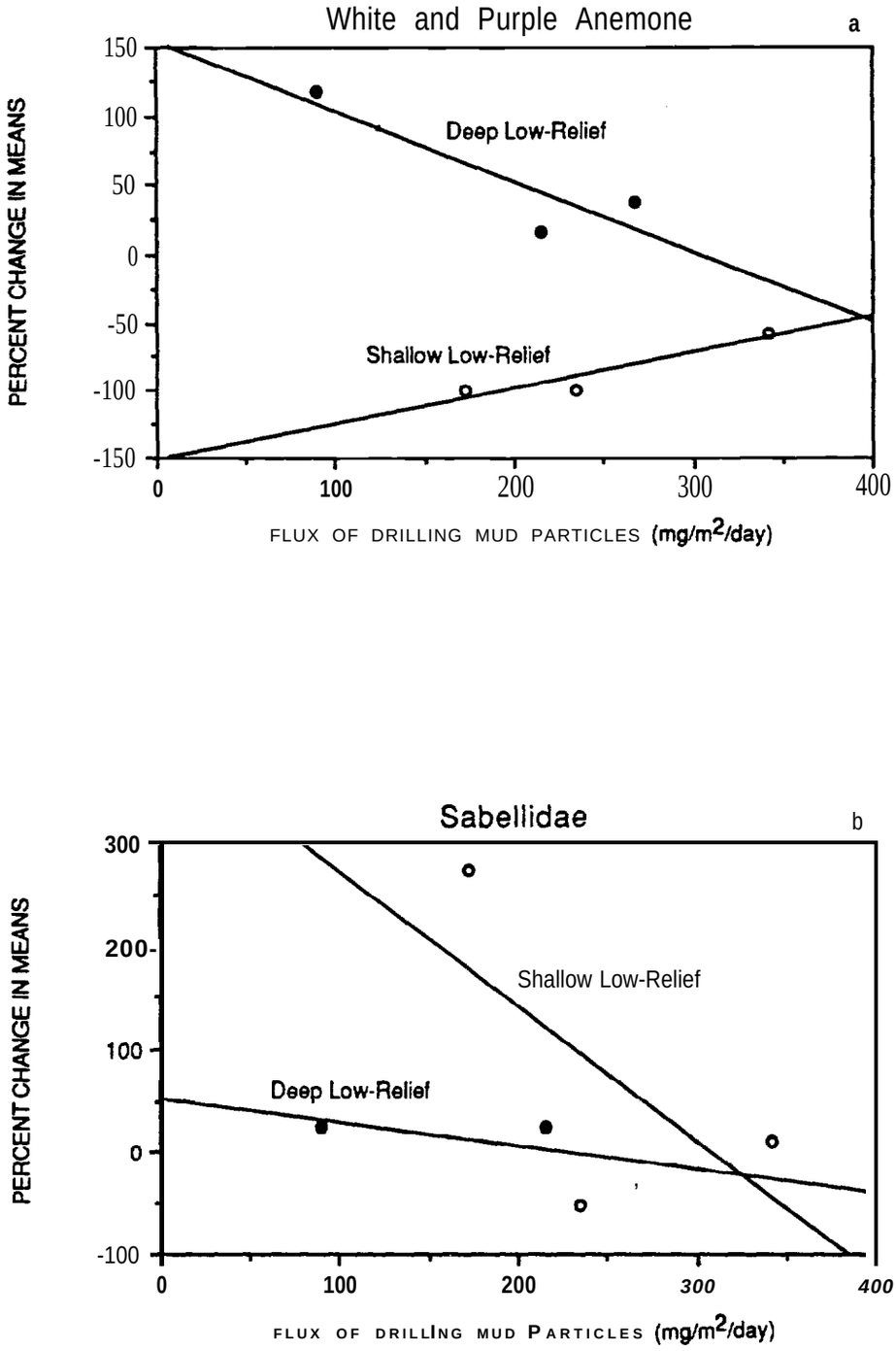

Figure 5. Relationships between estimated fluxes of drilling-mud particles and percent changes in species abundances at shallow low-relief (open circles) and deep low-relief (closed circles) stations. Lines were fit by the least-squares method. Y-axis values are the percent changes in mean abundances after initiation of drilling (average of October 1988, May 1989, October 1990) relative to the pre-drilling means (average of October 1986, July 1987, and November 1987).

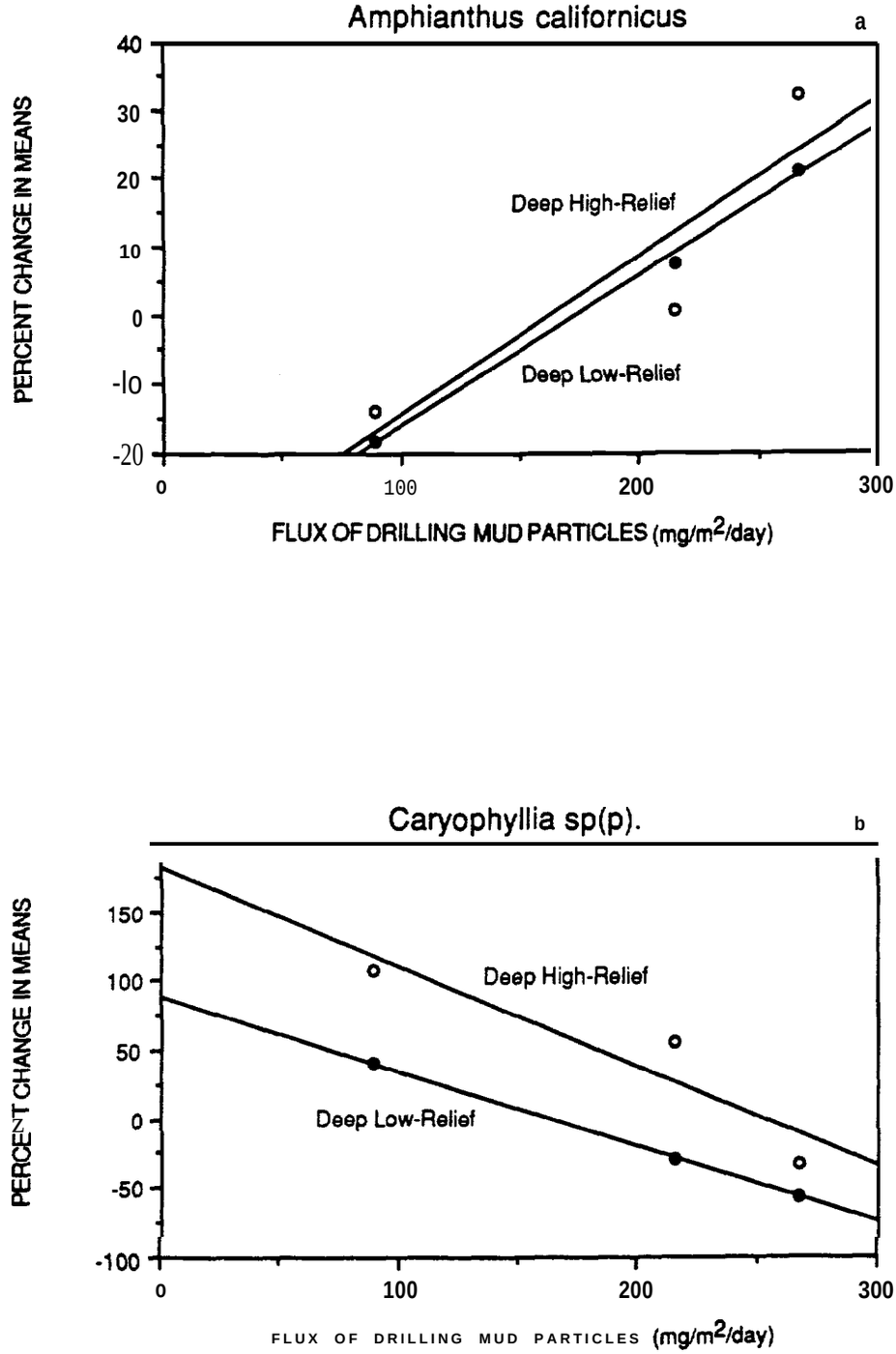

Figure 6. Relationships between estimated fluxes of drilling-mud particles and percent changes in species abundances at deep high-relief (open circles) and deep low-relief (closed circles) stations. Lines were fit by the least-squares method. Y-axis values are the percent changes in mean abundances after initiation of drilling (average of October 1988, May 1989, October 1990) relative to the pre-drilling means (average of October 1986, July 1987, and November 1987).

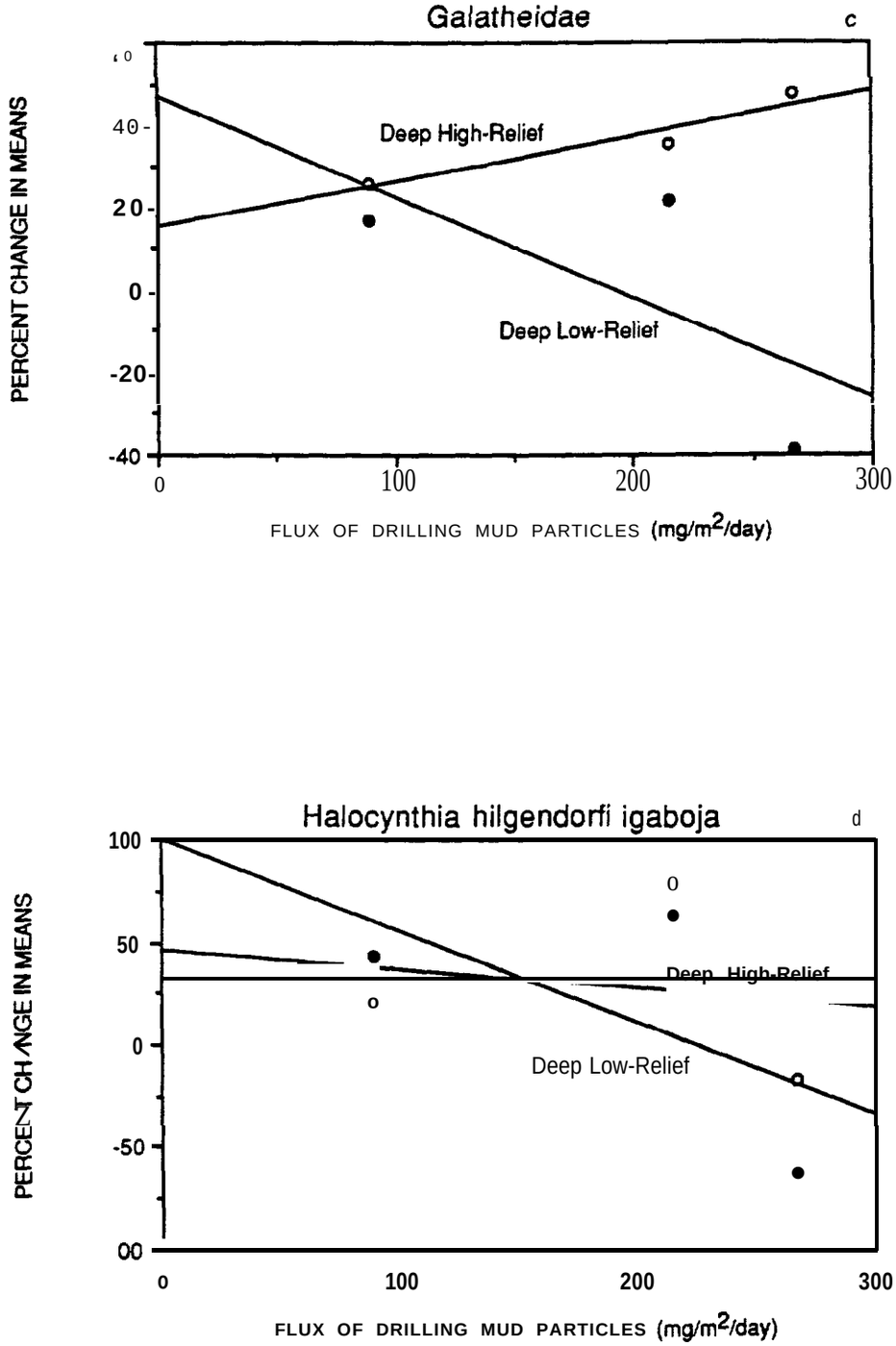

Figure 6. Relationships between estimated fluxes of drilling-mud particles and percent changes in species abundances at deep high-relief (open circles) and deep low-relief (closed circles) stations. Lines were fit by the least-squares method. Y-axis values are the percent changes in mean abundances after initiation of drilling (average of October 1988, May 1989, October 1990) relative to the pre-drilling means (average of October 1986, July 1987, and November 1987). (continued)

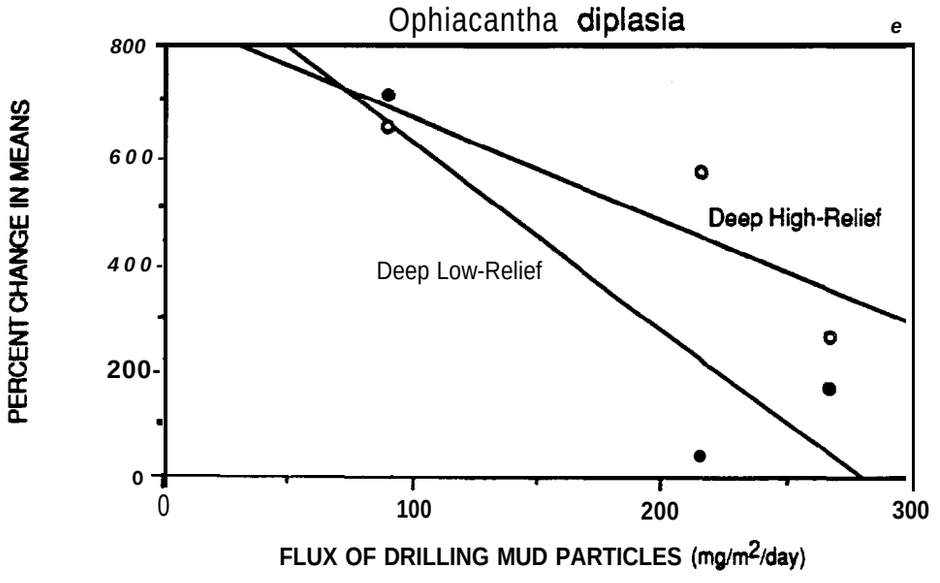

Figure 6. Relationships between estimated fluxes of drilling-mud particles and percent changes in species abundances at deep high-relief (open circles) and deep low-relief (closed circles) stations. Lines were fit by the least-squares method. Y-axis values are the percent changes in mean abundances **after** initiation of drilling (average of October 1988, May 1989, October 1990) relative to the **pre-drilling** means (average of October 1986, July 1987, and November 1987). (continued)